General Disclaimer

One or more of the Following Statements may affect this Document

- This document has been reproduced from the best copy furnished by the organizational source. It is being released in the interest of making available as much information as possible.

- This document may contain data, which exceeds the sheet parameters. It was furnished in this condition by the organizational source and is the best copy available.

- This document may contain tone-on-tone or color graphs, charts and/or pictures, which have been reproduced in black and white.

- This document is paginated as submitted by the original source.

- Portions of this document are not fully legible due to the historical nature of some of the material. However, it is the best reproduction available from the original submission.

Produced by the NASA Center for Aerospace Information (CASI)

CR-115111

Final Report Contract NAS 9-10484

EXTENDABLE NOZZLES FOR SPACE ENGINES

Volume 1: Program Studies

Report 10484-FR November 1970

FACILITY FORM 602

N71 31606 (ACCESSION NUMBER) (THRU)

362 (PAGES) 63 (CODE)

CR-115111 (NASA CR OR TMX OR AD NUMBER) 37 (CATEGORY)

AEROJET LIQUID ROCKET COMPANY

A DIVISION OF AEROJET-GENERAL

SACRAMENTO, CALIFORNIA

FINAL REPORT

EXTENDABLE NOZZLES FOR SPACE ENGINES

VOLUME I: PROGRAM STUDIES

Report 10484-FR
November 1970

Prepared Under
Contract NAS 9-10484

Prepared for

NATIONAL AERONAUTICS AND SPACE ADMINISTRATION
Manned Spacecraft Center
Houston, Texas

Report 10484-FR, Volume I

TABLE OF CONTENTS

		Page
I.	Introduction	1
II.	Summary	
	A. Configurations Analysis	4
	B. Tradeoff Studies	5
	C. Technical Analysis	5
	D. Experimental Hardware Design	6
	E. Experimental Hardware Fabrication and Checkout Testing	7
	F. Test Planning	8
	G. Experimental Testing	8
	H. Conclusions and Recommendations	8
III.	Discussion	
	A. Configuration Analysis	12
	B. Tradeoff Studies	22
	C. Technical Analysis	79
	D. Test Hardware Design	112
	E. Test Hardware Fabrication	139
	F. Demonstration Testing	145
References		146

APPENDICES

	Appendix
Bibliography	A
Test Plan	B
Predicted White Sands Diffuser Performance	C
Film Coolant Injector Design Calculations	D
Actuator Analysis	E
Thermal Stress Analysis	F

TABLE LIST

	No.
Sublimation of Metal in High Vacuum	I
Decomposition of Polymers in High Vacuum	II
Comparison of Lubricants for Bearings in Space	III
Radiation Tolerance for Various Materials	IV
Comparative Rating of Nozzle Extension Cooling Concepts	V
Standard Platings and Coatings for Metallic Seals	VI
Maximum Service Temperatures of Plastics and Elastomers	VII
Coefficient of Thermal Expansion for Different Materials	VIII
Linear Thermal Expansion of Typical Seal and Gland Materials	IX
Seal Comparison Chart	X
Comparison of Translation Systems	XI
Secondary Gas Coolant Properties and Engine and Gas Generator Operating Conditions	XII
Rao Nozzle Contours	XIII
Delivered Performance, R_T = 1.28 in.	XIV
Delivered Performance, R_T = 1.81 in.	XV
Extension Attachment Area Ratio Tradeoffs	XVI
Tradeoff Ratio for a Variation in Nozzle Throat Radius	XVII
Chamber Nozzle and Coolant Ring Data	XVIII
Test Engine Nozzle Contour	XIX

Figure List

Figure No.	Title
1	Phase I and II Master Program Schedule
2	Extendable Nozzle Test Engine Assembly
3	Extendable - Expandable Radiation Cooled Nozzle Extension in Test at Vacuum Conditions
4	Skybolt Extendable Nozzle Temperature Data
5	Airmat Reinforced Nozzle Extension - Solid Propellant Motor Design
6	Rib Skin Nozzle Extension, Retracted
7	Apollo SPS Engine Radiation Cooled Nozzle
8	Apollo Nozzle Steady-State Temperature Data
9	Apollo and Transtage Engine Radiation Cooled Nozzle Temperature Data
10	M-1 Gas Dump Cooled Extendable Nozzle
11	M-1 Gas Dump Cooled Nozzle Tube Design
12	Packaging Concepts
13	Fixed to Movable Transition Region
14	Elastomeric Face Seal in a "Cool" Region
15	Attachment Joint Cooling with Secondary Coolant
16	Tip Cooling by Injecting Secondary Coolant through Rigid Mesh and Supersonic Nozzle
17	Tip Cooling by Injecting Secondary Coolant through Rigid Mesh and Oriented Tube
18	Tube Cooling by Injecting Secondary Coolant through Rigid Mesh Alone
19	Propellant Injected through Simple Orifice
20	Propellant Injected through Rigid Mesh
21	Propellant Injected through Platelets
22	Propellant Injected through Bi-directional Orifices
23	Replaceable Tip Concept No. 1
24	Replaceable Tip Concept No. 2
25	Replaceable Tip Concept No. 3
26	Inflatable Elastomeric Seal Concept
27	Inflatable Metallic Seal Concept

Figure List (cont.)

Figure No.	Title
28	Ball Bushing Guide System
29	Extension Alignment Springs
30	Nozzle Extension Locking Device
31	Electrical Drive - Cable Tape or Chain Power Transmission
32	Electrical Drive - Rack and Pinion or Worm Gear Transmission
33	Electrical Drive - Internal Gear and Pinion - Ball Screw Power Transmission
34	Piston-Cylinder Scissors Drive
35	Piston-Cylinder Spring Drive Deployment System
36	Gas Drive Piston - Cylinder
37	Piston - Cylinder - Cable Drive
38	Gas Drive Rotary Motor
39	Bellows Drive
40	Telescoping Actuator Drive
41	Recommended Extension Translation System
42	Recommended Translation System Detail
43	Performance Study Base Case Design
44	Schematic Plot of Rao Nozzle Design Parameters
45	Minimum Length Rao Versus Expansion Ratio (γ = 1.22)
46	Nozzle Weight vs. Area Ratio Radiation - Film Cooled Extension Exit Area = 140
47	Nozzle Weight vs. Area Ratio - Tube Bundle Extension Exit Area = 140
48	Nozzle Weight vs. Area Ratio Radiation - Film Cooled Extension Exit Area = 180
49	Nozzle Weight vs. Area Ratio - Tube Bundle Extension Exit Area = 180
50	Nozzle Weight vs. Area Ratio Radiation - Film Cooled Extension Exit Area = 240
51	Nozzle Weight vs. Area Ratio - Tube Bundle Extension Exit Area = 240
52	Nozzle Weight vs. Area Ratio Radiation - Film Cooled Extension Exit Area = 280

Figure List (cont.)

Figure No.	Title
53	Nozzle Weight vs. Area Ratio - Tube Bundle Extension Exit Area = 280
54	Delivered Specific Impulse vs. Area Ratio R_T = 1.28, P_c = 300 psia
55	Delivered Specific Impulse vs. Area Ratio R_T = 1.28, P_c = 500 psia
56	Delivered Specific Impulse vs. Area Ratio R_T = 1.28, P_c = 1000 psia
57	Delivered Specific Impulse vs. Area Ratio R_T = 1.81, P_c = 300 psia
58	Delivered Specific Impulse vs. Area Ratio R_T = 1.81, P_c = 500 psia
59	Delivered Specific Impulse vs. Area Ratio R_T = 1.81, P_c = 1000 psia
60	Tradeoff Ratio vs. Area Ratio, P_c = 300 psia, R_T = 1.28
61	Tradeoff Ratio vs. Area Ratio, P_c = 500 psia, R_T = 1.28
62	Tradeoff Ratio vs. Area Ratio, P_c = 1000 psia, R_T = 1.28
63	Tradeoff Ratio vs. Area Ratio, P_c = 300 psia, R_T = 1.81
64	Tradeoff Ratio vs. Area Ratio, P_c = 500 psia, R_T = 1.81
65	Tradeoff Ratio vs. Area Ratio, P_c = 1000 psia, R_T = 1.81
66	$\Delta W/\Delta I_{sp}$ vs. Length
67	I_{sp} Delivered vs. Length
68	Area Ratio vs. Length
69	Gas-Side Bulk Film Coefficient
70	Stagnation Temperature for O_2/H_2, Mixture Ratio = 6.0
71	T_s/T_c vs. Area Ratio for O_2/H_2, Mixture Ratio = 6.0
72	DB Factor for O_2/H_2
73	Wall Discontinuities
74	Relative Heat Transfer Coefficient on the Downstream Face or a Rectangular Cavity, L/H = 5
75	Correlation of Maximum Heat Flux Upstream of Forward Facing Steps
76	Equivalent Rectangular Cavity
77	Radiation View Factors from Interior Nozzle Surface to Space
78	Radiation Equilibrium Temperature for a Thin Wall Nozzle
79	Entrainment Model Comparison with Hatch and Papell Model and Data
80	Fixed to Movable Transition Region
81	Variable Step Removable Tip Concept
82	Supersonic Coolant Injector Grooves

Figure List (cont.)

Figure No.	Title
83	Suggested Actuation System for Extendable Nozzle Tests at White Sands Test Facility
84	Typical Ablative and Regeneratively Cooled Chamber - Nozzle Interfaces
85	Separate and Integral Slide/Extension Interfaces
86	"D" and Tubular Seals as Used in the Extendable Nozzle Test Engine
87	Nozzle Wall Pressure Taps for Test Engine
88	Schematic of Flow Field and Pressure Profiles
89	Extendable Nozzle Test Engine Cooling
90	Heat Sink Design Transition Sections and Extendable Nozzle Temperature Response for a 30-sec Firing
91	Extendable Nozzle Attachment Region Flow Characteristics
92	Adiabatic Wall Temperature at the Attachment Region
93	Radiation Cooled Calorimeters for Use at the Nozzle Extension Attachment Region
94	Front View - Actuator Checkout System
95	Rear View - Actuator Checkout System
96	Actuators Extended
97	Actuators Retracted
98	Actuator Rods Constrained with Thin Aluminum Strip
99	Nozzle Extension as Received at White Sands Test Facility
100	Basic Engine Assembly as Received at White Sands Test Facility

I. INTRODUCTION

This report summarizes the technical accomplishments under Contract NAS 9-10484, extending from 12 January 1970 to 12 October 1970.

The objective of the Extendable Nozzles for Space Engines Program was to prepare a comprehensive design guide for extendable - retractable nozzle extensions for space applications. The program was accomplished in two phases: Phase I - Engineering Analysis and Experimental Hardware Design and Phase II - Experimental Engine Fabrication, Experimentation, Analysis (continued from Phase I), including nozzle heat transfer and performance studies, and Preparation of the Final Report and Design Guide. The program schedule displaying key tasks and mileposts is shown in Figure 1.

The objective of Phase I was to provide a comprehensive study effort which was conducted as follows:

1. Configurations analysis - Identified and evaluated literature from Aerojet, the government, and industry pertaining to the design and development of extendable - retractable nozzle extensions.

2. Tradeoff studies of the configurations identified in the literature survey were conducted.

3. Candidate nozzle extension cooling techniques, chamber - nozzle interface configurations, sealing concepts, and nozzle deployment and retraction techniques were selected for further evaluation during Phase II.

4. An experimental engine was designed to evaluate the effects of (a) contour mismatch at the chamber - nozzle attachment interface, (b) joint sealing, (c) film cooling of the nozzle extension injected at the nozzle extension attachment interface, (d) nozzle deployment and retraction, and (e) performance.

I, Introduction (cont.)

Phase II consisted of fabrication of the Phase I experimental engine design, technical analysis, experimentation, data evaluation, and documentation. It was conducted as follows:

1. The Phase I engine design was fabricated and delivered to NASA/WSTF for testing.
2. Studies of nozzle extension cooling techniques, chamber - nozzle interface and sealing concepts, and deployment and retraction concepts identified during Phase I were completed.
3. Nozzle optimization and nozzle heat transfer studies were completed.
4. The final report and design guide were completed.

The experimental engine was not test fired during this reporting period, but the nozzle translation system, including the hydraulic actuation system, was tested prior to its shipment to the NASA White Sands Testing Facility.

This report is presented in two volumes. Volume I details the total program accomplishments, while Volume II is a design guide for an extendable - retractable nozzle extension for a LO_2/LH_2 space engine. The technical analysis and tradeoff studies that are presented in detail in Volume I are the bases for the techniques of nozzle translation, guide and support, cooling, sealing, and alignment recommended in Volume II.

The technical analysis portion of the program was confined to an investigation of nozzle performance and the heat transfer characteristics of a deployable nozzle extension. The nozzle performance study established the general relationships between the parameters nozzle weight, length, delivered specific impulse, attachment area ratio, and exit area ratio.

I, Introduction (cont.)

The nozzle heat transfer studies were an evaluation of the chamber - nozzle extension joint area with respect to engine size, chamber pressure, nozzle attachment area ratio, and nozzle heat loads to provide thermal design requirements for the high heat transfer areas.

The technical analysis efforts are presented in Section III,C of Volume I of this report.

II. SUMMARY

A. CONFIGURATIONS ANALYSIS

The objective of the configurations analysis was to identify and evaluate, by means of a literature search, all available data related to extendable - retractable nozzle extensions. This information was to provide an overview of the extendable nozzle state-of-the-art and to identify those subjects pertinent to the design of an extendable nozzle for a rocket engine.

The survey was considered as the problem identification and summary phase of the program and was designed to provide candidate configurations and data input for the tradeoff studies.

The configurations analysis consisted of an extensive review of extendable - retractable nozzle development programs conducted by Aerojet and others in the space industry. Computerized literature searches were made of NASA and DDC data banks and the Aerojet library. Some 63 documents spanning a 10-year period were found. A complete listing is contained in the Bibliography, presented as Appendix A.

From the literature survey it was concluded that the data generated in other programs concerned with deployable nozzle extensions and systems were not of sufficient depth to permit a comprehensive tradeoff study. Consequently, a basic design analysis was conducted in parallel with the evaluation of information obtained from the literature survey and tradeoff studies. To provide data input for the tradeoff studies, specific design and study guidelines were established and followed. It was considered that these studies and guidelines would provide (1) a broader design base and (2) a greater quantity of details for the tradeoff studies. Section III,B elaborates on the specific studies and guidelines.

The literature review was continued throughout the program in an effort to uncover additional information of value to the program.

II, Summary (cont.)

B. TRADEOFF STUDIES

The tradeoff study effort was designed to evaluate the problems peculiar to design and use of certain combinations of nozzle geometry, cooling, and sealing techniques with various nozzle deployment and retraction schemes. Particular attention was given to (1) understanding the space environment and its effects on materials and component design; (2) identification and evaluation of design considerations affecting design of a nozzle extension cooling scheme, translation and actuation, travel guide, seals, and alignment and locking. The specific studies also included, but were not limited to, the evaluation of materials, weight, integrity, complexity, reliability, and the thermal limitations that could influence use of specific designs in the systems under consideration.

This effort was concluded with the identification of an optimum technique of nozzle deployment and retraction, sealing, nozzle cooling, locking, and alignment for use on an extendable nozzle space engine. This display of information is intended to allow the engine designer to assess the utility of the concepts presented for a particular engine and to provide guidelines for its design.

C. TECHNICAL ANALYSIS

The analyses performed encompassed the two major disciplines of nozzle performance and heat transfer and were confined to evaluation of the radiation and convection cooled nozzle extension concepts. Major emphasis was placed on LH_2/LO_2 systems for use in space and upper stage engines operating within the following limits: (1) chamber pressure from 300 to 800 psia, (2) thrust from 5K to 20K, and (3) nozzle expansion ratio from 50:1 to 300:1.

The nozzle performance study is presented in Section III,C. The final data presentation is in the form of nozzle length versus weight-to-performance tradeoff ratio ($\Delta w/\Delta I_s$). These data can be used directly to determine an optimum

nozzle length and configuration once a mission analysis has been conducted to define tradeoff ratio. The analysis defines the relationships between nozzle weight, delivered specific impulse, attachment area ratio, and overall area ratio. Consideration is also given to (1) real engine loss, boundary, divergence, injector, and film cooling losses, and (2) the weights of the gimbal actuation system, the nozzle actuation and guide system, and the nozzle attachment interface design with respect to performance.

The nozzle heat transfer studies are presented in Section III,C. Particular emphasis was placed on evaluation of heat transfer in the chamber - nozzle extension joint area with respect to engine size, chamber pressure and nozzle attachment area ratio, and the prediction of design and cooling requirements in the high heat transfer areas. The results of analysis can be used to define heat transfer in the chamber nozzle and chamber nozzle joint area with respect to the study limits as defined above.

D. EXPERIMENTAL HARDWARE DESIGN

An experimental engine was designed to incorporate an injector and chamber used during Contract NAS 9-8852. This engine design is shown in Figure 2. New designs were generated for the components directly related to the extendable nozzle. A primary criterion for the experimental engine design was that it yield the specific data necessary to evaluate (1) the effect of contour mismatch (divergent "steps") at the nozzle extension attachment point on heat transfer and gas dynamics, (2) joint leakage, (3) the feasibility of using film cooling at the nozzle attachment point, (4) nozzle deployment and retraction, and (5) performance. Also of importance was that the selected design permit evaluation of all these areas in a single nozzle test program. These factors led to the selection of the steel heat sink nozzle and skirt shown in Figure 2. The experimental engine was designed to provide data in the nozzle attachment area and to evaluate different fixed nozzle-to-extension interface geometries, both with and without secondary cooling. Further, the nozzle was made rigid, so as to present a known contour both in the fixed and extension sections, and was intended for relatively short duration (to 30 sec) operation only.

II, D, Experimental Hardware Design (cont.)

The experimental engine designed and fabricated for this program was intended primarily to obtain data on operation of components directly concerned with the extendable nozzle; accordingly, the engine incorporated high-response calorimeters and thermocouples, as well as pressure transducers, permitting accurate exhaust gas pressure and temperatures to be recorded at predefined axial stations of the nozzle extension. The engine was also designed to obtain empirical data on the effectiveness of several interface seals.

Special design studies were conducted in support of the test hardware design and in parallel with test planning. This effort provided specialized data for the test engine design and included (1) a performance evaluation and definition of the nozzle contour; (2) a heat transfer analysis to identify heat loads, nozzle cooling requirements, heat transfer instrumentation, and materials; and (3) a detailed stress analysis.

E. EXPERIMENTAL HARDWARE FABRICATION AND CHECKOUT TESTING

Fabrication, fitup assembly, checkout testing, and shipment of the test engine to the NASA White Sands Testing Facility was accomplished per schedule. The details of fabrication are discussed in Section III,E. Assembly and checkout testing was accomplished both at the Aerojet Liquid Rocket Company Physics Laboratory test facility and at the vendor's fabrication site. Aerojet testing consisted of demonstrating the operation of the nozzle hydraulic feed system and actuators.

The fitup, assembly, and checkout inspection of the test engine, necessary for project acceptance, was successfully accomplished at the vendor's fabrication site prior to shipment to the NASA White Sands test facility. The checkout inspection consisted of a dimensional inspection of all parts to establish conformance to drawings. Fitup-assembly consisted of a complete assembly of all engine components to ensure fitup of mating parts and operation of the nozzle translation and alignment mechanisms.

II, Summary (cont.)

F. TEST PLANNING

Test planning paralleled hardware design and supporting studies to ensure that the test program and hardware would provide the specific technical data desired. The detailed test plan was coordinated with NASA/MSC and the NASA White Sands Testing Facility. To ensure engine compatibility with the NASA White Sands diffusers, a diffuser performance analysis was conducted. Details of the proposed test program are presented in Appendix B. Details of the diffuser evaluation are presented in Appendix C.

G. EXPERIMENTAL TESTING

Testing was originally scheduled to commence 1 July 1970 at NASA/WSTF but conflicting programs resulted in slippage of the test schedule. Testing is now rescheduled to commence 15 November 1970.

H. CONCLUSIONS AND RECOMMENDATIONS

1. Conclusions

a. General

This section summarizes the significant conclusions drawn from the program. The design concepts presented are considered as optimum within the limits and guidelines established for conduct of the studies.

Metal parts which slide or roll on each other should be made of insoluble pairs and/or lubricated with a solid bonded or dry powder lubricant.

Radiation effects on organics and polymers should be considered when choosing materials for seal designs.

II, H, Conclusions and Recommendations (cont.)

The nozzle extension should be of a radiation cooled design.

It is suggested that the nozzle extension be made of Columbium C-103 and be coated with a silicide coating.

The nozzle should be designed for minimum discontinuity at the interface between the fixed portion of the nozzle and the movable nozzle extensions.

The seal design should be a gasket type face seal.

The seal should be elastomeric.

The elastomeric seal should be located in a cool or supplementary cooled region.

Leakage rates of the specific seal design must be evaluated by testing.

The actuator for nozzle deployment and retraction should be electrically powered.

The nozzle guide, support, power transmission, and nozzle locking features should be incorporated into one simple mechanism for simplicity, reliability, ease of development, and low weight. (The use of a jack screw is recommended.)

The use of lubricants on the power transmission system and mating moving parts is required.

II, H, Conclusions and Recommendations (cont.)

Nozzle alignment should be accomplished by radial expanding springs located around the outer diameter of the fixed position of the nozzle. Nozzle locking is accomplished by using threaded rods as jack screws for translation.

The nozzle performance study determined nozzle performance and weight for various extensions attached at various expansion ratios for different engines representing a range of parameters. The data are presented in terms of delivered impulse, nozzle weight, and change in impulse for change in weight ($\Delta I_s/\Delta W$).

Heat transfer analysis evaluated the heat flux values at the reattachment area of flow onto the extension and the effect of secondary coolant injected into the gas stream at the attachment point.

2. Recommendations

a. Prototype Design

It is recommended that a prototype design be fabricated and tested which embodies the design concepts evolving from this program. The successful demonstration of such an engine would reinforce the conclusions reached in this program and provide an off-the-shelf design capability for related space programs.

b. Subscale Laboratory Testing

The prediction of heat transfer rates for design of the extendable nozzle system is complicated by the existence of a discontinuity in the nozzle wall surface at the joint between the fixed and extendable portions of the nozzle. The flow in the boundary layer and the mechanism of heat transfer to the wall are disrupted at the discontinuity, and sufficient data do not exist to enable

II, H, Conclusions and Recommendations (cont.)

an empirical prediction of the heat transfer rate. When film cooling is used to supplement the basic cooling method, the situation is further complicated, and here also sufficient experimental data do not exist.

The data which are required to enable general empirical correlations to be developed can be obtained from relatively simple experiments in which the supersonic flow over the wall discontinuity is simulated using a two-dimensional nozzle and test setup. Heated gas can be used rather than combustion products and, thus, considerable simplification is possible in the test setup.

It is recommended that a subscale laboratory test program be conducted in addition to the currently scheduled White Sands testing to more fully describe the nozzle flow reattachment phenomena and the effect of secondary coolant injection.

The current test engine design provides the desired information on the flow reattachment phenomena with respect to (1) a fixed nozzle extension attachment area ratio, (2) a fixed coolant injection method, (3) a fixed angle of coolant injection relative to the mainstream flow, and (4) fixed coolant injection velocities for the designed-in nozzle wall discontinuities at the area ratio of nozzle attachment and cooled injection.

The proposed laboratory program should include provisions for varying the Mach number of the nozzle flow, the geometry of the nozzle wall discontinuity, attachment and coolant injection area ratio, and the method for introducing the film coolant. The film coolant parameters--injection Mach number, angle of injection, and coolant mass flow rate--should be varied over a sufficiently wide range to permit generalized correlations to be developed.

The test section instrumentation should include static pressure taps and thermocouple calorimeters located throughout the nozzle joint region and downstream of the joint where film cooling effects are to be established.

III. DISCUSSION

A. CONFIGURATION ANALYSIS

1. Introduction

The configuration analysis consisted of an extensive research into extendable - retractable nozzle development programs. Aerojet data were reviewed and computer tape searches were made of data banks at NASA and DDC. Programs dealing with extendable - retractable nozzle concepts and with nozzle optimization studies, heat transfer, radiation-cooled nozzle extensions, design, sealing techniques, and the space environment were reviewed. A bibliography of all literature reviewed is presented in Appendix A.

2. Histories

a. General

In general, the development programs evaluated confined their analyses to nozzle extension performance and heat transfer studies for the specific program's objectives. Studies of nozzle sealing requirements, deployment techniques and cooling requirements, where applicable, were secondary. Consequently, little detail of the design analysis was included in much of the literature.

Nozzle heat transfer and performance analyses (considering a wide range of propellant usage) were extensive, but the problems associated with discontinuities in the divergent section of the nozzle (nozzle extension attachment point) were not pursued, usually being considered beyond the scope of the particular program. The concensus was that the radiation equilibrium temperature level would be higher at the point of gas reattachment downstream of a discontinuity and could be minimized by designing the nozzle contour to be as continuous as possible.

III, A, Configuration Analysis (cont.)

It was concluded that the lack of depth in the presentation of specific design details and analysis of sealing concepts, techniques of nozzle deployment and retraction, and cooling necessitates a more in-depth evaluation of the various subsystems associated with the design of an extendable - retractable nozzle system.

The literature survey appeared to indicate that, in most programs, a significant portion of the design is performed by the project designer and is based upon his experience and the requirements of the particular program. In addition to being directed along very narrow requirements guidelines, the analyses appeared to be poorly documented and perhaps perfunctory.

b. Summary of Related Experience

(1) Extendable and Expandable Nozzles - General

Considerable experimental extendable nozzle work was performed under contract by Aerojet for both liquid rocket and solid rocket engine applications. These investigations began in January 1960 and, initially, were concerned with the development of an extendable nozzle system which might be employed with the Titan II second stage engine and have continued intermittently through the present Extendable Nozzles for Space Engines contract. The nozzle designs which were tested during this period employed two cooling methods: (1) radiation-cooled nozzles and (2) ablation-cooled nozzles. The radiation-cooled nozzles were constructed of C-103, a columbium alloy, which was coated with a thin layer of a silicide base coating. The coating provided chemical protection for the nozzle walls from the corrosive environment of the chamber gases and also increased the emissivity characteristics of the nozzle. This emissivity enhancement was advantageous thermally since it increased the radiant heat flux from the nozzle wall to the environment and thereby reduced the nozzle wall temperatures. The ablation-cooled designs that were tested employed a thin shell of a nitrile-butadiene

III, A, Configuration Analysis (cont.)

elastomeric material, which had been developed by General Tire for extendable nozzle applications and was called Gengard V-44. The Gengard nozzle was fabricated by forming the material to the required nozzle shape and attaching the nozzle to the upstream chamber using conventional flanging techniques. The nozzle was then folded and packaged as an integral unit with the chamber section of the engine. Deployment could be accomplished either by a pneumatic actuating system or by engine ignition. Nozzle wall cooling was accomplished by ablation of the inner surface of the elastomeric wall. The thickness of the nozzle walls were designed to provide sufficient material to ensure a rigid structure for the duration of the firing. The details of these programs will be discussed in the next two sections.

(2) Solid Rocket Motor Experience

(a) Radiation Cooling

A C-103 radiation-cooled extendable nozzle that was fabricated for testing with a Skybolt solid rocket engine is shown in Figure 3. The extendable nozzle was attached at area ratio 20:1 and, when fully expanded, provided an extension to area ratio of 50:1. The cold worked convoluted shape of the nozzle was designed to maintain the diameter of the nozzle before deployment at approximately 20:1. After nozzle deployment and engine ignition had occurred, the high nozzle wall temperatures and the internal pressure caused the convolutions to expand and the nozzle to assume a conical shape. A thin layer of Velvet Black* was applied to the exterior surface of the nozzle in the nozzle attachment region. This coating, which is capable of withstanding a nozzle temperature of 3000°F, increases the emissivity of the nozzle surface from 0.7 to approximately 0.9 and in so doing reduces the steady-state nozzle operating temperature to approximately 2500°F. High temperature tungsten-rhenium thermocouples were located at area ratios 21:1, 35:1, and 46:1 in order to measure the outer shell temperatures at these locations.

*A 3-M brand product that consists of 20% C and 80% SiO_2.

III, A, Configuration Analysis (cont.)

A transient thermal analysis was conducted to predict the response of the thermocouples at the three locations. The analysis included the effects of a thin (0.015 in. to 0.020 in.) layer of Al_2O_3 which was deposited from the propellant gases onto the nozzle walls. The thermocouple predictions are compared to the experimental data in Figure 4, displaying reasonable agreement between the data and predictions. The maximum or steady state temperature predictions shown in the table on Figure 4 appear to be slightly higher with the exception of the 46:1 data area ratio than the experimental maximum temperatures. Of particular interest is the fact that the thermocouple data obtained at area ratio 21:1, the nozzle attachment region, did not deviate much from the predicted data which were calculated by ignoring the effect of the step discontinuity in the nozzle contour at the attachment point of the extendable portion of the nozzle. This particular concept had been designed so that the joint contour was as continuous as possible.

(b) Ablation Cooling

An ablation-cooled nozzle having a Gengard ablative liner and a Goodyear AIRMAT outer shell was fabricated for testing with the Skybolt engine. The AIRMAT nozzle was integral with a fixed nozzle but could be folded and then deployed to its extended position by pressurizing the AIRMAT outer shell. Figure 5 shows the deployment of the AIRMAT nozzle. A Gengard ablative liner thickness of approximately 0.3 in. was estimated to be adequate for testing with the Skybolt engine system based on liner erosion data obtained from previous solid engine tests.

A single hot test was run with a Skybolt engine and premature failure of the AIRMAT nozzle occurred. The nozzle failure was attributed to excessive erosion of the Gengard ablative that appeared to be caused by solid particle (Al_2O_3) impingement on the Gengard liner. From the AIRMAT nozzle tests, it was concluded that: (1) an ablative extendable nozzle configuration would require further development for solid engine applications, and (2) the AIRMAT nozzle was less satisfactory than the columbium alloy radiation-cooled design.

III, A, Configuration Analysis (cont.)

(3) Liquid Rocket Engine Experience

(a) Titan II Experience

A variety of extendable and expandable nozzles were designed for testing with a Titan II second stage liquid rocket engine. Two of these designs were very similar to the C-103 radiation-cooled and AIRMAT ablative-cooled nozzles that had been tested with the Skybolt solid engine. A third design, shown in Figure 6, was tested successfully with a full-scale engine. The latter design included an ablation-cooled Gengard V-44 liner in the high heat flux region beginning at the nozzle attachment point and a thin-walled C-103 radiation-cooled section further downstream. Approximately one-half of the skirt was retractable and was hydraulically deployed prior to ignition. The thin-walled C-103 segment was convoluted in order to reduce the diameter of the retracted nozzle. The nozzle test data obtained from the Titan II engine test showed that the ablative liner erosion was more severe than had been anticipated.

The extendable - expandable nozzle investigations indicated that the thin metal wall, radiation-cooled nozzles were more satisfactory than the AIRMAT ablative designs. The ablative liner designs were heavier, more difficult to deploy, and might be limited to very short firing durations because of the high ablative liner erosion rates encountered during nozzle hot testing.

(b) Apollo SPS Nozzle Extension

The Aerojet Apollo SPS engine that is discussed in Reference 1 employs a radiation-cooled nozzle extension. The Apollo nozzle extension, which is shown in Figure 7, consists of a thin-walled, high temperature metal alloy skin which attaches to an ablative-cooled nozzle at area ratio 6:1 and extends to area ratio 62.5:1. The nozzle is fabricated from sheets which have been preformed and are welded together to form the nozzle contour. The forward section

III, A, Configuration Analysis (cont.)

of the nozzle from area ratio 6:1 to 40:1 employs columbium alloy C-103 because of its high strength characteristics at very high ($\leq$2500°F) temperatures. A titanium alloy was employed for the aft section of the nozzle because of the lower density of this material, and this permitted a reduction in nozzle weight. The titanium alloy can be used at these higher area ratios of the nozzle because of the reduced heat flux which results in lower nozzle wall temperatures. The "J" flange design employed for the nozzle provided for a conventional bolted joint which was designed to be thermally remote from the heated nozzle surfaces so that heat soakback into the joint region would be low. Reducing heat soakback prevents overtemperature of the joint components and ensures that the joint stresses that occur with thermal expansion are not excessive. A reliable wall coating was also required that would provide oxidation protection for the high temperature columbium nozzle wall in the corrosive propellant gas environment and which would also enhance the emissivity of the nozzle surfaces. The NAA-85 silicide-base coating was developed by North American Aviation for the Apollo nozzle. This coating exhibited adequate high temperature properties and possessed the chemical properties required to protect the nozzle wall from the hot gases. NAA-85 also increased the coated wall emissivity from 0.7 to approximately 0.9. Another high emissivity coating, S-31, was also employed for the outer surface of the titanium portion of the nozzle. This coating increased the emissivity of the titanium portion of the nozzle from 0.6 to approximately 0.9.

Steady-state nozzle wall thermocouple data, which were obtained during Apollo engine tests, are compared to the predicted axial temperature distribution in Figure 8. The thermocouple data shown in Figure 8 are seen to be consistently lower than the predictions. The data scatter (approximately 400°F) was attributed primarily to thermocouple anomalies. The data also indicate that the one-dimensional heat balance which was employed for steady-state nozzle temperature predictions overpredicts the maximum nozzle wall temperatures by approximately 200°F. This effect was also noted in the solid engine extendable

III, A, Configuration Analysis (cont.)

nozzle tests that were discussed previously. It is concluded from the experimental radiation cooling data that a one-dimensional heat balance provides a reasonable method of predicting steady-state nozzle wall temperatures which are slightly conservative but generally accurate enough for design purposes.

(c) Transtage and Delta Nozzle Extensions

The Transtage and Delta engines both employ thin-walled, coated metal wall radiation-cooled nozzle extensions that are similar to the Apollo nozzle but are smaller because the thrust of these engines is lower than the Apollo SPS engine. The design details for the Transtage engine and nozzle system are discussed in Reference 2. Each of these engines employs the same propellants, N_2O_4/AeroZINE 50, and operate at the same chamber pressure, 100 psia, as the Apollo engine. Therefore, the fact that the steady-state nozzle temperatures for these engines are close to those for the Apollo nozzle would be expected.

The Transtage and Apollo engine data and also the steady-state temperature predictions for the Apollo nozzle are compared in Figure 9. The Transtage temperatures are seen to be slightly higher overall than the Apollo temperatures. The higher wall temperatures are attributed to the reduced Transtage nozzle size, which results in a lower hot gas Reynolds number and a correspondingly increased film coefficient. This produces higher wall heating rates and increased nozzle wall temperatures.

(d) Agena

The radiation-cooled nozzle for the Agena engine is similar in design to the Apollo/Transtage/Delta nozzles in temperature capability and operating characteristics. The major difference between the Agena nozzle and the Apollo design is that the Agena employs a regeneratively cooled chamber whereas the other engines are ablation cooled. The regeneratively cooled chamber with a

radiation-cooled nozzle requires a different attachment joint design than an ablation-cooled chamber with a radiation-cooled nozzle. The regenerative chamber and radiation nozzle combination generally is more severe from a stress viewpoint since the temperature difference between the upstream and downstream segments of the flange tends to be higher, which causes a stress buildup in the flange components when they reach operating temperature. This difficulty would be more pronounced for a regenerative chamber employing a cryogenic coolant such as liquid hydrogen since the very low coolant temperatures usually produce very low temperatures in the upstream flange components. Some aspects of the Agena design are classified and, therefore, are not discussed fully in this report. Further information on the Agena nozzle design may be obtained from Reference 3.

(e) F-1 Booster

A film-cooled nozzle extension design has been used successfully on the Rocketdyne F-1 booster engine. Fuel-rich gas generator gas is manifolded for injection at several locations along the contour of a stainless steel nozzle and the gas film maintains the nozzle wall within its temperature design limits. The F-1 nozzle is fixed and does not have the capability of deployment. Details of the F-1 nozzle design are discussed in References 4 and 5.

(f) M-1 Engine

Figure 10 is a schematic diagram which shows the cooling system for a dump-cooled nozzle that was designed for the M-1 engine. The M-1 is a high thrust, upper stage engine system designed to operate with O_2/H_2 propellants. Oxidizer turbine exhaust gases were circulated through thin-walled nozzle tubes in a single pass from the nozzle attachment to the exit. Although not shown in the figure, a restriction was located at the exit of each tube in order to supersonically expand the coolant into the low pressure environment and increase the nozzle thrust. The nozzle tube design, which is shown in Figure 11,

III, A, Configuration Analysis (cont.)

consisted of 1-in. OD thin-walled stainless steel tubes that were flattened near the nozzle attachment and circular at the nozzle exit. Tube flattening was required to form the nozzle contour at the smaller nozzle diameter near the nozzle attachment. The flattened tubes increase the coolant gas velocity and, thus, the cooling capability at the high heat flux zone of the nozzle which also occurs near the attachment location.

3. Conclusions

The conclusions reached from the study of existing design data are as follows:

a. The chamber - nozzle extension attachment area had not been adequately studied.

b. The study of actuators, power transmission, and nozzle travel guide systems required a better definition of engine operating requirements and basic design analysis investigation.

c. The thermal environment dictating seal and seal interface design requirements had not been adequately studied.

d. The seals and sealing techniques had not been studied sufficiently.

e. Supplemental nozzle cooling, if required (function of engine operating cycle, duty cycle, and nozzle extension attachment area ratio), could not be defined without adequate heat flux test data and basic design analysis.

III, A, Configuration Analysis (cont.)

f. Deployable, flexible, nonmetallic nozzles were not applicable to reusable, long life duty cycle requirements because of the way they cool themselves (ablation).

g. Deployable, flexible (expandable), metallic nozzles were limited to extension and expansion (assuming fixed nozzle storable diameter) and not retraction.

h. Deployable, fixed (rigid) ablative nozzle extensions were also use-life limited by the cooling mechanism (ablation).

i. Deployable, fixed (rigid) heat sink nozzle extensions were use-life limited and/or limited to short periods of engine operation.

j. Deployable radiation-cooled nozzle extensions have been successfully demonstrated in test.

k. General design considerations dictating materials and material limitations for use in the space environment had not been compiled.

III, Discussion (cont.)

B. TRADEOFF STUDIES

1. Guidelines

The findings of the configuration analysis showed that basic design analysis should be conducted in parallel with evaluation of the literature survey data for a broader design base. Accordingly, specific studies and study guidelines were established. They were:

Special Studies

The space environment
Nozzle design
Seal design
Actuator design
Nozzle travel guide design
Nozzle extension locking device design
Nozzle interface and alignment design

Study Guidelines for Engine and Nozzle Operating Conditions and Design Considerations

Propellants: LO_2/LH_2

Chamber Pressure (P_c): 300 to 800 psia

Thrust (F): 5K to 20K

Nozzle Expansion Ratio (ϵ): From 50:1 to 300:1

Operating Environment: Space (vacuum)

Nozzle Operation: The nozzle is deployed prior to engine firing and is retracted following engine firing or prior to vehicle reentry.

Nozzle Gimballing: The nozzle will not be gimballed during the time of nozzle deployment or retraction.

III, B, Tradeoff Studies (cont.)

Nozzle Cooling:

Radiation, self
Convection
Ablation, self

Supplemental Nozzle Cooling:

None
Gas
Propellant

Seal Cooling:

None
Gas
Propellant

Nozzle Weight: To be established during final design.

"G" Loads (to be defined): During engine operation
Engine not operating - main stage operation

Structure: Nozzle extension and adjacent sealing interfaces are assumed to be round following initial fabrication but, because of (use) service requirements, no parts are assumed to be round following repeated engine operation. The seal designs will be interchangeable and the ability to compensate for out-of-roundness or local discontinuity will be built into the seal or sealing interface design.

Temperature and Pressure Environment of the Nozzle Seal:

(1) Temperature:

Prior to sealing: To be established
Sealing (prior to engine start): To be established
Sealing (engine on):

Cooled:	Turbine exhaust:	$\leq 1000^{\circ}R$
	Propellants:	$\leq 700^{\circ}R$
Uncooled:		$\leq 2500^{\circ}R$

(2) Pressure:

Prior to and following engine operation: Vacuum
During engine operation: 10 psia

Seal: The seal will be designed to have the required service life. Acceptable leakage rate will be evaluated at time of specific design.

Power Supply for Actuators: Electrical
Gas

Engine Service Life: Reusable

III, B, Tradeoff Studies (cont.)

Nozzle Extension Translation Time: Function of actuator power supply and system design. As an example, if turbine exhaust gas is used as the power source and provisions are not made for gas storage, the period of time available for nozzle translation becomes quite small due to the short period of time between turbopump start and engine ignition to develop the required power drive source.

The engine shall be incapable of automatically retracting the nozzle extension to the stowed and locked position without external command signal upon a system or engine failure.

A single point failure of the nozzle extension deployment and retracting mechanism shall not prevent the nozzle from translation and locking.

The deployment system shall have a minimum number of supporting mechanical devices and/or moving components for increased reliability.

The extreme space environment shall not cause deployment or retraction or alignment problems.

Expansion of the nozzle or chamber due to heat soak from engine firing will not affect or cause to bind the translation system.

The mechanical power drive system shall be designed for redundancy to assure nozzle translation in the case of component failure.

2. <u>The Space Environment</u>

a. Sublimation of Metals in Vacuum

The effects of vacuum on the sublimation rate of metals can be calculated from the Langmuir Equation, assuming that none of the molecules leaving the surface return to it.

$$G = \frac{P_v}{17.14}\sqrt{\frac{M}{T}}$$

III, B, Tradeoff Studies (cont.)

where G = weight loss rate per unit of exposed surface, $gm\text{-}cm^{2}\text{-}sec^{-1}$

P_v = vapor pressure of metal at temperature, T, mm Hg

M = molecular weight of the metal in the gas phase

T = absolute temperature, ^{o}F

From the above equation, it is seen that weight loss rate increases directly with increasing vapor pressure. Table I is a listing of several metals and their corresponding sublimation rates for different temperatures. These data indicate that cadmium, which is often used for plating parts, is a poor material for extended use in a high vacuum. Metals that sublimate from a warm surface will have a tendency to plate out on cooler surfaces, possibly causing electrical short circuiting, change in surface emissivities, or changes in optical properties of mirrors and lenses. Sublimation of the base material can be retarded by the use of surface coatings with low vapor pressures (for example, inorganic coatings).

b. Plastics and Elastomers in the Space Vacuum

Because the Langmuir Equation is not applicable to the organic materials of engineering interest, determining weight loss of organic materials requires empirical data. The weight reduction exhibited by organic polymers is usually the result of the loss by evaporation of relatively lower molecular weight fractions, unreacted additives, contaminants, adsorbed and absorbed gases, moisture, etc. The loss of these additives and contaminants, however, can change important properties of the polymers. For example, the loss of a plasticizer by evaporation in a vacuum environment will produce a more rigid or brittle part with a corresponding decrease in elongation and increase in tensile and flexure strength.

The rate of weight reduction at a given pressure and temperature varies as a function of time. The initial weight loss is usually high and is due to the evaporation of absorbed and adsorbed gases, water, and other contaminants.

III, B, Tradeoff Studies (cont.)

During this stage, the total weight loss may be as great as 3% for some polymers. This relatively high initial weight loss will drop to a very low value when the loss of weight is due primarily to degradation of the basic polymer.

In general, polymers of relatively high molecular weight, such as Teflon, do not evaporate or vaporize in vacuum; however, when supplied with sufficient thermal energy, they decompose or depolymerize. These polymers have such low vapor pressures that the thermal energy required to cause evaporation exceeds that required to break the chemical bonds of the polymer. Many polymers of engineering importance do not sublime or evaporate in high vacuum environments, and the thermal stability of these polymers should be at least as good in high vacuum as in the earth's atmosphere.

Weight loss of several purity polymers are given in Table II. The weight loss data are given as 10% per year at some temperatures. Normally, a 1 or 2% weight loss is not considered detrimental to materials for engineering applications; however, 10% weight loss can result in considerable change in the engineering properties of organic materials. Table II should be used with caution, since much of the data are of questionable quality. Teflon and Mylar are materials which show promise for space vacuum exposures.

In general, the following eight points should be noted:

High molecular weight polymers apparently do not evaporate or sublime in vacuum.

The thermal stability of these polymers should be at least as good in vacuum as in air.

The weight loss by engineering plastics in vacuum is the result of evaporation of relatively lower molecular weight fractions, unreacted additives, contaminants, etc.

The rate and amount of weight loss are greatest early in the test period when the materials at or near the surface evaporate. These loss factors subsequently decrease to a rate determined principally by diffusion rates through the polymer to the surface.

III, B, Tradeoff Studies (cont.)

Rigid plastics are generally preferred over flexible, elastomeric materials.

Materials with a minimum number and quantity of additives and modifiers are preferred.

Complete cure of the plastics must be obtained by extended time and/or elevated temperature post-curing to ensure the elimination of unreacted, low molecular fractions in the product.

Those materials exhibiting high loss rates, but considered necessary for use in space vehicles because of special desirable properties, should be preconditioned in vacuum at elevated temperatures to reduce, as much as possible, the potential loss of the material to space.

c. Lubricants in the Space Vacuum

Conventional lubricants are generally not suitable for use in the space vacuum because of their high vapor pressure which results in the dissipation of fluid by evaporation. Even if the rate of evaporation of a fluid lubricant is acceptable, the vapors may condense on cooler surfaces such as lenses, relay contacts, or other sensitive components essential to the operation of the equipment. Other problems associated with using a lubricant in a vacuum are (1) the absence of oxygen--essential to forming a metallic soap, and (2) poor thermal conductivity due to the absence of convective gases, resulting in high thermal gradients due to friction. Also, the lack of absorbants in space will prevent the use of such bearing materials as graphite, which depends on absorbed water vapor for its lubricating properties.

The environmental conditions of space (namely vacuum, radiation, and zero gravity) affect the performance of bearings, particularly in their lubrication. A comparison of a few lubricants for space application are shown in Table III.

Vacuum detrimentally affects bearing materials and lubricants by (1) failure to replenish the oxide layer on the bearing surface, and (2) evaporation or sublimation of the lubricant or bearing metal. The lack of an oxide layer

III, B, Tradeoff Studies (cont.)

allows the metal surfaces to join by cold welding or, if a liquid lubricant is present, to react more readily with the lubricant to form a varnish-like coating on the bearing surfaces. The effect of vacuum on the removal of the oxide layer from metal surfaces is measured by changes in coefficients of friction. Since friction is considered to be the result of shearing of metallic junctions formed by cold welding of asperities, any method that can be devised to contaminate the surfaces will aid in reducing friction.

Wear is also aggravated when the oxide layers are removed between the sliding surfaces. Wear particle size formed between the metallic surfaces is believed to be maximum in vacuum. The same methods used to reduce friction will also help in reducing wear.

Lubrication with respect to usage and state of development is further discussed in Section III,B,5,c,(3).

d. Cold Welding

Cold welding--often referred to as pressure bonding--may be defined as the joining of two solid metallic elements without the use of heat to produce a liquid or melting phase at the interface. In the earth's atmosphere, metal parts have a natural surface oxide coating and their surfaces are normally contaminated. The detailed mechanisms involved in cold welding of metallic elements are not well understood; however, it is generally accepted that the surface contamination and oxide layers play an important part in preventing bonding of materials in static or dynamic contact.

Normally, solid metal surfaces are neither perfectly clean nor perfectly smooth. Under normal atmospheric conditions, oxygen molecules are adsorbed and react with the metal atoms to form oxides. On top of this oxide layer, a condensed adsorbed moisture layer is formed. The moisture layer varies in thickness with the relative humidity of the atmosphere. These surface layers are often referred to as surface contaminants.

III, B, Tradeoff Studies (cont.)

The conventional process of welding two metals requires heat in sufficient quantity to remove the surface oxide layers and reduce the metal at the interface to a liquid phase. It should be noted that the liquid phase does not promote the joining of two metals but only allows complete contact of the surfaces. It is only the removal of the surface oxides that allows the metals to be joined.

If the oxide films removed from the metal surfaces are not quickly replaced, the metals will cold weld when in static or dynamic contact. Because surfaces are not perfectly smooth, the real area of contact between parts is limited to the contact of surface asperities. Under the high bearing pressures that can occur at these points, brittle oxide layers are fractured because they cannot conform to the changing surface contours. If the metal surfaces remain free of contaminants (oxides, moisture, etc.), metal-to-metal contact occurs and a metallic junction is formed. Continued removal of oxide layers eventually results in appreciable welding and the parts may seize.

Although there is little useful design data on cold welding, limited experimental results indicate that:

> The degree of cold welding may be a function of solubility between mating materials, as indicated by phase diagrams. The results of one investigation of various clean metals coupled under static pressure in a vacuum showed joining of the following soluble couples: iron/aluminum, copper/silver, nickel/copper, and nickel/molybdenum. No joining occurred between the following insoluble couples: copper/molybdenum, silver/molybdenum, silver/iron, and silver/nickel.
>
> Hard materials which have good wear resistance also show resistance to cold welding. Limited data on 42100 steel, a common ball and roller bearing material, indicates that this material is relatively resistant to cold welding in a vacuum.
>
> Although some materials are less susceptible to cold welding than others, it is advisable, whenever possible, to provide lubrication when sliding surfaces are exposed to vacuum conditions.

III, B, Tradeoff Studies (cont.)

e. Radiation in Space

Radiation may be defined as the emission and propagation of energy through either space or a material medium. The space radiation environment is composed of cosmic rays, electromagnetic radiation, Van Allen belt radiation, auroral particles, and solar flare particles. Radiation types may be generally classified as either electromagnetic or particulate. Electromagnetic radiation includes ultraviolet light, X-rays, and gamma rays. Particulate radiation consists of electrons, protons, neutrons, alpha particles, and a smaller quantity of higher atomic number particles.

The space radiation environment is characterized by the earth radiation zone (Van Allen belts), the auroral zone, and the interplanetary zone. The evaluation of radiation in space will be with respect to the earth radiation zone and the effects of radiation on materials.

The earth radiation zone is characterized by magnetically trapped electrons and protons. This zone, often referred to as the Van Allen belt, is made up of two concentric belts: the inner belt and the outer belt. The inner belt extends approximately 4000 miles with intensity reaching a maximum at 1800 to 2000 miles above the geomagnetic equator. The inner belt is sometimes referred to as the hard belt and contains high energy protons having energies to 700 Mev, with electrons in the 20 Kev to 1 Mev range. The outer belt extends about 8000 to 37,000 miles, where the region of high intensity is at 10,000 to 15,000 miles and up. This belt, called the soft belt, consists primarily of electrons from 20 Kev to 5 Mev and some protons over 60 Mev.

An important factor in determining the effect of radiation on materials is the range or penetrating power. Metals are considerably more resistant to radiation damage than most other classes of solids, showing little damage due to radiation except when exposed to the radiation in the heart of nuclear reactors (fast neutron exposure).

III, B, Tradeoff Studies (cont.)

Organic materials, as a class, are the least stable in a radiation field. Radiation damage to organic materials is dependent upon the total energy absorbed and sometimes upon the radiation intensity; damage is usually not dependent upon the type of radiation.

Polymers may be degraded by a loss in mechanical strength, an increase in vapor pressure and viscosity, and a reduction in molecular weight. Most elastomeric materials are not satisfactory in a radiation environment. Natural rubber is the most radiation-resistant of the elastomers, while silicones and fluorine-based polymers are below average in radiation resistance. Table IV presents the radiation resistance data of some plastics and elastomers.

Ceramic materials, in general, are not seriously affected by radiation.

f. Conclusions and Design Recommendations

The following conclusions and recommendations can be drawn about the usage of materials in the design of vehicles for use in the space environment:

Metals, in general, are not subject to weight loss by sublimation.

To restrict weight loss or subsequent loss of material properties caused by evaporization of organic compounds, those compounds having high molecular weights and the lowest content of additives and contaminants should be used when possible.

Organic components should be space prepared by prolonged storage in hard vacuum.

Hard or rigid polymers should be used when possible.

The use of lubricants should be restricted or avoided where possible. When the use of lubricants is mandatory, those developed for use in space must be used.

III, B, Tradeoff Studies (cont.)

Metal parts which roll or slide on each other should be made of insoluble pairs where possible to prevent "cold welding".

Friction between parts may be eliminated by using a combination of materials, e.g., hard roller bearings moving over Teflon-coated rails or guides.

Metals and ceramics are usually not affected by space radiation, but radiation effects on organics and polymers should be considered.

It is concluded that practical, workable designs for the space environment can be developed by recognizing and allowing for the limitations imposed by space environment.

3. Nozzle Extension Design

a. Packaging

For space applications, performance of a rocket motor can be enhanced by increasing the expansion ratio of the exhaust nozzle. This is feasible out to area ratios of perhaps 200 or 300. Unfortunately, such area ratios also mean exit diameters or nozzle lengths which are difficult to fit within the physical dimensions of the vehicle at liftoff or prior to staging.

One means of satisfying both performance and geometry requirements is to "package" a portion of the exit cone (or nozzle extension) in some manner as to fit the desired vehicle dimensions and then deploy it to the correct configuration for thrusting periods. As shown in Figure 12, the extension can be packaged longitudinally and extended or retracted to and from firing position. Such an arrangement would be practical when vehicle length is of prime consideration. If, however, diameter rather than length is the critical parameter, the extension can be packaged so that it can be expanded radially to form the desired nozzle contour (also shown in Figure 12). Obviously, the third packaging concept illustrated is a combination of these two in which the extension is both extended and expanded. This allows storage with no loss in usable volume.

III, B, Tradeoff Studies (cont.)

A mission analysis is required to determine which would be the most desirable packaging method. Nozzle extensions to provide greater expansion ratios, as well as the methods of packaging described above, have been previously demonstrated and are considered state-of-the-art.

b. Cooling Concepts Evaluation

There are five basic cooling concepts that can be considered for use with nozzle extensions:

Transpiration cooling.

Convective cooling (tube bundle).

Ablation cooling with or without coolant injected at the nozzle extension attachment point.

Radiation cooling with or without coolant injected at the nozzle extension attachment point.

Heat sink with or without coolant injected at the nozzle extension attachment point.

Of these five types, the heat sink design can be eliminated for use because either (1) the surface will reach melting temperature in a matter of seconds, or (2) the mass (thickness) of a highly conductive material required to withstand a longer duration would be prohibitive from a weight standpoint.

A comparison of the remaining four candidates is made in Table V. The points assigned to the rating factors are arbitrary and are meant merely to indicate general importance. It is also conceivable that the lowest rated concept from the table may be the only suitable concept because of special design considerations.

III, B, Tradeoff Studies (cont.)

The chart indicates that radiation- and convective-cooled extensions are the better of the four and should be considered for design purposes, while the transpiration-cooled extension should be eliminated from consideration because of greater complexity, higher cost and weight, lower reliability, and more development required. The table also indicates that the ablative extension is either duration limited or of such thickness that the weight is prohibitive.

The following is a discussion of some of the design factors in the chart (by number) with comments applicable to the different concepts.

1. Light Weight

The lightest design is the radiation-cooled extension. This design should weigh less than one-half of a comparable tube bundle design. The ablative extension has a prohibitive weight if duration requirements are met.

2, 4, 10, 12. Cost, Reliability, Fabrication and Complexity

These factors are interconnected to a large degree. The more complex transpiration-cooled concept, for instance, would also cost more because of resulting fabrication requirements and would likewise suffer decreased reliability. On the other hand, the simplest concepts, radiation cooled and ablative, are fairly equal in these ratings because the simplicity lends itself to lower cost and greater reliability.

3. Ease of Development

This factor indicates the amount of development required for the concept. The transpiration-cooled concept requires the most development and the ablative the least.

III, B, Tradeoff Studies (cont.)

5, 6. Cooling Effectiveness

The ablative and radiative concepts are self cooled by design and require no secondary coolant, either turbine dump gas or other, although such cooling might enhance their operation. The convective design requires a coolant, either dump gas or other, as does the transpiration-cooled concept.

7, 8, 11. Extended Operation, Recycling and Exhaust Compatibility

The transpiration, convection, and radiation designs reach equilibrium and theoretically are not duration limited. The radiation-cooled extensions are subject to corrosive attack (loss of material and penetration) by water vapor and oxygen. This rate of attack is small, however ($\sim$60 $Mg/cm^2/hr$), and can be delayed by silicide or aluminide coatings, such as were used on the Apollo skirt. The ablative design cools by ablating material at a certain rate and is therefore duration limited for a given thickness. Also, certain ablative materials are subject to severe corrosion in exhaust gases containing water vapor. None of the concepts are severely affected by recycling; however, the coatings used in protecting radiative extensions may be subject to flaking after cycling. A thousand-cycle capability is considered a reality.

9. Clusterability

All concepts must function and be storable in a hard vacuum (space). This space environment restriction will affect only ablatives to some degree. The radiative concept is restricted, however, insofar as it cannot be used where surrounding components are temperature limited and, since it requires a good "view factor" to be radiation cooled, there is some limit as to how close it may be placed to another radiation-cooled extension.

13. Size Limitation for a Given Coolant Flow

The transpiration and convection extensions have some maximum area that can be cooled for a given amount of coolant. The ablative and radiative concepts, being self operating, have no such restriction.

III, B, Tradeoff Studies (cont.)

A distinction must be made on the basis of the foregoing tradeoff as to what constitutes the best extension to meet a given set of objectives. For instance, in flight application, the following requirements are intuitively predominant:

(1) Light weight.

(2) Capable of long durations (equilibrium state).

(3) Preferably capable of self operation, once deployed, without need of assistance such as cooling.

It can be seen that the selection of an extension filling these demands leans toward the radiation-cooled concept. Other mission factors must be considered, of course, such as the effect of locally high backside nozzle temperatures on surrounding equipment, which may dictate the use of the convectively cooled tube bundle or transpiration-cooled extensions.

c. Nozzle - Chamber Interface Design

(1) Design Considerations

The attachment joint can be described as all of that area which generally extends from the forward end of the movable extension to the aft edge of the fixed portion of the nozzle. This statement is based on the fact that the two parts must overlap in order to meet certain joint requirements or features. These features are interrelated and the influence of each must be considered in the design of the attachment area. The major factors to be considered in the joint design are (1) location, (2) sealing, (3) nozzle alignment and support, and (4) whether or not a means of providing injection of secondary coolant at the joint is required. These four factors will be discussed later in this section.

III, B, Tradeoff Studies (cont.)

A fifth factor of importance, although not necessarily interrelated with the previous four, has to do with minimizing the flow discontinuities as the exhaust gases move from fixed to moving parts. It is assumed that, for liquid rocket applications, the fixed portion extending from the combustion chamber to the attachment area will probably be regeneratively cooled and likely of a tube bundle or slot design. Good design practice here dictates that the tube bundle or a tip cooled by the bundle be carried out to as near a point as possible--in other words, to a minimum discontinuity (Figure 13). Whatever the final resulting step height may be is then to be considered in calculating the heat fluxes associated with reattachment of flow to the extension as discussed in Section III,C,3.

It is otherwise assumed that the regeneratively cooled section is of conventional design.

(2) Joint Location

Some general comments are necessary concerning the axial location of the "joint" between the fixed and extendable portion of the nozzle. For least weight, the joint should be made at as low an area ratio as physically possible. This also has the benefit of keeping seals and concentric hardware sections on a small diameter.

The first restriction on attachment at this low area ratio is that the extension must still pass forward around the thrust chamber on some system of guides. Therefore, the thrust chamber diameter for a given system can be the lower limit.

Secondly, the specific thermal and operating conditions and configurations for a given engine may be such that it is impossible--or at least impractical--to effect the joint at lower area ratios where, for instance, heat fluxes to the extension reattachment sections would be extremely high for the selected extension material or gimbal or pump equipment may interfere.

III, B, Tradeoff Studies (cont.)

Finally, how long (physically) is the total nozzle expansion compared to the length of the thrust chamber? If the real purpose of packaging is to reduce nozzle length for vehicle accommodation, it would be impractical to make the joint just aft of the thrust chamber if the thrust chamber represents, say, only 10% of the total nozzle length.

It is more likely that the vehicle system analyst, restricted to a vehicle with a given length and diameter (and therefore volume), is looking for the nozzle which occupies the least amount of this available volume in the retracted position for the lowest weight while still delivering the required performance. Actual joint location then becomes a function of vehicle systems analysis and is probably near the one-half total nozzle length.

If the thermal or thrust chamber diameter restrictions on attachment joint location outlined above make it necessary to locate the joint at a point significantly aft of one-half total nozzle length, serious thought should be given as to whether or not a movable extension is beneficial to engine performance. It might well be that a lightweight radiation or other fixed extension might be more desirable.

(3) Cooling

The design philosophy associated with cooling of various components in and around the extension attachment joint can be summarized as follows:

(a) If a coolant source is available without imposing additional penalties on the vehicle system (turbine exhaust gas, for instance), MAKE USE OF IT.

III, B, Tradeoff Studies (cont.)

(b) If a free coolant source is not available, make every effort to design the various components SO THAT NONE IS REQUIRED.

In other words, if coolant is available, even turbine dump gas at 600 to 800°F, it can always be used with benefit to either reduce temperatures of the components or to allow them to be positioned in areas of greater heat input. An example might be that of placing the attachment joint at an area ratio of 15:1 and still have the extension operate at the same temperature it would have uncooled at an area ratio of perhaps 20:1. Or perhaps the use of a coolant would allow substitution of more desirable materials which could not withstand the temperatures that would be reached without cooling.

On the other hand, if a "free" coolant is not available, it is not likely that the benefits derived from cooling could possibly offset the disadvantages--such as increased weight, complexity, and cost of having to provide a separate coolant supply system.

The three different joint components which can benefit most from cooling are the seal, the fixed tip (trailing edge of the fixed portion of the nozzle), and the moving extension. The joint design should be so integrated that the coolant can effectively cool each of them as required.

It should be mentioned here that some provision must be made to preclude a catastrophic engine failure in case the coolant is lost. If the coolant is turbine exhaust gas, loss of coolant probably means engine failure anyway, but components should not be designed so that loss of coolant from other sources will cause total and immediate engine failure.

Nonmetallic seals generally have some temperature limit above which they should not be operated because of either loss of sealing capability or a decrease in use life. One method of being able to place nonmetallic seals in

III, B, Tradeoff Studies (cont.)

regions which would normally prove too hot for the seal is to effect a local cooling of the region by directing a coolant on or passing it near the metal surfaces which touch the seal. For instance, if an elastomeric face seal is used in conjunction with a radiation-cooled extension and a fixed regeneratively cooled tube bundle nozzle as shown in Figure 14, the fixed nozzle portion touching the seal will probably remain fairly cool but the heat will work its way forward to the seal area through the extension material. By merely dumping the coolant into the annulus formed between fixed and moving nozzle parts as shown in Figure 15, this portion of the extension can be kept at a lower temperature, enabling seal usage.

Figure 15 also depicts other methods which might be employed to cool with a secondary coolant.

The design of the tip of the fixed portion of the nozzle represents another paradox to the engineer. It is desirable to have this tip machined to essentially a feather edge with the gas surface tangent to that of the extension so that flow discontinuities are minimized. On the other hand, these very thin sections can become very hot and melt because the heat cannot be conducted away from the thin section quickly enough. Even when the tip is brazed or welded to a specially designed tube bundle, it is unlikely that the very sharp point will remain cool enough to survive under the heating conditions present at the joint attachment area.

If no "free" coolant is available, the designer must determine how thin the tip may be so as to survive steady-state temperatures and yet represent a minimum flow discontinuity which, in turn, helps minimize heat flux increases to the extension upon reattachment of the flow. If a "free" coolant is available, however, it may be utilized to keep a sharp, thin tip cool enough to survive by properly injecting in, around, or through the tip area. Several different injection schemes for use with tip cooling are shown in Figures 16 through 18. It is generally agreed that coolant supersonically injected at angles nearly tangent to the gas surface is most effective.

III, B, Tradeoff Studies (cont.)

Still another method of cooling the tip would be to transpiration cool it by forcing a small amount of propellant from the tube bundle through a Rigimesh or other orifice system as shown in Figures 19 through 22. Figures 23 through 25 show how a replaceable tip can be employed to compensate for any eventual material loss due to overheating, corrosion, etc.

As defined in Section III,B,3,b, nozzle extensions are generally classified as to the basic method by which they are cooled. Closer examination of the different types resulted in the recommendation of two for use with movable extensions--namely, convection and radiation cooled.

The convection concept naturally requires a coolant source for operation, whether turbine exhaust or some other fluid, and the extension can be designed by conventional methods based on the coolant used and the heating conditions. It must be remembered that a means of getting the coolant into the movable extension must be found, which may result in complex flexible piping or ducts. Also, if a "free" coolant is not available, a coolant source must be provided, which may or may not penalize engine performance in some manner.

The real application of cooling as outlined in this section is to the radiation-cooled nozzle which normally is cooled or achieves a temperature balance by radiating heat from its outer surface. For a given material, there is a thickness range for a given heat input and set of load conditions. That is, the material must be thin enough so that, when a heat balance is achieved, the inner surface does not start to melt and it must be thick enough to be able to carry expected loads at a predicted average temperature.

If a "free" coolant is available and it is injected upstream of this type of extension so as to provide a certain amount of film cooling, then (1) the local thickness of the material at the attachment point can be increased. (2) the same thickness of material can be operated at a lower temperature, or (3) the attachment point can be moved upstream to a smaller area ratio since a higher

III, B, Tradeoff Studies (cont.)

attachment heat flux can now be accepted. Additionally, no complicated ducting is necessary since the coolant can be injected through the fixed portion of the nozzle.

Final emphasis should be made again that, whether a coolant is used or not, every effort should be made to provide as smooth a transition from fixed to movable portion as possible to minimize heating at the joint attachment area. Again, the same coolant supply can and should be used to cool all components in the joint area in an integrated design.

d. Conclusions and Design Recommendations

The following conclusions and recommendations can be drawn concerning the selection and design of extendable nozzles:

(1) The extension should be of radiation-cooled design when possible with tube bundle and transpiration-cooled designs as alternatives when a cooling source is available.

(2) If a cooling source is available at no penalty to the engine or system, it should be used to cool the fixed tip, joint seals, and extension if required.

(3) Discontinuities at the fixed tip should be minimized to reduce increased heat fluxes due to reattachment.

(4) The location of the attachment joint should be in the vicinity of the midpoint of the total nozzle length.

(5) The extension should be coated to prolong resistance to possible corrosive attack.

III, B, Tradeoff Studies (cont.)

(6) A columbium alloy such as C-103 is recommended for the initial design of radiation-cooled extensions.

4. Seal Design

a. Design Considerations

The design guidelines established for the tradeoff studies did not require nozzle sealing during deployment or retraction; only during engine operation. Static seals are common to most fluid components. Their importance in design cannot be overemphasized, as seal leakage constitutes a major cause of malfunctions. A static seal is a device used to prevent leakage of a fluid through a mechanical joint in which there is no relative motion of the mating surfaces other than that induced by changes in the operating environment.

The degree to which seal leakage is eliminated depends on the seal's capability to effect continuous mating of the sealing surfaces. Seal and gland mating can be accomplished by (1) making one surface relatively soft and compliant so that it will readily conform to the harder surface irregularities, (2) providing sufficient sealing load to plastically deform the softer of the two sealing surfaces, or (3) carefully finishing both surfaces so that good mating can be achieved without high sealing loads. The stress required at the sealing interface to afford good mating depends both on the physical properties and the surface finishes of the mating materials. Resilience of the seal material ensures that adequate sealing stress is maintained, in spite of relative movement of the joint surfaces caused by changes in the operating environment.

Metal seal materials are normally used for high pressure, high temperature, and/or corrosive fluid applications. The most commonly used materials for metallic seals are steels, copper alloys, aluminum alloys, Monel, Inconel, gold, silver, and nickel. Selection of metallic seal materials must include consideration of the thermal environment, since the levels of creep

III, B, Tradeoff Studies (cont.)

strength, fatigue strength, and notch sensitivity of metallic materials may be adversely affected by extremes in temperature. Differences in thermal expansion, if not compensated for, can result in seal failure through structurally damaging loads or load relaxation.

The material of the seal must be chemically compatible with the sustained media and with the surrounding environment. Material combinations which promote corrosion must be avoided, particularly those combinations of materials which would promote galvanic action, oxidation, or stress corrosion.

In metallic seals, plastic flow of one of the materials at the seal interface is usually required to obtain an effective seal. Softer materials with a desirable high plastic strain range will usually have a low ultimate strength level. To balance the requirements of high strength in the seal body and good plastic flow under low stress at the interface, high strength materials are often plated with a thin coating of a softer material. Plating materials and their recommended applications are given in Table VI.

b. Seal Leakage

Of primary consideration in seal design is the determination of the amount of leakage which can be tolerated. The design must be examined with respect to the total system and mission requirements in order to arrive at an acceptable leakage rate. Since reduction of the leakage rate requires a reduction in the size of the potential leak path (which, in turn, necessitates higher seal loads, smoother surface finishes, or softer seal materials), setting an overly restrictive leakage rate could result in an excessively complicated and costly design because of the need for close manufacturing control.

III, B, Tradeoff Studies (cont.)

The factors that will determine the amount, or rate, of leakage that can be accepted include fluid loss allowance, system performance, corrosion and erosion considerations, and hazards associated with subsystems or components in the environment or leak path.

In establishing an acceptable leakage rate, a common tendency is to state that the leakage shall be zero; however, it should be recognized that an absolute seal is an impossibility. Gaseous leakage inspection of a part by immersion may show a zero bubble count over an extended period of time, while mass spectrometer inspection of the same part may show a relatively high leakage rate. To determine or predict an absolute value for leakage rates, measurement of actual performance by testing will be required.

c. Reusability

The degree to which seal components may be reused after disassembly is an economic consideration, particularly for separable connector applications. In general, when plastic deformation of one or both of the components is required to effect a seal, the components are not reusable; if the deformation is in the elastic range, the components may be reusable. In those areas where plastic deformation is required, considerations should be given in material selection to limiting the plastic deformation to one component only. The component that is most easily replaced, the seal element, should be designed or selected on the basis of plastic deformation occurring in the component, with little, if any, occurring in the mating gland interface. The relative relationship of plastic deformation of two interfaces will govern the number of times that the seal can be replaced without a major rework of the component.

Nonmetallic seals, particularly elastomers, are generally reusable; however, because of their low cost, this type of seal is often replaced when an installation is disassembled in order to improve the reliability of the seal joint.

III, B, Tradeoff Studies (cont.)

Soft metal plating is often used on metallic seals in order to reduce the contact stress required for sealing. Because of this plating, many of these seals may be reused if the base structure is not plastically deformed.

d. Temperature Environment

In addition to the effects of high and low temperature on materials (see Table VII for the operating limits of some organic materials), consideration must be given to the affects on dimensional stability of temperature changes.

Where materials having different thermal expansion coefficients are in contact, thermal stress and subsequent dimensional changes can occur. When a component must operate over a wide temperature range, care must be taken to assure that differential expansion (contraction) will not result in detrimental dimensional changes, particularly where moving parts and close tolerances are involved. Where elastomers or plastics are used for seals, increases or decreases in temperature will affect the sealing forces in a closure because of a corresponding increase or decrease in the seal volume with relation to the groove. This is caused by the fact that all polymeric materials have a much higher thermal expansion coefficient than metals. In some elastomeric materials at certain rates of cooling, the rate of return of the material at the low temperature is less than the rate of shrinkage due to cooling. Consequently, the sealing force may be lessened to the point where leakage occurs. The coefficient of thermal expansion of several materials are given in Table VIII.

It should be noted that the selection of seal materials with appropriate coefficients of thermal expansion can increase the seal load under temperature extremes as well as decrease it. Thermal expansion data for typical seal and gland material are shown in Table IX.

III, B, Tradeoff Studies (cont.)

In the design of a seal joint, care must be taken to ensure that the required seal load is maintained throughout the operating environment of the seal. Two temperature conditions which could affect the stability of the seal load are the steady-state effects at temperature extremes and the transition effects during temperature change. One of the chief problems associated with the thermal gradients is the possibility of a momentary shifting of the sealing surface, which may destroy the surface mating achieved in original seating. This would result in a shift of the plastically deformed interface and a corresponding change in the leakage path.

e. Pressure Environment

Design of the structure surrounding the seal element must take into account the effects of continued operation at pressure as well as the possibility of pressure surge effects. The surrounding structure must be sufficiently rigid to ensure that any deformation of one of the seal interfaces will not allow the seal load to drop below that value required for the sealing application.

The differential pressure across the seal is a factor in establishing the maximum allowable leakage and its related apparent seating stress. The higher the differential pressure, the higher the leakage rate will be through a given size leak path.

The pressure-energized seals utilize increases in the magnitude of pressure differential to increase the seal load. In O-ring design, the elastomer acts as a highly viscous liquid with high surface tension and transmits the increased pressure load to the sealing surface. In flexible metallic seals, the interface contact area is designed much smaller than the area of the flexible member exposed to the contained fluid. Increase in the fluid pressure results in correspondingly higher loads at the contact interface.

III, B, Tradeoff Studies (cont.)

The rate of pressure change must be considered when using elastomers in a high temperature gas system. The gases absorbed by the seal material will expand and the forces generated can rupture the material if the decompression rates are high.

f. Resiliency

The resiliency of the seal is a measure of its capability to accommodate interface deflection (temperature and pressure) without reducing seal loads to a level where the allowable leakage rate is exceeded. Resiliency may be expressed as the ratio of energy given up on recovery from deformation to the energy required to produce the deformation.

In nonmetallic designs, particularly those utilizing elastomers, the seal load due to deflection of the seal during installation results in a significant portion of the stress necessary for sealing. The natural resilience of nonmetallic materials, the effective pressure actuation, and the initial deflection act to reduce the problem of increased leakage due to motion of the sealing interfaces.

In metallic designs, there is little or no resilience in the material itself. A measure of resilience may be provided by designing the seal so that a flexible member is deformed elastically in a cantilever type of deflection by the mating parts.

g. Commercial and New Design Seals Investigation

In parallel with identifying the above seal design considerations, an investigation was initiated to identify and evaluate commercially available seals as well as new seal concepts for potential use in an extendable nozzle design.

III, B, Tradeoff Studies (cont.)

In addition to the guidelines established for the tradeoff studies, specific obvious seal design requirements were formulated to assist in the identification process. They are as follows:

- The seal design must require only a minimum of unit loading to accomplish sealing. This relaxes the load required to be input by the nozzle deployment system to accomplish sealing and increases the radial tolerance between fixed and moving portions of the nozzle extension. The seal design will be insensitive to surface scratches. The scratches on the seal surface interfacing with the sealing gland will not affect or prevent positive sealing.
- The seal design must seal or accommodate out-of-roundness and distortion of mating surfaces resulting from thermal cycling of the nozzle.
- The seal design must seal against low pressure differentials.
- The seal design must accommodate radial thermal expansion of the nozzle extension during periods of engine operation, i.e., sealing must be positive.
- The seal gland must not require a critical surface finish. This requirement goes in hand with the out-of-roundness requirement.

Of the 34 commercially available seals evaluated, none satisfied the above design requirements. Table X is a listing of typical available seals and their gland design and separation requirements, in addition to applicable remarks.

The new seal concepts evaluation identified three potential candidates. They are the inflatable elastomeric, the inflatable metallic, and an elastomeric gasket employed as a face seal concept. The inflatable concepts are not new to the sealing industry, but because they are not considered as off-the-shelf items and require special design considerations, they are called new sealing techniques.

III, B, Tradeoff Studies (cont.)

The inflatable concepts, shown in Figures 26 and 27, require some auxiliary or supporting system for inflation that takes place following positioning of the nozzle extension for firing, whereas the elastomeric face gasket--once positioned--remains sealed.

h. Conclusions

For extendable nozzle applications, it is concluded that the fixed-to-movable-extension seals in the attachment region should be designed or selected in accordance with the following criteria:

- The seal should be a face seal if possible to eliminate the clearance and compression problems associated with piston (diameter) seals.
- The seal should be elastomeric if possible to provide good sealing characteristics for the low compression forces allowed and because of the low differential pressures for which it must seal.
- The seal should be of the gasket type to eliminate the need for very close tolerance controls.
- If a piston type seal is employed, the use of an inflatable elastomeric or metallic seal is warranted to allow free movement of the extension and to overcome tolerance and clearance problems.
- Leakage rates of specific seals and seal interface designs must be evaluated by testing.
- If an elastomeric seal is used, it should be located in a cool or cooled region.
- If an elastomeric seal is used, it should probably be replaced after a mission as a "soft goods" item.
- The maximum operating temperature environment for an elastomeric seal is approximately 700°F.
- The maximum operating temperature for metallic seals is approximately 1500 to 1800°F, depending upon the seal design and coating.

III, B, Tradeoff Studies (cont.)

5. Nozzle Extension Translation System

a. Introduction

The nozzle extension translation system can be described as those mechanical devices required to deploy, retract, support, and guide during travel of the nozzle extension from its stowed (retracted) to firing (deployed) position. This system consists of a mechanical drive (actuation) device, a traveling mechanism, and a guide and support structure. This section serves to identify and evaluate these design considerations and requirements most obvious, within the established design guidelines, for design of a nozzle extension translation system.

b. Actuator Design

(1) Definitions

An actuator is a power unit which provides a mechanical operating force to position some element or device; the actuator may be direct acting or piloted. The direct-acting actuators are piston - cylinders, solenoids, electric motors, and servo-torque motors, each used independently. Piloting, which involves the use of a small power input to control a larger power source, is common with piston - cylinder actuators which include the electrohydraulic, electropneumatic, pneumatic - hydraulic, or pneumatic - pneumatic combination.

Most aerospace systems are powered by remotely controlled, or automatic, actuators. Linear actuators used in aerospace systems include solenoids, piston - cylinders, bellows, and diaphragms. Rotary actuators include electric motors and servo-torque motors. Rotary actuators can also be used to impart linear motion through, for example, a rack and pinion. Linear actuators can be used to impart rotary motion by driving an internally threaded shaft sttachment with a threaded rotating shaft. The actuator may be either an integral part of the system or a separate device mechanically linked.

III, B, Tradeoff Studies (cont.)

Positioning requirements can be broadly divided into two groups: (1) two-position or nonmodulating, and (2) modulating (used for discrete positioning). The design or selection of an actuator is at best a tradeoff among several interrelated factors. Typical mechanical factors which must be considered in the design and selection of an actuator include length of stroke desired, locking requirements, speed required, limitation of envelope size and weight, and magnitude of the force that must be provided. If a long stroke is required, a solenoid is automatically eliminated. If fast response times are desired, an electric motor, solenoid, or explosive charge should be considered. If high forces must be overcome, either hydraulic or pneumatic pressure must be used.

(2) Power Requirements and Sources

The choice of an actuator is limited by readily available power sources. Solenoids, electric motors, and servo-torque motors can be used with electric power. Piston-cylinders, diaphragms, and bellows might be selected as the actuator with hydraulic and pneumatic pressure. In a rocket system, power sources available might include high pressure gas used for propellant tank pressurization systems, and hydraulic pressure and electrical power used for thrust chamber gimballing. Other power sources available include 28 VDC electric power, sometimes converted to AC, and hydraulic pressure of the propellant from the propellant feed system downstream of the turbopump. Also to be considered is the use of hot gas either from gas generators or from thrust chamber bleed. The stroke of an actuator is measured in terms of length of travel in the case of linear actuators or angle of rotation in the case of rotary actuators.

(3) Locking Ability and Devices

The ability of an actuator to hold a constant position independent of varying forces impressed upon it is called the locking ability. The best type of actuators for maintaining constant position are actuators with screw

III, B, Tradeoff Studies (cont.)

outputs and piston - cylinder actuators utilizing relatively incompressible fluids (e.g., hydraulic oil). For varying actuator loads, air cylinders and electric motors require mechanical locking devices for accurate positioning. Actuator locking mechanisms include toggles or linkages and pin and ball locks which are spring or piston actuated. Solenoid actuators can be locked in the closed air gap position by the use of a second coil to hold the plunger (holding coil) or to disengage a locking mechanism such as a detent.

(4) Actuator Speed

The speed of an actuator should be considered in terms of initial response, total response time, acceleration, speed, uniformity, and ease of adjustment.

The solenoid actuator and the electric motor have higher speeds than other types of actuators. The electric motor actuator has the highest initial acceleration and the best uniformity of response. The uniformity of response is best with induction motors because constant force is produced at every position along its entire length of stroke. Piston - cylinder actuators respond instantly, but because the maximum acceleration is not reached until the end of the stroke, it has a very poor uniformity of response. The initial response of piston - cylinders is limited by the time lapses in the system valving and/or transmission system. Hydraulic cylinders generally have a faster initial response than pneumatic cylinders. The total response time, particularly for relatively long strokes, is commonly shorter for pneumatic cylinders than for hydraulic cylinders.

The speed of piston - cylinder actuators is easiest to adjust, followed in order by electrical motor actuators. The actuator must provide sufficient force to overcome the weight and inertia of the moving element and friction forces. The weight load exists where the unbalanced weight of moving parts must be supported by the actuator, and the inertial load exists due to acceleration

III, B, Tradeoff Studies (cont.)

of moving parts. Friction forces include viscous friction loads which exist even in well-lubricated actuators, such as hydraulic cylinders, and static friction loads which are apparent at startup.

(5) Actuator Output

The electrical induction motor maintains a constant output force if the applied voltage is constant. Fluid cylinders will have a constant force output if the pressure in the cylinder and the effective area are constant.

Relative size for actuators is based on the total energy that can be obtained per actuator volume. The total energy for linear actuation is the output force times the stroke and, for rotary actuators, output torque times the angle of rotation (in radians).

High pressure hydraulic and pneumatic cylinders provide the highest ratio of total energy to volume. Electrical motors have a low force-to-volume ratio but require less auxiliary equipment than cylinder actuation. Electrical actuators require batteries, while cylinder actuators require external pumps, accumulators, and fluid lines. The ability of the actuator to utilize the same power to produce the same force, speed, and stroke is called repeatability. Electrical motors have the best repeatability because they have few critical parts and exhibit constant force at every position.

Piston - cylinder actuators do not rate high in repeatability because the working fluids are very sensitive to temperature changes and the pressure drops through valving and connecting lines do not vary linearly with flow rate.

III, B, Tradeoff Studies (cont.)

(6) Environmental Considerations

The environment to which an actuator can be exposed includes temperature, vacuum, corrosive atmosphere, radiation, vibration, and shock. Temperature variations and extremes will adversely affect performance characteristics such as repeatability and response. With electric actuators, increases in temperature increase electrical resistance and also increase the amount of current necessary to obtain a desired output force. Manufacturers usually indicate operating characteristics close to normal room temperature and apply correction factors for different temperatures. Low temperatures eliminate the use of hydraulic cylinders and oil-lubricated screw drives unless heat is supplied.

Special design considerations are required for actuators which must operate under vacuum conditions. Electrical actuators may arc or exhibit a corona discharge if subjected to a partial vacuum. Electrical devices should be encapsulated and supplied with a blanket of helium or nitrogen. Vacuum adversely affects sealing of a piston - cylinder, increasing fluid permeation and seal degradation. Screw drives, if not lubricated, will cold weld. For extended periods of vacuum service, solid lubricants should be considered.

In general, rotary actuators have greater resistance to shock and acceleration than linear actuators because the rotor (in the case of an electric motor) is very closely balanced. Shock in cylinder actuators can result from a sudden pressure buildup caused by the load reacting against the actuator.

(7) Reversability

The previously mentioned actuators all have reversability built in. Some DC motors can be reversed while running. All series DC motors can be reversed if first allowed to come to a stop. Reversability is a basic selection and design requirement for an extendable - retractable nozzle actuator.

III, B, Tradeoff Studies (cont.)

(8) Conclusions and Design Recommendations

Based on the general observations regarding actuation systems presented in this section, the following conclusions can be summarized concerning their design usage for extendable nozzle applications. The actuation or power drive system should:

- Be designed based on system requirements and available power sources.
- Be electrically powered if possible.
- Incorporate actuation source, guides, rails, and locking features into one simple mechanism for simplicity, reliability, ease of development, and low weight.
- Be self-positioning in two positions only (retracted and deployed).
- Feature known, reliable, and repeatable operating characteristics under any conditions or loads.

c. Guide and Support Systems

(1) Purpose

The purpose of the guide and support system is to support or hold the nozzle extension at any point in its travel from the retracted to the extended position and to hold the extension in a proper relation to the fixed portion of the nozzle during deployment. The guides and/or supports may be a part of the actuation system as discussed in Section III,B,5,d. Likewise, the guide-support system may include alignment and locking features. Support systems and alignment and locking mechanisms are discussed in the following sections.

(2) Guides and Supports

The guide and support system can be any mechanism which holds the nozzle extension radially around the fixed portion of the nozzle and guides it during translation from retracted to extended position. The typical

III, B, Tradeoff Studies (cont.)

system usually consists of rails attached to the engine or the fixed portion of the nozzle and bearings which ride these rails and support the extension. The number of rails is usually three or four. Such a system, which uses hardened steel shafts for the rails and ball bushings for the bearings, is shown in Figure 28. This section is rigid enough that it could be used to align the extension.

A major problem with this type of system is the potential of cold welding between certain metal pairs--the steel ball bearings and the hardened steel shafts, for instance. The wiser course appears to be a support system which supports the extension adequately but somewhat loosely and allows final alignment to be accomplished by engagement of mating parts at the end of travel. If such a "loose" type of support can be utilized, thin-walled hollow tubes can be used to replace the shafts and Teflon sleeves can be used to replace the ball bushings. In other words, when the requirement for close tolerances is removed, the system can be made lighter and more inexpensively.

If threads are formed in the inside of the bearing and the outside of the tube rail, the rail not only serves as a support but can be used to translate the extension when turned by motor or rotary actuator. When this system is carried to its simplest form, a cylinder with threads formed in it can be placed around the fixed portion of the nozzle and a concentric cylinder with matching threads placed around it with lubricating material in between. If the nozzle extension is now attached to the outer cylinder, the entire extension can then be "threaded" or rotated into the extended position.

Any of the systems described are considered suitable for use as a guide system. The main thing is that the system support the extension against vehicle "g" and vibrational loads in the retracted position and be capable of support while in its extended position.

III, B, Tradeoff Studies (cont.)

(3) Lubrication

Several different types of lubricants have been developed and found suitable for elevated temperature operation in space vacuum, as well as standard conditions. These lubricants are required in at least two specific areas of the guide and support system. The first is at the interface of the guide or support rod and the bushing which rides on it and supports the extension. The second is at the interface between the extension and the springs or other devices on the fixed nozzle which accomplish final alignment.

The lubricants that are now available and are most suited to this rubbing or sliding type of friction are the so-called bonded solid films and the dry powder lubricants that are usually sprayed on the metal surface. In addition, several types of filled tapes and coatings of Teflon or Teflon TFE filled materials are in use.

Graphite bearing lubricants were purposely omitted from consideration in this instance because of the general incompatibility of graphites and carbons with the combustion products of LO_2/LH_2 engines.

The most promising solid bonded and dry powder lubricants available incorporate molybdenum disulfide (MoS_2) either alone or in combination with other constituents. The bonding agent for the solid bonded type can be a resin or polyimide or boric oxide (B_2O_3). The dry powder types are applied by several methods with impingement plating being the most popular.

The solid bonded types which have undergone extensive testing under different environmental conditions are: (1) $PbS\text{-}MoS_2\text{-}B_2O_3$ and (2) $MoS_2\text{-}SbO_3$-polyimide (MIL-MLR-2). Both exhibit good wear life and low friction coefficients from -100°F to 1000°F at standard and vacuum conditions. In general, friction decreases and wear life increases at higher temperatures and reduced atmosphere.

III, B, Tradeoff Studies (cont.)

One of the better dry powder lubricants that has successfully been used in the Apollo and other space programs is Microseal 200-1 (MIL-L-8937), manufactured by the Microseal Corporation. This compound uses MoS_2 as its lubricating solid and is applied by an impingement plating process that is proprietary to Microseal.

Both the solid and dry powder lubricants are applied or deposited to depths ranging from 0.0001 to 0.001 in., depending on the usage and the material to which the lubricant is being applied. Surface preparation of the material is usually very exacting with very smooth, treated surfaces required for good adhesion or dispersion.

The possibility of using one of the many available Teflon or TFE tapes or coatings currently on the market should not be overlooked. The major problem associated with use of these products is their tendency to "cold flow" under heavy or repeated loading. Fillers, such as fiberglass matrices within the material, have eliminated this problem in many instances.

It is undesirable to use solid bonded coatings in conjunction with friction-eliminating devices (such as ball bushings or bearings) and therefore the dry powder types are recommended where these devices are used.

Finally, although cold welding of interfacing parts may be a problem, the useful life of a ball bushing and rod or other guide system in a vacuum without a lubricant should be experimentally measured to determine whether a lubricant of some type is definitely required.

(4) Nozzle Alignment

Nozzle alignment is concerned primarily with the angular difference between a theoretical centerline through the nozzle throat and injector

III, B, Tradeoff Studies (cont.)

end of the thrust chamber and the theoretical centerline through the throat and the exit plane of the nozzle. For any motor configuration, the tolerance on misalignment is usually specified by the customer and must be met by the manufacturer.

Misalignment tolerances are usually quite small, perhaps on the order of 0.25 degrees or less. This is because the engine is usually mounted in the vehicle using the thrust chamber centerline as the mounting guide, generally placing it in parallel with the vehicle centerline. For single-nozzle vehicles, these centerlines are also coincident. It can readily be seen that, for a fixed single-nozzle application, any misalignment built into the nozzle now represents a moment arm of the resultant thrust vector about the vehicle center of gravity. Similarly, thrust misalignment in a multi-engine vehicle might result in undesirable turning moments or thrust losses.

If the engine is not fixed, but gimballed, a slight movement of the gimbal actuators will compensate for small amounts of misalignment. This action reduces total gimbal movement in that direction by a like amount, however.

For an extendable nozzle, it can be assumed that misalignment in the fixed portion of the engine is small and can be held to conventional tolerances by conventional methods. This is not true of the extendable exit cone or moving portion, however. This section, supported by some sort of guides and moved into position by an actuation system, must be carefully designed so as to reduce misalignment between it and the fixed portion of the nozzle. It is true that, if the extendable nozzle motor is gimballed, this misalignment can be corrected for by slight gimbal motion. It must be remembered, however, that the misalignment of the extendable nozzle occurs within the divergent portion of the nozzle itself, at the joint attachment line and probably at a fairly high area ratio. Therefore, a severe misalignment at this point could result in a loss of performance.

III, B, Tradeoff Studies (cont.)

In any case, it is important to keep misalignment between fixed and moving portions of an extendable nozzle to a minimum, probably meeting a tolerance on the order of that allowed for conventional nozzles.

The nozzle extension can be aligned with the fixed portion of the nozzle in two ways: through the guide and support system or directly to the fixed portion. The use of the guide and support system to accomplish alignment is a poor choice because the guide and supports must first be aligned with the fixed part of the nozzle and then the extension aligned with the guides. Alignment of the guide rods or screws to the fixed portion of the nozzle is very difficult no matter how many rods are employed. Alignment of the extension to the rod is generally accomplished by line-boring the bearing holders in relation to the extension centerline.

A much better system is to align the extension directly to the nozzle. Since both parts are concentric and turned on a lathe or spun, it is more natural to interface the two parts and accomplish alignment with the interface.

The spring-loaded system of Figure 29 holds the nozzle in as perfect alignment as possible within the machining tolerances of the two parts and also establishes a moment arm to resist lateral forces imposed on the extension due to gimballing and other vehicle imposed loads. Figure 29 is an integrated design which also illustrates the gasket seal and shows how a secondary coolant can be used to cool all attachment joint components.

(5) Nozzle Locking System

The nozzle locking system must function as the name implies--it must lock and hold the nozzle extension in either the deployed or retracted position for certain periods of time and, upon command, unlock to allow motion of the nozzle extension.

III, B, Tradeoff Studies (cont.)

Like the nozzle actuator, this system requires an electrically powered actuator to position a locking mechanism to lock and hold the nozzle extension in a fixed position. Because this system is so interrelated with the nozzle translation system, several design techniques could be employed to hold or lock the nozzle extension in a fixed position. The locking devices could be designed into (1) the nozzle deployment actuators or mechanical power transmission system or (2) into the nozzle extension itself.

The technique of designing the locking device into the nozzle extension (Figure 30) presents design and use problems that could readily be eliminated by designing the locking device so that it is integral with the nozzle translation system. The problems presented are:

- The electrical power supply becomes a traveling cord or line.
- If the locking device is to maintain the nozzle in a fixed, sealed, aligned, and firing position--assuming that a face sealing concept is employed--this dictates that the nozzle is held in some preloaded condition to effect sealing and that the device must maintain this position. To unlock the nozzle, then, requires that the actuator retract the locking mechanism (which is under load), or that the nozzle deployment actuators be actuated to reduce this preload to facilitate removal of the locking mechanism.
- Thermal expansion of the nozzle extension is also a potential problem because it could also cause the locking mechanism to bind. This situation also dictates that the solenoids have sufficient power to unlock the locking mechanism.
- When the locking device is designed into the nozzle extension, a separate actuator and locking mechanism is required. This technique requires additional system controls because of the increased components and sequence of events during nozzle unlocking, deployment and locking.

It is obvious that the technique of nozzle deployment and retraction confines the option of the nozzle locking technique. As an example, with the chain, tape or cable drive system, a locking system designed into the

III, B, Tradeoff Studies (cont.)

nozzle extension is a must unless the power drive mechanism (actuator) preloads the transmission system to a load greater than that imposed by the pressure load imposed on the transmission system from the engine firing, compensating for elongation of the power transmission system.

It can be concluded from the above discussion, that, if the locking technique is incorporated into the nozzle deployment actuators and/or mechanical power transmission system, a locking system requiring a separate actuator and controls will be eliminated, simplifying total engine operation, design and development, minimizing cost and weight of the total system, and increasing reliability.

(6) Conclusions and Design Recommendations

The following conclusions and design recommendations can be summarized concerning the design and use of a nozzle guide and support system, lubricants, and nozzle alignment and locking techniques.

(a) Guide and Support

The guide and support system is used only as the name implies--to guide and support the nozzle extension from its stowed to extended position--and is not used to accomplish final alignment of the nozzle extension with respect to the combustion chamber. The guide and support and power transmission systems, for simplicity and reliability, should be combined.

(b) Lubricants

The use of lubricants in the space environment, particularly on the power transmission system, should be restricted to commercially available solid bonded and dry powder lubricants. The particular problems (cold flow and adherence) associated with use of bonded Teflon and similar materials should be avoided.

III, B, Tradeoff Studies (cont.)

(c) Nozzle Alignment

Alignment in the extended position should be repeatable within the allowed tolerance. Minor eccentricities should have little effect on nozzle alignment.

Alignment should be accomplished so that it is unaffected by the extreme temperature differentials expected from both the space environment and heat soakback from engine or nozzle extension. Finally, alignment methods should be independent of the deployment system when possible.

(d) Nozzle Locking

The locking mechanism must maintain the nozzle extension in a fixed, defined position during engine operation.

The locking device must be designed to be fail safe; that is, the ability to translate the nozzle extension must not be impaired by the loss or interruption of power. Operation must not be affected by environmental conditions (space and earth).

Devices must be located in a cool zone and be unaffected by heat soakback from the engine. Adequate insulation will preclude possible binding due to thermal expansion of the nozzle extension.

Nozzle lock and unlock shall be upon command. The same locking device should be used for locking the nozzle in the extended or stowed position if the design warrants it. The locking system must be designed to satisfy system requirements and to operate with available power sources.

III, B, Tradeoff Studies (cont.)

Incorporating the nozzle locking feature into the actuator or actuator power transmission system will provide one simple mechanism for operation, increased reliability, simplicity, ease of development, and low weight.

Redundant locking devices are required for both the extended and stowed position of the nozzle extension. The number of devices will depend upon the particular design.

d. Comparison of Translation Systems

Twelve different nozzle deployment and retraction concepts were evaluated and comparisons made. They are named after the basic element they use to perform the task:

(1) Electrical drive, steel wire cable (Figure 31)
(2) Electrical drive, steel tape (Figure 31)
(3) Electrical drive, steel chain (Figure 31)
(4) Electrical drive, rack and pinion or worm gear (Figure 32)
(5) Electrical drive, internal gear and pinion, ball screw (Figure 33)
(6) Piston - cylinder scissor drive (Figure 34)
(7) Piston - cylinder spring drive (Figure 35)
(8) Piston - cylinder cable drive (Figures 36 and 37)
(9) Hydraulic or pneumatic torque motor drive (Figure 38)
(10) Bellows drive (Figure 39)
(11) Diaphragm drive
(12) Telescoping hydraulic or pneumatic drive (Figure 40)

The bases of comparison were: simplicity, historical background, weight, reliability, ease of development, environmental design problems, and system design problems.

III, B, Tradeoff Studies (cont.)

Of the candidate systems evaluated, the electrical motor - screw drive concepts seemed to best satisfy the design requirements established by the nozzle translation systems tradeoff studies.

The hydraulic cylinder, pneumatic torque motors, diaphragm, and bellows drive systems were eliminated because they require a greater number of support systems, controls, and components, which increases weight and design and development problems and decreases reliability. An additional disadvantage of the bellows and diaphragm power drive systems is their length of stroke limitation.

Figures 32 and 33 identify the electrical mechanical systems determined to be suited for nozzle deployment. Included in the figures are weight estimates and the identification of the number of mechanical components required to conform to the study guidelines. The comparative weight estimates are based on the following assumptions:

That the nozzle translation scheme, regardless of engine size, would weigh the same percentagewise.

That a minimum of two extension travel guide columns were required for support if the design warranted it.

That a minimum of two power drive devices are required if the design warrants it.

That the combustion chamber diameter is 1 ft (established for weight calculations).

That the nozzle extension has a total travel from deployed to extended position of three feet (established for weight calculations).

That common devices between concepts all weigh the same (e.g., the nozzle travel guide columns).

A comparison of the twelve candidate systems is presented in Table XI. The following is a discussion of some of the comparison factors with comments applicable to the different concepts:

III, B, Tradeoff Studies (cont.)

- Drive or Actuator Mechanism: The device that drives the mechanical power transmission system, deploying and retracting the movable nozzle extension.

- Energy Source and Type: The drive or actuator system power and its source.

- Supporting Power Supply Systems: The power supply supporting systems for the power drive mechanisms which include the systems required to transmit power to the actuator as well as the power transmission system from actuator to nozzle extension. This comparison is to show the extent of the various systems required to transmit power to and from the actuator to deploy the nozzle.

- Relative Total System Weight: Comparison of estimated weights of the individual deployment systems.

- Relative System Complexity: Identifies the number of major components of the undeveloped drive systems and compares them. The system having the greatest number of controls and devices is the most complex.

- Ease of Development: Inversely proportional to complexity.

- Environmental Problems: A function of specific mechanical design problems for operation in the space environment. It does not indicate the degree of the problem nor does it indicate if the problem can be solved; it just displays the problem.

- Relative Reliability of System: Reliability and complexity are interconnected to a large degree. The more complex piston - cylinder drive concept, for instance, would be less reliable because of the greater number of supporting controls components and systems.

- System Design Problems: The most obvious system design problems associated with the individual power drive concepts are identified for comparison. The problems range from controls redundancy problems associated with the use of LO_2/LH_2 products of combustion as a power media.

- Nozzle Locking: It has been established that, during periods of thrusting, the nozzle extension must be firmly held in a fixed, extended, aligned, and sealed position. To accomplish this task, several techniques could be employed. The locking device could be designed into the actuation power device or into the mechanical power transmission system or, as a third choice, a separate locking concept could be fixed to the nozzle

III, B, Tradeoff Studies (cont.)

extension. With tape, chain, or cable power transmission systems, it is obvious that separate locking devices are required.

6. Summary of Tradeoff Conclusions and Design Recommendations

a. Summary of Tradeoff Conclusions

(1) General

This section serves to summarize the significant conclusions and design recommendations concluded from the tradeoff studies. The design recommendations presented are considered as optimum within the limits and guidelines established for conduct of the studies.

(2) Space Environment

Metal parts which slide or roll on each other should be made of insoluble pairs and/or lubricated with a solid bonded dry lubricant to prevent the possibility of cold welding in the space vacuum environment. Space lubricants have been developed and are commercially available (see Sections III, B, 2, c, (a) and III, B, 5, C, 3, (c) and Table III).

Radiation effects on organics and polymers should be considered when choosing materials for seal designs.

(3) Nozzle Extension Design

The nozzle extension should be of a radiation cooled design. It is considered as the lightest in weight, higher in reliability (because of its simplicity of construction), relative ease of development, least in total cost, and is easier to fabricate than the transpiration, tube bundle and ablative concepts considered for possible use as a deployable nozzle extension.

III, B, Tradeoff Studies (cont.)

It is recommended that the nozzle extension (possible material C-103) be coated with silicide and/or aluminide coatings to prolong resistance to possible fatigue, grain growth and grain boundary layer contamination.

The nozzle should be designed for a minimum of discontinuity at the interface between the fixed portion of the nozzle and the movable nozzle extension. That is, that the nozzle contour should be as continuous as possible, particularly at the interface, and that rapid divergent or convergent steps be eliminated to insure as continuous a contour as possible. These step conditions create undesireable heat loads that could result in destruction of the nozzle extension.

In selection of the nozzle extension attachment area ratio, consideration must be given to the specific thermal and operating condition of the engine and nozzle contour. It may be impossible to effect a joint at lower area ratios because of the normal heat flux at that station. The material may be the limiting factor. If the requirement is that the attachment area ratio be small, then consideration should be given to supplimental cooling in and around the extension attachment joint (Figure 29).

(4) Seal Design

Gasket face seals eliminate the problems of clearance, compression, and seal interface concentricity associated with piston or diameter seals (Figure 29). The seal should be elastomeric to provide good sealing characteristics for low compression forces and because of the low differential pressure for which it must seal. Further, the elastomeric seal should be located in a cool (or cooled) area. Leakage rates of the specific seal design must be determined by testing.

III, B, Tradeoff Studies (cont.)

(5) Nozzle Extension Translation System

The actuator for nozzle deployment and retraction should be electrically powered.

The nozzle guide, support, power transmission and nozzle locking features should be incorporated into one simple mechanism for simplicity, reliability, ease of development and low weight.

The use of lubricants on the power transmission system and mating moving parts is required and restricted to commercially available, proven solid bonded lubricants.

Nozzle locking requirements such as (1) maintaining the extension in a fixed firing position, (2) power drive fail safe, (3) lock and unlock upon command, (4) unaffected by operating environment, (5) locking redundancy, and (6) using the same locking device or technique for both the nozzle stowed or extended position, are satisfied by incorporating the locking device with the nozzle power transmission system, as shown in Figures 41 and 42.

(6) Nozzle Alignment

Nozzle alignment should be repeatable, unaffected by the concentricity of mating parts, unaffected by the extreme operating temperature environment and independent of the power transmission system (Figure 29).

b. Design Recommendations

(1) General

In view of the preceding summary of conclusions, it becomes obvious that (1) the nozzle extension should be radiation cooled, (2) the

III, B, Tradeoff Studies (cont.)

seal should be a face seal, and (3) the nozzle, actuator, guide, support, power transmission system, and nozzle locking features should all be designed into one simple mechanism. The techniques felt to most satisfy the above summary of tradeoff conclusions is displayed in Figures 29, 41 and 42.

(2) Nozzle Extension Cooling Scheme

As stated above, it is recommended that the nozzle extension be radiation cooled and possibly fabricated of C-103. It is also recommended that the extension be coated with a silicide or aluminide coating to prolong resistance to fatigue, grain growth, and grain boundary layer contamination.

The nozzle should be designed for a minimum of discontinuity at the interface between the fixed portion of the nozzle and the movable nozzle extension. That is, that the nozzle contour should be as continuous as possible, particularly at the interface and that rapid divergent or convergent steps be eliminated to ensure as continuous a contour as possible. "Steps" create undesirable heat loads that could damage the nozzle extension and possibly result in degradation of nozzle performance ($I_{sp\ (del)}$).

In selecting the nozzle extension attachment area ratio, consideration must be given to the specific thermal and operating condition of the engine and nozzle contour. It may be impossible to effect a joint at lower area ratios because of the heat flux at that station. If such is the case, consideration should be given to supplemental cooling in and around the extension attachment joint and of a portion of the nozzle extension itself (Figure 29).

III, B, Tradeoff Studies (cont.)

(3) Nozzle Extension Sealing

The tradeoff studies concluded that the nozzle extension joint should be sealed by an elastomeric gasket type face seal. The sealing concept satisfying these recommendations is shown in Figure 29.

The joint is sealed by an elastomeric face seal in the form of a silicone rubber gasket. The gasket seals both from the mounting ring to the flange brazed to the tube bundle and from the extension to the mounting ring. A positive seal is assured by serrations machined in the surfaces of all parts that contact the seal. The amount of gasket "crush" between extension and mount ring is controlled by interlocking lips.

The seal is located in a cool area well removed from the heat input to the extension. A thermal analysis must be performed to make sure that this region does not reach a steady-state temperature of more than 600°F to 700°F without benefit of a secondary coolant.

To replace the seal, the extension is fully retracted and unbolted from the mounting ring. The seal is then cut and removed. The new seal is stretched over the fixed portion of the nozzle, inserted in the flange, and the bolts replaced. On small diameters, it may be necessary to split the seal on the bias and to reseal on assembly with a silicone rubber adhesive.

This sealing technique is both positive and insensitive to machining tolerances. It does required that the translation system lock or hold the seal in compression during engine firing modes.

(4) Proposed Nozzle Deployment and Retraction System

The tradeoff studies have identified the optimum

III, B, Tradeoff Studies (cont.)

translation system as that system which incorporates into one simple design the nozzle power drive, guide, support, power transmission, and nozzle locking device. Such a system is shown in Figures 41 and 42.

(a) Description

The concept consists of three (for stability) electrically motor-driven, tubular steel jack screws located 120° apart around the fixed portion of the nozzle. A single jack screw is shown in Figure 41.

The 28 volt power drive motors have integral spur reduction gear sets. The mounting flange is also integral with the housing. The motor is mounted to the engine structure by means of an elastomeric, flexible, load cell device similar to those used to mount engines in aircraft or automobiles. This type of mount allows for thermal expansion and contraction, minimizing undesirable loads on the translation system.

The hollow steel screw is mounted in an elastomeric supported sleeve bearing located in the brazed flange fixed to the tube bundle (Figure 42). The other end of the threaded shaft is rigidly connected to the output shaft of the motor gearbox, which provides a simple support at both ends of the shaft.

The moving extension is attached to and supported by the mounting ring which has integral threaded lugs or nuts through which the threaded shafts pass. Thus, the extension is guided, supported, and translated by the threaded shaft.

To maintain shaft synchronization during operation and to provide for redundancy in case of a single motor failure, each shaft has incorporated a pulley for use with a timing belt which passes around all the shafts. This represents the basic translation system.

III, B, Tradeoff Studies (cont.)

(b) System Redundancy

The tradeoff studies recommended that a redundant system be added to retract the extension in case of complete power failure. Looking at the problem realisitically, it is difficult to imagine a situation in which total craft power is lost and the urgency of the situation is not far greater than that of retracting a nozzle extension. Additionally, since the circuitry to the drive motors is probably contained in the same harness as the circuitry for engine control, because of the location, it is difficult to imagine an accidental occurrence disrupting power to the drive motors without disrupting engine operation--a far greater emergency than an extended nozzle. The situation seems to then concern itself with assuring reliable operation as long as power is available.

It is likely that all of the mechanical components can be designed to function reliably and the problem, therefore, is concerned with an electrical feature, such as an open circuit, in the windings or coils of one of the motors. This failure mode is precluded by giving any two motors the capability of retracting the system, merely rotating the third motor armature and shaft by means of the synchronizing belt.

(c) Motor Drive Design Requirements

Assuming that the extension is translated only during nonfiring periods, what then are the loads that the translation system must withstand and overcome?

The first load consideration is the friction forces due to turning the shaft in the support nuts and the bearings and/or bushings. Assuming that the shafting has been design so that it is structurally capable of supporting the extension against external acceleration loads, these

III, B, Tradeoff Studies (cont.)

loads merely increase the resistance torque due to friction. If the threaded shaft is made of steel and the ring mount and nuts of titanium and the surface of the threaded shaft is treated with a dry powder lubricant such as described in Section III, B, 2, c, the friction loads can be reduced to a small value.

Recent work in which molybdenum disulfide was placed in the matrix of a pressed and sintered refractory metal has proven to provide an excellent lubricated bushing or wear resistant material (Ref. 6).

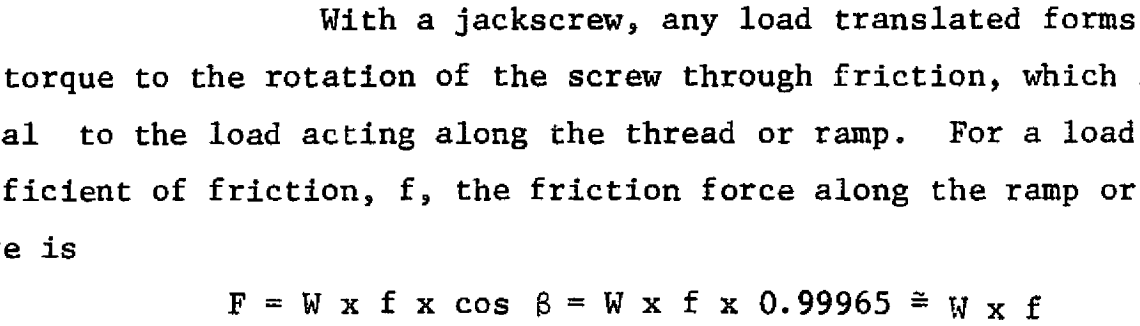
It is possible that threaded inserts made of these materials could be placed in the mounting ring loop to ride the threaded shafts and that the ends of the shafts could be supported in plain bushings of the same material.

It can be appreciated that the largest loads, friction or otherwise, which must be overcome are probably those associated with the vehicle standing on the earth during system checkout--and then primarily if the nozzle happens to be in a horizontal position. It is unlikely that, when the nozzle is being deployed in space, there will be any "g" loads to be overcome and, therefore, the system may have to be designed for the "worst" case of deployment on earth.

The force available with the system is high. For instance, a 1/5 HP motor with a 5:1 spur gear reduction delivers about 5 lb-in. of torque at 500 rpm continuously at 28 vdc. If a threaded shaft having a 1-12 UNF thread is attached to it, the motor and shaft can move about 200 lb at a speed of about 40 in./min. This can be determined as follows.

For the jackscrew design illustrated, the diameter is 1 in. and there are 12 threads to the inch. For one revolution, then the axial motion of the load is 1/12 of an inch or 0.0833 in., having ridden up a ramp 1 in. or 3.1416 in. length.

III, B, Tradeoff Studies (cont.)



The tan of $\beta = 0.0833/3.1416 = 0.0265$ and therefore $\beta \cong 1.5°$ = jackscrew lead angle.

With a jackscrew, any load translated forms a resisting torque to the rotation of the screw through friction, which is proportional to the load acting along the thread or ramp. For a load, W, and a coefficient of friction, f, the friction force along the ramp or thread shown above is

$$F = W \times f \times \cos \beta = W \times f \times 0.99965 \cong W \times f$$

This force is located on a 1/2 in. radius and therefore the resisting torque is W x f/2 lb in.

The torque available in the electric motor for the system illustrated was 5 lb in. and f for the molybdenum disulfide impregnated refractory metal sintered bearings suggested for use if 0.05 in vacuum or air, at room temperature or up to 2200°F. Therefore, the weight or load that one jackscrew can move is slightly less than the weight found by the equation:

$$\text{Friction Torque} = \text{Motor Torque} = \frac{W \times f}{2}$$

$$W = \frac{\text{motor torque} \times 2}{f} = \frac{5 \times 2}{0.05} \text{ lb}$$

$$= 200 \text{ lb}$$

Therefore, the three jackscrew translation systems proposed would be capable of lifting slightly less than 600 lb. This is for the "worst case" ground checkout since translation in space would be for essentially a no-load condition.

The final question is whether or not the jackscrew system is capable of holding the extension in place against thrust loads without keeping the motor energized. If the inertia of the system is neglected, we are really asking if the load will slide back down the ramp or thread, causing the jackscrew to rotate.

III, B, Tradeoff Studies (cont.)

It was shown above that the tangent of the equivalent ramp angle for the 1-12 UNF jackscrew illustrated was Tan β = 0.0265. By definition, the coefficient of friction is defined as the tangent of an angle for which a load will just slide down a ramp.

Since Tan^{-1} 0.0265 or 1.5° is less than Tan^{-1} 0.05 or 3°, the load cannot slide and it can be seen that the 1-12 UNF jackscrew with a coefficient of friction of 0.05 can support or hold by friction against any load up to the point where the jackscrew fails.

It can readily be seen that in space, if no "g" loads are present, one motor of a three-system could readily rotate all three shafts and move the largest extension. It is only in a gravity field that motor size to accomplish translation becomes an important criterion.

It is assumed that the motor selected is suitable for vacuum operation as regards bearings, arcing, etc. If arcing of brushes is a severe problem, the use of synchronous ac motors should be investigated.

(d) Locking

As shown above, the system is self-locking; that is, there is enough friction present in the system to prevent firing loads acting upon the extension in an axial direction to rotate the shafts, gears, armatures, etc. Travel is controlled in each direction by limit switches which open the motor circuit.

Mounting each end of each shaft in an elastomeric holder allows a pretension to be put on the timing belt and also allows the nozzle some radial movement as it centers around the alignment springs. There

is no size limitation to the approach so long as the shafting and bushings can support the extension and the motors can move it in at least a vertical mode on the ground for checkout purposes and maintenance.

It should be remembered that the extension is best supported near the ends of the shaft, that is, in the retracted or extended position. In the center of travel, especially in a "g" field, the nozzle weight can be allowed to sag or cause a slight deflection in the shafting as long as binding does not occur. This is allowed because of the flexible end supports. If sagging or deflection of the shafting is not desirable for any reason, the threaded shaft can be cut and then splined together through a supported bushing whose outer diameter is less than the minimum thread diameter. The nut or lug on the mounting ring can then be slotted to allow it to pass by the intermediate support.

(4) Nozzle Alignment

In view of the established nozzle alignment design requirements that nozzle alignment be repeatable and concise, little affected by mating parts, unaffected by the extreme operating temperature environment, and independent of the power transmission system, it is recommended that the nozzle extension be aligned by a device designed into the chamber-nozzle interface. It is also recommended that the aligning surfaces between fixed and movable portions of the nozzle be as shown in Figure 29. The two alignment springs contained in the cylindrical guide surfaces in conjunction with the suggested seal and nozzle deployment concepts provide for repeatable and accurate nozzle alignment. The springs push radially outward with a uniform force which is sufficient to keep the extension centered about the fixed portion of the nozzle under normal engine loads and operating conditions. The spring force is not so great, however, as to create undue frictional forces which might tend to prevent nozzle extension or retraction. To help reduce the frictional forces, the use of a dry powder or solid bonded lubricant can be employed.

III, B, Tradeoff Studies (cont.)

The guide and support system is designed to be "loose" enough so as to allow the interfacing spring surfaces to accomplish final alignment at the end of nozzle travel. The metal spring is designed to yield slightly during seating and alignment so that the lack of exact concentricity of parts will not be a problem. Finally, even though both the fixed and moving parts should be heated or cooled together in an ideal situation, the cylindrical springs have the ability to compensate for differential temperatures between the mating surfaces, allowing the parts to seat at slightly different longitudinal and radial position.

C. TECHNICAL ANALYSIS

1. Introduction

The technical analysis performed encompassed two major disciplines: (1) performance and gas dynamics, and (2) heat transfer.

Primary emphasis was placed on evaluation of the two nozzle extension cooling concepts (radiation and convection) identified as most promising in the tradeoff studies for a LO_2/LH_2 propellant space engine. The data derived from this effort can be used directly to determine optimum nozzle length and cooling requirements with respect to performance and weight once a mission analysis has been conducted.

The performance analysis established the relationships between nozzle weight, delivered specific impulse, attachment area ratio, and overall area ratio. Consideration was also given to real engine losses, boundary, divergence, injector and film cooling losses.

The thermal analysis placed emphasis on evaluationof heat transfer in the chamber nozzle extension joint area with respect to engine size, chamber pressure and nozzle attachment area ratio, and the prediction of design and cooling requirements in the high heat transfer areas.

III, C, Technical Analysis (cont.)

The technical analysis was to be accomplished by (1) a review of available literature pertaining to heat transfer to the nozzle wall as well as the discontinuities caused by the joint for attachment of the extendable to fixed portion of the nozzle, (2) establishment of study models from the literature review, and (3) comparison of the test results from the White Sands testing effort with the predicted results and an upgrading of the study models to reflect this new data.

As a result of slippage in the schedule at NASA White Sands Test Facility, there was no testing and the study results could not be compared with empirical data. Therefore, the heat transfer studies provide only a summary of existing thermal technology that is applicable to the design of extendable nozzle systems and to indicate those technical areas in which existing data need to be supplemented by development testing. The nozzle performance studies are completed with the exception of identifying the possible performance loss associated with nozzle wall discontinuities. This data also was to have been derived from experimental testing.

2. Performance Analysis

a. General

The objective of the performance analysis was to establish the general relationships between the parameters nozzle weight, delivered specific impulse, attachment area ratio and exit area ratio for an extendable - retractable nozzle extension for space applications. These relationships are defined and presented in the form of parametric design data intended for use by a design engineer during the preliminary design phase of a LO_2/LH_2 space engine employing an extendable - retractable nozzle extension. This task was accomplished by designing and evaluating nozzles for a given engine operating cycle and within specific ranges of design variables. The nozzles were designed using the Rao optimum nozzle design technique and evaluated using standard ICRPG techniques (Ref. 7).

III, C, Technical Analysis (cont.)

The basic data presented is in the form of specific impulse and nozzle weight as a function of overall area ratio. This data is also presented in the form of tradeoff ratio as a function of overall area ratio; tradeoff ratio is defined as $\Delta W/\Delta I_{sp}$, where W is nozzle weight. The parameter "tradeoff ratio" is included here because it is a convenient link between specific vehicle mission characteristics and optimum engine design.

b. Technique of Analysis

In order to examine the overall effects of incorporating an extendable nozzle extension into the design of an otherwise conventional rocket engine, the analysis considered different overall nozzle expansion ratios and attachment ratios (expansion ratio at extendable nozzle flange) for a typical O_2/H_2 engine having the following range of operating parameters:

P_c = 300 psia to 800 psia
F = 5K to 20K
ε = 50:1 to 300:1
minimum attachment ε = 80:1
range of attachment ε_i = 100:1, 140:1 and 180:1
Two thrust chamber designs corresponding to F/P_c ratios of 10 and 20

To accomplish this task, a midpoint or base case design was formulated. This design is shown in Figure 43. The characteristics of operation and the basic values of weight and performance for the design were identified as necessary so they could be used throughout the operating range of interest. The operating characteristics for the midpoint design were as follows:

III, C, Technical Analysis (cont.)

1. Gas generator cycle
2. GO_2/GH_2 propellants at the injector
3. Injector mixture ratio = 6.27
4. Nozzle is regeneratively cooled to the extension attachment point.
5. Turbine exhaust gas used for nozzle coolant

   MR = 1

   $\dot{w}$ = 0.311

   T = 860°R

The secondary gas coolant properties and engine operating conditions are summarized in Table XII.

Nozzle weights were calculated based on nozzle surface areas and estimated weights per unit area. Three different nozzle cooling modes were considered in calculating both nozzle performance and weight. The thrust chamber from the injector to the attachment point was assumed to be regeneratively cooled and weight 0.0204 lb/in.^{2} in all cases. The retractable nozzle extension was assumed to be cooled using turbine exhaust gases either by radiation/film cooling or by dump cooling. The estimate of weight for the radiation and dump-cooled sections was 0.0096 lb/in.^{2} and 0.0164 lb/in.^{2}, respectively. In the case of radiation/film cooling the turbine exhaust gases were assumed to be injected into the main flow at the attachment point. In the case of dump cooling the turbine exhaust gases were used to internally cool the extension via a tube bundle, entering at the attachment point and being exhausted to the atmosphere through a number of small nozzles located at the nozzle exit plane.

c. Method of Analysis

(1) Determination of Nozzle Contours and Weights

The overall nozzle area ratios (ε_o) considered in this study were 80, 140, 180, 240, 280 and 300. For each area ratio, nozzle

III, C, Technical Analysis (cont.)

length ratios (L/L_{min}) of 1.00, 1.25, and 1.50 were designed and analyzed. Furthermore, for each combination of length ratio and area ratio above, nozzles of two different throat radii, 1.28 and 1.81 in., were also considered. These throat radii were calculated assuming thrust to chamber pressure ratios (F/P_c) of 10 and 20, respectively.

$$R_t = \left(\frac{F/P_c}{C_f \pi} \right)^{1/2}$$

The thrust coefficient (C_f) is representative of the approximate range of nozzle area ratios enumerated above. The above geometric parameters defined a total of 30 different basic nozzle configurations.

The ramifications with respect to weight and performance were investigated for attachment area ratios (ε_i) of 100, 140, and 180, where applicable ($\varepsilon_i < \varepsilon_o$). The effects of performance and weight were also considered for the two types of extension cooling mode, i.e., dump cooling and radiation/film cooling. The performance of each nozzle configuration was evaluated at three different chamber pressures: 300, 500, and 1,000 psia. The corresponding nominal thrust levels were 3,000, 5,000, and 10,000 lb for F/P_c = 10, and 6,000, 10,000, and 20,000 lb for F/P_c = 20. In all cases the injector mixture ratio was assumed equal to 6.27.

Some discussion is in order to clarify the parameter "length ratio" (L/L_{min}) used to define nozzle geometry. Length (L) is defined as the absolute axial distance from nozzle throat to exit. The parameter L_{min} is the length, throat to exit, of the "Rao minimum length nozzle", and is unique (within the conditions of this study) for a given overall area ratio and throat radius. In order to define "Rao minimum length nozzle" it is desirable to present some background information. For this, the reader is referred to the schematic plot of Figure 44 which represents various combinations of area ratio and L/R_t for Rao nozzles. By definition (Reference 8), the Rao nozzle produces

III, C, Technical Analysis (cont.)

maximum specific impulse for a given L/R_t and ambient pressure (in this case $P_a = 0$). For this reason, then, the lines of constant I_{sp} are shaped as shown in Figure 44, with a point of infinite slope corresponding to $P_a = 0$.

Consider a series of nozzle configurations of various lengths (L/R_t) with a constant overall area ratio equal to ε as represented by Points A, B, and C in Figure 44. For any length (e.g. L_c/R_t) greater than L_B/R_t, it may be seen from the figure that a decrease in area ratio will result in a <u>decrease</u> in specific impulse. Conversely, for any length (e.g. L_A/R_t) will result in an <u>increase</u> in specific impulse. Therefore, the latter family of nozzles ($L < L_B$) should not be considered since a higher performance could be realized for a given length by reducing area ratio. Thus, L_B/R_t (identical to L_{min}/R_t) is the minimum length which should be considered for the overall area ratio ε. Since the minimum length (L_{min}/R_t)varies with expansion ratio, it is a convenient normalizing parameter when considering nozzles of various lengths and area ratios. It should be noted that it is impertinent to consider nozzle lengths greater than the "Rao minimum length". As indicated in Figure 44, performance increases with length for the constant area ratio ε ($I_{SP_C} > I_{SP_B} > I_{SP_A}$). This effect is due to a reduction in the flow divergence loss as length increases. Thus, performance may generally be increased by increasing either length or area ratio or both.

Nozzle contours were determined through use of the Rao optimum nozzle computer program (Aerojet Program E21207). A constant ratio of specific heats (γ) of 1.22 was selected for use in the computer program as representative of GO_2/GH_2 propellants at a mixture ratio of 6.27 and chamber pressures of 300 to 1000 psia. The radii of curvature of the contour adjacent to the throat plane, upstream and downstream, were taken as $R_u/R_t = 2.0$ and $R_d/R_t = 1.0$, respectively. The Rao minimum length contours were computed by inputting the desired area ratio and P_a = Zero. The contours of lengths 25% and 50% greater than the minimum length were computed by inputting the desired area ratio and length where the minimum lengths are defined in Figure 45.

III, C, Technical Analysis (cont.)

The contour coordinates normalized with throat radius are presented in Table XIII for the stated ranges of area ratio and length ratio (L/L_{min}). Also shown in this table are surface areas from the throat to the given axial location. As noted the surface areas are, however, dimensional corresponding to a throat radius of 1.28 inches. Surface areas may be scaled to represent nozzles of different throat radii using the following relationship:

$$A_s = A_s' \, (R_t/1.28)^2$$

where

A_s' = Surface area ($in.^2$) corresponding to a throat radius of 1.28 inches taken from Table XIII.

A_s = Surface area ($in.^2$) corresponding to throat radius R_t of a geometrically similar nozzle.

As previously mentioned for all nozzles under consideration, the weight per unit area of the regeneratively cooled portion of the nozzle (throat to attachment point) was assumed to be 0.0204 $lb/in.^2$; the weight per unit area of the extension was assumed to be 0.0164 $lb/in.^2$ for the dump cooling mode and 0.0096 $lb/in.^2$ for the combined radiation/film cooling mode.

Nozzle weights for intermediate ratios (as opposed to exit area ratio) are presented in the curves of Figures 46 through 53 for the assumed weights per unit area. Curves are presented for overall area ratios of 140, 180, 240, and 280, each for the two different cooling modes. The branch curves are due to the reduced weight per unit area of the extension. Attachment area ratios of 100, 140, and 180 are shown where appropriate ($\varepsilon_i < \varepsilon_o$). Curves are shown only for R_t = 1.28 in.; however, weights (W) for throat radii other than 1.28 in. may be simply calculated by:

III, C, Technical Analysis (cont.)

$$W = W' \, (R_t/1.28)^2$$

where

W' = Nozzle weight corresponding to a throat radius of 1.28 in.

W = Nozzle weight corresponding to throat radius (R_t) of a geometrically similar nozzle.

(2) Delivered Performance Determination

(a) ODK Computer Program

The delivered performance ($I_{sp(del)}$) for each nozzle configuration was calculated using the ICRPG One-Dimensional Kinetic Nozzle Analysis Computer Program (ODK) (Ref. 1) which is designated Aerojet Program Number #23401 and subtracting the various real engine losses as indicated below.

$$I_{sp(del)} = I_{sp(odk)} - \Delta I_{sp(er/mrd)} - \Delta I_{sp(bl)} - \Delta I_{sp(div)} - \Delta I_{sp(c)}$$

where

$I_{sp(odk)}$ = One-dimensional kinetic vacuum specific impulse based on injector mixture ratio.

$\Delta I_{sp(er/mrd)}$ = Specific impulse loss due to energy release and mixture ratio maldistribution.

$\Delta I_{sp(bl)}$ = Specific impulse loss due to boundary layer effects.

$\Delta I_{sp(div)}$ = Specific impulse loss due to flow divergence at the nozzle exit.

$\Delta I_{sp(c)}$ = Specific impulse loss due to extension cooling.

The theoretical performance value, $I_{sp(odk)}$, in the above equation includes the effect of a 0.6% (by weight) Argon impurity which is normally found in oxygen propellants.

III, C, Technical Analysis (cont.)

(b) Energy Release and Mixture Ratio Maldistribution Loss

This loss is a function of injector/combustion chamber design and for this reason was considered constant. A value equal to 1% of equilibrium performance was chosen as being realistic for injector designs. This loss was included only to make absolute engine performance calculations more realistic. Since this loss is incurred in the combustion chamber and is constant, the absolute magnitude of performance values of this report may be adjusted either up or down to reflect the loss for a specific thrust chamber. However, the tradeoff ratio values resulting from the study will not be affected by this loss.

(c) Boundary Layer Loss

The boundary layer loss results from three effects.

(1) Shear drag and heat transfer at the nozzle wall.

(2) Increased enthalpy of incoming propellants due to heat addition in the regenerative cooling system.

(3) Alteration of nozzle effective expansion ratio due to the boundary layer displacement thickness.

The performance loss due to shear drag and heat transfer was calculated using the ICRPG Turbulent Boundary Layer Reference Program TBL, Ref. 10 (Aerojet Program Number E24204). Since this computer program considers only a constant ratio of specific heats (γ) it was necessary to select a single representative value of γ to approximate the mass flux per unit area (ρV) profile along the nozzle wall for a reacting flow from the injector to the nozzle exit. This was accomplished by first calculating the

III, C, Technical Analysis (cont.)

reacting flow mass flux per unit area profile along the wall using the TDK, Ref.13, computer program and then superimposing upon it mass flux per unit area profiles for various values of constant γ. The reacting flow mass flux distribution was then used to input the TBL program.

In order to calculate the shear drag and heat transfer loss it was necessary to specify a wall temperature distribution. For the regeneratively cooled initial nozzle portion a constant wall temperature of 800°R was assumed. The wall temperature of the extension was assumed to be a constant 1200°R for the dump cooled cases and 2500°R for the combined film and radiation cooled case. The higher temperature of the radiation/film cooled extension resulted in slightly smaller boundary layer loss than for the dump cooled extension.

The heat transfer from the hot boundary layer gases to the regenerative coolant increases the enthalpy of the coolant (propellant) and thus tends to increase delivered specific impulse of the flow outside the boundary layer. The heat transferred to the coolant was calculated using the TBL computer program. The increase in specific impulse was then calculated using the ODK computer program inputting propellant heats of formation which included the heat acquired in the cooling tubes.

The performance loss due to alteration of the effective expansion ratio was calculated using boundary layer displacement thicknesses (δ^*) obtained from the TBL computer program. This loss was found to be small compared to the two previously mentioned components of the boundary layer loss.

(d) Divergence Loss

The divergence loss accounts for nonaxially directed momentum at the nozzle exit and a nonplanar sonic surface. The

III, C, Technical Analysis (cont.)

divergence efficiency (η_{div}) of each nozzle configuration was computed with Aerojet Program E21213, which uses the method of characteristics to evaluate the axisymmetric flow properties.

$$\eta_{div} = I_{sp\ (2\ dim)}/I_{sp(1\ dim)}$$

where

$I_{sp(2\ dim)}$ = Two-dimensional vacuum specific impulse calculated using the method-of-characteristics

$I_{sp(1\ dim)}$ = One-dimensional vacuum specific impulse

The divergence loss was then calculated from the following relation.

$$\Delta I_{sp(div)} = I_{sp\ (del)} \frac{(1 - \eta_{div})}{\eta_{div}}$$

where

$I_{sp(del)}$ = delivered specific impulse

(3) Cooling Loss

Two different techniques were considered for cooling the nozzle extension: (1) combined film and radiation cooling, and (2) dump cooling. In the case of the film/radiation cooled skirt, coolant is injected into the gas stream approximately parallel to the nozzle wall at the attachment point. In the case of dump cooling, the coolant enters a tube bundle at the attachment point and is ejected at the nozzle exit plane through small nozzles.

It was assumed that the engine utilized a gas generator cycle to provide power to the pumps and that the turbine exhaust was used as the coolant. The mass flow rate from the turbines was estimated to be 0.311 lb/sec for a typical engine with P_c = 1000 psia and F = 10,000 lb. Flow rates at other thrust levels and chamber pressures were calculated assuming that flow rate was directly proportional to both thrust (F) and chamber pressure (P_c).

III, C, Technical Analysis (cont.)

The performance loss ($\Delta I_{sp(c)}$) due to the cooling of the nozzle extension was calculated using the following relationship (Ref. 12).

$$\Delta I_{sp(c)} = I_{sp(inj\ MR)} - \frac{1}{\dot{w}_{inj} + \dot{w}_c} \left(I_{sp(inj\ MR)} \times \dot{w}_{inj} + I_{sp(c)} \times \dot{w}_c\right)$$

where

$I_{sp(inj\ MR)}$ = Equilibrium one-dimensional vacuum specific impulse based on the effective nozzle expansion ratio and the injector mixture ratio.

$I_{sp(c)}$ = Equilibrium one-dimensional vacuum specific impulse of the coolant

$\dot{w}_{inj}$ = Total (O_2 + H_2) injector mass flow rate

$\dot{w}_c$ = Coolant (gas generator cycle) mass flow rate

The above equation has been generalized to apply to both modes of cooling the extension. In the case of film cooling it was assumed that the coolant expands isentropically to the nozzle exit pressure and does not mix or exchange energy with the main flow. However, it was assumed to displace the mainstream and thus slightly reduce the main stream expansion ratio (referred to as effective expansion ratio). The dump coolant was assumed to expand to the same exit pressure as the film coolant. Thus, the performance loss for both the film and dump cooling modes were the same except for the relatively small effect of reduction in mainstream expansion ratio in the case of film cooling.

(f) Wall Discontinuity Loss

In a retractable - extendable nozzle there will be a small discontinuity between the extension and the fixed nozzle segments. The magnitude and location of the discontinuity will determine the magnitude of the associated performance loss. Neither analytical techniques nor experimental

data are available for predicting this loss. It is expected, however, that the loss would be small for properly designed joints; consequently, it was assumed equal to zero for this study. For this reason, the validity of this assumption requires verification through experimentation.

d. Discussion of Results

A complete summary of delivered performance values for each nozzle configuration considered in this study may be found in Tables XIV and XV. In addition to delivered performance values, these tables also present theoretical specific impulse and the various losses which were used to calculate delivered performance. These values were derived through use of the techniques explained in the previous section. The performance values were computed for an attachment area ratio (ε_i) of 100 for each overall area ratio (ε_o). They may be adjusted for the samll change in performance caused by use of a different attachment area ratio. Figures 54 through 59 are plots of delivered performance versus overall area ratio for the combinations of throat radii of 1.28 and 1.81 inches and P_c's of 300, 500, and 1000 psia.

The main study tradeoff to be evaluated was nozzle length. As the nozzle length is increased for a constant overall area ratio, the divergence loss is reduced. This performance gain must be traded off with the increase in nozzle weight associated with lengthening the nozzle. The length tradeoff ratio was determined in the following manner. Weights for nozzles with radiation/film cooled extensions and attachment area ratios of 100 were found from end points in Figures 46, 48, 50 and 52. The weight of each nozzle was plotted against its corresponding delivered specific impulse. The tradeoff ratios were then determined by calculating the slopes on the weight-versus-performance curves at each overall area ratio. Curves of length tradeoff ratio versus overall area ratio are provided for all combinations of throat radii of 1.28 and 1.81 inches and P_c's of 300, 500, and 1000 psia in Figures 60 through 65. If, for a given system, extension weight per unit area values differ from those assumed for the radiation/film cooled extension (0.0096 lb/in.^{2}),

III, C, Technical Analysis (cont.)

the tradeoff ratios presented need only be ratioed to account for the new value.

The tradeoff ratio curves are intended for use in nozzle optimization. To aid in understanding how these curves and all other data included may be used in designing an optimum rocket nozzle, a few sample techniques are presented. For example, to determine absolute nozzle lengths, the tradeoff ratio versus area ratio curve can be plotted as a tradeoff ratio versus length curve with lines of constant overall area ratio. These relationships are depicted in Figure 66 for the example case of P_c = 1000 and throat radius equal to 1.28 inches. The lengths were determined by multiplying the length ratio value for a particular area ratio from Table XIII by the value for throat radius. A plot of delivered specific impulse versus length was constructed for constant overall area ratio from the delivered specific impulse curves of Figures 54 through 59. This curve is shown in Figure 67. Figures 66 and 67 were combined to form the plot of area ratio versus length of Figure 68. Lines of constant tradeoff ratio and lines of constant performance are shown on this plot. This curve is then used to determine the area ratio and length of the optimum nozzle for a given system tradeoff ratio. It should be pointed out that the delivered specific impulse data shows that, in general, increasing the nozzle length beyond approximately one and one half times the Raominimum length would not benefit overall vehicle performance. That is, the small increase in performance with increased nozzle length would be more than offset by the increased nozzle weight.

The type of nozzle extension cooling selected for a given system affects the weight of the nozzle configuration under consideration. Since a film radiation-cooled extension provides the greater weight savings, when compared to dump cooling of the extension, it is necessary to determine if there are performance penalties which would negate this advantage. The model described

III, C, Technical Analysis (cont.)

previously for predicting the performance loss associated with cooling the extension indicates that the losses for the two cooling modes are very nearly equal. The film cooling mode tends to produce a slightly greater loss due to the fact that the coolant displaces the main flow reducing the main flow effective area ratio. However, this performance reduction is approximately offset by the slightly greater boundary layer loss due to the lower wall temperatures associated with the dump cooling mode. This, then, indicates a net advantage of for the radiation/film cooling mode as compared to the dump cooling mode due to the reduced weight of the former. It should be noted that this analysis considered only the performance aspects of cooling the extension. Heat transfer analysis would be required to verify the adequacy of the flow rates for cooling the extension. It was merely assumed that all the available turbine exhaust products were utilized for cooling, whether dump cooling or film cooling.

The next question to be considered was optimum location of the extension attachment point. The primary considerations associated with selecting the extension attachment point are cooling and packaging. The minimum attachment area ratio considered was 100 to insure that the extension wall at the attachment point would be at a temperature low enough to permit adequate cooling by radiation/film cooling. From a weight standpoint it is obvious that the closer to the throat that the extendable nozzle is attached, the lighter the complete nozzle assembly. Nozzle performance is slightly affected by attachment point location due to heat transfer to the nozzle wall. One of the basic assumptions in this study was that the regeneratively cooled region extended to the attachment point. Thus, heat lost to the regenerative coolant would be recycled to the combustion chamber, minimizing the performance loss; whereas, heat lost to the radiation/film cooled extension is non-recoverable.

One of the extension attachment point tradeoff ratios was the weight gain due to a change in attachment area ratio divided by the performance gain associated with this change. This tradeoff ratio for all study configurations is shown in Table XVI. If the mission tradeoff ratio for

III, C, Technical Analysis (cont.)

a given system is higher than the value listed in Table XVI, it is advantageous to extend the attachment point to a higher area ratio. If envelope considerations limit the maximum attachment area ratio of a configuration under consideration, Table XVI will aid in determining if there will be a performance loss associated with this limitation.

Two different throat radii were used for all study combinations of P_c, overall area ratio, and length ratio. Tables XIV and XV, for systems if similar P_c, area ratio and length ratio, show performance differences attributable solely to a change in throat radius. With an increase in throat radius, there is both a performance gain and a weight gain due to increasing the nozzle surface area. For the two throat radii considered, tradeoff ratio was defined as the change in nozzle weight divided by the change in performance attributable to the throat radius change. Values for this tradeoff ratio are shown in Table XVII.

For each nozzle configuration delivered performance was evaluated for three different chamber pressures: 300, 500 and 1000 psia. Tables XIV and XV show specific impulse increase due to an increasing P_c. This performance gain must be balanced against possible weight gains. The weight variations with varied P_c are due primarily to pump and turbine hardware and were not evaluated in this study.

e. Summary and Conclusions

Estimated performance and weight values have been presented for a wide range of nozzle design parameters including overall area ratio, attachment area ratio, throat-to-exit length, thrust level, and chamber pressure. The primary influences on both nozzle performance and weight are due to nozzle overall area ratio and length. Nozzle performance increases with length and overall area ratio; however, at very high area ratios a unit increase in specific impulse with area ratio is accomplished by a larger increase in nozzle weight. Thus, there is an optimum length and area ratio beyond which

III, C, Technical Analysis (cont.)

the increase in weight more than offsets the small increase in nozzle performance. The object of this study was to provide data regarding this effect and other nozzle design tradeoffs to facilitate systems analyses. In this regard the basic data is also presented in the form of tradeoff ratio ($\Delta W/\Delta I_{sp}$) versus overall area ratio for three different nozzle length ratios.

In addition to the primary nozzle design parameters of length and area ratio, several other parameters also impact the nozzle optimization. The attachment area ratio has a small effect on delivered specific impulse but a significant effect on nozzle weight. Considering only nozzle weight and performance effects, it is desirable to have a small attachment area ratio due to the weight savings associated with the low weight per unit area of the extension. Similarly, the method of cooling the extension, either dump or radiation/film cooling, has a negligible effect on performance but significant effect on weight.

Based on this study, which considers only performance and weight, the radiation/film cooling mode is superior to the dump cooling mode due to the greater weight of the latter.

Chamber pressure has a small effect on performance in that the theoretical specific impulse increases only slightly with chamber pressure. The influence of chamber pressure on engine weight was, however, not evaluated since it is due primarily to effects other than those associated with the nozzle (e.g. gas generator, pumps, turbine). Increasing throat radius for a constant chamber pressure and nozzle geometry results in only a very small increase in delivered performance. The nozzle weight increases proportionally to the square of the throat radius.

III, C, Technical Analysis (cont.)

The absolute magnitudes of the specific impulse and weight values presented in this study are, of course, subject to the stated assumptions. The performance losses which were calculated for each configuration are included for reference in the performance data of Tables XIV and XV. The specific impulse for a given engine system which deviates from the assumed system may then be calculated by modifying the various losses as needed.

The nozzle weights also may be simply recalculated to reflect structural characteristics which are different from those assumed in the study. For this purpose nozzle surface areas as a function of distance from the throat are included in Table XIII.

3. Thermal Analysis

a. Introduction

The objective of the thermal analysis study effort was to provide a summary of existing thermal technology which is applicable to the design of extendable nozzle systems and to indicate those technical areas in which existing data need to be supplemented by development testing.

The heat transfer to the walls of rocket engines in the absence of mass transfer is well understood and adequate correlations exist for the film coefficient. An extendable nozzle system differs from the usual rocket engine system by the requirement for a joint in the supersonic portion of the nozzle so that a part of the nozzle can be retracted. The joint results in a discontinuity of the nozzle wall contour which disturbs the boundary layer flow and thus modifies the heat transfer. Analytical solutions do not exist for the flow and heat transfer characteristics at such discontinuities. Only limited experimental data for such configurations exist; consequently, general empirical correlations also are unavailable. The data which do exist can be

III, C, Technical Analysis (cont.)

used to establish limits for the expected heat transfer coefficient; however, these limits are so broad that the resulting engine design may be penalized by the need to overdesign the cooling system.

The heat flux limits which are established for wall discontinuities are given as the ratio of the heat transfer coefficient to the heat transfer coefficient for a smooth wall. Thus, parametric smooth wall heat transfer data is provided for use in design studies.

b. Thermal Design Criteria

(1) Nozzle Wall Heat Transfer

The thermal design of an extendable nozzle requires that the heat flux to nozzle wall be established for both the smooth wall portions and at the discontinuity caused by the joint for attachment of the extendable portion to the fixed part of the nozzle. The heat flux to the smooth wall portions of the nozzle can be established with good reliability using existing film coefficient correlations. The accuracy of these methods has been verified in the course of development of many liquid propellant rocket engines.

The heat flux in the attachment region must be estimated using the limited amount of experimental data which exists for supersonic flow over cavities. These data have been referenced to the smooth wall heat transfer as a means of correlation. Thus, the smooth wall heat transfer coefficient also is used in establishing the heat transfer to the joint or cavity flow regions of the extendable nozzle.

Heat transfer from the hot exhaust gas to the nozzle wall occurs mainly by convection. The nozzle wall usually is at some temperature below the mainstream gas temperature, which results in a temperature differential across the nozzle wall boundary layer. This temperature gradient produces a transfer of heat from the hot gas to the nozzle wall. In addition,

III, C, Technical Analysis (cont.)

the high temperature exhaust gas will radiate heat to the nozzle wall. Gas radiation is not as well understood as simple convection, but is known to be a second-order effect for LO_2/LH_2 propellants and usually may be neglected in design calculations.

The convective heat transfer rate per unit area, Q_c, from the combustion gases to the nozzle wall is predicted using the familiar Newton's Law equation:

$$Q_c = h_g \, (T_r - T_{wg}) \qquad \text{(Eq 1)}$$

In this equation, h_g is the hot gas film coefficient and T_r is the gas recovery temperature. The chamber wall temperature, T_{wg}, will depend on the method of cooling the wall, the wall thermal properties, and other factors.

The recover temperature is calculated using Equation 2.

$$T_r = \eta^2 \, [T_s + Pr_s^{1/3} \, (T_o - T_s)] \qquad \text{(Eq 2)}$$

$$\eta = \frac{c^*_{chamber}}{c^*_{theo}}$$

The combustion efficiency, also known as the c* efficiency, is calculated as the square root of the ratio of engine c* to theoretical c*. The stagnation temperature or flame temperature, T_o, is the theoretical combustion temperature of propellants at the combustion temperature of propellants at the combustion chamber pressure and injector mixture ratio. T_o is obtained from thermochemical calculations, which include the effect of pressure and temperature on the equilibrium chemical composition of the gases. The gas stream static temperature, T_s, usually is calculated assuming isentropic gas flow with shifting chemical equilibrium. The Prandtl number (Pr) is relatively insensitive to pressure and temperature and may be evaluated at local conditions. Equation 2 is applicable only to the turbulent flow in the expansion region of thrust chambers.

III, C, Technical Analysis (cont.)

Many investigators have attempted to correlate data for the hot gas film coefficient in rocket engine environments and, as a result, a number of h_g correlations are in general use. The correlation recommended for use in the smooth contour region of extendable nozzles is the simplified form Bartz equation (Eq 3) with a modification to account for two-dimensional gas flow effects in the expansion region of the nozzle.

$$h_g = \frac{0.026}{D_c 0.2} \left[\frac{\mu^{0.2} C_p}{Pr^{0.6}}\right]_f (\rho v)^{0.8} \left(\frac{T_{2-d}}{T_f}\right)^{0.8} \qquad \text{(Eq 3)}$$

and

$$T_f = 0.5 (T_r + T_w) \qquad \text{(Eq 4)}$$

In Equation 3, the two-dimensional mass velocity, $(\rho v)_{2-D}$, has been substituted for the one-dimensional mass velocity employed by Bartz. This modification results in an h_g prediction and convective heat flux that is as much as 30% higher than predictions using the one-dimensional Bartz equation. The temperature ratio accounts for the gas density gradient in the thermal boundary layer. The improved correlation obtained by inclusion of the two-dimensional mass velocity term in Equation 3 has been well substantiated by rocket engine test data.

The Bartz film coefficient correlation has been used to prepare a parametric plot of the smooth wall film coefficient for the range of parameters of interest in this design study. The values of the parameters or range of parameters for which the parametric data have been prepared are: propellants LO_2/LH_2, MR = 6.0, chamber pressure 200 to 800 psia, area ratio 50 to 300, and thrust 5K to 20K lb.

The film coefficient is obtained from Figure 69 using the values of area ratio, chamber pressure, and thrust for a particular case. The factor $(F/P_c)^{0.1}$, which appears in the ordinate, is a scale factor to account for the variation of nozzle size. The correlation has been found to

III, C, Technical Analysis (cont.)

be most accurate when the gas properties are evaluated at the film temperature, $T_f = (T_r + T_w)/2$, which is defined as the arithmetic mean temperature between the free-stream recovery temperature, T_r, and the wall temperature, T_w. In order to accomplish this correction, the film coefficient for bulk conditions, obtained from Figure 69, is multiplied by the ratio of the DB factor for the film temperature to the DB factor for bulk conditions. The DB factor is defined by the following equation:

$$DB = 0.026 \frac{C_p \mu^{0.2}}{Pr^{0.6}} \left(\frac{4}{\pi}\right)^{.8}$$

which contains the fluid property terms from Equation 3 that are a function of temperature. The recovery temperature is calculated using Equation 2 with T_s determined from Figures 70 and 71. The DB factors corresponding to film and bulk temperatures are obtained from Figure 72.

(2) Attachment Region Heating

The joint between the fixed and extendable portions of the nozzle results in a discontinuity in the nozzle wall contour. The discontinuity will cause some disturbance of the boundary layer flow and if the size of the discontinuity is much larger than the boundary layer thickness the main flow will be affected also. Small discontinuities which affect only the boundary layer will have a relatively small effect on the heat transfer, but will result in increased heat flux over that for a smooth wall. Large discontinuities will cause boundary layer flow separation at the upstream edge of the discontinuity followed by reattachment of the flow near the downstream edge. A region of separated flow will exist within the cavity of the wall discontinuity. The heat transfer is reduced in the separated flow region, but at the point of flow reattachment the heat transfer is increased by a factor from 1 to 3 times the flux for a smooth wall.

III, C, Technical Analysis (cont.)

The heat transfer mechanism within cavities, such as those associated with the nozzle wall joint, is very complex and insufficient data exist to permit a correction to be developed which includes the effect of all pertinent variables. However, the available data can be used to establish limits for the maximum heat flux to be encountered within a cavity. The variables which have a significant effect on the heat transfer include the size of the cavity relative to the approaching boundary layer thickness, the Mach number of the approach flow, the length to depth ratio of the cavity and the shape of the cavity in the vicinity of the reattachment point.

A typical extendable nozzle attachment point wall discontinuity with the associated flow field is illustrated in Figure 73. Several general configurations of wall discontinuity for which heat transfer data are available and which bear similarities to the extendable nozzle joint configuration also are shown in Figure 73. The extendable nozzle wall discontinuity is most nearly like the open cavity shown on Figure 74.

It is reported by Nestler (Ref 13) that the maximum heat flux for open cavity flow occurs near the corner of the downstream edge of the cavity. The heat transfer coefficient referenced to the value for undisturbed flow is shown plotted in Figure 75 as a function of distance down the downstream face. Only data for two approach flow Mach numbers, 6.3 and 8.5, are given; however, data of Holloway, et al., Burbank, et al., and Gadd, et al., (Ref. 14, 15 and 16) show that the relative heat flux for flow over forward facing steps is lower for lower Mach numbers (see Figure 75). Thus, the data of Nestler can be used to establish an upper limit for the heat flux amplification in rectangular cavities, since the Mach number at the extendable nozzle attachment point generally will be less than 8.5.

III, C, Technical Analysis (cont.)

The wall cavities which occur at the joint between the extendable and fixed portions of the nozzle will not be rectangular. The main difference is that the actual cavity will have a wedge rather than a rectangular step at the downstream edge. A comparison of the actual cavity to an equivalent rectangular one is shown in Figure 76. The effect of the ramp will be to reduce both the pressure rise and the heat flux at the point of flow reattachment. Charwat (Ref 17) presents data at low Mach numbers for a cavity having a wedge downstream face. The data show a marked reduction in average heat flux in the vicinity of the flow reattachment point.

At the present time, insufficient data exist to accurately define the maximum heat transfer coefficient which will occur within a cavity of the extendable nozzle type for an arbitary configuration and Mach number. However, it is possible to place an upper limit on the relative heat transfer coefficient by using the rectangular cavity data. Thus, a conservative estimate for the heat flux is obtained. This limit is estimated to be 3.0 times the heat transfer coefficient for a smooth wall (see Figure 74).

The heat flux within the separated flow region is also of interest, since some cooling may be required in the joint region of the cavity as well as at the point of maximum heat flux. Generally, the heat transfer coefficient within the separated flow region of the cavity is less than the heat transfer for a smooth surface. A value for the heat transfer coefficient between 0.6 and 0.8 that of the smooth wall value is reported in References 13 and 17. Here again, because of inadequate data, it is necessary to choose the higher value for design purposes.

The increased heat flux at the extendable nozzle joint over that for a smooth wall affects the selection of the area ratio at which a radiation cooled extension can be attached. A radiation cooled nozzle extension is limited, usually, by the temperature and heat flux at the attachment point.

III, C, Technical Analysis (cont.)

Therefore, with a cavity at the attachment point, the limiting attachment area ratio increases to a point at which the smooth wall heat flux is 1/3 the maximum for radiation cooling. This effect can be reduced or eliminated through the use of supplemental film or transpiration cooling to reduce the maximum heat flux.

(3) Cooling Methods

(a) General

Both the extendable nozzle attachment region and extension must be cooled by some means because the adiabatic wall temperature of most rocket systems exceeds the temperature limits of all but the most exotic materials. The simplest cooling method for the nozzle extension is radiation to space. Radiation cooled nozzles are light in weight and have high reliability because of the passive cooling method. The maximum heat flux for use of radiation cooled nozzles is set by the temperature limit of the material, thus supplemental cooling or other methods of cooling may be required for some systems.

The nozzle extension also can be cooled by regenerative or dump cooling systems if the heat flux or other factors prevent the use of radiation cooled extensions. These systems generally will be heavier, but have the advantage that less severe material and environmental problems are encountered.

Film cooling is one of the best methods for supplemental cooling of the nozzle attachment region since the heat flux in the region of separated flow and the heat flux to the nozzle extension at the point of flow attachment is reduced. Cooling methods such as regenerative systems and transpiration cooling require relatively complex flow passages in the joint region and, for this reason, result in increased nozzle weight and complexity.

III, C, Technical Analysis (cont.)

(b) Nozzle Extension Cooling

Convection cooling systems such as regenerative or dump cooling for the nozzle extension are designed using the same methodology as that for the fixed portion of the nozzle. The hot gas film coefficient is accurately predicted by the procedure outlined in Part (1) of this section. For these reasons, convective cooling will not be discussed further.

The most desirable nozzle extension cooling system, conditions permitting, is radiation cooling. This technique is completely passive and results in a mechanically simple system. However, materials selection becomes very important since the nozzle is required to operate at high temperature in a corrosive atmosphere.

The equilibrium wall temperature of a radiation cooled nozzle wall is established by equilibration of the heat flux to the nozzle wall due to convection and the heat flux from the wall due to radiation. In the analysis of this process, the temperature drop across the nozzle wall can be ignored because of the relatively low heat flux and the high conductivity of the metal wall. The axial conduction along the nozzle wall is also neglected because of the small temperature gradient along the wall.

The nozzle wall temperature is calculated by a heat balance on the wall. The radiant heat flux from a unit area element of the nozzle wall is given by:

$$q_{rad} = \Sigma_{all\ i} \mathcal{F}_{Wi} \sigma \ (T_w^4 - T_i^4) \qquad \text{(Eq 5)}$$

III, C, Technical Analysis (cont.)

where $\mathcal{F}_{wi}$ = Surface View Factor

σ = 3.306×10^{-5} Btu/sec-in.^{2}-°R Stefan Boltzman constant

T_w = Wall temperature

T_i = Temperature of surface to which energy is being radiated

It can be shown that energy radiated between any element of the nozzle and any other element may be neglected compared to the energy radiated to space. Simplification of the above expression and assuming a view factor of unity for radiation from the outer surface yields an expression for the energy radiated to space.

$$q_{rad} = (F_o + 1)\ \sigma\ \varepsilon_w\ T_w^4 \qquad \text{(Eq 6)}$$

where

F_o = View factor from inner surface to space

The view factor from the inner surface to space is a function of the nozzle geometry and is shown plotted in Figure 77 as a function of the nozzle area ratio for three overall nozzle area ratios.

At equilibrium the radiant heat flux is equal to the convective heat flux to the nozzle wall. Thus,

$$q_{conv} = h_g\ (T_r - T_w) = q_{rad} = (F_o + 1)\ \sigma\ \varepsilon_w\ T_w^4 \qquad \text{(Eq 7)}$$

or

$$\frac{T_r - T_w}{T_w} = \frac{(F_o + 1)\ \sigma\ \varepsilon_w\ T_w^4}{hg} \qquad \text{(Eq 8)}$$

The equilibrium wall temperature, T_w, is shown plotted in Figure 78 as a function of the right-hand side of Equation 8 and for three values of the recovery temperature.

III, C, Technical Analysis (cont.)

The nozzle wall material most commonly used is silicide-coated columbium alloy (C-103) for high temperatures. Titanium and stainless steel can be used at lower temperatures.

(c) Film Cooling

1 General

Film cooling is a form of mass transfer cooling in which the coolant is introduced on the surface to be cooled through discrete slots or holes. Film cooling is contrasted with transpiration cooling in which the coolant is introduced uniformly over the cooled surface by injection through a porous media. Because of the weight usually associated with the porous wall, transpiration cooling does not appear to be attractive for application to extendable nozzles. Generally, transpiration cooling is better suited to high heat flux applications in which other methods of cooling are inadquate.

Either a gas or a liquid may be used as a film coolant. The coolant is injected in such a manner that a protective layer is formed between the surface to be cooled and the hot gas stream. As the film coolant flows along the wall, it is both heated by the hot gas stream and dispersed by turbulent mixing with the high velocity nozzle flow. The mixing process continues until all of the film coolant is dispersed homogeneously in the high temperature nozzle gas. Additional coolant must be supplied at intervals in order to provide continuous cooling. Because of the relatively large mass of coolant that is required, rocket systems suffer a penalty in specific impulse when film cooling is used as a primary cooling system. Therefore, film cooling usually is employed as a supplement to some other primary means of cooling such as a regenerative system.

III, C, Technical Analysis (cont.)

The simplest film coolant injection design for chamber region cooling consists of a row of fuel or oxidizer film cooling injector orifices that are designed to apply the coolant film directly on the chamber wall downstream of the injector. The film coolant orifices must be small since film cooling rates are required to be low compared to the injector flow in order to minimize performance losses. The orifices also must be located close together in order to ensure complete coverage of the chamber surfaces by the coolant film. When liquid is used as the film coolant, a portion of the filmcooled zone adjacent to the injector will be covered by liquid. The chamber walls in this zone will be at temperatures close to the temperature of the injected coolant. The addition of heat from the chamber gases increases the liquid film temperature and causes the liquid to gasify. Chemical reaction and decomposition of the coolant film promotes the formation of a gas film from the liquid film coolant until the phase change is completed. The process of heat addition and mixing causes the temperature of the coolant film to increase. The ratio of the injection velocity of the film coolant to the mainstream velocity has been found to be an important parameter in determining the effectiveness of film cooling. The effectiveness is maximum when this ratio is near unity, i.e., the velocities of the mainstream and the coolant are equal. This result occurs because the fluid shear between the two streams is minimum for a ratio of one and thus mixing is retarded.

The primary applications of film cooling for the extendable nozzle are as supplemental cooling schemes for the joint region and possibly the extendable portion of the nozzle. Both of these applications differ from rocket combustion chamber cooling by the fact that the mainstream gas flow is supersonic. Only limited experimental work is available for this condition and thus accurate film cooling effectiveness predictions are not possible. In addition, for film cooling at the nozzle attachment point, the film coolant must negotiate some turning and merging with the supersonic mainflow.

III, C, Technical Analysis (cont.)

Both the gas flow and heat transfer are very complex in this region which further complicates the prediction of film cooling effectiveness. What data exist for film cooling in supersonic flows has been obtained for highly idealized configurations in which the coolant has been injected tangentially to the nozzle wall and insufficient data exists to indicate what definite effect such important variables as velocity ratio will have on the film coolant effectiveness. The additional data which are required to provide a sound thermal design must be obtained experimentally.

Although either a gas or a liquid film coolant could be used, the use of a liquid has a number of difficulties which reduce its attractiveness relative to gaseous coolants. These include: (1) coolant injection orifices must be very small in order to obtain uniform distribution of the coolant over the surfaces to be cooled; (2) the performance loss with liquid film cooling in the supersonic nozzle will be significantly greater than with gaseous film cooling; and (3) analytical methods for predicting liquid film cooling effectiveness in the supersonic nozzle are nonexistent. These problems are encountered to a lesser degree when a gaseous film coolant is employed.

2 Analysis

Early subsonic film cooling analyses were generally based on the model of Hatch and Papell (Ref. 18) and Papell (Ref. 19). In order to apply this model to a rocket nozzle geometry, it was necessary to modify the model slightly to account for variations in the nozzle gas mass velocity, since this variation had not been included in the model. More recently, the data of Seban (Ref. 20) of the asymtotic boundary layer model of Stollery and El-Ehwany (Refs. 21 and 22) have been employed to predict film cooling effectiveness in a subsonic gas stream. Recent work done at Aerojet Liquid Rocket Company indicate that a mixing model such as that of Stollery

III, C, Technical Analysis (cont.)

and El-Ehwany provides better accuracy in the film cooling effectiveness range of 0.2 to 0.5. The improvement of the correlation of Hatch and Papell's data which is obtained by using a mixing (entrainment) correlation in this effectiveness range is shown in Figure 79. The effective film coefficient, h_{eff}, which is contained in the abcissa of Figure 79, is defined as

$$h_{eff} = h \left(W_e \frac{Pr_c}{\mu_c}, \frac{U_e}{U_c}\right)^{0.125} f_1 \left(\frac{U_c}{U_e}\right) \qquad \text{(Eq. 9)}$$

where:

h = convective heat transfer coefficient for no film cooling

W_c = coolant flow rate

Pr_c = coolant Prandtl number

μ_c = coolant viscosity

U_e = mainstream edge velocity

U_c = coolant injection velocity

The function, f_1, is such that it is a maximum for a value of the velocity ratio near unity. Thus the effect of velocity ratio on the coolant effectiveness is evident for the case of subsonic flow. The remaining parameters of the abscissa in Figure 79 are

Cp_c Specific heat of the coolant

X Distance from point of injection

X^1 Isothermal length parameter

The limited amount of experimental data for film cooling in a supersonic air stream was obtained from air turbine nozzle experiments conducted at the General Electric Co. (Ref. 23 and 24). Recently, Goldstein, et. al., experimentally investigated film cooling injection

III, C, Technical Analysis (cont.)

from a rearward facing step into a supersonic air stream (Refs. 25 and 26). Zakkay et. al., (Ref. 27) has conducted experiments similar to those of Goldstain but using supersonic coolant injection velocities. The air film cooling data of Reference 25 were correlated using the following equation:

$$\eta \doteq \frac{T_{wa} - T_r}{T_c - T_r} = \left(\frac{15.5}{\xi}\right)^{2.5}, \text{ for } 15.5 < \eta > 39 \qquad \text{(Eq 10)}$$

where $\xi = \left(\frac{x}{h}\right)\left(\frac{T_o}{T_c}\right)\left(\frac{1}{M}\right)^{0.27}$

x = Film cooled length

h = Coolant slot height

T_o = Mainstream gas stagnation temperature

T_c = Coolant supply temperature

M = Ratio of coolant to mainstream mass velocity

T_{wa} = Adiabatic wall temperature

T_r = Free-stream recovery temperature

and $\eta = 1.0$ for $\xi \leq 15.5$ (Eq 11)

The ratio of the coolant injection velocity to mainstream velocity does not appear explicitely in Equation 10, but is contained in the parameter M and, in contrast to the subsonic data, Equation 10 predicts a continuous increase in effectiveness with increased coolant injection velocity if the density is held fixed. This result probably is due to the fact that test data only exist for velocity ratios less than unity and thus the behavior at higher values is unknown. A similar trend has been noted in subsonic film cooling data for velocity ratios less than unity. In this case, a peak effectiveness is observed for velocity ratios slightly greater than one.

No data exist which show the effect of injection angle on the film cooling effectiveness for supersonic film cooling, however, some reduction in effectiveness is to be expected with increasing injection angle in a manner similar to the subsonic case.

III, C, Technical Analysis (cont.)

Although the existing correlations for supersonic film cooling data do not apply to a situation as complex as the flow at the joint between the fixed and extendable portions of the nozzle, it is possible to draw certain conclusions with respect to the design of a film cooling system: (1) the static pressure of the coolant at the point of injection should match the static pressure of the main nozzle flow at the injection point. This will assure minimum disturbance of main flow which will reduce the rate of mixing between the two streams and will result in minimum performance degradation due to disturbance of the main nozzle flow; (2) the coolant should be injected at the highest possible velocity, up to a velocity equal to that of the main flow, consistent with matching of static pressures, and (3) the coolant should be injected in a direction as nearly parallel to the main-stream as possible in order to reduce interaction losses.

The correlation given by Equations 10 and 11 can be used to estimate the film cooling effectiveness, if an effective slot height, h, is used i.e., the equivalent annular slot height for the coolant exit. The predicted effectiveness parameter defines the local adiabatic wall recovery temperature, T_w, which should be used in the Newton's cooling law, i.e.,

$$q = h_g(T_{wa} - T_w)$$

where h_g is the convective film coefficient without film cooling. The heat flux, q, which is predicted in this manner should be regarded as an optimistic estimate since the specific nature of the coolant injection geometry is not considered due to insufficient data.

(d) Prediction of Nozzle Heat Flux

The methods which have been discussed for prediction of smooth wall convective film coefficient, separation-reattachment

III, C, Technical Analysis (cont.)

region heating and film coolant effects on the heat transfer must be combined in order to obtain an estimate for the expected heat flux in the attachment region and the nozzle extension of the extendable nozzle. The smooth wall convective film coefficient is the basis for the method. The peak heat transfer coefficient at the point of flow reattachment is obtained as an amplification to the smooth wall value. Because of limited data, a conservative estimate for the amplification factor should be used. A value equal to 3.0 is recommened.

The effect of film cooling on the nozzle wall heat flux is predicted by means of the film cooling effectiveness parameter, η, which is used to determine the adiabatic wall temperature. The effectiveness parameter is established from existing correlations and is a function of length from the coolant injection point. At each axial station the local adiabatic wall temperature is established and, when combined with the estimate for the convective film coefficient, can be used to estimate the heat flux using Newton's cooling law:

$$q = h\ (3.0)\ \ (T_{wa} - T_w)$$

where:

h	= Smooth wall convective film coefficient
3.0	= Amplication factor for reattachment point
T_{wa}	= Adiabatic wall temperature
T_w	= Cooled wall temperature

III, Discussion (cont.)

D. TEST HARDWARE DESIGN

1. Nozzle Extension

a. Design Considerations

One of the primary purposes of this program was to investigate analytically and to evaluate through appropriate tests the problem areas associated with reattachment of the mainstream fluid flow on a nozzle extension downstream of a rapidly diverging step (Figure 80). In addition, a second purpose was to evaluate the erfect of auxiliary film cooling in this high heat flux region while varying the geometries of the steps and the step heights.

To satisfy this objective, it makes little difference if the nozzle is extendable or expandable or both, since the reattachment area for all is identical when deployed and constitutes only a small axial region.

Indeed, if geometry changes, seals, actuation, guides, and film cooling were not of interest, the joint and reattachment area for the purpose of this program could be an instrumented step groove machined into the ID of a steel exit cone.

The use of a retractable extension, however, does allow study of different step heights and coolant injection as well as evaluation of the other items such as seals and retraction mechanisms.

The design considerations and selected approach for each of the major components of the extendable nozzle test e gine shown in Figure 2 are discussed below.

III, D, Test Hardware Design (cont.)

In order to fulfill the program objectives, the following design criteria for a nozzle extension must be satisfied:

(1) Must be considered a test "tool".

(2) Must be low cost.

(3) Weight not important.

(4) Must provide valid data in reattachment area.

(5) Must evaluate or demonstrate seals and actuation mechanisms (secondary considerations).

(6) Must evaluate different fixed nozzle-to-extension-tip geometries (step heights).

(7) Must evaluate secondary cooling.

(8) Must present a known contour both in fixed and extension sections (rigid).

(9) Need survive only relatively short durations, repeatedly.

b. Selected Approach

All of the above factors lend themselves to the selection of a heavyweight, low cost, steel heat sink nozzle. The test engine for this program (Figure 2) has been designed around such an exit cone. This "tool" meets all of the objectives of this program, and the data gathered and mechanical evaluations performed will be applicable to all design concepts.

A heat-sink extension is one in which sufficient mass (thickness) is provided to absorb heat transferred by conduction from the gas-side surface. Since conduction is considerably faster than radiation, a heat sink is quite effective for short durations. Such a structure could be steel or steel lined with graphite. The duration of firing is limited by the temperature which the material may be allowed to safely reach. Since this type of extension is rigid (i.e., faithfully represents a desired contour) and relatively inexpensive, it is quite suitable for short duration test work.

III, D, Test Hardware Design (cont.)

The extension was made of 347 stainless steel. It has a cylindrical section several inches long so as to put the attachment flange in a cooler area. Nine calorimeters, 24 thermocouples, and 14 pressure taps are used to monitor thermal and pressure conditions throughout the extension for the different test conditions. A "Rao" contour was selected for the entire nozzle assembly and the rigid, heat-sink extension duplicates this contour from an area ratio of approximately 22:1 out to 37:1.

Instrumentation is concentrated in the reattachment locations predicted for the different fixed-nozzle step conditions to be evaluated.

A flange is incorporated at the exit plane to facilitate the use of a sealing fixture to permit pressure checking the entire assembly. The extension is mounted to and positioned by a "slide section" that will be discussed later.

The constant extension thickness of 0.200 in. makes it a rigid "heat sink" design with predictable characteristics. The particular calorimeters used will yield data applicable to radiation cooled and other designs.

2. LEM Thrust Chamber and Modifications

a. Design Considerations

This program required a reliable thrust chamber which could produce low pressure, low mass flow exhaust gas, preferably using O_2/H_2 propellants.

Reliability was a must since the purpose of the program was to evaluate different fixed-to-movable nozzle joint conditions and not a particular thrust chamber design. Therefore, it was advisable to select a chamber design with proven reliability and adapt it for use in this program.

III, D, Test Hardware Design (cont.)

b. Selected Approach

A Lunar Excursion Module (LEM) ascent thrust chamber with all necessary hardware, injectors, valves, etc., was located which was available for use on this program at no cost. It was determined that operating characteristics of the chamber were suitable for the program and that the N_2O_4/AeroZINE 50 propellant system would provide data which could be used for analyzing O_2/H_2 systems. The chamber is also shown in Figure 2. Operating characteristics are as follows:

Chamber pressure	100 psia
Propellants	N_2O_4/A-50
Mixture ratio	1.6
Operating temperature	5610°R
Throat diameter	4.944 in.

The only rework required was refitting the thrust chamber valves and machining the exit portion of the silica phenolic barrel or liner to match the Rao contour selected for the test engine.

3. Chamber - Nozzle Adapter

a. Design Considerations

The chamber - nozzle adapter can also be called a transition section or the fixed portion of the nozzle. Its chief function is to physically bridge the area from thrust chamber to the movable extension and to maintain the desired contour in this region.

III, D, Test Hardware Design (cont.)

In the design of a flightweight engine assembly, this part would probably be eliminated since the thrust chamber would likely be designed to extend out to the fixed-movable interface and could be either regeneratively cooled or ablative in nature. An ablative transition would have the advantage of providing cooling pyrolyzed gases to the reattachment area--an advantage purposely avoided in the test hardware so as not to influence the heat transfer and other data obtained.

The adapter used in the test design represents the nozzle contour from an area ratio of about 3.5:1 to 22:1. Additionally, other factors were considered of prime importance in the design of the test engine adapter section.

Because of the weight of the entire assembly, the adapter must serve as the backbone of the design, supporting all other components and mounting the entire assembly to a mounting system provided by the test facility. Further, it must provide the capability of delivering a secondary cooling flow to the reattachment area for evaluation of this cooling technique. It must also support the guide and actuation systems required to translate the nozzle, and it must serve as a support for the seals necessary to seal the moving and fixed portions. Finally, it should have variable geometry at the end of the fixed portion or tip in order to determine the effect of different fixed-to-movable transition dropoff or step heights.

b. Selected Approach

The adapter design satisfying all of these requirements is shown in Figure 2. Since the inner contour could not be ablative in nature and since no cooling source was available, the design is for a Type 347 stainless steel heat sink.

III, D, Test Hardware Design (cont.)

On the forward end, the LEM chamber is mounted by sixteen 1/4-in. bolts and sealed by a standard O-ring. RTV-60 silicon rubber compound is used to fill any voids remaining at this interface.

On the aft end, the contour blends into the movable nozzle which is bolted to a slide section which, in turn, is supported by bearings on guides mounted to the adapter support gussets. The slide section and guides are discussed in a following section.

These three support gussets transmit the weight of the entire assembly from adapter to mounting flange. Bolted to the mounting flange are the supports for the actuation system. On the OD of the adapter tip and on the forward face of the tip, grooves are machined to support the seals between fixed and moving components. The sealing technique is also discussed in a later section.

Eight 1/2-in. stainless steel tubes feed a manifold in the adapter with nitrogen which is injected supersonically at the tip of the adapter to determine its cooling effects. The injector design is also discussed in the following section. Pressure in the manifold is monitored through two additional tubes, while temperatures in all sealing areas and of the nitrogen in the manifold are monitored by chromel-alumel thermocouples.

Design details of the removable adapter tips are shown in Figure 81. By proper tip removal and replacement, a full contour can be presented to the gas flow in an uncooled configuration and 1/4-in., 1/2-in., and 3/4-in. steps can be provided for testing in nitrogen-cooled or uncooled states.

III, D, Test Hardware Design (cont.)

4. Nozzle Film Coolant Injector

a. Design Considerations

The supersonic injector used for injecting nitrogen coolant into the reattachment area is an integral part of the nozzle - chamber adapter, as mentioned previously. The following design requirements were placed on the injector by heat transfer specialists in order to obtain necessary data:

Capable of supersonic injection.

Integral with removable step rings in adapter tip.

Provide slightly different injection velocity at each step for the same manifold pressure.

Provide nitrogen mass flows from 0.1 to 0.5 lb/sec.

Provide uniform peripheral nitrogen flow around injector diameter. (Groove width to be at least two times web width if discrete nozzles are used.)

A sixth and obvious condition is that the exit pressure of the nitrogen from the groove be equal to or greater than the static pressure of the exhaust gas in the nozzle at the point of injection. It was also decided to inject aft, parallel with the nozzle centerline.

b. Selected Approach

At first, it was decided that an annulus would give the full peripheral coverage desired. Preliminary calculations, however, showed that the machining and concentricity tolerances required to guarantee even distribution of the coolant would be too restrictive. It was therefore decided to make the injector of a number of discrete supersonic nozzles, satisfying the conditions listed above.

III, D, Test Hardware Design (cont.)

Several different numbers of grooves were investigated from 120 to 240. One hundred eighty grooves were decided upon as best satisfying the above conditions, having physical dimensions that could be more easily machined and still not being too numerous.

Appendix D shows the calculations made in determining the exact geometry of the grooves. The 180 resulting two-dimensional nozzles depicted in Figure 82 are located on a mean diameter of 22.086 in. are 0.019 in. deep, have a throat width of 0.215 in. and an exit width of 0.266 in.

Table XVIII lists the relative main nozzle and injector information for the 5 psia heat pressure used to size the grooves for the minimum mass flow of 0.1 lb/sec at the three different tip step heights. The grooves are machined through all removable tips; therefore, injector performance varies as the tips are removed.

III, D, Test Hardware Design (cont.)

The width of the material separating the grooves is about 0.119 in., which satisfies the fifth design consideration, and should provide uniform peripheral coverage.

From the 5 psia minimum, the head pressure can be increased to produce any desired mass flow, although it is expected that 25 psi or 0.5 lb/sec mass flow will be an upper limit (as defined by the heat transfer analysis).

5. Nozzle Deployment and Retraction

There are three separate items to be discussed under the heading of deployment and retraction. They are the actuation system, the guide and support system, and the piece of nozzle hardware that ties the preceding two together, allowing the extension to be mounted and moved. This component has been arbitrarily named the slide section. These three items are discussed in the following paragraphs.

a. Actuation System

(1) Design Considerations

There are probably as many actuation schemes theoretically possible to provide translatory motion to an exit cone as there are designers to design them. They all have at least two things in common--they require a power source and they provide axial motion. There the commonality seems to cease.

The most commonly used sources of power are electric, pneumatic, fluid (hydraulic), and--in the case of one-way travel--springs. Some of the schemes which employ these sources to produce axial movement to an extension were discussed in Section III,B,5,c, together with appropriate design comments.

III, D, Test Hardware Design (cont.)

The system decided upon for an actual application must be based upon the requirements of that application. The physical forces that must be overcome, the length of travel involved, the power sources available, the space available adjacent to the engine assembly, the required time for deployment, whether or not the extension must also be retracted, allowable system weights--all must be evaluated in order to design the actuator best suited for the application.

This program placed the following requirements on an actuator system:

Low cost.
Simple and reliable.
Any power source which would do the job.
12-in. travel.
6 in./sec actuation speed minimum.
Must fit in available test stand space.

(2) Selected Approach

Considering the above requirements, the actuation system for the extendable nozzle test engine was formulated. It was immediately decided that the most simple and reliable system would be that of connecting actuators directly from the movable portion to the fixed portion of the nozzle--thus requiring an actuator with a 12-in. stroke.

Next, the power source was considered. Springs were eliminated since two-way operation was required. Electrical, hydraulic, and air sources were all available in the test facility. Electric actuators were eliminated because of the high cost of units guaranteed for vacuum operation. This left actuators which could be operated either hydraulically or pneumatically.

III, D, Test Hardware Design (cont.)

Since, to keep cost low, no feedback potentiometers or servo-actuators were to be employed, the travel speed of all actuators would have to be orifice matched and controlled. This eliminated a compressible fluid as a motive source and led to the selection of low-cost hydraulic actuators.

It was decided to use three actuators to distribute loads equally about the three rails used in the guide system (discussed later). The actuator would be attached to the main engine mounting flange on the fixed end and attached to the slide section on the rod end as shown in Figure 2. Three Flairline F-1-1/8-12 HC (1-1/8 in. bore, 12 in. stroke, oil-cushioned stops each end), single rod and actuators were decided upon. These actuators can operate on up to 200 psi air or oil; so hydraulic fluid at 175 psi system was selected as the operating fluid. The design of the hydraulic system is shown in Figure 83.

An analysis was then conducted to predict the actuation system operating characteristics. The nozzle was to be fired down and the weight of the moving parts were known to be about 164 lb. It was calculated that, if the nozzle was moving while the engine was running, gas loads on the exit could reach as high as 400 lb, tending to retract. These factors were considered in the analysis, which is attached as Appendix E.

The analysis predicts that all loads can be adequately handled and that orificing is required to limit velocities to the approximate 6 in./sec desired.

b. Guide and Support System

(1) Design Considerations

The guide and support system must function as the name implies--support the moving hardware (in this case, the slide section and exit cone attached to it) at all times under all loads, whether extended or retracted,

III, D, Test Hardware Design (cont.)

and guide it so as to achieve proper radial clearances and alignment when deployed. Equal clearance between fixed and moving nozzle parts is essential to properly seal the nozzle and to ensure there is no physical obstruction to prevent deployment. Proper alignment of the extension is necessary to guarantee thrust vector alignment.

In addition, it is desirable that the guide system have minimum friction characteristics in any position and provide rigid support, preferably without any lash or relative clearances.

As was the case with actuation systems, there are many schemes available to support and guide the moving parts of an extendable nozzle assembly. Also, as with actuation systems, the guide system must finally be designed on the basis of requirements of the specific application.

Roller or ball bearings must be used to support the required loads with minimum friction and must be oriented to support and guide in both transverse planes. Finally, the guide system must be adjustable in the transverse planes to compensate for machining tolerances and normal wear.

An additional specific requirement for this program was that the system be low in cost, implying commercial availability.

(2) Selected Approach

The guide/support system selected for the test nozzle in this program was the Thomson Industries ball bushing system, well noted for low friction, long life service, and rigidity in machinery applications. The rails or guides consist of case hardened, centerless ground steel rods which are mounted to the three support gussets of the chamber/nozzle adapter by bolts

III, D, Test Hardware Design (cont.)

and spacers, allowing shims to be added for final adjustment. The ball bushing is open, permitting the stands of the rail to pass through the longitudinal slot in the bushing.

The bushing is a housing which supports rows of longitudinally recirculating ball bearings which roll between the shaft and the housing, contacting the shaft around 75 to 80% of its circumferential surface. The housing (bushing) is, in turn, held and clamped in the hardware to be moved (slide section and extension).

c. Slide Section

(1) Design Considerations

In any extendable nozzle design, there is generally a piece of hardware that serves four distinct functions:

It holds the bearings or bushings which ride the guides or rails and is, in turn, supported by them.

It is either an integral part of or serves as a fixture to which the extension is mounted and sealed.

It serves as the movable sealing surface for the fixed-to-moving nozzle seals.

It serves as the point of attachment for the actuation system.

In any extendable nozzle, this versatile ring must be designed to transmit all transverse loads on the extension to the guides and all longitudinal loads to the actuation system or to the rails (guides) through a brake or other locking device.

III, D, Test Hardware Design (cont.)

In an extendable nozzle, this versatile ring must be designed to transmit all transverse loads on the extension to the guides and all longitudinal loads to the actuation system or to the rails (guides) through a brake or other locking device.

(2) Selected Approach

In this program, this ring section has been dubbed a slide section, since it does "slide" on the guide rails by means of the roller bushings. As shown in Figure 2, the six roller bushings are securely clamped and locked in three holders welded to the ring section. The holders also have detent bolts mounted in them so that the extension may be securely locked in the fully extended, 4-in. retracted, and fully retracted positions.

The ring section has a large OD flange to which the nozzle is bolted and sealed. A lip on the flange ensures concentricity whenever reassembled and assures that the ID of the slide and extension represents a continuous smooth sealing surface for the seals mounted on the OD of the nozzle/chamber adapter.

A small flange on the ID serves as a sealing surface for the conventional O-ring mounted on the forward-looking face of the adapter. Three threaded blocks are welded to the ring section to accept the rod ends of the hy raulic actuators.

The weight of the components in the test nozzle requires that the slide section be sturdy and, consequently, heavy. For flightweight applications, much lighter sections can be used and may be an integral part of the extension.

III, D, Test Hardware Design (cont.)

d. Seals

(1) Design Considerations

In an extendable nozzle design, there are generally three joints to be sealed. First, where the fixed nozzle portion attaches to the thrust chamber as shown in Figure 84, unless the fixed portion has been especially designed as part of the thrust chamber (also shown), which is desirable if the extension/fixed joint is at a fairly low area ratio. Second, where the extension attaches to the slide section (Figure 85), unless the two parts have been designed to be integral (again, also shown). Finally, between the fixed and movable parts of the nozzle.

The first two joints mentioned can generally be designed using conventional O-ring seals should the design require seals in these areas. The fixed-to-movable seal, however, is required to generally accommodate conditions beyond the capability of standard O-rings, but even these conditions may not be too stringent, depending on proper design and usage.

For instance, it seems illogical to extend or retract the extension while the thrust chamber is operating. Depending on whether the vehicle is in space or in the earth's atmosphere, the actuation forces required could be quite large, which would increase weight of the system. Also, the fixed-to-movable seal becomes a dynamic seal, with an increased chance of leakage and burnthrough. The logical approach is to, at least momentarily, shut down and to reposition the extension before restarting. For such a mode of operation, only minimal actuator loads and a static seal would be required.

III, D, Test Hardware Design (cont.)

Secondly, through proper design techniques, the seal can be kept in a relatively cool area (as was depicted in Figure 14), allowing the possible use of elastomeric seals. It can be readily seen that, if the nozzle can be fully extended and locked before firing and the rest of the design considerations allow the use of an elastomeric O-ring face seal in the cool area as shown, the seal problem of fixed-to-movable nozzle parts has suddenly been eliminated by proper design and usage.

If, however, design considerations require that the seal be of the piston type, located between the OD of the fixed part and the ID of the movable part, the seal requirements become very stringent. First, a radial gap must be left between the diameters of the two parts to ensure that there is not interference to relative movement caused by machining tolerances, normal wear, or slight distortion. This gap is likely to be far larger than those normally accommodated by standard elastomeric O-rings where radial clearances are on the order of two or three thousandths of an inch and so will probably result in seal "roll-out" with any relative movement.

Next, a standard O-ring must be compressed at least 10% to effect a good low-pressure seal. This can require as much as 7 lb axial force per running inch of seal to accomplish, or, for example, nearly 500 lb force to effectively seal a 23-in. diameter.

Finally, if the seal is not placed in a cooler region, or if exhaust gases circulate in the clearance between the two parts, the seal must withstand very high temperatures. Such high-temperature seals as metallic O-rings and V-seals are available. Their major drawback is that they are generally used in face seal applications and require high clamping loads to effect the metal-to-metal seal. It is true that a minimal amount of leakage would not damage such seals.

III, D, Test Hardware Design (cont.)

All things considered, if the face gasket seal shown in Figure 29 cannot be used and a piston-type seal is required, it would seem wise to follow these guidelines:

(a) No translation during thrust chamber operation.

(b) Place the seal in as cool a region as possible, even for long duration thrusting.

(c) Use an elastomeric seal that requires minimum force to compress, will seal large radial clearances, and will not tend to roll out during relative part movement.

(2) Selected Approach

An elastomeric seal satisfying (c) would be one which is deeply set or glued in a groove on the OD of the fixed part to prevent rollout, is hollow to minimize compression forces required, and is made from a high operating temperature compound such as silicone rubber. Such a seal has been designed for the test engine and is shown in Figure 86. Also shown is a tubular O-ring in a standard O-ring groove which will be evaluated for comparison purposes.

The nozzle also incorporates a standard commercial O-ring in the safer face seal configuration.

A tubular O-ring is again used under the movable slotted groove cover ring as shown in Figure 81 to minimize the compression problems that zero clearance may present while assembling the ring to the adapter in a wrap-around manner. Conventional O-rings are used to seal the adapter to the thrust chamber and the nozzle extension to the slide section.

III, D, Test Hardware Design (cont.)

e. Supporting Design Analyses

(1) Nozzle Performance Analysis

The nozzle for the test engine incorporates a Rao optimum contour designed for an area ratio of 48.3, but truncated at an area ratio of 36.8. The larger area ratio nozzle was truncated so as to reduce the fabrication cost and to make the nozzle compatible with existing altitude simulation facilities at White Sands Test Facility. The fact that the nozzle is truncated will in no way detract from the test objectives since it is performance differences that are important, not absolute performance. The nozzle throat radius was chosen equal to 2.472 in. to produce a chamber pressure of 100 psia, which is the design pressure for the LEM injector. The contour coordinates (X and R) and wall angles (Θ) for the test nozzle are shown in Table XIX. Also shown are Mach numbers and static pressures at the wall for frozen flow conditions with $\gamma = 1.22$, which is representative of N_2O_4/A-50 propellants at $P_c = 100$ psia.

From Table XIXit may be seen that the predicted wall pressure at the nozzle exit is 0.42 psia for the design chamber pressure of 100 psia. For this reason (i.e., to avoid flow separation), the nozzle must be tested in a simulated altitude facility. An analysis of test engine compatibility with the White Sands Test Facility diffusers is given in Appendix C. A wall pressure tap located near the nozzle exit will serve as a check that the nozzle is flowing full. The wall angle at the nozzle exit is 13.76°, which is less than the 15° suggested by White Sands personnel as a maximum for efficient diffuser operation.

The interface, or junction, between the fixed base nozzle and movable extension was located at an expansion ratio of 20.5. This choice was a compromise between practical considerations and a desire to

III, D, Test Hardware Design (cont.)

simulate flow conditions in a high expansion ratio nozzle designed for vacuum operation. In the analytical performance/weight study in this report, interface area ratios of 100, 140, and 180 were considered. Interface area ratios of this magnitude were obviously not feasible for the test engine. The Mach number and free stream wall pressure at the interface were calculated to be 3.52 and 0.84 psia, respectively, as indicated in Table XIX.

One of the primary objectives of the test program will be to develop a relationship between performance and the magnitude of the wall discontinuity at the interface between the stationary base nozzle and the extension. This relationship will be determined by testing with three different step heights (0.75, 0.50, and 0.25 in.), first without film cooling, and comparing the measured performances with the performance for the zero step height (continuous contour). These data would then yield a relationship between performance decrement and step height which can be extrapolated to other flow conditions.

The extrapolation would consider (1) boundary layer thickness as compared to step height, (2) flow reattachment criteria, (3) potential flow conditions adjacent to the wall, and (4) oblique shock effects downstream of the reattachment point. Previous analyses using potential flow techniques to evaluate small discontinuities in nozzle contours have indicated little or no effect on performance. This, however, may have been due to a limitation of the potential flow analysis. No experimental data have been found to either refute or verify these analyses.

To afford an insight into the flow processes associated with both the step and the film cooling, a series of pressure taps are being located in the test nozzle. A total of 14 pressure taps will be instrumented: six on the cylindrical surface of the step and eight at progressively increasing distances downstream of the step. Figure 87 shows the exact locations of the 14 pressure taps with respect to the face of the largest (0.75 in.) step. All pressure taps, with the exception of two, will be located in line with coolant passages.

III, D, Test Hardware Design (cont.)

Figure 88 is a schematic of the flow field in the region of the step, assuming no film cooling. Also shown in this figure is a schematic of the pressure profile at the wall. For comparison, the pressure profile and contour are also shown for the continuous contour. The flow expands at Point A, producing a reduced (compared to continuous contour) pressure along the base of the step. The separated region within the step is characterized by low-velocity recirculating flow. At Point B, the flow reattaches and is turned to the axial direction, causing the oblique shock and pressure spike. At Point C, the flow again expands to follow the nozzle contour as is indicated by the latter half of the pressure spike (decreasing pressure). The flow will initially over-expand downstream of Point C and then approach the undisturbed pressure profile denoted by the dashed line in Figure 88. The reduced pressure on the vertical face at Point A and along the contour downstream of Point C will tend to produce a performance decrement as compared to the continuous contour.

For the tests with film coolant injected at the interface, it may not be possible to separate the effects on performance of the film coolant from that of the step since both will contribute to a performance loss (based on total weight flow). The hardware design will not permit baseline tests with film coolant on the continuous contour. It may, however, be possible to infer an approximate performance decrement, depending on the magnitude of the decrement, for a given film coolant flow rate by extrapolating the data for the three step heights to zero step height. Qualitatively, the film coolant would tend to reduce the performance decrement due to the step by essentially filling the discontinuity.

The fact that the injection velocities are different for each step height (see Section III,D,4,a) should have a negligible effect on performance decrement due to either film cooling or step height. The injection velocities vary from 1485 ft/sec for the 0.25-in. step to 1290 ft/sec for the 0.75-in. step, whereas the adjacent freestream velocity is approximately 9000 ft/sec.

III, D, Test Hardware Design (cont.)

Injection velocity would, of course, be affected only by area ratio of the injection tip and not by the pressure at which it is injected.

(2) Heat Transfer Analysis

The extendable nozzle test engine consists of three major components: the ablative chamber, the adapter transition section, and the extendable nozzle. The cooling mechanism for each of these three segments is shown schematically in Figure 89. The injector and chamber subassemblies consist of a Lunar Module Ascent (LMA) engine injector and chamber supplied by NASA for the extendable nozzle program. The remainder of the components are being fabricated under the cognizance of this program. The transition section and extendable nozzle subassemblies mate with the LMA engine system upstream and will serve as workhorse hardware to obtain nozzle test data. The engine system operates with N_2O_4/A-50 propellants at the following chamber conditions:

Chamber pressure	100 psia
Mixture ratio	1.6
Injector gas barrier cooling	3% of fuel
Max. designed test duration	30 sec per test
Planned test duration	15 sec max/test

The LMA injector employs a conventional orificed injector pattern and has an AeroZINE 50 regeneratively cooled face. The injector has been designed to operate in the chamber pressure range of 100 to 120 psia at a nominal MR of 1.6. Since injectors of this particular design have been successfully fired in excess of 600 sec of accumulated test duration, no cooling difficulties are anticipated. Approximately 3% of the fuel flow is injected as a coolant barrier to cool the flange region of the ablative chamber.

III, D, Test Hardware Design (cont.)

The LMA chamber consists of a silica-reinforced phenolic ablative shell supported by a steel shell. This chamber terminates at an area ratio of approximately 2.4:1 and is designed to fire for a total of 600 sec in either a continuous or pulsed mode. The current extendable nozzle test plan calls for 20 test firings of approximately 15 sec duration each; therefore, the chamber will be adequate for the planned duration.

The nozzle extension transition section (adapter) extends between the LMA ablative chamber and the extendable portion of the nozzle which attaches at an area ratio of 20:1. In addition to serving as the support structure for the extendable nozzle, the metal transition section allows the ablative chamber pyrolysis gases and residual barrier cooling gases, which are entrained in the low velocity boundary layer, to diffuse into the main gas stream, permitting thermal test data to be obtained that are independent of the thermal and flow anomalies that are peculiar to the LMA injector - chamber system. It is necessary that thermal data by unencumbered by these effects, since the experimental data must be generalized to apply to different propellants, chamber pressures, and mixture ratios.

For simplicity of design and fabrication and to minimize the cost, heat sink cooling was selected for the transition section. Two materials were considered: stainless steel and copper.

Typical temperature response curves for these two transition section heat sink designs are shown in Figure 90. These curves show the temperature response at an area ratio of 2.4:1--the most severe thermal environment in the transition section--for both the stainless steel and copper designs over a range of wall thicknesses. Figure 90 shows that the stainless steel design has a high gas-side wall temperature (T_{wg}) which becomes independent of wall thickness when the thickness is made greater than 1.00 in. at this area ratio. The ambient-side temperature (T_{wo}) response of the stainless steel design

III, D, Test Hardware Design (cont.)

is delayed as the nozzle wall is made thicker, the outer wall of a 2.00-in.-thick section remaining at ambient temperature during the 30-sec test period. With copper walls, the curves show that T_{wg} continuously decreases as the nozzle wall thickness is increased. The temperature drop through the copper is seen to be much less than for stainless steel of comparable thickness. Both the reduction of wall temperature drop and the continuous influence of wall thickness on T_{wg} noted with the copper design are attributed to the very high thermal conductivity of copper, nearly 20 times that of stainless steel.

Figure 90 indicates that a thick-walled copper transition section might be employed for long duration tests (30 to 60 sec) without melting the copper walls, but the rapid temperature response of the copper T_{wo} is a disadvantage, since the service temperatures of the O-ring and ablative liner that are in contact with the adapter would be exceeded unless the nozzle wall thickness was greater than 2.00 in. at the 2.4 area ratio. Figure 90 shows that the stainless steel section approaches the service temperature limit of the material after a 30-sec test. Because the steel section T_{wg} is independent of wall thickness for a design greater than 1 in. thick, the test duration with a stainless design is limited to approximately 30 sec. Mechanical strength, thermal expansion characteristics, weight, cost, and attachment considerations finally lead to the selection of a stainless steel transition section for the test engine.

There are two distinct rates of heating on the nozzle extension: the flow attachment region which occurs at area ratio 20:1 and the remainder of the extension downstream. The two heating zones result from the discontinuity at the point of nozzle attachment. The nozzle discontinuity produces abnormal hot gas flow effects and high heat transfer rates at the attachment region. Downstream of area ratio 20:1, the attachment region flow and heating effects are dissipated, and heat transferred from the hot gases to the nozzle walls may be predicted using conventional developed-flow heat transfer correlations.

III, D, Test Hardware Design (cont.)

The nozzle gas flow characteristics that occur in the attachment region are shown schematically in Figure 91. The gas flow is characterized by expansion of the hot gases into the cavity formed by the adapter step or tip upstream and the extension downstream, producing a region of separated gas flow with high gas temperatures but low heat fluxes. Immediately downstream of this region, the supersonic mainstream gases change flow direction, causing an oblique gas shock to be formed. The shock attachment region is characterized by high gas pressures and very high local heating rates. Still further downstream, as the original contour is resumed, the cavity gas flow must again change direction, which extends the region of high local heating rates for an additional distance downstream. The high heat fluxes in this region are due to formation of a laminar boundary layer. When the laminar boundary layer downstream of the nozzle shoulder becomes very thick, it becomes unstable, and transition to a turbulent boundary layer occurs.

An investigation was conducted to establish the approximate hot gas heating rates at the attachment region of the nozzle extension. This investigation showed that some experimental and analytical work had been performed with rearward facing, 90° steps with supersonic gas flow; however, it was concluded that a thermal design correlation that could be used to design the attachment region cooling system was not available, and that some development testing was required. The lack of design data available in the literature did not seriously hamper the thermal design effort, since a major goal of the test program requires acquisition of region thermal data.

Downstream of the reattached region, following the transition from a laminar to a turbulent boundary layer, the nozzle flow is fully developed and behaves in a predictable manner. The fully developed flow region extends to the end of the nozzle. In the fully developed flow region, heat transferred from the hot gases to the nozzle walls may be predicted using conventional heat transfer correlation.

III, D, Test Hardware Design (cont.)

The supply system was designed to inject the nitrogen so as to obtain complete coverage of the base of the adapter step or attachment region cavity. The nitrogen is injected at supersonic velocities for two reasons: (1) the momentum of the film coolant must be high enough to penetrate the region where impingement and reattachment of the main gas stream occurs (see Figure 91), otherwise the coolant may effectively be destroyed by the high pressures at this point; and (2) since the nozzle gas pressure is ≯1 psia, it would be impossible to design and control a subsonic injection velocity system.

The cooling requirements of the vertical surface (base) of the cavity was ignored in designing the cooling system. Since this is a low heat flux region, the heat sink effect provided by the transition section wall will be adequate to maintain reasonable temperatures in this region. For an engine system design, cooling of this portion of the cavity will depend on the cooling method employed upstream of the attachment zone and must be considered separately.

The coolant flow rate requirements are estimated using the data of Goldstein*. The adiabatic wall temperature for GN_2 flow rates of 0.1 lb/sec and 0.5 lb/sec are plotted as functions of dimensionless distance in Figure 92. The heating rates for fully developed flow at an area ratio of 20:1 were used to perform the calculations. The abnormal heating rates that occur at the base of the cavity were ignored since the low heat fluxes that occur near the coolant injection point tend to compensate for the higher fluxes that occur closer to the shoulder of the cavity. From the curves of Figure 92, it is concluded that the GN_2 film coolant supply system should be designed to provide flow ranging from 0.1 lb/sec to 0.5 lb/sec. These film coolant flows are nominally 1% to 5% of the propellant flow rate.

*Goldstein, et al., Film Cooling in Supersonic Flow, University of Minnesota Heat Transfer Laboratory Technical Report No. 54, Contract NONR 710(14), December 1963.

III, D, Test Hardware Design (cont.)

Two types of instruments will be used to measure the nozzle extension temperatures: gas-side thermocouples and radiation-cooled calorimeters. The calorimeters have been designed specifically for this application and will supply thermal data having special significance for extendable nozzle design work.

The gas-side thermocouples are 0.020 in. OD, stainless-sheathed-type chromel-alumel, fast-response design. The thermocouples will be installed so as to be flush with the gas-side surface of the extension wall. The design of the radiation-cooled calorimeters is shown in Figure 93, which also shows the predicted temperature response curves. The calorimeter has been designed for operation at the extension attachment area ratio of 20:1 and has the capability of operating at element temperatures in excess of 3000°F. This high temperature element capability is required for attachment region testing because of the high heat fluxes which will be encountered. As shown in Figure 93, the calorimeter element would reach a steady-state temperature of approximately 2200°F if the more severe attachment region heating conditions were not encountered. The calorimeter data will provide steady-state radiation-cooled nozzle wall temperature data and will permit calculation of the hot gas film coefficient and recovery temperature at a steady measured value of the wall temperature. These data will be especially valuable for use in the design of a radiation-cooled nozzle extension. The calorimeters will also be used to obtain film cooling data at the attachment region.

(3) Stress Analysis

The purpose of this analysis was to identify any critical areas of the test engine design, establish structural adequacy, and provide recommended design changes as required.

III, D, Test Hardware Design (cont.)

The analysis of the nozzle was conducted in two phases: a mechanical load and a combined mechanical-thermal evaluation. The mechanical load evaluation was conducted using conventional structural theory. The combined thermal mechanical solution was conducted on the basis of the finite element method of analysis. The time period chosen for evaluation was the maximum expected operating time of 15 sec from an ambient temperature condition. Less firing time provides lower thermal gradients and reduced strains.

The pressure/thrust loads do not subject the nozzle itself to any significant stress levels. The major source of stresses are those thermally induced by the operating conditions. The largest strain level is near the forward flange where the CRES 347 chamber adjoins the LEM chamber. The design was modified after preliminary analyses revealed that very high stresses would be developed at this location. The modification consisted of extending the ablative chamber aft which resulted in a decrease in maximum temperatures and gradient. The maximum effective strain at the forward flange was determined to be 1.43% with an effective stress of 27,000 psi at 1200°F, resulting in a margin of safety of +0.65. A separation between the CRES 347 nozzle and the ablative liner at this location is desirable to preclude local crushing of the silica liner. The condition is satisfied by the nominal clearance provided by the tolerances on the drawings.

A complete stress analysis is included as Appendix F.

III, Discussion (cont.)

E. TEST HARDWARE FABRICATION

1. Nozzle Deployment and Retraction

a. Actuation

Actuation for deployment and retraction is accomplished by three Flairline F-1-1/8-12-HC actuators. The actuators were attached to the thrust takeout ring by Flairline mounting pads which were bolted to welded plate brackets which were, in turn, bolted to the ring. The actuator rod was attached to the slide section by welding three drilled and tapped stainless blocks to the slide section into which the rod end was threaded.

Operation of the actuators was bench checked to determine if uniform and simultaneous motion of the three actuators and the required actuation times could be obtained. Turbine oil at 150 psi was used during testing. A 3/8-in.-port 4-way valve was used for switching instead of the four 1/2-in. valves that will be used during White Sands testing. Consequently, the feed lines from valve to cylinder manifolds and from cylinder to dump orifice were 3/8-in. tubing instead of the 1/2-in. tubing to be used for White Sands testing. It was felt that, if satisfactory operation could be obtained under these conditions, the units would be acceptable.

Another major difference between the two systems was the elimination of all individual check valves and orifices and substitution of a single orifice in the dump line to control actuator speed. The individual orifices and check valves were originally thought necessary to ensure that all actuators acted together; later, it was decided to determine if this condition could be met through the use of equal feed line lengths and proper fluid distribution.

III, E, Test Hardware Fabrication (cont.)

The checkout system as fabricated is shown in Figures 94 and 95. Special distribution manifolds were fabricated from 3/8-in. fittings by welding a union on one side and boring a hole through, ensuring equally distributed flow to each cylinder. The 6-in.-long 1/4-in. lines used to connect the cylinders required tight bends on the center cylinder.

The accumulator was filled and pressurized with available 150 psi nitrogen. The system on-off valve was then opened, allowing the cylinders to extend, at which time the extending side of the system was bled. The 4-way valve was then actuated, which retracted the cylinders and the retracting side of the system was bled. Due to the size of the accumulator, the actuators could be cycled only three times before the accumulator had to be recharged. The actuators are shown in the extended and retracted positions in Figures 96 and 97.

With the dump orifice completely removed, actuation times of 2 sec were obtainable. This flow would be increased using the 1/2-in. valves and lines. The two outboard actuators moved simultaneously with the center actuator lagging slightly in first motion, possibly due to the bends in the inlet lines. It was decided to see if a thin (0.020 in.) piece of aluminum secured across the actuator rod ends, as shown in Figure 98, would equalize all three actuators without any flexure of the aluminum. This objective was achieved. It is considered that the extendable portion of the nozzle represents a considerably stiffer structure than the aluminum sheet; therefore, the results were considered satisfactory.

III, E, Test Hardware Fabrication (cont.)

b. Guide Rail and Support

The guide and support system for the extendable nozzle was assembled from commercially available products made by Thompson Industries Incorporated. As shown in Figure 2, centerless ground, hardened shafting was used for the three guide rails. The 0.75-in.-dia shafting is machined to accept the standoff bolts and end retainer clips and to provide detent holes.

Essentially friction-free movement was provided by three pairs of Thompson ball bushings mounted in 347 stainless steel bearing blocks which were welded to the slide section.

2. Nozzle Extension

The nozzle extension (Figure 2) was fabricated from rolled and welded 347 stainless steel which was then stress relieved. First, the preform was rough machined on the ID to within 0.040 in. of the finished contour. The rest of the extension was then finish machined, with the exception of the mounting flange surface.

The nine 1/4-in. Swagelok fittings for the calorimeters, the 24 1/8-in. Swagelok fittings for the thermocouples, and the 14 1/4-in. AN fittings for the pressure taps were then welded on and the through-holes finish reamed. At this point, the part was again stress relieved and the inner contour and mounting flange surface finish machined. This process eliminated any distortion of the inner contour attributable to welding of the fittings.

III, E, Test Hardware Fabrication (cont.)

3. Slide Section

The slide section was also machined from a 347 stainless steel rolled and welded ring, which was then finish machined on noncritical surfaces and rough machined to within 0.030 in. of critical surfaces. The bearing blocks and actuator rod end blocks were then welded on. After welding, the part was stress relieved and the critical surfaces machined; this included the extension attachment flange and O-ring groove and the line boring of the bearing blocks.

4. Chamber - Nozzle Adapter

The main body of the adapter was machined from a 347 stainless steel forging. The inner contour was machined last after fabrication and installation of the coolant injector tips described in the next section. Prior to final machining, the thrust mount gussets and coolant feed tubes were welded in place and the part stress relieved.

5. Film Coolant Injector

The film coolant injector feed tubes and distribution manifold were machined as an integral part of the adapter. Each of the removable tips were machined on the fore and aft surfaces from rolled and welded 347 stainless steel strips. After all rings had been notched together as shown in Figure 62, the OD was machined and the groove cover (machined from rolled and welded 347 stainless steel flat stock) was installed and the 13 rows of bolt holes drilled and tapped. With the bolts installed, the inner contour of all tips and the adapter were then machined. Finally, the groove cover was slit and removed and the 180 grooves, or two-dimensional nozzles, were machined in the OD of the assembly.

III, E, Test Hardware Fabrication (cont.)

6. Thrust Structure

The thrust structure was made entirely from 5/8-in. 347 stainless steel plate and consisted of the three mounting gussets welded to the adapter (which also mount the guide rails) and the mounting flange or ring which was, in turn, welded to the gussets. The gussets and flange were then drilled to accept the guide rail bolts, actuator bracket bolts, and mounting bolts.

7. Thermal Instrumentation

The thermal instrumentation is shown in Figure 93. It consists of 1/4-in. OD calorimeters and 1/8-in. OD thermocouples that were inserted flush to the inner contour through the appropriate Swagelok fittings welded to the extension shell.

In fabricating the calorimeter, a 0.250-in. OD stainless rod was machined so as to have a 0.040-in. hole through a 0.125-in.-dia x 0.125-in.-deep chamber and a recessed shelf as shown. A nickel (used with chromel-alumel thermocouples) or tantalum (used with tungsten/tungsten rhenium thermocouples) disk, 0.150-in.-dia x 0.010-in.-thick, was then drilled to accept the two thermocouple wires from the 0.040-in.-dia sheathed thermocouple. These wires were surface welded to the disk and the thermocouple and the disk was lowered into the through-hole and recessed shelf, respectively. The disk sits in a layer of zirconium oxide ceramic adhesive which insulates and seals it to the 0.250-in. stainless steel rod.

The calorimeter chamber was spray-coated with a material called "velvet black", as was exposed thermocouple wires. This makes the chamber an effective "black box" to which the disk radiates heat. A lip on the rod was then rolled around the disk to retain it and the ceramic adhesive is cured.

III, E, Test Hardware Fabrication (cont.)

Prior to assembly, both sides of the disk surface were sprayed with a silicide coating to provide protection and to increase its emissivity.

The thermocouples were made from two sizes of stainless tubing. The larger tubing was 1/8-in. OD. The inner tubing was about 1/2-in. long and bridged the gap between the ID of the outer tubing and the 0.020-in. OD of the chromel-alumel thermocouple. The entire assembly was then furnace brazed so that the thermocouple would indicate the bulk temperature of the mass of stainless steel at the tip.

8. LEM Chamber Modifications

The only modification required for LEM components was the recontouring of the silica phenolic barrel liner as shown in Figure 2.

9. Engine Assembly

A fitup assembly and inspection of all engine components were accomplished at the subcontractor's plant prior to shipment to White Sands Test Facility. All parts were found acceptable and fitup was determined to be good. The components were then shipped to White Sands Test Facility, and Figures 99 and 100 show the basic engine assembly and one extension as received there.

Final assembly of the engine as shown in Figure 2 was accomplished by Aerojet personnel at White Sands.

III, Discussion (cont.)

F. DEMONSTRATING TESTING

1. Test Plan

Twenty tests are planned for the extendable nozzle test effort at the NASA White Sands Test Facility. The test plan and operational procedures were detailed to NASA/MSC and are presented as Appendix A.

2. Test Program

Testing is currently scheduled to commence 15 November 1970 and be completed 15 December 1970. The proposed test plan has the following objectives:

a. To demonstrate the operation of an extendable - retractable nozzle at simulated altitude conditions.

b. To evaluate the effects of nozzle contour mismatch at the nozzle extension attach interface on heat transfer and performance. .

c. To evaluate the feasibility of film cooling at the nozzle attachment interface.

d. To evaluate nozzle sealing.

REFERENCES

1. A. L. Feldman and D. David, "Design of the Apollo Service Module Propulsion System Rocket Engine for Manned Operation," Second International Conference on Space Engineering (Venice, Italy), May 1969.

2. AJ 10-138 Transtage Engine Data, Aerojet-General Corp., Propulsion Division, April 1969.

3. Agena Propulsion System Engineering Analysis Report, Lockheed Missiles and Space Division, Report LMSD-446439, Contract AF 04(647)-558, -563, and -564, 30 July 1960.

4. F-1 Rocket Engine Program, Final Report, North American Aviation (Rocketdyne), Report NAA-R R-1437, September 1959.

5. F-1 Design Information, North American Aviation (Rocketdyne), Report NAA-R R-2823-1, 23 August 1961.

6. "Refractory Metal Plus MOS_2 Yields Rugged Self-Lubricating Material," Design News, 15 September 1970.

7. J. L. Pieper, ICRPG Liquid Propellant Thrust Chamber Performance Evaluation Manual, CPIA Publication No. 178, September 1968.

8. G.V.R. Rao, "Exhaust Nozzle Contours for Optimum Thrust," Jet Propulsion, Vol. 28, No. 6, 1958.

9. The ICRPG One-Dimensional Kinetic Nozzle Analysis Computer Program, July 1968.

10. The ICRPG Turbulent Boundary Layer Reference Program, Pratt & Whitney Aircraft, East Hartford, Connecticut, July 1968.

11. Two-Dimensional Kinetic Nozzle Analysis Computer Program, ICRPG Performance Standardization Working Group (available through Dynamic Science Corporation), AD 841200, 30 July 1968.

12. G. A. Hosack and R. R. Stormsta, "Analytical Methods for Computing the Effects of Turbine Exhaust and Film Cooling Injection on Rocket Engine Performance," North American Rockwell Corp (Rocketdyne), Canoga Park, California, presented at AIAA Fifth Propulsion Joint Specialist Conference, June 1969.

13. D. E. Nestler, A. R. Saydah, and W. L. Auxer, "Heat Transfer to Steps and Cavities in Hypersonic Turbulent Flow," AIAA Fluid and Plasma Dynamics Conference, Paper No. 68-673, June 1968.

REFERENCES (cont.)

14. P. F. Holloway, J. R. Sterrett, and H. S. Creekmore, An Investigation of Heat Transfer Within Regions of Separated Flow at a Mach Number of 6.0, NASA TN D-3074, November 1965.

15. P. D. Burbank, R. A. Newlander, and I. K. Collins, Heat Transfer and Pressure Measurements on a Flat-Plate Surface and Heat Transfer Measurements on Attached Proturbances in a Supersonic Turbulent Boundary Layer at Mach Numbers of 2.65, 3.51, and 4.44, NASA TN D-1372, December 1962.

16. G. E. Gadd, W. F. Cope, and J. L. Attridge, Heat Transfer and Skin-Friction Measurements at a Mach Number of 2.44 for a Turbulent Boundary Layer on a Flat Surface and in Regions of Separated Flow, ARC R&M No. 3148, 1960.

17. A. F. Charwat, "Supersonic Flows with Imbedded Separated Regions," Advances in Heat Transfer, Vol. 6, 1970.

18. J. E. Hatch and S. S. Papell, Use of a Theoretical Flow Model to Correlate Data for Film Cooling or Heating an Adiabatic Wall by Tangential Injection of Gases of Different Fluid Properties, NASA TN D-130, November 1959.

19. S. S. Papell, Effect on Gaseous Film Cooling of Coolant Injection Through Angled Slots and Normal Holes, NASA TN D-299, September 1960.

20. R. A. Seban, "Heat Transfer and Effectiveness for a Turbulent Boundary Layer with Tangential Fluid Injection," J. Heat Transfer, Vol. 82, Series C, No. 4, 1960, pp 303-312.

21. J. L. Stollery and A. A. M. El-Ehwany, "A Note on the Use of a Boundary Layer Model for Correlating Film Cooling Data," Int. J. Heat and Mass Transfer, Vol. 8, No. 1, 1965, pp 55-65.

22. J. L. Stollery and A. A. M. El-Ehwany, "On the Use of a Boundary Layer Model for Correlating Film Cooling Data," Int. J. Heat and Mass Transfer, Vol. 10, 1967, pp 101-105.

23. B. Cockshutt, Film Cooling Tests with a Two-Dimensional Convergent-Divergent Nozzle, Part I: Single Slot, General Electric Co., 15 August 1958.

24. F. Burggraf, Design and Analysis of Cooled Turbine Blades, Part III: Transpiration and Multiple Small Hole Film Cooled Nozzles and Buckets, General Electric Co., Contract NAS 3-7278, 1 January 1968.

25. R. J. Goldstein, F.K. Tsou, E.R.G. Eckert, Film Cooling in Supersonic Flow, U. of Minnesota, Report HTL TR No. 54, December 1963.

REFERENCES (cont.)

26. R. J. Goldstein, E.R.G. Eckert, F. K. Tsou, A. Haji-Sheikh, Film Cooling with Air and Helium Injection Through a Rearward-Facing Slot into a Supersonic Air Flow, U. of Minnesota, Report HTL TR No. 60, February 1965.

27. V. Zakkay, et al., "An Experimental Investigation of Supersonic Slot Cooling," Proceedings of the 1970 Heat Transfer and Fluid Mechanics Institute, Naval Post Graduate School, Monterey, California, June 1970.

SUBLIMATION OF METAL IN HIGH VACUUM

Element	TEMPERATURE °F AT WHICH GIVEN SUBLIMATION RATE OCCURS			Melting Point °F
	10^{-5} Cm/yr (3.94×10^{-6} in/yr)	10^{-3} Cm/yr (3.94×10^{-4} in/yr)	10^{-1} Cm/yr (3.94×10^{-2} in/yr	
Cadmium	100	170	250	610
Zinc	160	260	350	790
Magnesium	230	340	470	1200
Silver	890	1090	1300	1760
Aluminum	1020	1260	1490	1220
Beryllium	1140	1300	1540	2330
Copper	1160	1400	1650	1980
Gold	1220	1480	1750	1940
Chromium	1380	1600	1840	3410
Iron	1420	1650	1920	2800
Nickel	1480	1720	2000	2650
Titanium	1690	1960	2280	3040
Miozybdenum	2520	2960	3450	4730
Tantalum	3250	3700	4200	5400
Tungsten	3400	3900	4500	6200

TABLE I

DECOMPOSITION OF POLYMERS IN HIGH VACUUM

Polymer	Temperature (°F) for 10% Weight Loss per Year	Quality of Data
Benzyl	540	B
Butadiene	490	B
Butadiene - Acrylonitrile (NBR Rubber)	300-450	B-D
Butadiene - Styrene (SBR Rubber)	460	B
Carbonate	350	D
CFE	490	A
CFE-Vinylidene Fluoride	500	A
Epoxy	100-460	B-C
Ethylene, High Density	560	A
Ethylene, Low Density	460-540	A
Ethylene Terephthalate (Mylar, Dacron)	400	A
Isobutylene	400	B
Isobutylene-Isoprene (Butyl Rubber)	250	D
Isoprene	380	B
Methyl Styrene	350-420	A
Neoprene	200	C
Nylon	80-410	A
Phenolic	270-510	B-D
Propylene	370-470	A
Rubber, Natural	380	B
Silicone Elastomer	400	D
Styrene	270-420	A
TFE (Teflon)	710	A
Trivinyl Benzene	560	A
Vinyl Acetate	320	A

From "Chemical Engineering Progress", Symp. Series, L. D. Jaffe, Vol. 59, No. 40

TABLE III

COMPARISON OF LUBRICANTS FOR BEARINGS IN SPACE

Lubricant	Temp (°F)	Vacuum	Radiation	Sliding Contact	Rolling Element
Diester-oil-based greases	-65 to 350	P	P	G	E
Mineral-oil-based greases	-40 to 250	P	P	G	E
Silicone-oil based greases	-100 to 400	P	P	G	E
Molybdenum Disulfide	-300 to 750	E	E	E	P
Graphite	-300 to 1200	P	E	G	P
Tungsten Disulfide	850	E	E	U	U
Teflon		G	G*	E	E
Nylon-bonded coatings with:	-40 to 200	P	G	E	P
Organic Binders	-100 to 500	P	P	E	P
Inorganic Binders	-300 to 1000	E	E	G	P

*Teflon is relatively resistant to radiation alone; however, if teflon is in contact with an oxidizer while being irradiated, it rapidly deteriorates.

E = Excellent
G = Good
P = Poor
U = Unknown

RADIATION TOLERANCE FOR VARIOUS MATERIALS

ELASTOMERS	25% DAMAGE	REMARKS
Natural Rubber	2.5×10^9 ergs/gram (C)	Damage to all properties.
Styrene-Butadiene	1×10^9	Damage to all properties.
Silicone Rubber	10^9	
Viton A	9×10^9	Hardness increases 25%, elongation decreases 80%.
PLASTICS		
Teflon	3.5×10^6	
Nylon	5×10^9	

NOTE: 25% damage is the amount of radiation exposure required to change a physical property of the material by 25%.

TABLE IV

TABLE V

COMPARATIVE RATING OF

NOZZLE EXTENSION COOLING CONCEPTS

	RATING FACTOR	POINTS POSSIBLE	COOLING CONCEPT			
			TRANSPIRATION	TUBE BUNDLE	ABLATIVE	RADIATION
1.	Light Weight	30	6	15	0	25
2.	Low Cost	10	2	6	8	10
3.	East of Development	20	8	16	20	18
4.	Reliability	30	15	30	30	30
5.	Cooling Effectiveness Using Dump Gas	10	5	10	10	10
6.	Cooling Efficiency With Other Coolants	10	10	10	10	10
7.	Extended Duration Capability	30	30[1]	30[1]	0	30
8.	Recycling Capability	30	30	30	30	24[2]
9.	Clusterability	20	20	20	20	14
10.	Ease of Fabrication	20	6	10	14	20
11.	Compatibility with Exhaust	20	20	20	16[3]	16[3]
12.	Not Complex	20	4	10	16	20
13.	Not Size Limited for Given Coolant Mass Flow	10	5	7	10	10
	TOTAL	260	161	214	184	237

1. Dependent on coolant flow.
2. Questionable if coating required.
3. Rate of attack must be determined for material used.

STANDARD PLATINGS AND COATINGS FOR METALLIC SEALS

Plating or Coating	Temperature Range (°F)	General Recommendations
Silver	-325 to +1650	Excellent general purpose plating for high temperature resistance, but generally less suitable for cryogenic temperatures than gold or Teflon. Excellent chemical and radiation resistance.
Gold	-423 to °1850	Similar to silver but somewhat better resistance to certain corrosive fluids. Improved high and low temperature resistance but higher in cost thar silver.
Teflon (TFE)	-423 to +500	Excellent coating for applications up to +500°F. Excellent chemical resistance. Particularly suitable for cryogenic applications.
Teflon (FEP)	-432 to +400	Similar to Teflon (TFE) but somewhat softer and more dense. High temperature resistance lower than Teflon (TFE).
Kel-F	-423 to +300	Similar to Teflon, but more resilient and plastic at low temperatures, and generally higher in cost than Teflon.
Platinum	-423 to °3100	Highest temperature-resistant plating. Normally limited to use with ultra high temperature base metals
Nickel (soft)	-325 to +2500	High temperature-resistant plating but slight sacrifice in softness and ductility compared to other platings.
Lead	-65 to +450	Very soft plating but limited temperature resistance. Excellent radiation resistance.
Indium	-320 to +300	Very soft plating but limited temperature resistance. Suitable for cryogenic applications.
Aluminum	-423 to +900	Compatible with most oxidizers and fuels, but extremely costly as a plating material. Particularly suitable for liquid and gaseous fluorine.
Tin pure)	-32 to +350	Very ductile, but limited temperature resistance. Usage limited to a few corrosive chemicals.
Copper	-423 to °1900	Suitable for vacuum applications; resistant to fluorine and certain other corrosive chemicals.

MAXIMUM SERVICE TEMPERATURES OF PLASTICS AND ELASTOMERS

Material	Temp (°F)	Material	Temp (°F)
Butadiene-acrylonitrile foams	210	Polyvinylidene chloride film	290
Rubber hydrochloride film	205	Melamines, fabric-filled	250
Acrylics	200	Melamines, shock res	250
Polystyrenes, glass-filled	200	Nitrile rubber	250
PVC-nitrile rubber blend film	200	Nylons 6 and 11	250
Urethane foams, flexible	200	Polyethylene film	250
Modified polystyrenes	190	Polysulfide rubber	250
Acetal	185	Neoprene rubber	240
Polystyrene foamed-in-place, rigid	185	Urethane rubber	240
Natural rubber	180	Polyvinyl chloride	220
Neoprene foams	180	Methylstyrenes	212
Polystyrenes, GP	180	Vinylidene chloride	212
Polyvinyl chloride film nonrigid	180	Melamines, GP	210
Styrene-butadiene rubber	180	Silicones (molded)	>700
Epoxies (cast, GP	175	TFE film	585
Prefoamed polystyrene, rigid	175	Silicone rubber	550
Polyvinyl formal	165	Plastics laminates, low pressure	500
Butadiene-styrene foams	160	TFE fluorocarbons	500
Natural rubber foam	160	Polyester film	490
Cellulose nitrate	140	Diallyl phthalate	450
Epoxies (cast), resilient	122	Fluorinated acrylic rubber	450
Polyvinyl butyral	115	Phenolics, shock and ht res	450
Prefoamed cellulose acetate, rigid	350	Viton rubber	450
Alkyds, GP	345	Cellulosic films	400
Alkyds, elec	300	Epoxies (cast), ht res	400
Allyls (cast)	300	FEP fluorocarbons	400
Butyl rubber	300	Melamines, glass-filled	400
Diallyl phthalate, orlon-filled	300	Nylon, glass-filled	400
Nylons 66 and 610	300	Phenolics (molded), shock and heat	400
Phenolic foamed-in-place, rigid	300	Plastics laminates, elec	400
Polypropylene film	300	Urethane foamed-in-place, rigid	400
Rubber phenolics	300	CFE film	395
Plastics laminates, GP	295	Melamines, cellulose or mineral-filled	395
Polyester (cast), rigid	295	CFE fluorocarbons	380
		Nylon 6 film	380
		Alkyds, high str	350
		Phenolics (molded), GP	350

NOTE: Values represent high side of a range of typical values.

TABLE VII

COEFFICIENT OF THERMAL EXPANSION FOR DIFFERENT MATERIALS (10^{-6} in/in/°F)

Material	High	Low	Material	High	Low
Silicone rubber	670	-	Aluminum bronzes (cast)[c]	9.5	9
Nitrile rubber	390	-	Cobalt-base supperalloys[d]	9.4	6.8
Neoprene rubber	340	-	Beryllium Copper[c]	9.3	-
Butyl rubber	320	-	Cupro-nickels and nickel silvers[c]	9.3	9
Polypropylene	170	-	Nickel and its alloys[d]	9.2	6.8
Polyethylenes, medium and high density	167	83	Cr-Ni-Co-Fe superalloys[d]	9.1	8
Polyethylenes, low density	110	89	Alloy steels[d]	8.6	6.3
Vinylidene chloride	87.8	-	Carbon free-cutting steels[d]	8.4	8.1
Nylons 6 and 11	71	46	Alloy steels (cast)[d]	8.3	8
Phenolics (cast)	66	33	Age hardenable stainless steels[c]	8.2	5.5
Nylons 66 and 610	55	-	Gold[c]	7.9	-
TFE fluorocarbons	55	-	High temperature steels[d]	7 9	6.3
Acrylics and epoxies (cast)	50	30	Titanium carbide cermet[d]	7.5	4.3
CFE fluorocarbons	38.8	-	Wrought irons[c]	7.4	-
Silicones (molded)	32.2	4.5	Titanium and its alloys[d]	7.1	4.9
Phenolics (molded)	25	8.3	Cobalt[d]	6.8	-
Zinc and its alloys[c]	19.3	10.8	Martensitic stainless steels[c]	6.5	5.5
Nylon, glass-filled	17	12.5	Nitriding steels[d]	6.5	-
Lead and its alloys[c]	16.3	14.4	Ferritic stainless steels[c]	6	5.8
Magnesium alloys[b]	16	14	Gray irons (cast)[c]	6	-
Epoxies (molded)	14	-	Low expansion nickel alloys[c]	5.5	1.5
Aluminum and its alloys[c]	13.7	11.7	Columbium and its alloys	4.1	3.8
Tin and its alloys[c]	13	-	Titanium carbide[d]	4.1	-
Tin and aluminum brasses[c]	11.8	10.3	Tungsten carbide cermet[c]	3.9	2.5
Plain and leaded brasses[c]	11.6	10	Alumina ceramics[c]	3.7	3.1
Silver[c]	10.9	-	Zirconium and its alloys[b]	3.6	3.1
Cr-Ni-Fe superalloys[d]	10.5	9.2	Molybdenum and its alloys	3.1	2.7
Stainless steels (cast)[d]	10.4	6.4	Borosilicate glasses[c]	2.5	1.8
Tin bronzes (cast)[c]	10.3	10	Aluminum silicate glass[c]	2.3	-
Austentic stainless steels[c]	10.2	9	Tungsten[b]	2.2	-
Phosphor silicon bronzes[c]	10.2	9.6	Invar (free cutting)	0.8	-
Coppers[c]	9.8	-	Silica glasses[c]	0.5	0.3
Nickel-base superalloys[d]	9.8	7.7	Silica, vitreous[e]	0.28	-

[a]Values represent high and low sides of a range of "typical" values. Values for plastics materials are for a range of temperatures between -22 and 86F (ASTM D696).

[b]Value at room temperature only.

[c]Value for a temperature range between room temperature and 212-750 F.

[d]Value for a temperature range between room temperature and 1000-1800 F.

[e]Value for a temperature range between room temperature and 2200-2875 F.

TABLE VIII

LINEAR THERMAL EXPANSION OF TYPICAL SEAL AND GLAND MATERIALS

Material	Contraction +75 to -65°F (in/ft)	Expansion +75 to +375°F (in/ft)	Coefficient of Expansion (in/in °F)
Teflon	.093	0.148	5.5×10^{-5}
Nitrile, General Purpose	0.218	0.468	13.0×10^{-5}
Chloroprene	0.190	0.407	11.3×10^{-5}
Viton-A	0.130	0.277	9.0×10^{-5}
Kel-F	0.064	0.137	3.5×10^{-5}
Silicone	0.252	0.540	15.0×10^{-5}
High Temp AL, 2017	0.022	0.047	13.0×10^{-6}
Stainless Steel, 302	0.016	0.035	9.6×10^{-6}
Steel, Mild	0.011	0.024	6.7×10^{-6}
Invar.	0.001	0.002	6.0×10^{-7}

TABLE IX

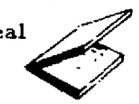
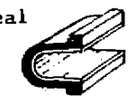
	SEAL TYPE	NAME	GLAND DESIGN: Surface Fin. (Micro inches)	Flatness (in.)	Allowable Separation (in.)	Base Material	REMARKS
GASKETS	Face	Corrugated 	64	.002	.005	All Metals	1. Seal could act as labyrinth 2. Various manufacturers
	Face	Jacketed 	64 - 125	.005	.005-.010		1. Various Manufacturers 2. Various Core Materials
	Face	"O" Ring 	32 - 64	.004	.004	Elastomeric or Plastic	1. Various Manufacturers
FLEXIBLE METALLIC	Face or Radial	Del TAU C 	16 - 32	.0002	.002	Various Metals	1. Made by Pressure Science Inc. 2. Can be plated with silver, gold and teflon 3. Sensitive to radial scratches
	Face	Del TAU E 	16 - 32	.001	.006	Various Metals	1. Made by Pressure Science Inc. 2. Higher resiliency than "O" ring 3. Can be plated with silver, gold and teflon
	Face	"K" Seal 	2 - 32	.0005	.002	Stainless Alloys	1. Same as Haskel Seal 2. Sensitive to handling and requires critical gland finish control. 3. Made by Harrison Mfg. Co. 4. Can be plated
	Face	"V" Seal 	16 - 32	.0005	.008	Various Metals	1. Similar to "K" Seal
PLASTIC SPRING LOADED	Face	Omniseal 	63	.005	.020	Teflon Jacket over flat stainless Helical spring	1. Similar to Bal-Seal 2. Manufactured by Aeroquip Corp. 3. Sensitive to scratches 4. Temperature limited
	Face	Raco Seal 	32	.005	.015	Teflon jacket over stainless finger spring	1. RACO Mfg. Co. 2. Manufactured by RACO Mfg. Co. 3. Sensitive to scratches

TABLE X

SEAL COMPARISON CHART

TABLE XI

DRIVE	ENERGY SOURCE AND TYPE	SUPPORTING POWER SUPPLY SYSTEMS	RELATIVE SYSTEM WEIGHT	RELATIVE COMPLEXITY *	RELATIVE EASE OF DEVELOPMENT *	POWER DRIVE AND TRANSMISSION ENVIRONMENTAL DESIGN PROBLEMS *Ta,Tb: VIBRATION SENSITIVITY	TEMPERATURE	COLD WELDING LUBRICATION REQUIRED	RADIATION	CORROSIVE ATMOSPHERE	SHOCK SENSITIVITY	SYSTEM DESIGN PROBLEMS *	RELATIVE RELIABILITY *	NOZZLE LOCKING *
Piston - Cylinder	Pneumatic N_2 - Storage Container H_2 or O_2 - Heat Exchanger Hot Gas (U) Turbine Exhaust T. C. Bleed Pyrotechnic Hydraulic Pump Discharge Stored Fluids - Container Reqd.	Source to Drive Electrical Controls, Valves and Plumbing Drive to Nozzle Extension Rod Scissor Cable - Pulleys and Tightening Devices Spring	Rod - Low	A,B,C	D,E,G	High	Yes	Yes	Yes	No	Yes	B,C,D,E,F,G	H,I,J	K,L,M
			Scissor - Heavy	A,B,C	D,E,G	High	Yes	Yes	Yes	No	Yes	B,C,D,E,F,G	H,I,J	K,L,M
			Cable - Medium	A,B,C	D,E,G	Medium	Yes	Yes	Yes	No	Yes	B,C,D,E,F,G,P	H,I,J	K,L,M,Q
			Spring - Low + Medium	A,B,C	D,E,G	High	Yes	Yes	Yes	No	Yes	B,C,D,E,F,G	H,I,J	K,L,M,Q
			NOTE: See Figures 31 thru 41 for controls reqts and weight estimates.											
Electrical Motor	Batteries Generator - Gas Driven	Source to Drive Electrical Controls and Wiring Drive to Nozzle Extension Cable Chain Tape Rack and Pinion Ball Screw Scissor	Cable - Med, Fig 31	A,C,N	G,N	Medium	Yes	Yes	No	No	Yes	P,G,N	S	(Tb,H) Q,M
			Chain - High, Fig 31	A,C,N	G,N	Medium	Yes	Yes	No	No	Yes	P,G,N	S	Q
			Tape - Med, Fig 31	A,C,N	G,N	Medium	Yes	Yes	No	No	Yes	P,G,N	S	Q
			Rack and Pinion - Low, Fig 32 & 33	A,C,N,O	G,N	Low	No	Yes	No	No	No	G,N	S,V	R,M
			Ball Screw - Low Fig 33	A,C,N,O	G,N	Low	No	Yes	No	No	No	G,N	S,V	R,M
			Scissor - High	A,C,N,O	G,N	High	Yes	Yes	No	No	Yes	G,N	S	R,M
			NOTE: See Figures 31 thru 41 for controls reqts and weight estimates.											
Hydraulic or Pneumatic Torque Motors - Require complex systems in conjunction with design problems, power supply better accomplished by electric motor.														
Diaphragms - Diaphragm Drive System stroke limited, power supply better accomplished with piston-cylinders or electric motor.														
Bellows - Difficult to achieve without extensive development, stroke limited, better accomplished with piston-cylinder or electric motor.														

COMPARISON OF NOZZLE TRANSLATION SYSTEMS

Report 10484-FR

COMPARISON OF NOZZLE TRANSLATION SYSTEMS

*A - System requires minimum of two power drives (for scissor drive, requires 2 ea per transmission system - redundancy considerations).

B - More complex than electrical drive.

C - Requires special electrical control circuitry for controls sequencing.

D - More difficult due to number of auxiliary controls.

E - Critical nozzle deployment sequence problem with pneumatic power.

F - Products of combustion (LO_2/LH_2) freeze problem - possible heaters required for actuators.

G - Redundancy problems with components - component failure considerations.

H - Respect to number of components, less reliable than electrical drive.

I - Piston/cylinder systems have proven reliability.

J - Poor reliability with respect to water freezing problem.

K - Simply designed into actuators.

L - Must use incompressible fluid for constant positioning.

M - Very good locking ability.

N - Minimum number of critical components (see Figures 31 through 41).

O - Requires individual motor drive.

P - Nozzle size limitation (weight consideration) with respect to size of cable, tape or chain.

Q - Requires locking device other than drive system.

R - Does not require other locking devices.

S - Electrical motors have demonstrated repeatability and reliability in the space environment. Have fewer critical parts and exhibit constant force at every position.

T - (a) See Section III, B - The Space Environment
(b) See Section III, B - Nozzle Locking

U - At all LO_2/LH_2 M.R.'s, H_2O vapor is present in products of combustion. At MR = 1, H_2O concentration ≈12%.

V - The best type of actuators for constant positioning are actuators with screw outputs and piston-cylinder utilizing relatively incompressible fluids.

Report 10484-FR, Volume 1

Secondary Gas Coolant Properties and Engine and Gas Generator Operating Conditions

SECONDARY GAS COOLANT PROPERTIES

T_o = 860°R

c^* = 4735 ft/sec

γ = 1.40

A^* = 2.407 $in.^2$

$$P_{o,\ turbine} = \frac{(c^*)\ (\dot{w})}{(A^*)\ (q_c)}$$

ENGINE AND GAS GENERATOR OPERATING CONDITIONS

	P_c (psia)	Mass Flow Rates (lbm/sec)	
		Thrust Chamber	Gas Generator Combustor
R_t = 1.28 in.	300	6.71	0.028
	500	11.11	0.0778
	1,000	22.09	0.311
R_t = 1.81 in.	300	13.42	0.056
	500	22.22	0.1566
	1,000	44.18	0.622

TABLE XII

Report 10484-FR, Volume 1

RAO NOZZLE CONTOURS
AREA RATIO = 80, MINIMUM LENGTH

R/R_t	Z/R_t	Surface* Area, in^2
1.0000	.00000	.00000
1.2138	.61802	7.3548
1.2690	.68877	8.5044
1.3558	.80046	10.420
1.4484	.92026	12.610
1.5480	1.0501	15.138
1.6585	1.1925	18.093
1.7769	1.3493	21.562
1.9054	1.5233	25.666
2.0479	1.7185	30.572
2.2037	1.9379	36.460
2.3756	2.1864	43.579
2.5665	2.4698	52.264
2.7784	2.7952	62.942
3.2321	3.5331	89.719
3.5423	4.0718	111.39
3.9823	4.8869	147.24
4.4115	5.7450	188.69
4.7865	6.5492	230.69
5.0688	7.1906	266.23
5.2807	7.6936	295.30
5.6019	8.4934	343.58
5.9260	9.3497	397.90
6.1193	9.8859	433.24
6.4607	10.881	501.37
6.7200	11.682	558.48
6.9155	12.314	604.93
7.2120	13.322	681.33
7.5107	14.403	766.32
7.7149	15.184	829.60
7.8938	15.899	888.80
8.2089	17.234	1002.5
8.4448	18.304	1096.4
8.7994	20.045	1254.1
8.9435	20.810	1325.2

* For R_t = 1.28 inches, Surface Area is Proportional to R_T^2

Table XIII

RAO NOZZLE CONTOURS (CONT'D)

AREA RATIO = 80, 150% MINIMUM LENGTH

R/R_t	Z/R_t	Surface Area*, in^2
1.0000	.00000	.00000
1.1414	.51257	5.8039
1.1833	.58242	6.7788
1.2428	.68037	8.2101
1.3066	.78435	9.8112
1.3754	.89561	11.617
1.4500	.10158	13.674
1.5311	1.1469	16.040
1.6201	1.2910	18.786
1.7181	1.4506	22.004
1.8264	1.6287	25.804
1.9461	1.8284	30.324
2.0788	2.0537	35.741
2.2264	2.3096	42.287
2.3910	2.6025	50.271
2.7463	3.2636	70.105
2.9905	3.7444	86.026
3.3387	4.4698	112.24
3.6812	5.2330	142.45
3.9818	5.9476	173.03
4.2091	6.5177	198.90
4.3802	6.9649	220.07
4.6407	7.6765	255.26
4.9049	8.4393	294.91
5.0629	8.9173	320.74
5.3429	9.8056	370.63
5.5562	10.521	412.52
5.7179	11.087	446.67
5.9634	11.990	502.92
6.2117	12.959	565.64
6.3820	13.661	612.44
6.5318	14.304	656.32
6.7960	15.505	740.70
6.9946	16.470	810.59
7.2945	18.041	928.26
7.5917	19.759	1061.9
7.7655	20.852	1149.3
7.9160	21.861	1231.6
8.0464	22.787	1308.5
8.2708	24.513	1454.7
8.4344	25.898	1574.6
8.6713	28.145	1773.5
8.8917	30.578	1994.4
8.9432	31.213	2052.9

* For R_T = 1.28 inches, Surface Area is Proportional to R_T^2

TABLE XIII

RAO NOZZLE CONTOURS (CONT'D)

AREA RATIO = 140, MINIMUM LENGTH

R/R_t	Z/R_t	Surface Area *, in^2
1.0000	.00000	.00000
1.2350	.64407	7.7780
1.2733	.68986	8.5506
1.3681	.80379	10.571
1.4694	.92620	12.897
1.5784	1.0591	15.599
1.6968	1.2048	18.767
1.8262	1.3661	22.520
1.9712	1.5464	27.015
2.1324	1.7492	32.435
2.3061	1.9775	38.981
2.4984	2.2368	46.957
2.7127	2.5336	56.763
2.9518	2.8758	68.923
3.4689	3.6572	99.848
3.8257	4.2316	125.22
4.3369	5.1065	167.76
4.8411	6.0344	217.63
5.2865	6.9099	268.82
5.6245	7.6114	312.54
5.8794	8.1633	348.53
6.2692	9.0449	408.80
6.6662	9.9930	477.23
6.9048	10.589	522.07
7.3292	11.699	609.13
7.6542	12.596	682.68
7.9014	13.306	742.90
8.2788	14.442	842.55
8.6627	15.664	954.27
8.9277	16.550	1038.0
9.1616	17.363	1116.8
9.5772	18.886	1269.0
9.8921	20.111	1395.8
10.372	22.112	1610.4
10.855	24.307	1855.9
11.140	25.706	2017.7
11.390	27.001	2170.6
11.609	28.193	2314.0
11.832	29.476	2471.2

* For R_T = 1.28 inches, Surface Area is Proportional to R_T^2

TABLE XIII

RAO NOZZLE CONTOURS (CONT'D)

AREA RATIO = 140, 125% MINIMUM LENGTH

R/R_t	Z/R_t	Surface Area*, in^2
1.0000	.00000	.00000
1.1793	.57134	6.6394
1.1881	.58395	6.8267
1.2595	.68600	8.3961
1.3359	.79435	10.167
1.4183	.91067	12.188
1.5076	1.0367	14.514
1.6052	1.1745	17.218
1.7121	1.3266	20.392
1.8300	1.4956	24.149
1.9605	1.6848	28.634
2.1055	1.8981	34.030
2.2669	2.1399	40.571
2.4472	2.4161	48.571
2.6495	2.7339	58.452
3.0893	3.4576	83.450
3.3947	3.9889	103.90
3.8343	4.7971	138.12
4.2711	5.6547	178.26
4.6585	6.4638	219.49
4.9539	7.1129	254.77
5.1778	7.6242	283.88
5.5207	8.4413	332.67
5.8713	9.3212	388.21
6.0829	9.8751	424.69
6.4601	10.908	495.67
6.7501	11.743	555.80
6.9710	12.406	605.13
7.3095	13.466	686.96
7.6552	14.610	778.99
7.8944	15.441	848.15
8.1060	16.203	913.34
8.4833	17.633	1039.6
8.7701	18.786	1145.1
9.2091	20.671	1324.3
9.6520	22.743	1530.0
9.9153	24.067	1665.9
10.146	25.293	1794.7
10.349	26.422	1915.7
10.704	28.534	2147.7
10.968	30.235	2339.8
11.360	33.012	2662.1
11.740	36.041	3025.1
11.832	36.847	3123.5

* For R_T = 1.28 inches, Surface Area is Proportional to R_T^2

TABLE XIII

RAO NOZZLE CONTOURS (CONT'D)
AREA RATIO = 140, 150% MINIMUM LENGTH

R/R_t	Z/R_t	Surface Area *, in^2
1.0000	.00000	.00000
1.1569	.53771	6.1533
1.1861	.58336	6.8071
1.2506	.68307	8.2966
1.3199	.78903	9.9717
1.3947	.90264	11.872
1.4760	1.0256	14.050
1.5649	1.1599	16.571
1.6626	1.3079	19.516
1.7704	1.4722	22.987
1.8898	1.6559	27.115
2.0224	1.8626	32.060
2.1702	2.0966	38.032
2.3355	2.3634	45.309
2.5208	2.6699	54.261
2.9241	3.3661	76.796
3.2045	3.8762	95.153
3.6082	4.6510	125.78
4.0095	5.4718	161.59
4.3659	6.2457	198.32
4.6376	6.8660	229.70
4.8438	7.3547	255.58
5.1596	8.1352	298.93
5.4828	8.9757	348.26
5.6779	9.5047	380.65
6.0261	10.491	443.67
6.2938	11.289	497.04
6.4981	11.922	540.84
6.8112	12.936	613.51
7.1311	14.029	695.24
7.3527	14.822	756.67
7.5487	15.552	814.58
7.8986	16.919	926.83
8.1647	18.021	1020.6
8.5724	19.825	1179.9
8.9842	21.808	1362.9
9.2291	23.075	1483.9
9.4442	24.248	1598.5
9.6330	25.329	1706.3
9.9635	27.350	1912.9
10.210	28.979	2083.9
10.577	31.636	2370.9
10.932	34.534	2694.0
11.168	36.694	2941.3
11.370	38.708	3176.1
11.540	40.573	3397.0
11.684	42.287	3602.6
11.832	44.212	3836.2

* For R_T = 1.28 inches, Surface Area is Proportional to R_T^2

TABLE XIII

RAO NOZZLE CONTOURS (CONT'D)

AREA RATIO = 180, MINIMUM LENGTH

R/R_t	Z/R_t	Surface* Area, in^2
1.0000	.00000	.00000
1.2454	.65623	7.9825
1.2748	.69020	8.5663
1.3736	.80517	10.639
1.4791	.92880	13.032
1.5928	1.0631	15.820
1.7162	1.2105	19.099
1.8513	1.3738	22.993
2.0001	1.5563	27.660
2.1644	1.7618	33.298
2.3545	1.9959	40.207
2.5606	2.2616	48.648
2.7864	2.5652	59.035
3.0386	2.9156	71.957
3.5859	3.7178	105.00
3.9646	4.3090	132.26
4.5089	5.2115	178.18
5.0488	6.1720	232.35
5.5273	7.0802	288.20
5.8916	7.8096	336.11
6.1673	8.3843	375.66
6.5900	9.3039	442.10
7.0216	10.294	517.79
7.2820	10.918	567.55
7.7464	12.082	664.45
8.1033	13.023	746.58
8.3754	13.770	813.98
8.7923	14.965	925.85
9.2181	16.254	1051.7
9.5128	17.190	1146.3
9.7737	18.050	1235.4
10.239	19.662	1408.3
10.593	20.960	1552.6
11.137	23.085	1797.9
11.686	25.420	2079.6
12.015	26.912	2265.9
12.300	28.293	2442.5
12.553	29.565	2608.5
12.996	31.946	2926.9
13.328	33.866	3190.9
13.417	34.411	3267.0

* For R_T = 1.28 inches, Surface Area is Proportional to R_T^2

TABLE XIII

RAO NOZZLE CONTOURS (CONT'D)

AREA RATIO = 180, 125% MINIMUM LENGTH

R/R_t	Z/R_t	Surface Area, in^2 *
1.0000	.00000	.00000
1.1864	.58146	6.7901
1.1882	.58399	6.8283
1.2620	.68676	8.4240
1.3410	.79595	10.230
1.4263	.91323	12.295
1.5188	1.0404	14.679
1.6199	1.1796	17.458
1.7310	1.3334	20.728
1.8537	1.5045	24.612
1.9897	1.6963	29.263
2.1409	1.9127	34.875
2.3096	2.1584	41.702
2.4983	2.4394	50.077
2.7106	2.7635	60.462
3.1742	3.5035	86.894
3.4974	4.0485	108.65
3.9647	4.8799	145.27
4.4313	5.7651	188.50
4.8471	6.6028	233.15
5.1652	7.2762	271.53
5.4069	7.8074	303.29
5.7783	8.6580	356.72
6.1595	9.5760	417.79
6.3901	10.155	458.02
6.8028	11.236	536.59
7.1209	12.111	603.37
7.3642	12.807	658.32
7.7381	13.922	749.75
8.1214	15.127	852.95
8.3876	16.003	930.75
8.6237	16.808	1004.2
9.0464	18.321	1147.1
9 3690	19.542	1266.8
9.8657	21.543	1470.9
10.370	23.747	1706.4
10.672	25.157	1862.6
10.938	26.464	2011.0
11.172	27.670	2150.8
11.585	29.982	2419.7
11.894	31.751	2643.1
12.359	34.732	3019.7
12.813	37.991	3446.0
13.120	40.429	3774.0
13.383	42.705	4086.7
13.417	43.014	4129.5

* For R_T = 1.28 inches, Surface Area is Proportional to R_T^2

TABLE XIII

RAO NOZZLE CONTOURS (CONT'D)

AREA RATIO = 180, 150% MINIMUM LENGTH

R/R_t	Z/R_t	Surface Area, in^2 *
1.0000	.00000	.00000
1.1637	.54830	6.3040
1.1870	.58363	6.8157
1.2537	.68409	8.3305
1.3254	.79088	10.038
1.4029	.90548	11.981
1.4872	1.0296	14.213
1.5794	1.1653	16.802
1.6809	1.3149	19.836
1.7930	1.4812	23.422
1.9175	1.6674	27.699
2.0561	1.8772	32.840
2.2106	2.1150	39.067
2.3838	2.3864	46.679
2.5784	2.6989	56.081
3.0037	3.4107	79.889
3.3003	3.9337	99.394
3.7295	4.7304	132.13
4.1582	5.5772	170.65
4.5405	6.3778	210.37
4.8333	7.0211	244.47
5.0558	7.5284	272.67
5.3979	8.3405	320.07
5.7492	9.2167	374.23
5.9618	9.7689	409.91
6.3428	10.801	479.56
6.6367	11.637	538.77
6.8616	12.301	587.49
7.2075	13.366	668.58
7.5622	14.517	760.11
7.8087	15.353	829.13
8.0276	16.123	894.35
8.4196	17.569	1021.2
8.7191	18.736	1127.4
9.1805	20.650	1308.8
9.6498	22.758	1518.2
9.9307	24.108	1657.1
10.178	25.359	1789.1
10.397	26.513	1913.6
10.782	28.675	2152.9
11.071	30.421	2351.9
11.505	33.274	2687.3
11.930	36.393	3067.0
12.218	38.725	3359.1
12.465	40.903	3637.5
12.676	42.924	3900.5
12.857	44.784	4146.2
13.162	48.262	4613.7
13.377	51.053	4996.0
13.417	51.615	5073.8

* For R_T = 1.28 inches, Surface Area is Proportional to R_T^2

TABLE XIII

RAO NOZZLE CONTOURS (CONT'D)

AREA RATIO = 240, MINIMUM LENGTH

R/R_t	Z/R_t	Surface * Area, in^2
1.0000	.00000	.00000
1.2593	.67183	8.2515
1.2761	.69049	8.5801
1.3803	.80680	10.723
1.4917	.93200	13.206
1.6116	1.0682	16.112
1.7419	1.2178	19.542
1.8845	1.3838	23.631
2.0416	1.5695	28.547
2.2156	1.7788	34.507
2.4092	2.0166	41.792
2.6254	2.2885	50.765
2.8655	2.6014	61.896
3.1607	2.9698	76.093
3.7455	3.8002	112.05
4.1514	4.4132	141.85
4.7361	5.3504	192.28
5.3181	6.3502	252.06
5.8357	7.2975	313.96
6.2312	8.0598	367.26
6.5314	8.6614	411.40
6.9925	9.6253	485.74
7.4654	10.666	570.77
7.7516	11.322	626.82
8.2631	12.548	736.28
8.6579	13.542	829.39
8.9597	14.331	906.00
9.4237	15.596	1033.5
9.8992	16.963	1177.4
10.230	17.957	1285.9
10.523	18.871	1388.4
11.049	20.587	1587.7
11.450	21.972	1754.7
12.069	24.243	2039.6
12.700	26.744	2368.4
13.078	28.344	2586.6
13.412	29.828	2793.9
13.706	31.197	2989.3
14.226	33.761	3365.5
14.617	35.832	3678.4
15.207	39.220	4206.2
15.492	40.995	4490.4

* For R_T = 1.28 inches, Surface Area is Proportional to R_T^2

TABLE XIII

RAO NOZZLE CONTOURS (CONT'D)

AREA RATIO = 240, 125% MINIMUM LENGTH

R/R_t	Z/R_t	Surface * Area , in^2
1.0000	.00000	.00000
1.1946	.59280	6.9619
1.2647	.68754	8.4532
1.3467	.79766	10.299
1.4353	.91603	12.415
1.5315	1.0445	14.867
1.6367	1.1853	17.733
1.7526	1.3409	21.117
1.8807	1.5144	25.148
2.0229	1.7090	29.992
2.1814	1.9290	35.859
2.3586	2.1792	43.022
2.5575	2.4659	51.848
2.7814	2.7970	62.831
3.2728	3.5559	90.981
3.6169	4.1165	114.30
4.1170	4.9751	153.84
4.6186	5.8921	200.83
5.0680	6.7629	249.67
5.4130	7.4645	291.85
5.6760	8.0192	326.88
6.0813	8.9089	386.05
6.4990	9.8713	453.97
6.7525	10.479	498.89
7.2077	11.617	586.92
7.5601	12.540	662.06
7.8304	13.275	724.08
8.2471	14.455	827.62
8.6760	15.732	944.94
8.9750	16.662	1033.7
9.2410	17.518	1117.8
9.7191	19.128	1281.7
10.086	20.430	1419.6
10.653	22.569	1655.8
11.234	24.930	1929.7
11.583	25.445	2112.2
11.892	27.850	2286.1
12.166	29.148	2450.3
12.651	31.582	2767.4
13.017	33.551	3032.0
13.571	36.776	3479.9
14.121	40.312	3990.0
14.496	42.963	4384.3
14.821	45.443	4761.8
15.102	47.751	5119.8
15.345	49.879	5455.5
15.491	51.237	5672.3

* For R_T = 1.28 inches, Surface Area is Proportional to R_T^2

TABLE XIII

RAO NOZZLE CONTOURS (CONT'D)

AREA RATIO = 240, 150% MINIMUM LENGTH

R/R_t	Z/R_t	Surface * Area, in^2
1.0000	.00000	.00000
1.1716	.56014	6.4751
1.1877	.58384	6.8227
1.2569	.68513	8.3665
1.3314	.79285	10.111
1.4120	.90854	12.102
1.4997	1.0340	14.396
1.5958	1.1712	17.065
1.7017	1.3227	20.202
1.8189	1.4913	23.922
1.9491	1.6802	28.373
2.0943	1.8934	33.740
2.2567	2.1355	40.267
2.4390	2.4123	48.275
2.6444	2.7315	58.206
3.0949	3.4609	83.517
3.4108	3.9988	104.40
3.8697	4.8206	139.66
4.3306	5.6974	181.45
4.7434	6.5287	224.80
5.0607	7.1983	262.19
5.3027	7.7275	293.23
5.6759	8.5761	345.61
6.0607	9.4940	405.73
6.2944	10.073	445.47
6.7142	11.158	523.33
7.0396	12.039	589.81
7.2894	12.740	644.68
7.6745	13.865	736.29
8.0714	15.083	840.14
8.3484	15.971	918.73
8.5948	16.788	993.17
9.0381	18.326	1138.4
9.3784	19.570	1260.7
9.9054	21.614	1470.2
10.445	23.871	1713.3
10.771	25.320	1875.4
11.059	26.664	2029.9
11.314	27.906	2175.9
11.766	30.236	2457.8
12.108	32.120	2693.2
12.627	35.208	3091.9
13.141	38.594	3546.0
13.493	41.132	3897.3
13.798	43.506	4233.5
14.062	45.714	4552.4
14.290	47.750	4851.3
14.680	51.565	5423.2
14.961	54.636	5893.8
15.361	59.645	6677.9
15.491	61.483	6970.5

* $R_t = 1.28$ inches. Surface Area is Proportional to R_t^2

RAO NOZZLE CONTOURS (CONT.'D)

AREA RATIO = 280, MINIMUM LENGTH

R/R_t	Z/R_t	Surface* Area, in^2
1.0000	.00000	.00000
1.2697	.68310	8.4510
1.2766	.69059	8.5853
1.3850	.80786	10.780
1.5008	.93421	13.334
1.6255	1.0718	16.329
1.7610	1.2230	19.876
1.9094	1.3909	24.115
2.0729	1.5790	29.224
2.2539	1.7913	35.433
2.4553	2.0325	43.038
2.6797	2.3085	52.420
2.9348	2.6273	64.124
3.1889	2.9920	78.549
3.8634	3.8592	117.16
4.2944	4.4909	148.98
4.9038	5.4521	202.64
5.5102	6.4768	266.29
6.0498	7.4477	332.25
6.4624	8.2290	389.07
6.7759	8.8460	436.17
7.2580	9.8348	515.55
7.7531	10.903	606.44
8.0530	11.577	666.41
8.5902	12.837	783.67
9.0052	13.859	883.51
9.3230	14.671	965.75
9.8123	15.974	1102.8
10.315	17.383	1257.7
10.665	18.408	1374.6
10.976	19.351	1485.1
11.534	21.123	1700.4
11.961	22.554	1881.0
12.622	24.903	2189.7
13.297	27.493	2546.7
13.703	29.152	2784.1
14.062	30.692	3009.9
14.380	32.112	3223.0
14.942	34.777	3633.9
15.367	36.930	3976.3
16.010	40.457	4555.2
16.647	44.322	5213.6
16.733	44.881	5310.8

* For R_T = 1.28 inches, Surface Area is Proportional to R_T^2

TABLE XIII

RAO NOZZLE CONTOURS (CONT'D)

AREA RATIO = 280, 125% MINIMUM LENGTH

R/R_t	Z/R_t	Surface * Area , in^2
1.0000	.00000	.00000
1.1995	.59928	7.0613
1.2661	.68794	8.4689
1.3498	.79860	10.337
1.4404	.91759	12.484
1.5388	1.0468	14.975
1.6464	1.1885	17.893
1.7650	1.3452	21.343
1.8963	1.5200	25.461
2.0421	1.7163	30.418
2.2049	1.9383	36.433
2.3870	2.1910	43.795
2.5914	2.4808	52.880
2.8222	2.8161	64.218
3.3292	3.5854	93.370
3.6855	4.1550	117.62
4.2040	5.0286	158.86
4.7257	5.9637	208.06
5.1942	6.8531	259.37
5.5546	7.5706	303.79
5.8297	8.1385	340.76
6.2545	9.0503	403.33
6.6930	10.038	475.32
6.9596	10.662	523.02
7.4392	11.831	616.69
7.8111	12.782	696.81
8.0968	13.538	763.03
8.5380	14.755	873.80
8.9931	16.072	999.58
9.3110	17.033	1094.9
9.5941	17.917	1185.3
10.104	19.583	1361.9
10.496	20.931	1510.8
11.104	23.148	1766.4
11.729	25.598	2063.5
12.105	27.171	2261.9
12.440	28.632	2451.2
12.736	29.982	2630.3
13.263	32.516	2976.7
13.662	34.568	3266.4
14.269	37.932	3757.9
14.874	41.625	4319.3
15.290	44.397	4754.4
15.651	46.993	5171.8
15.966	49.410	5568.5
16.238	51.641	5941.1
16.705	55.829	6655.7
16.734	56.107	6703.8

* For R_T = 1.28 inches, Surface Area is Proportional to R_T^2

TABLE XIII

RAO NOZZLE CONTOURS (CONT.'D)

AREA RATIO = 280, 150% MINIMUM LENGTH

R/R_t	Z/R_t	Surface *2 Area, in^2
1.0000	.00000	.00000
1.1761	.56669	6.5708
1.1880	.58392	6.8255
1.2586	.68567	8.3854
1.3347	.79391	10.151
1.4170	.91019	12.169
1.5067	1.0363	14.498
1.6050	1.1744	17.212
1.7133	1.3269	20.408
1.8333	1.4968	24.203
1.9668	1.6873	28.752
2.1158	1.9023	34.249
2.2825	2.1467	40.945
2.4698	2.4264	49.178
2.6812	2.7494	59.411
3.1459	3.4886	85.582
3.4725	4.0346	107.25
3.9480	4.8703	143.96
4.4269	5.7636	187.64
4.8570	6.6121	233.09
5.1882	7.2964	272.39
5.4410	7.8376	305.07
5.8317	8.7065	360.35
6.2354	9.6473	423.93
6.4809	10.242	466.04
6.9229	11.356	548.72
7.2660	12.262	619.46
7.5299	12.983	677.94
7.9374	14.142	775.76
8.3582	15.398	886.87
8.6524	16.314	971.10
8.9146	17.158	1051.0
9.3871	18.748	1207.2
9.7507	20.035	1339.0
10.315	22.152	1565.2
10.896	24.492	1828.6
11.246	25.996	2004.5
11.558	27.392	2172.5
11.834	28.684	2331.4
12.325	31.108	2639.1
12.698	33.071	2896.4
13.266	36.291	3333.4
13.832	39.827	3832.9
14.221	42.481	4220.1
14.561	44.965	4591.7
14.856	47.279	4944.8
15.112	49.414	5276.5
15.552	53.420	5912.6
15.872	56.649	6437.5
16.333	61.925	7315.4
16.733	67.320	8236.1

* For R_T = 1.28 inches, Surface Area is Proportional to R_T^2

TABLE XIII

a. P_c = 300 psia

	ϵ = 80 L/L Minimum			ϵ = 140 L/L Minimum			ϵ = 180 L/L Minimum			ϵ = 240 L/L Minimum			ϵ = 280 L/L Minimum			ϵ = 300 L/L Minimum		
	1	1.25	1.50	1	1.25	1.50	1	1.25	1.50	1	1.25	1.50	1	1.25	1.50	1	1.25	1.50
ISP, THEØ	461.4	461.4	461.4	470.2	470.2	470.2	473.7	473.7	473.7	477.4	477.4	477.4	479.2	479.2	479.2	479.9	479.9	479.9
ISP, ØDK	449.2	449.6	449.9	456.7	457.2	457.4	459.6	460.1	460.4	462.7	463.2	463.5	464.2	464.7	464.9	464.9	465.4	465.8
ISP, TBL	3.32	3.43	3.82	4.06	4.53	5.01	4.95	5.51	6.10	5.96	6.65	7.35	6.45	7.19	7.95	6.64	7.41	8.06
ISP, DIV	6.17	2.01	0.41	4.84	1.58	0.23	4.46	1.45	0.14	4.06	1.32	0.09	3.84	1.23	0.05	3.76	1.20	0.04
ISP,CØØL	0.84	0.84	0.84	1.08	1.08	1.08	1.05	1.05	1.05	1.02	1.02	1.02	1.01	1.01	1.01	1.00	1.00	1.00
ISP,ERL	4.61	4.61	4.61	4.70	4.70	4.70	4.74	4.74	4.74	4.77	4.77	4.77	4.79	4.79	4.79	4.80	4.80	4.80
ISP, DEL	434.3	438.8	440.2	442.0	445.3	446.4	444.7	447.4	448.4	446.9	449.5	450.2	448.1	450.5	451.1	448.7	451.0	451.9

b. P_c = 500 psia

	ϵ = 80 L/L Minimum			ϵ = 140 L/L Minimum			ϵ = 180 L/L Minimum			ϵ = 240 L/L Minimum			ϵ = 280 L/L Minimum			ϵ = 300 L/L Minimum		
	1	1.25	1.50	1	1.25	1.50	1	1.25	1.50	1	1.25	1.50	1	1.25	1.50	1	1.25	1.50
ISP, THEØ	462.1	462.1	462.1	470.8	470.8	470.8	474.2	474.2	474.2	477.9	477.9	477.9	479.7	479.7	479.7	480.6	480.6	480.6
ISP, ØDK	454.0	454.4	454.6	461.7	462.2	462.4	464.8	465.2	465.4	467.9	468.4	468.6	469.5	470.0	470.2	470.1	470.7	470.9
ISP, TBL	3.00	3.10	3.45	3.67	4.09	4.53	4.47	4.98	5.51	5.38	6.00	6.64	5.82	6.48	7.17	5.99	6.67	7.38
ISP, DIV	6.18	2.01	0.41	4.85	1.58	0.23	4.46	1.46	0.41	4.07	1.32	0.09	3.85	1.23	0.05	3.76	1.20	0.04
ISP,CØØL	1.59	1.59	1.59	1.75	1.75	1.75	1.71	1.71	1.71	1.67	1.67	1.67	1.66	1.66	1.66	1.65	1.65	1.65
ISP,ERL	4.62	4.62	4.62	4.71	4.71	4.71	4.74	4.74	4.74	4.78	4.78	4.78	4.80	4.80	4.80	4.80	4.80	4.80
ISP, DEL	438.6	443.0	444.5	446.7	450.1	451.2	449.4	452.3	453.3	452.0	454.6	455.4	453.3	455.8	456.5	453.9	456.4	457.

DELIVERED PERFORMANCE, R_T = 1.28 INCHES

Table XIV, Sheet 1 of 2

c. P_c = 1000 psia

	ϵ = 80 L/L Minimum			ϵ = 140 L/L Minimum			ϵ = 180 L/L Minimum			ϵ = 240 L/L Minimum			ϵ = 280 L/L Minimum			ϵ = 300 L/L Minimum		
	1	1.25	1.50	1	1.25	1.50	1	1.25	1.50	1	1.25	1.50	1	1.25	1.50	1	1.25	1.50
ISP, THEØ	462.9	462.9	462.9	471.5	471.5	471.5	474.9	474.9	474.9	478.4	478.4	478.4	480.2	480.2	480.2	480.9	480.9	480.9
ISP, ØDK	458.7	459.0	459.1	466.8	467.1	467.2	470.0	470.3	470.4	473.2	473.6	473.7	474.9	475.2	475.4	475.5	475.9	476.1
ISP, TBL	2.61	2.70	3.00	3.20	3.56	3.94	3.89	4.33	4.80	4.68	5.22	5.78	5.07	5.65	6.25	5.21	5.82	6.43
ISP, DIV	6.19	2.02	0.41	4.85	1.59	0.23	4.47	1.46	0.14	4.07	1.33	0.09	3.85	1.24	0.05	3.75	1.21	0.04
ISP, CØØL	3.10	3.10	3.10	3.36	3.36	3.36	3.32	3.32	3.32	3.27	3.27	3.27	3.25	3.25	3.25	3.25	3.25	3.25
ISP, ERL	4.63	4.63	4.63	4.71	4.71	4.71	4.75	4.75	4.75	4.78	4.78	4.78	4.80	4.80	4.80	4.80	4.80	4.80
ISP, DEL	442.2	446.5	448.0	450.7	453.9	455.0	453.5	456.4	457.4	456.4	458.8	459.8	457.9	460.3	461.0	458.5	460.8	461.6

a. P_c = 300 psia

	ϵ = 80 L/L Minimum			ϵ = 140 L/L Minimum			ϵ = 180 L/L Minimum			ϵ = 240 L/L Minimum			ϵ = 280 L/L Minimum			ϵ = 300 L/L Minimum		
	1	1.25	1.50	1	1.25	1.50	1	1.25	1.50	1	1.25	1.50	1	1.25	1.50	1	1.25	1.50
ISP, THEØ	461.4	461.4	461.4	470.2	470.2	470.2	473.7	473.7	473.7	477.4	477.4	477.4	479.2	479.2	479.2	479.8	479.8	479.8
ISP, ØDK	450.4	450.9	451.1	458.0	458.5	458.7	461.0	461.5	461.7	464.1	464.6	464.9	465.6	466.1	466.4	466.2	466.8	467.1
ISP, TBL	2.86	2.96	3.29	3.50	3.91	4.32	4.27	4.75	5.26	5.14	5.74	6.34	5.56	6.20	6.86	5.72	6.37	7.09
ISP, DIV	6.17	2.01	0.41	4.84	1.58	0.23	4.46	1.45	0.14	4.06	1.32	0.09	3.84	1.23	0.05	3.75	1.20	0.04
ISP, CØØL	0.92	0.92	0.92	1.01	1.01	1.01	0.99	0.99	0.99	0.97	0.97	0.97	0.90	0.90	0.90	0.85	0.85	0.85
ISP, ERL	4.61	4.61	4.61	4.70	4.70	4.70	4.74	4.74	4.74	4.77	4.77	4.77	4.79	4.79	4.79	4.80	4.80	4.80
ISP, DEL	435.9	440.4	441.9	444.0	447.3	448.5	446.5	449.6	450.6	449.1	451.8	452.7	450.5	453.0	453.8	451.1	453.6	454.3

b. P_c = 500 psia

	ϵ = 80 L/L Minimum			ϵ = 140 L/L Minimum			ϵ = 180 L/L Minimum			ϵ = 240 L/L Minimum			ϵ = 280 L/L Minimum			ϵ = 300 L/L Minimum		
	1	1.25	1.50	1	1.25	1.50	1	1.25	1.50	1	1.25	1.50	1	1.25	1.50	1	1.25	1.50
ISP, THEØ	462.1	462.1	462.1	470.8	470.8	470.8	474.2	474.2	474.2	477.9	477.9	477.9	479.7	479.7	479.7	480.3	480.3	480.3
ISP, ØDK	455.0	455.4	455.6	462.8	463.3	463.5	465.9	466.3	466.6	469.0	469.5	469.8	470.6	471.2	471.4	471.4	471.8	472.0
ISP, TBL	2.59	2.67	2.98	3.17	3.53	3.91	3.89	4.30	4.75	4.64	5.17	5.73	5.02	5.59	6.18	5.18	5.75	6.37
ISP, DIV	6.18	2.01	0.41	4.85	1.58	0.23	4.46	1.46	0.14	4.07	1.32	0.09	3.85	1.23	0.05	3.76	1.21	0.04
ISP, CØØL	1.51	1.51	1.51	1.65	1.65	1.65	1.62	1.62	1.62	1.60	1.60	1.60	1.52	1.52	1.52	1.47	1.47	1.47
ISP, ERL	4.62	4.62	4.62	4.71	4.71	4.71	4.74	4.74	4.74	4.78	4.78	4.78	4.80	4.80	4.80	4.80	4.80	4.80
ISP, DEL	440.1	444.6	446.1	448.6	451.8	453.0	451.2	452.2	455.3	453.9	456.7	457.6	455.4	458.0	458.8	456.2	458.6	459.3

DELIVERED PERFORMANCE, R_T = 1.81 INCHES

Table XV, Sheet 1 of 2

c.

P_c = 1000 psia

	ϵ = 80 L/L Minimum			ϵ = 140 L/L Minimum			ϵ = 180 L/L Minimum			ϵ = 240 L/L Minimum			ϵ = 280 L/L Minimum			ϵ = 300 L/L Minimum		
	1	1.25	1.50	1	1.25	1.50	1	1.25	1.50	1	1.25	1.50	1	1.25	1.50	1	1.25	1.50
ISP, THEØ	462.9	462.9	462.9	471.5	471.5	471.5	474.9	474.9	474.9	478.4	478.4	478.4	480.2	480.2	480.2	480.8	480.8	480.8
ISP, ØDK	459.3	459.6	459.7	467.5	467.8	467.9	470.7	471.0	471.1	474.0	474.3	474.5	475.6	476.0	476.1	476.2	476.6	476.8
ISP, TBL	2.25	2.33	2.59	2.76	3.07	3.40	3.35	3.73	4.14	4.04	4.50	4.98	4.37	4.87	5.39	4.50	5.02	5.56
ISP, DIV	6.19	2.02	0.41	4.85	1.59	0.23	4.47	1.46	0.14	4.07	1.33	0.09	3.85	1.24	0.05	3.76	1.22	0.04
ISP, CØØL	2.98	2.98	2.98	3.20	3.20	3.20	3.18	3.18	3.18	3.15	3.15	3.15	3.04	3.04	3.04	2.97	2.97	2.97
ISP, ERL	4.63	4.63	4.63	4.72	4.72	4.72	4.75	4.75	4.75	4.78	4.78	4.78	4.80	4.80	4.80	4.80	4.80	4.80
ISP, DEL	443.3	447.6	449.1	452.0	455.2	456.4	454.9	457.8	458 9	457.9	460.6	461.5	459.6	462.0	462.8	460.2	462.6	463.4

TABLE XVI

ε_o	L/L_{Min}	I_{sp}, sec			Δ Weight, lb		$\Delta W/\Delta I_{sp}$ (lb/sec)	
		ε_i = 100	ε_i = 140	ε_i = 180	ε_i = 100 - 140	ε_i = 100-180	ε_i = 100 - 140	ε_i = 100-180
				P_c = 300				
180	1.00	444.43	444.80	-	9.11	-	24.62	-
	1.25	447.38	447.79	-	11.49	-	28.02	-
	1.50	448.35	448.80	-	13.87	-	30.82	-
240	1.00	446.86	447.19	447.51	7.78	17.13	23.58	26.35
	1.25	449.46	449.85	450.19	9.34	21.24	23.95	29.10
	1.50	450.24	450.64	451.03	10.69	24.91	26.73	31.53
280		448.08	448.38	448.67	7.19	15.72	23.97	26.64
	1.25	450.48	450.81	451.14	8.55	17.03	25.91	28.83
	1.50	451.14	451.51	451.87	9.63	21 90	26.03	30.00
				P_c = 500				
180		449.37	449.70	-	9.11	-	27.61	-
	1.25	452.33	452.70	-	11.49	-	31.05	-
	1.50	453.34	453.75	-	13.87	-	33.83	-
240		451.99	452.29	452.57	7.78	17.13	25.93	29.53
	1.25	454.63	454.97	455.28	9.34	21.24	27.47	32.68
	1.50	455.44	455.81	456.16	10.69	24.91	28.89	34.60
280		453.22	453.49	453.75	7.19	15.72	26.63	29.66
	1.25	455.81	456.10	456.39	8.55	19.03	29.48	32.81
	1.50	456.53	456.86	451.18	9.63	21.90	29.18	33.69
				P_c = 1000				
180		453.52	453.81	-	9.11	-	31.41	-
	1.25	456.40	456.71	-	11.49	-	37.06	-
	1.50	457.39	457.75	-	13.87	-	38.53	-
240		456.44	456.70	456.99	7.78	17.13	29.92	31.15
	1.25	458.77	459.06	459.33	9.34	21.24	32.21	37.93
	1.50	459.81	460.13	460.44	10.69	24.91	33.41	39.54
280		457.90	458.14	458.37	7.19	15.72	29.96	33.45
	1.25	460.29	460.55	460.80	8.55	19.03	32.88	37.31
	1.50	461.03	461.33	461.60	9.63	21.90	32.10	38.42

NOTE: Values are also typical for R_t = 1.81 in.

TABLE XVII

TRADEOFF RATIO ($\Delta W/\Delta I_s$) FOR A VARIATION IN NOZZLE THROAT RADIUS (1.28 IN. TO 1.81 IN.)

	ε = 80 L/L Minimum			ε = 140 L/L Minimum			ε = 180 L/L Minimum			ε = 240 L/L Minimum			ε = 280 L/L Minimum		
	1.00	1.25	1.50	1.00	1.25	1.50	1.00	1.25	1.50	1.00	1.25	1.50	1.00	1.25	1.50
P_c = 300	16.69	20.94	24.78	23.62	28.75	33.81	21.72	25.78	29.65	24.86	29.55	33.98	38.05	45.36	53.14
P_c = 500	18.14	22.60	27.02	25.16	33.19	39.04	25.06	29.74	34.02	28.81	39.04	39.27	43.27	52.36	61.77
P_c = 1000	24.80	31.03	36.74	36.17	43.67	51.21	33.05	39.03	44.67	37.45	38.79	50.16	55.27	67.37	79.56

CHAMBER NOZZLE DATA

Step location		①	②	③
Height, in.		0.25	0.50	0.75
Nozzle radius at tip, in.		10.90	10.66	10.42
Nozzle wall pressure, psia		1.04	1.09	1.14
Nozzle Mach number		3.548	3.521	3.493

COOLANT RING INJECTION GROOVE DATA

Number of grooves	180			
*Groove depth, in.	0.019			
Groove exit width, in.		0.266	0.248	0.229
Groove throat width, in.	0.215			
Area ratio		1.238	1.153	1.065
Mach number		1.585	1.465	1.300
Velocity, ext, ft/sec		1485	1410	1291
Exit pressure for 5 psia and $\dot{w}$ = 0.1 lb/sec		1.20	1.435	1.752

*At 5 psia, groove dimensional tolerances of $\pm$0.001 can produce mass flows of 0.0944 to 0.1055 lb/sec and exit pressures at ① of 0.94 to 1.635 psia.

Chamber Nozzle and Coolant Ring Data

TABLE XVIII

TEST ENGINE NOZZLE CONTOUR

P_c = 100 psia

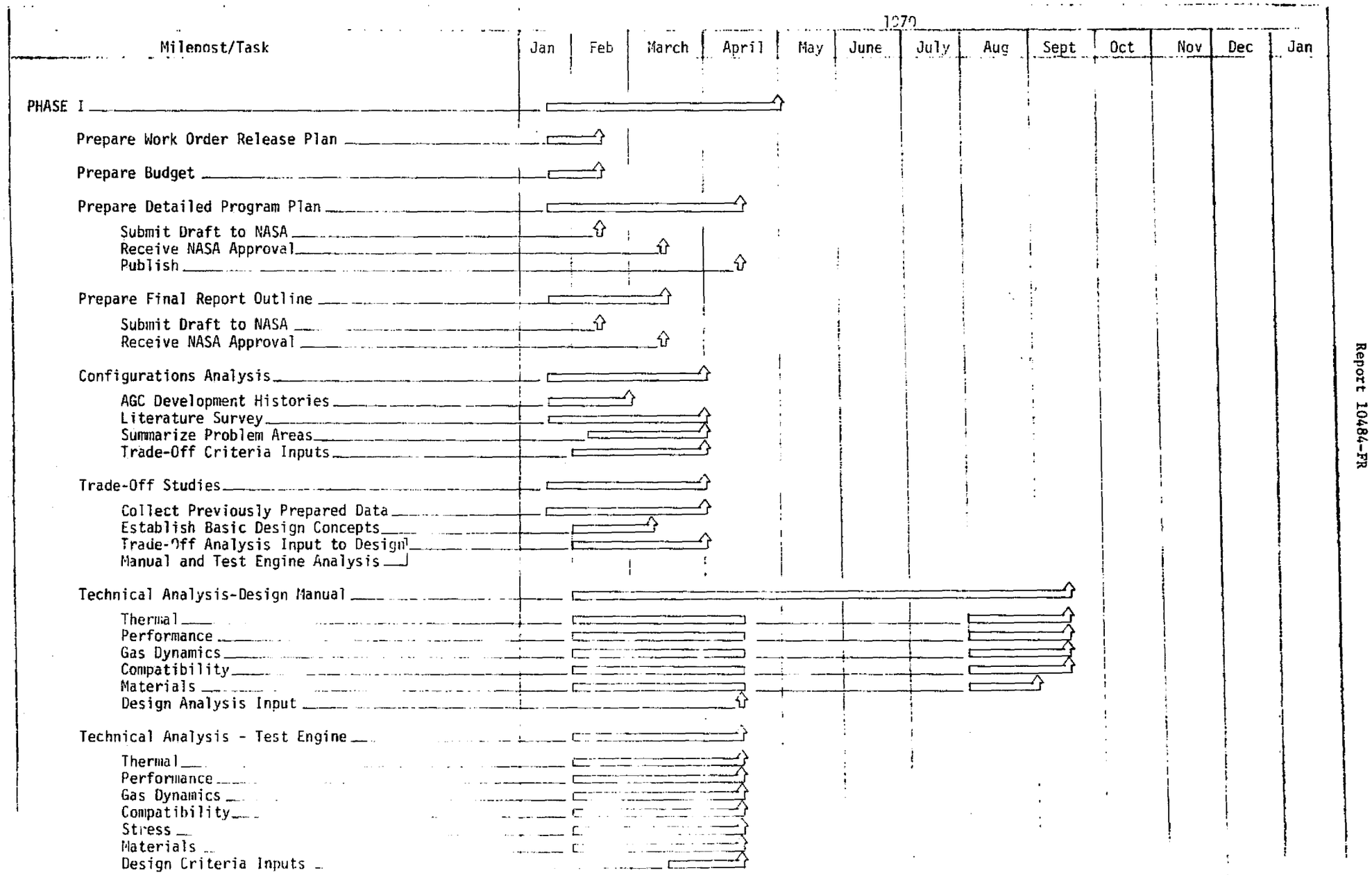
R_t = 2.472 inches

R_d = 0.704 inches

γ = 1.22

	Axial Coordinate (X, inches)	Radial Coordinate (R, inches)	Wall Angle (θ, degrees)	Mach Number (M)	Wall Pressure (P, psia)
Throat	0	2.47	0	1.20	44.2
Tangent	.387	2.587	33.29	2.19	9.49
	2.459	4.007	34.45	2.52	5.27
	4.587	5.412	32.23	2.78	3.32
	6.891	6.788	29.46	2.99	2.26
	9.404	8.127	26.69	3.16	1.63
	12.146	9.424	24.02	3.32	1.21
	15.131	10.677	21.57	3.45	.93
Interface	16.463	11.187	20.60	3.52	.84
	16.716	11.284	20.41	3.53	.83
	20.069	12.459	18.25	3.66	.66
	23.678	13.577	16.24	3.77	.54
Exit	29.018	15.000	13.76	3.91	.42

TABLE XIX



PHASE I AND II MASTER PROGRAM SCHEDULE

FIGURE 1

Report 10484-FR

Sheet 1 of 3

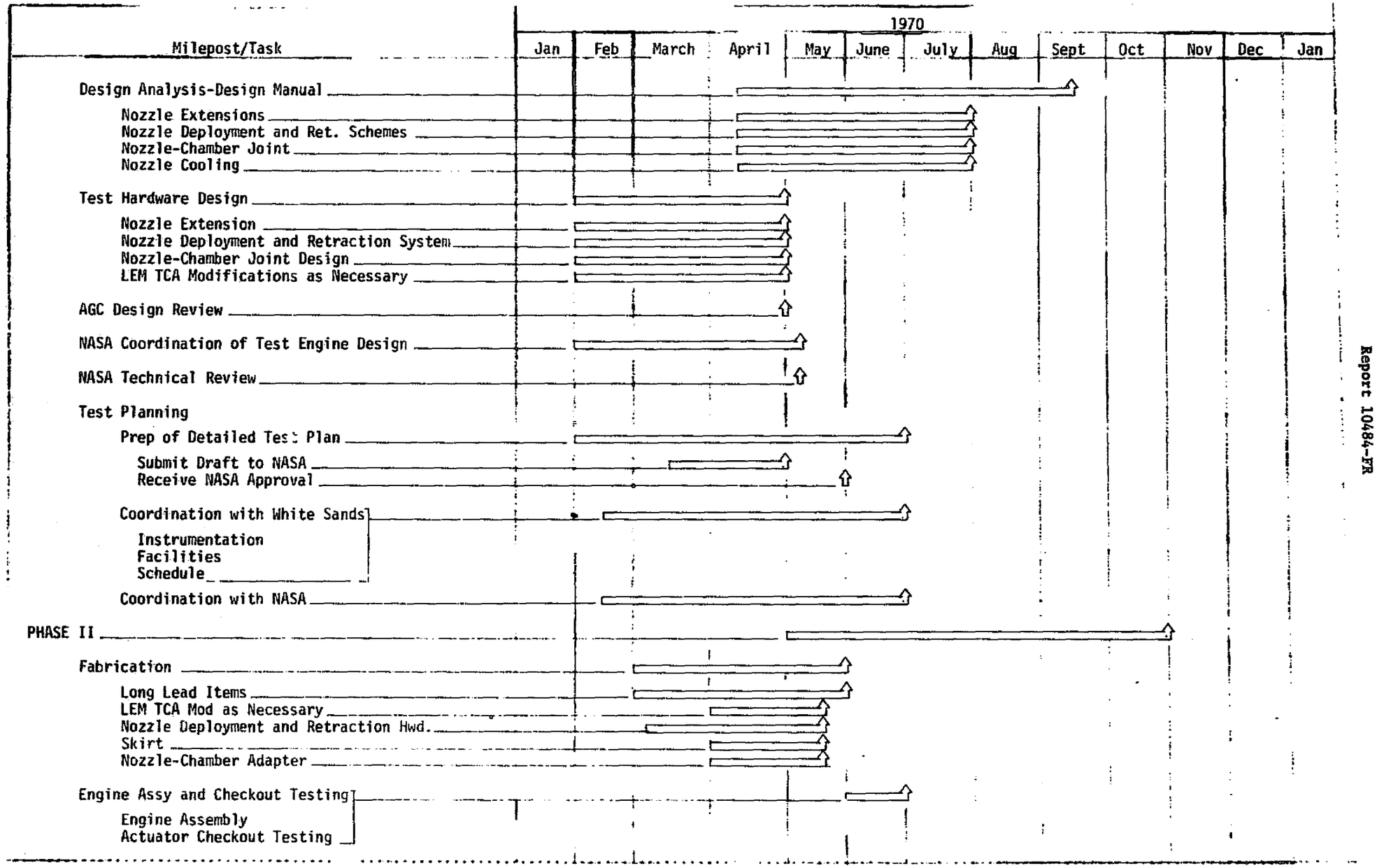


FIGURE 1

Sheet 2 of 3

Report 10484-FR

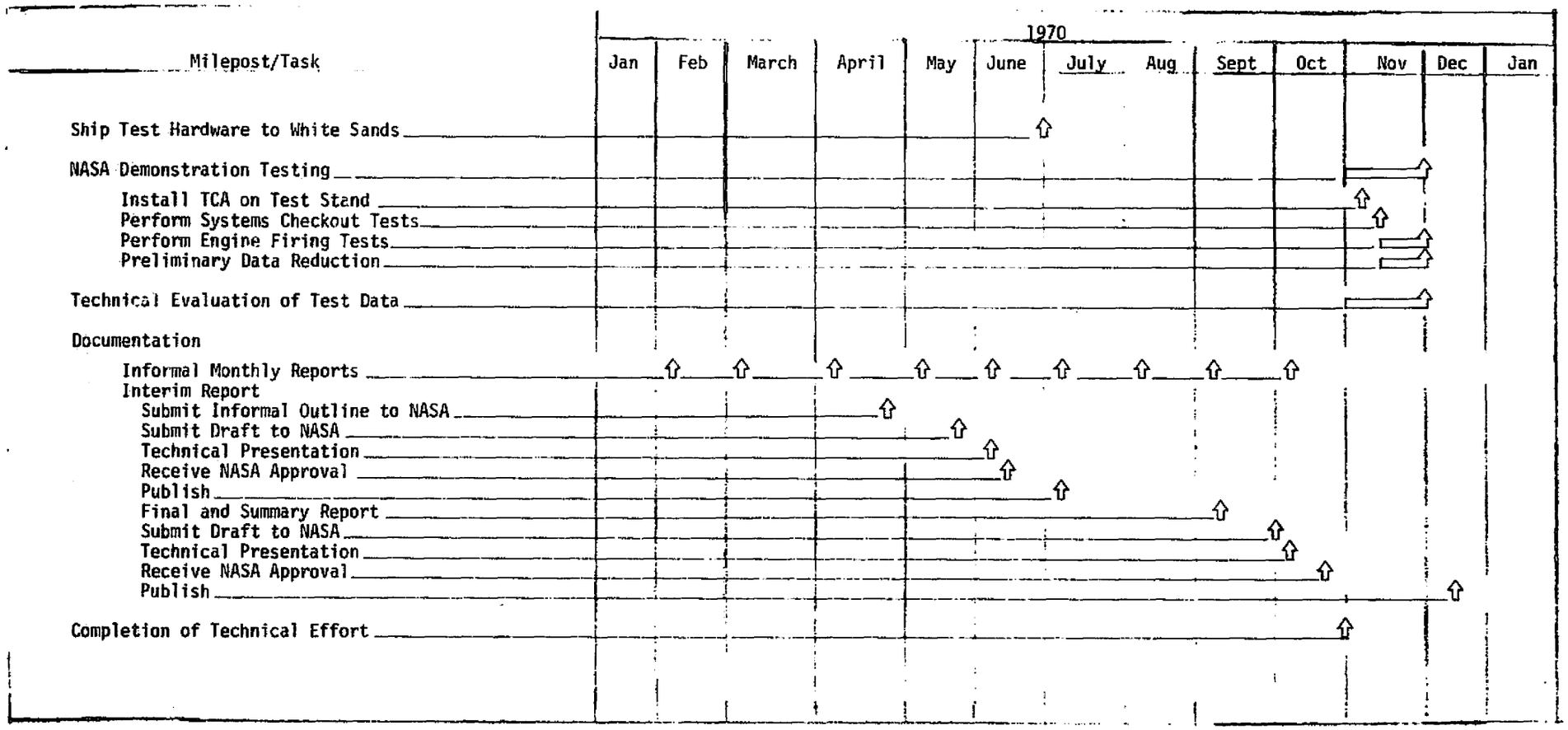

1970
Milepost/Task
Jan
Feb
March
April
May
June
July
Aug
Sept
Oct
Nov
Dec
Jan
Ship Test Hardware to White Sands
NASA Demonstration Testing
Install TCA on Test Stand
Perform Systems Checkout Tests
Perform Engine Firing Tests
Preliminary Data Reduction
Technical Evaluation of Test Data
Documentation
Informal Monthly Reports
Interim Report
Submit Informal Outline to NASA
Submit Draft to NASA
Technical Presentation
Receive NASA Approval
Publish
Final and Summary Report
Submit Draft to NASA
Technical Presentation
Receive NASA Approval
Publish
Completion of Technical Effort

FIGURE 1

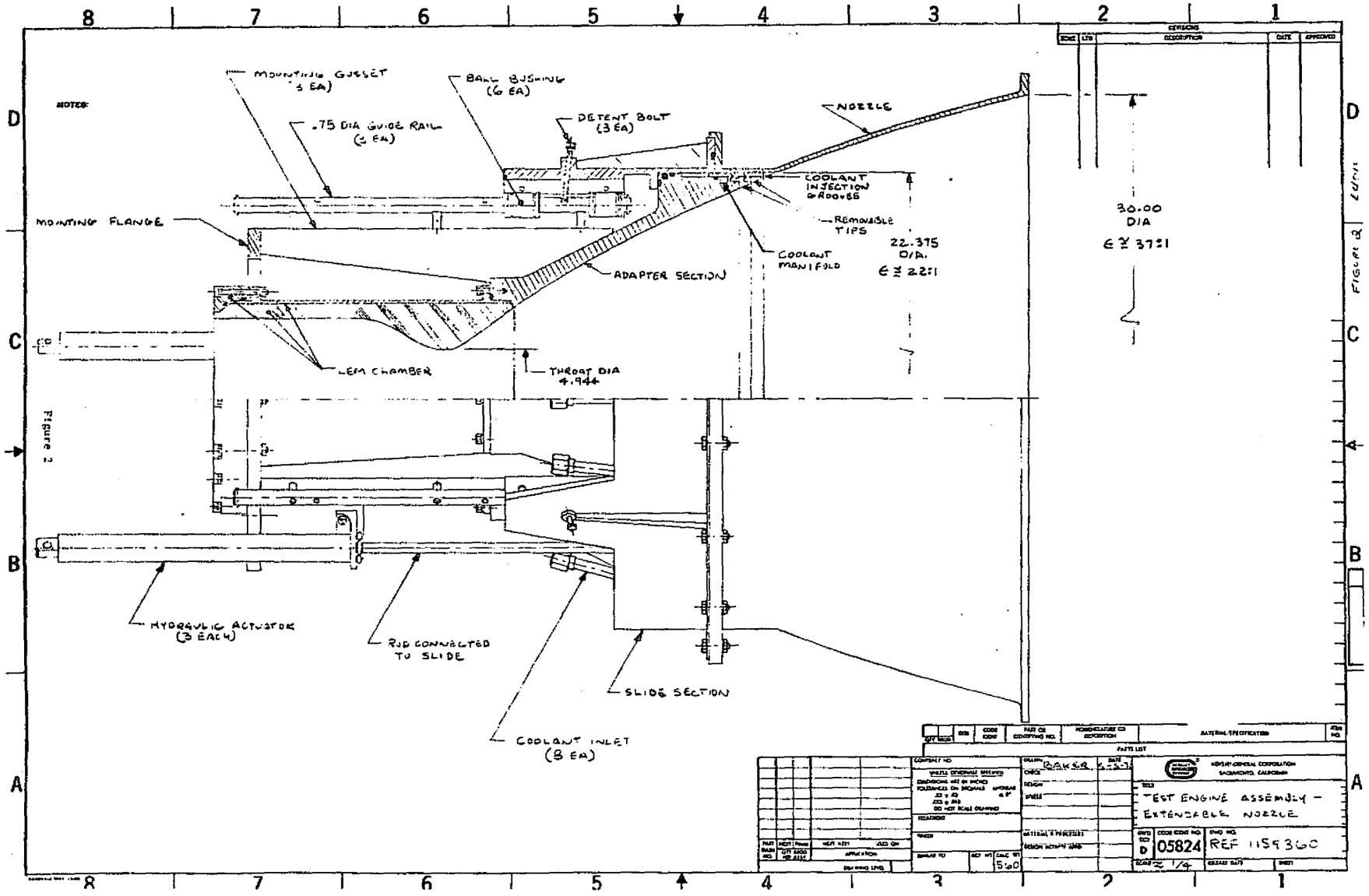
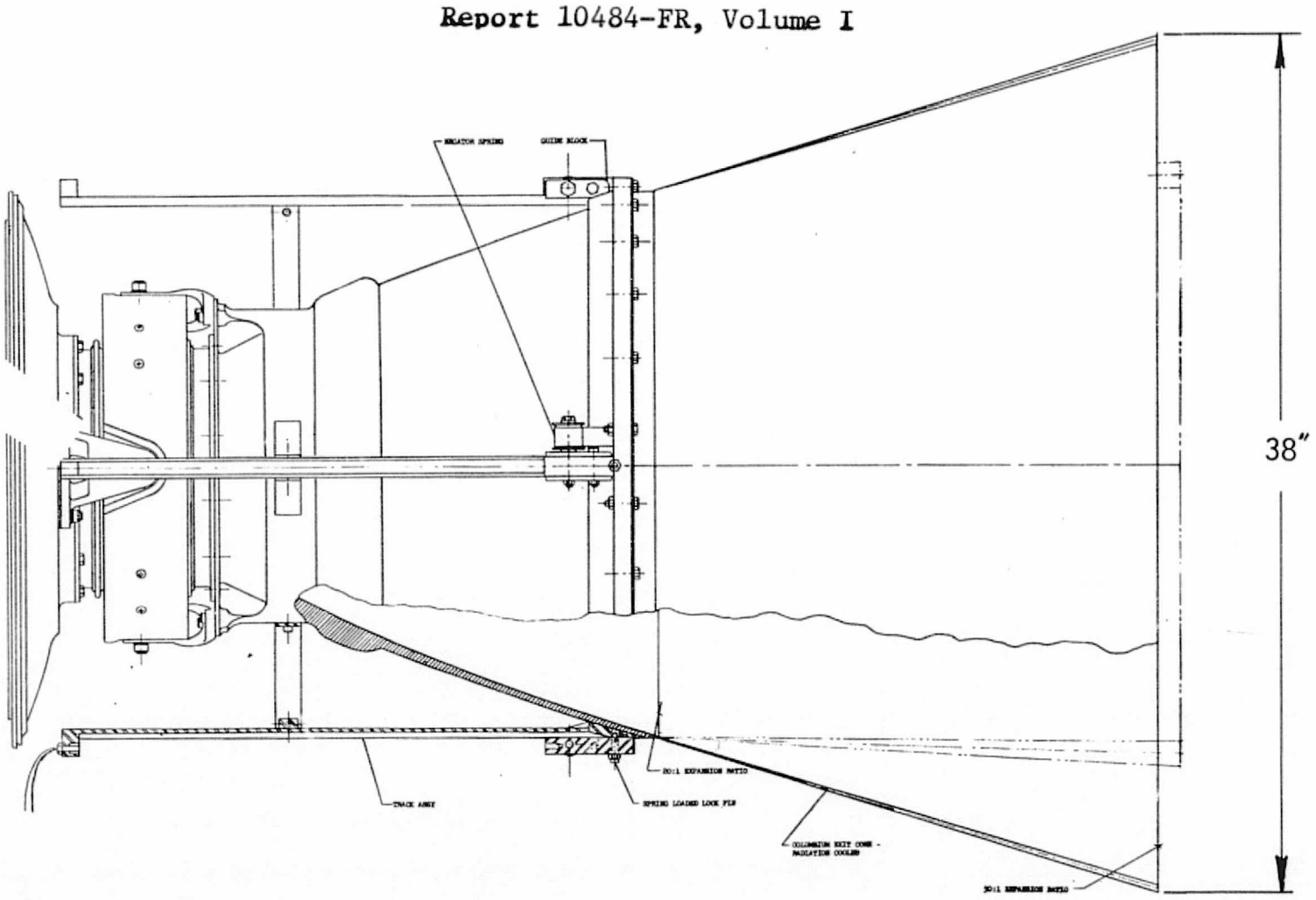


Figure 2

Extendable Nozzle Test Engine Assembly



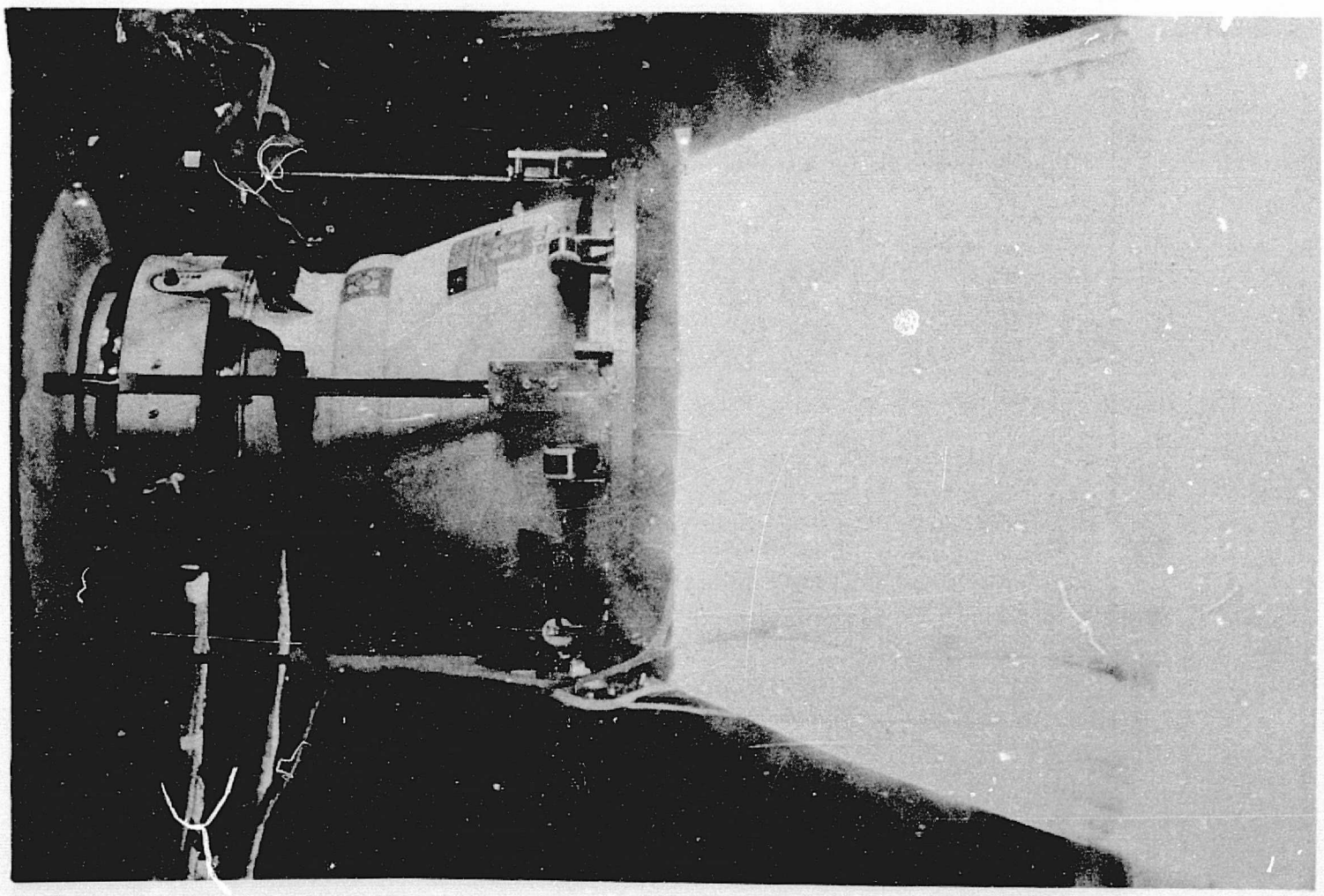


Figure 3. Extendable - Expandable Radiation Cooled Nozzle Extension in Test at Vacuum Conditions

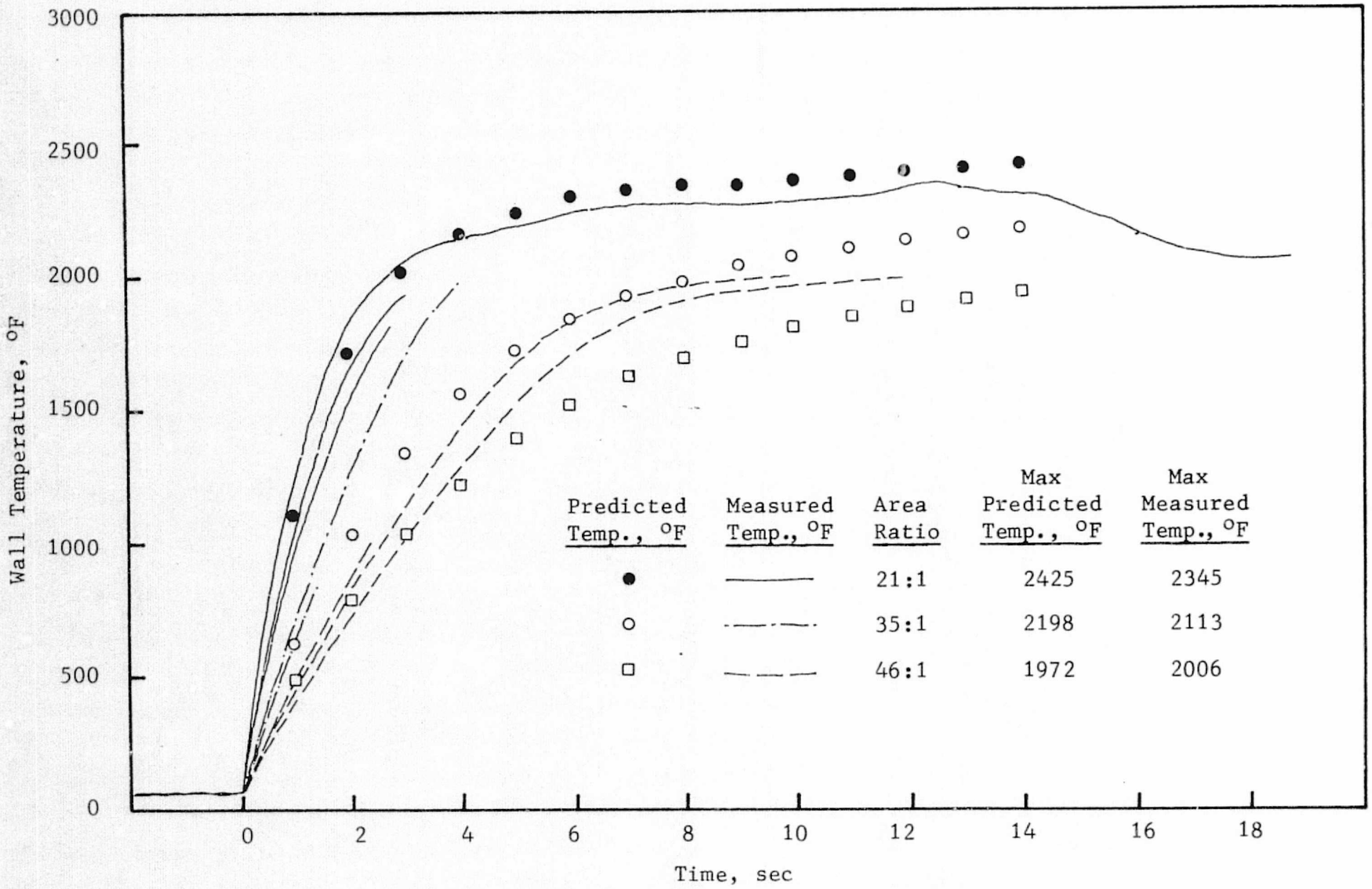


Figure 4

SKYBOLT EXTENDABLE NOZZLE TEMPERATURE DATA

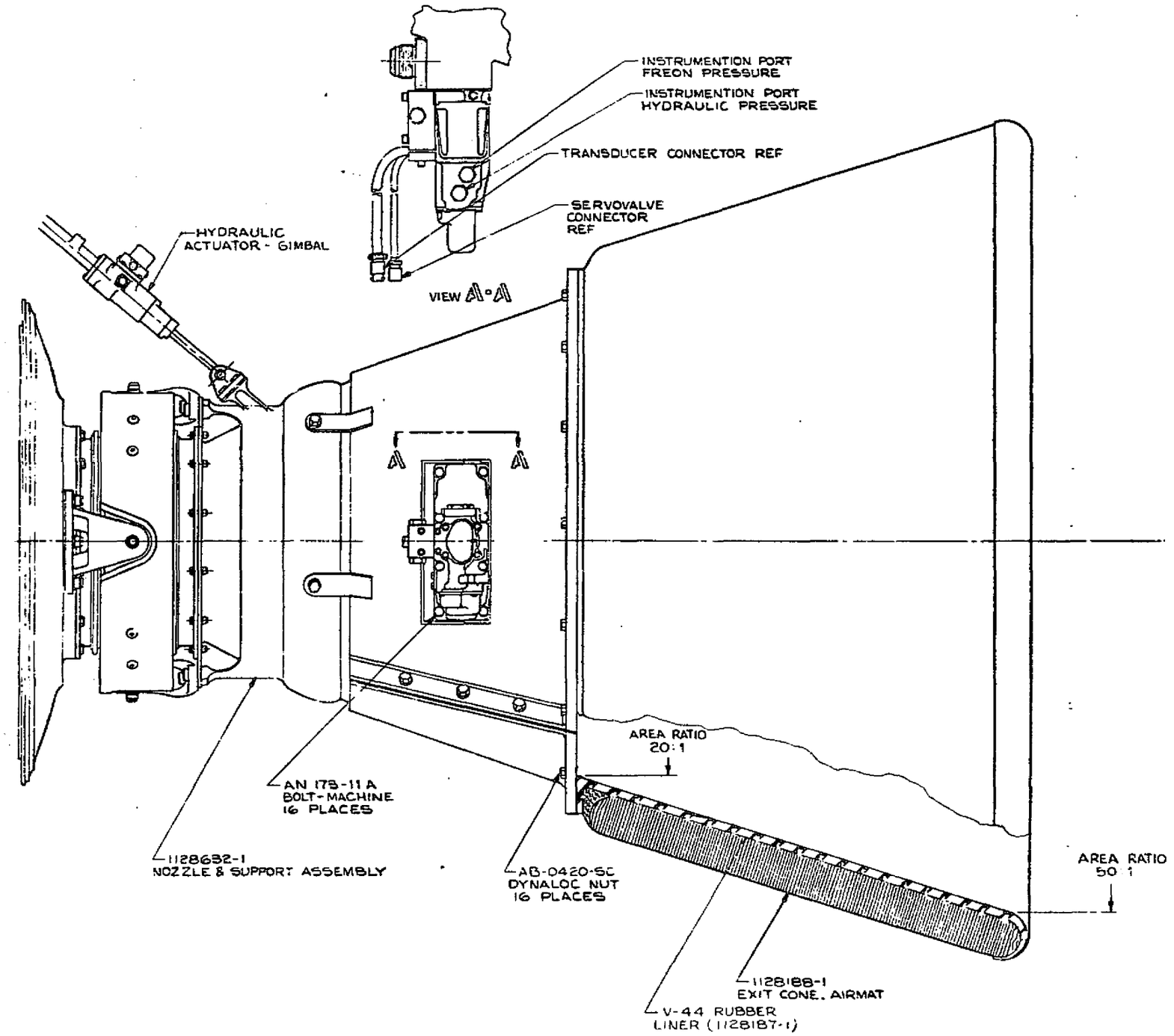


Figure 5

Airmat Reinforced Nozzle Extension - Solid Propellant Motor Design

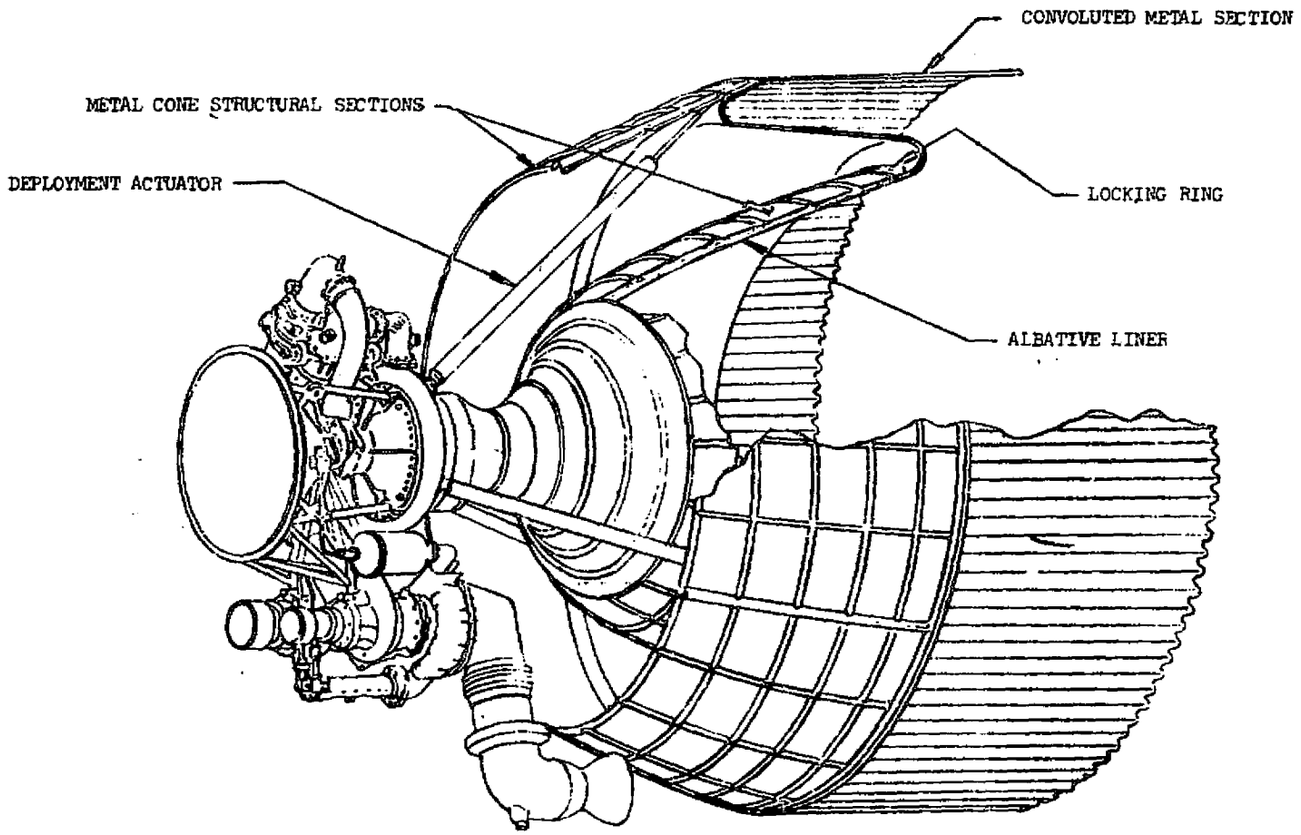
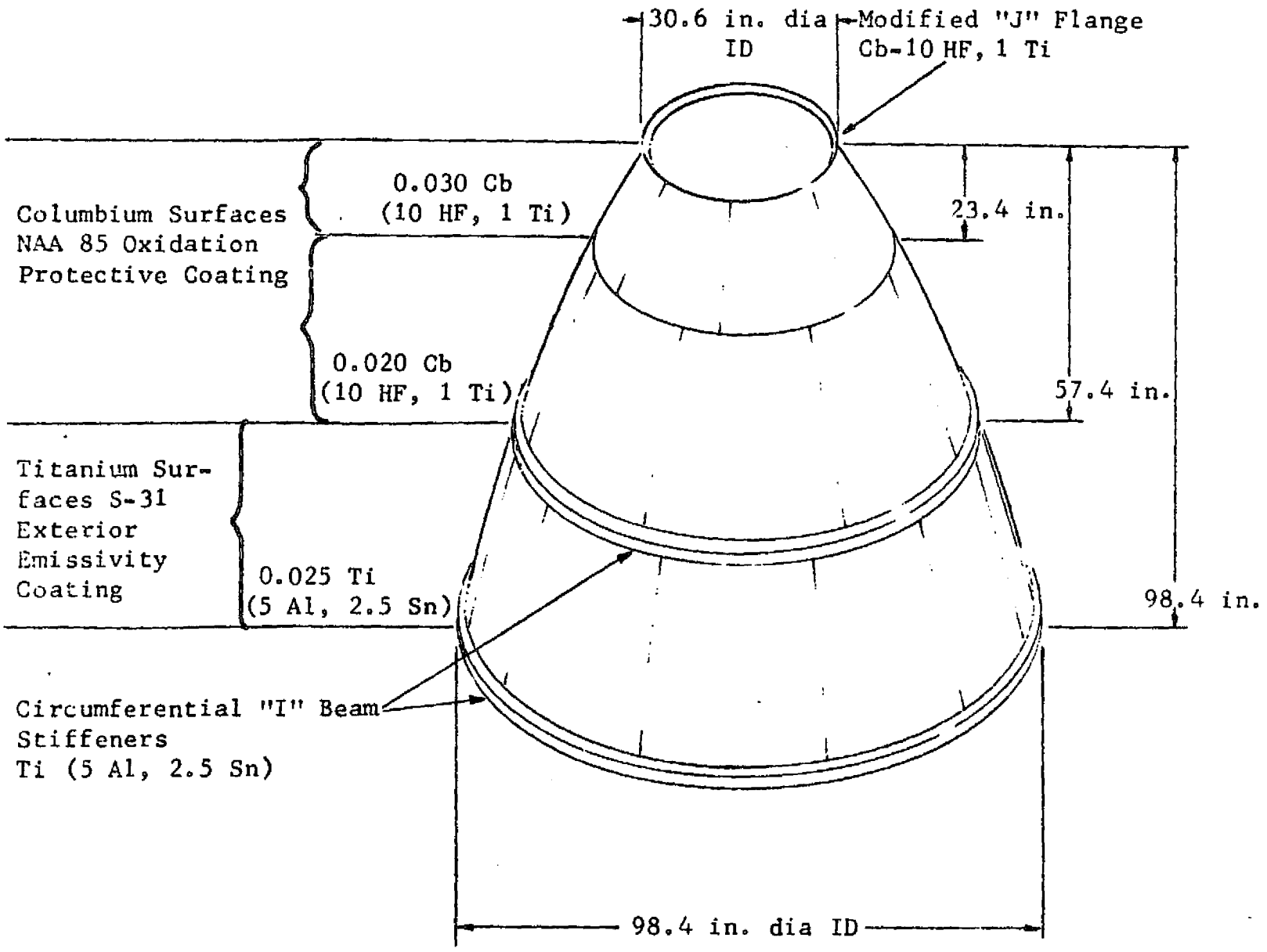


Figure 6

Rib Skin Nozzle Extension, Retracted



APOLLO SPS ENGINE RADIATION COOLED NOZZLE

Figure 7

APOLLO NOZZLE STEADY-STATE TEMPERATURE DATA

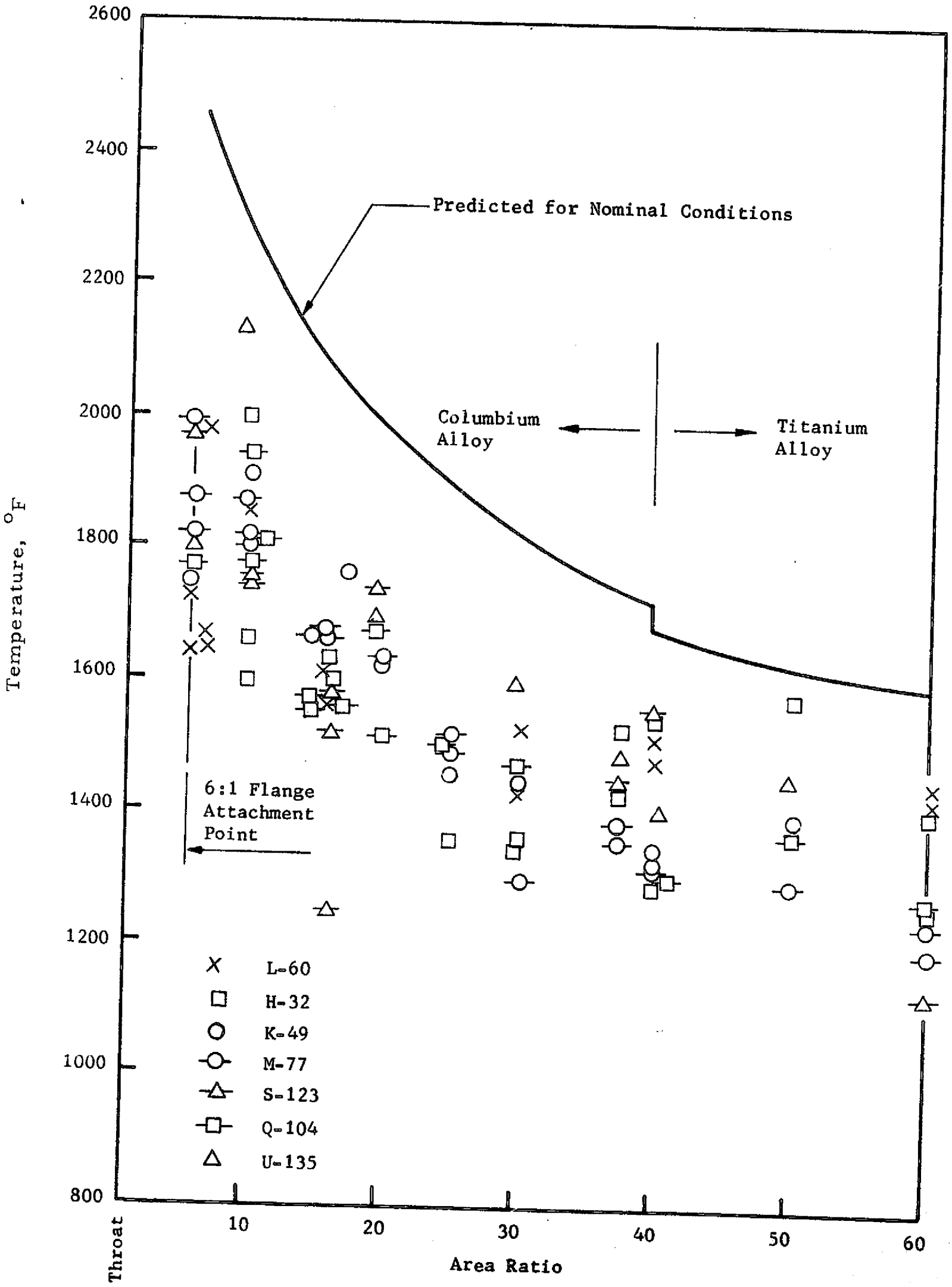
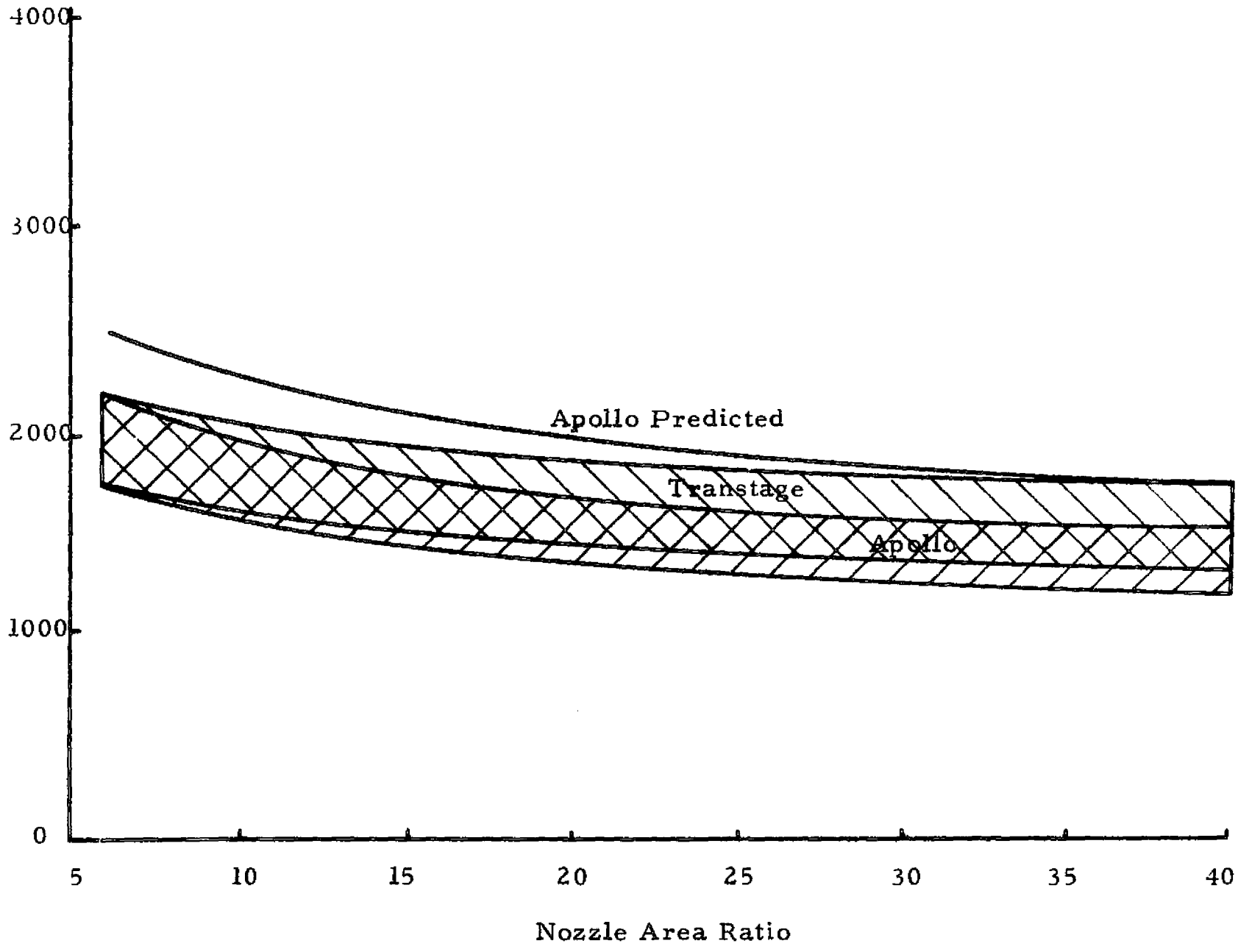


Figure 8

Report 10484-FR

APOLLO AND TRANSTAGE ENGINE RADIATION COOLED NOZZLE TEMPERATURE DATA



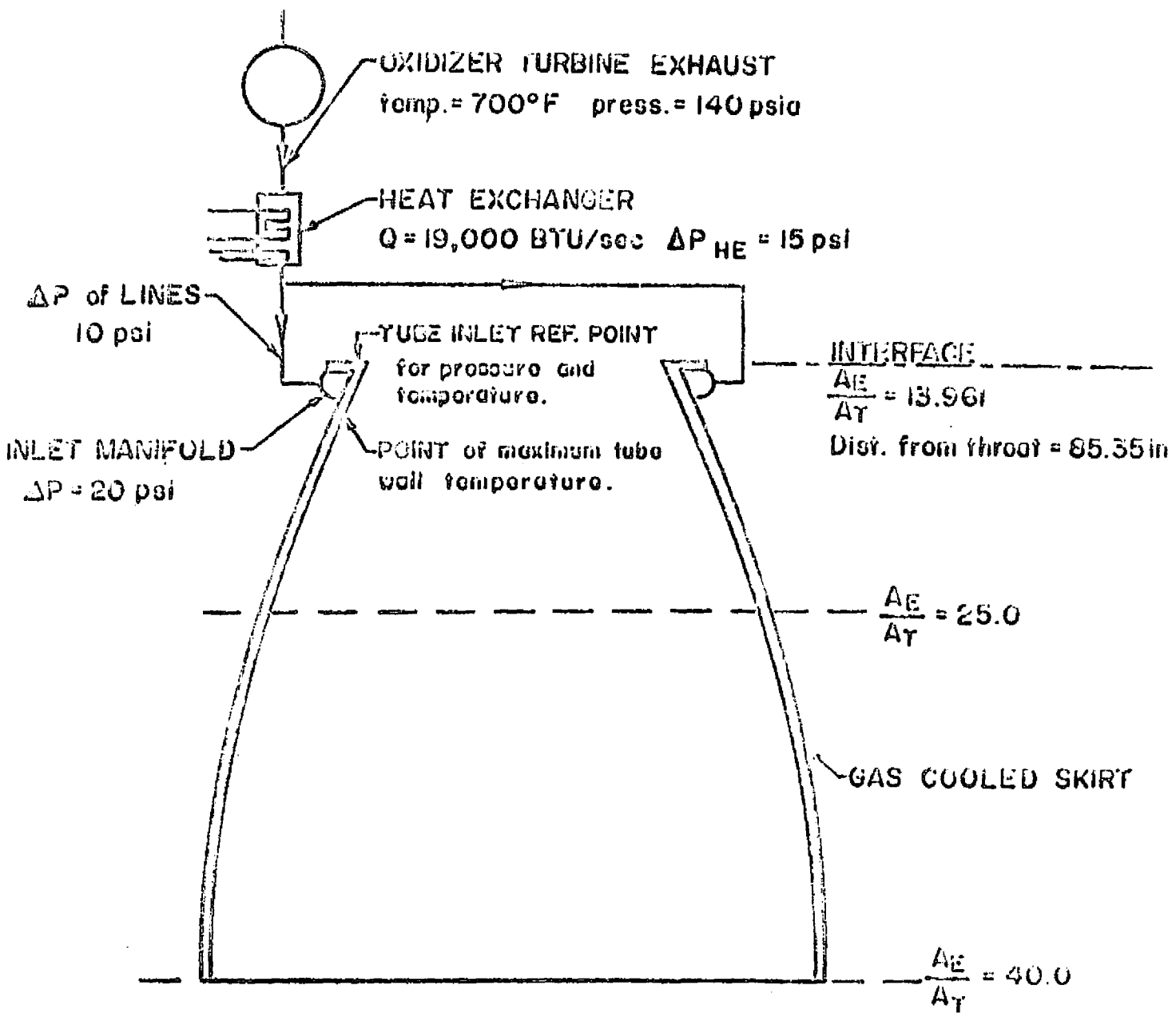
Legend:

Apollo predicted temperatures

Apollo experimental temperature data

Transtage experimental temperature data

Figure 9



M-1 GAP DUMP COOLED EXTENDABLE NOZZLE

Figure 10

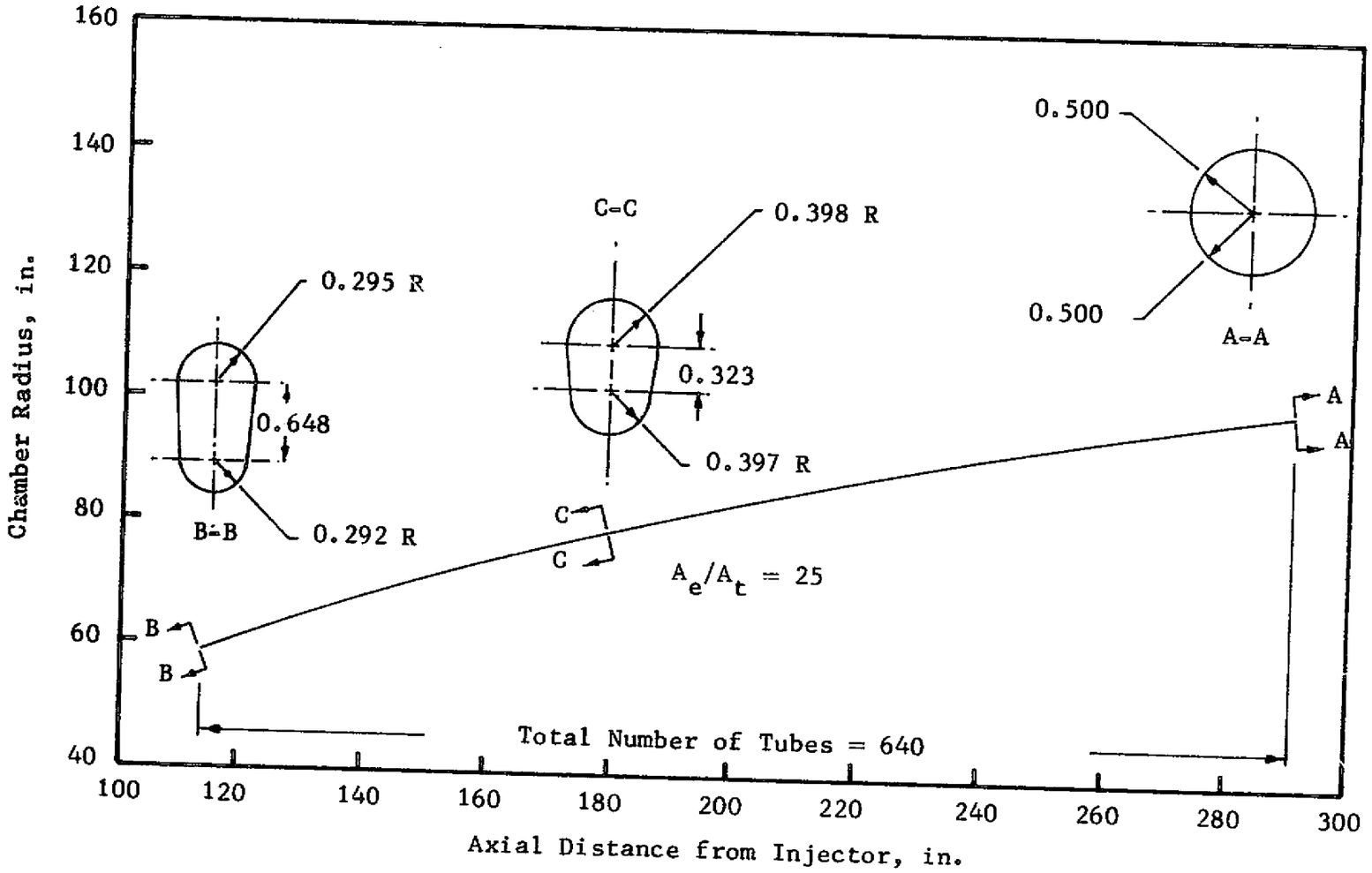
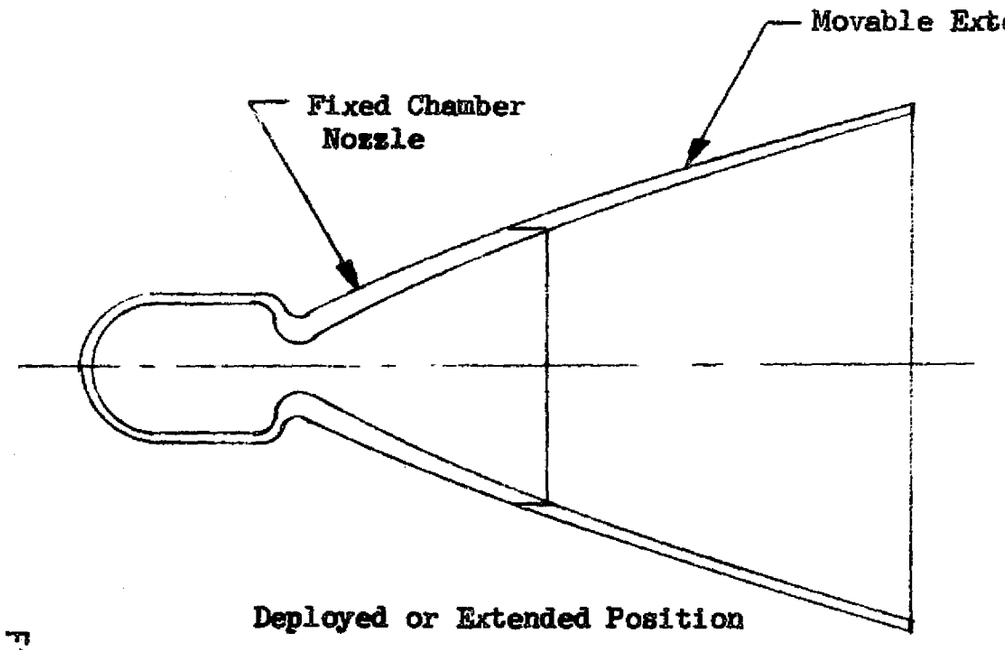
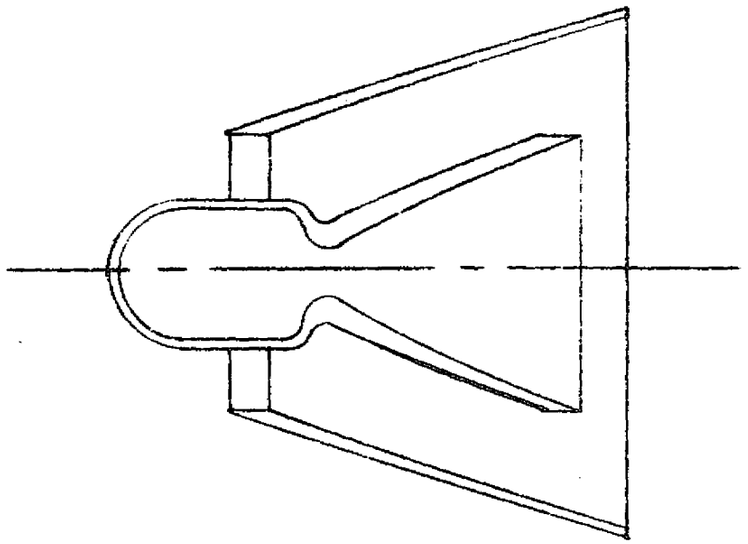


Figure 11

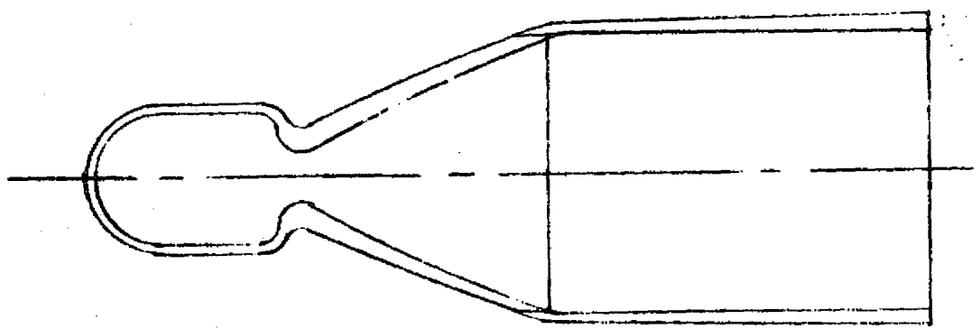
M-1 GAS DUMP COOLED NOZZLE TUBE DESIGN



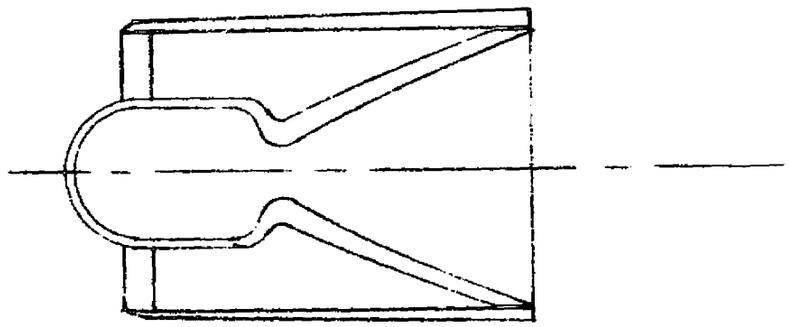
Deployed or Extended Position



Longitudinal Extension Packaging



Radial Expansion Packaging



Longitudinal and Radial Packaging

Packaging Concepts

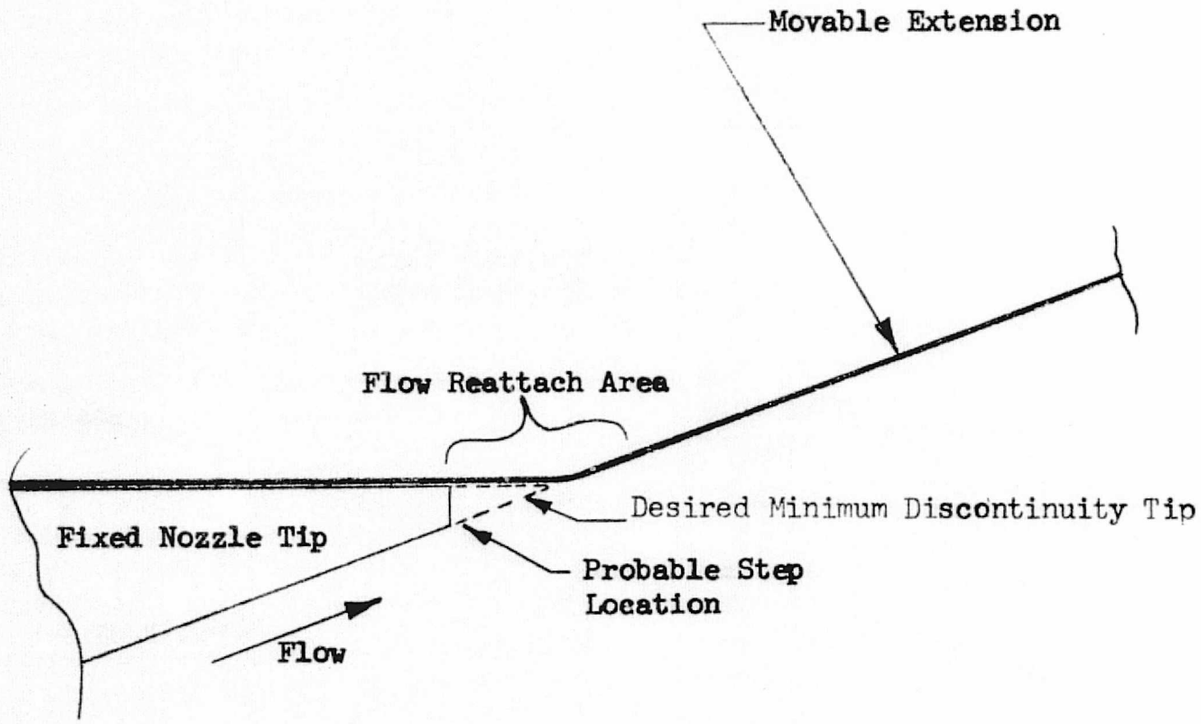


Figure 13 Fixed to Movable Transition Region

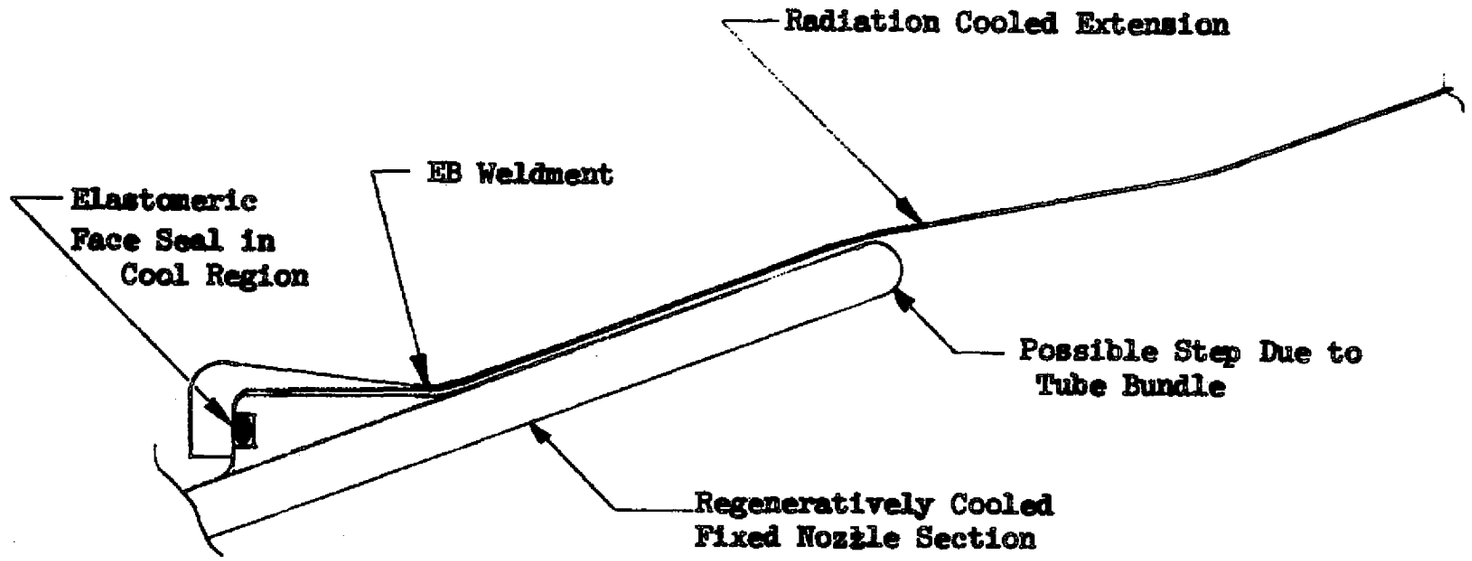
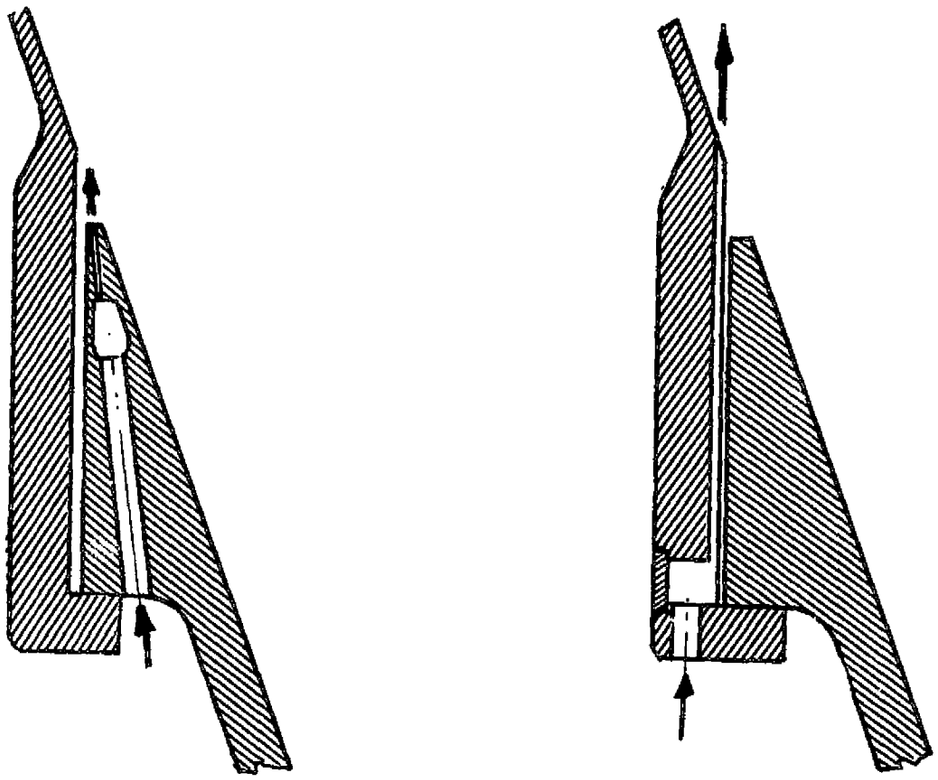


Figure 14 Elastomeric Face Seal in a "Cool" Region



ATTACHMENT JOINT COOLING WITH SECONDARY COOLANT

Figure 15

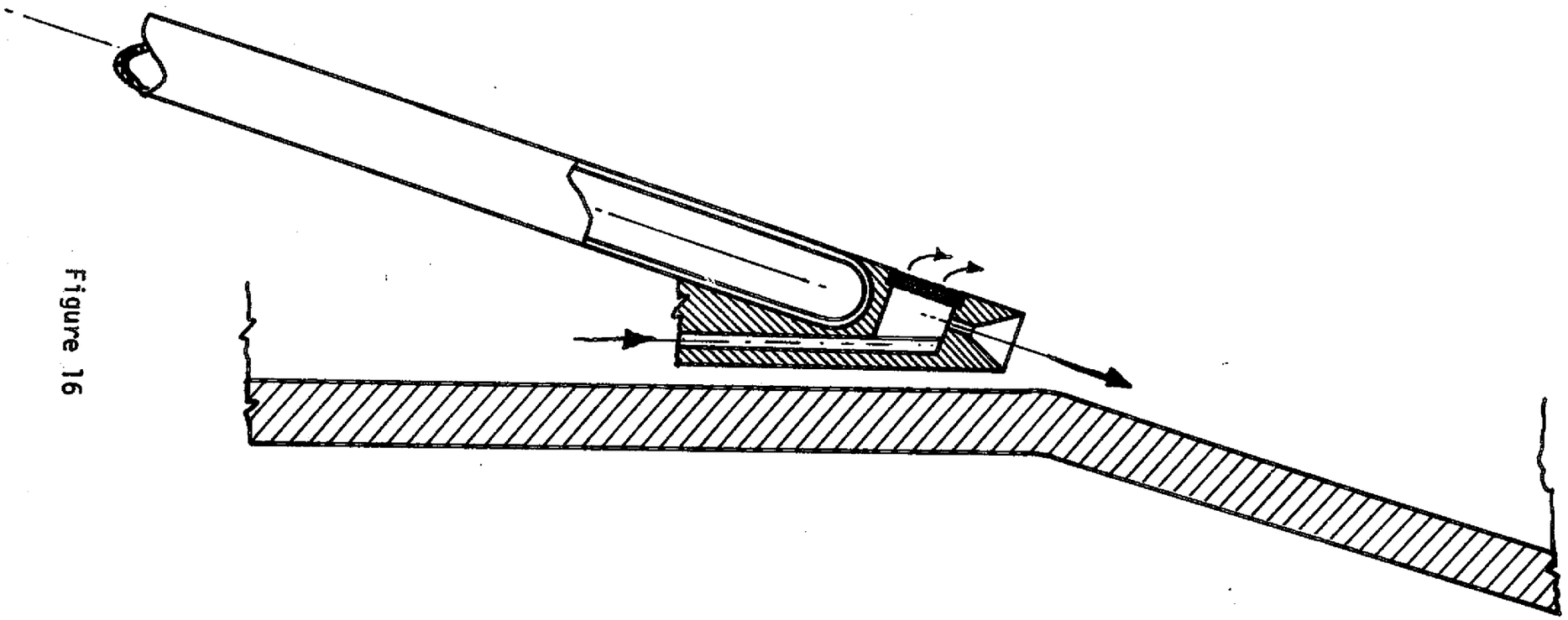
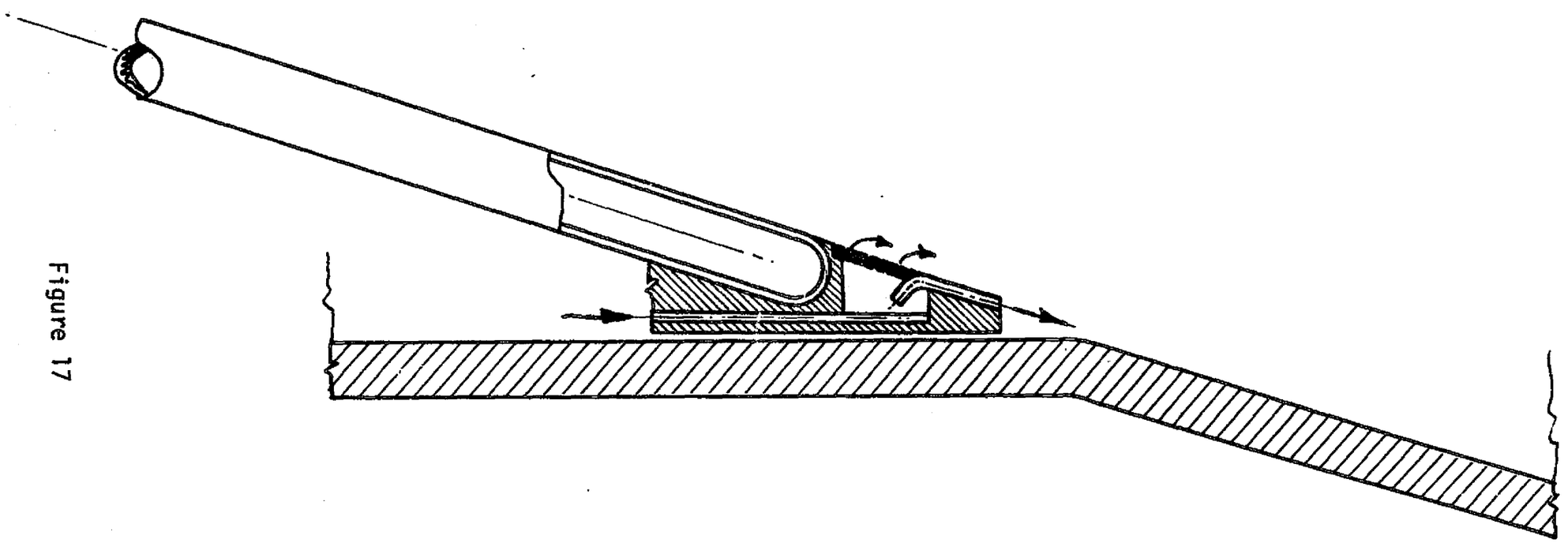


Figure 16

TIP COOLING BY INJECTING SECONDARY COOLANT THROUGH
RIGID MESH AND SUPERSONIC NOZZLE



Report 10484-FR

Figure 17

TIP COOLING BY INJECTING SECONDARY COOLANT THROUGH
RIGID MESH AND ORIENTED TUBE

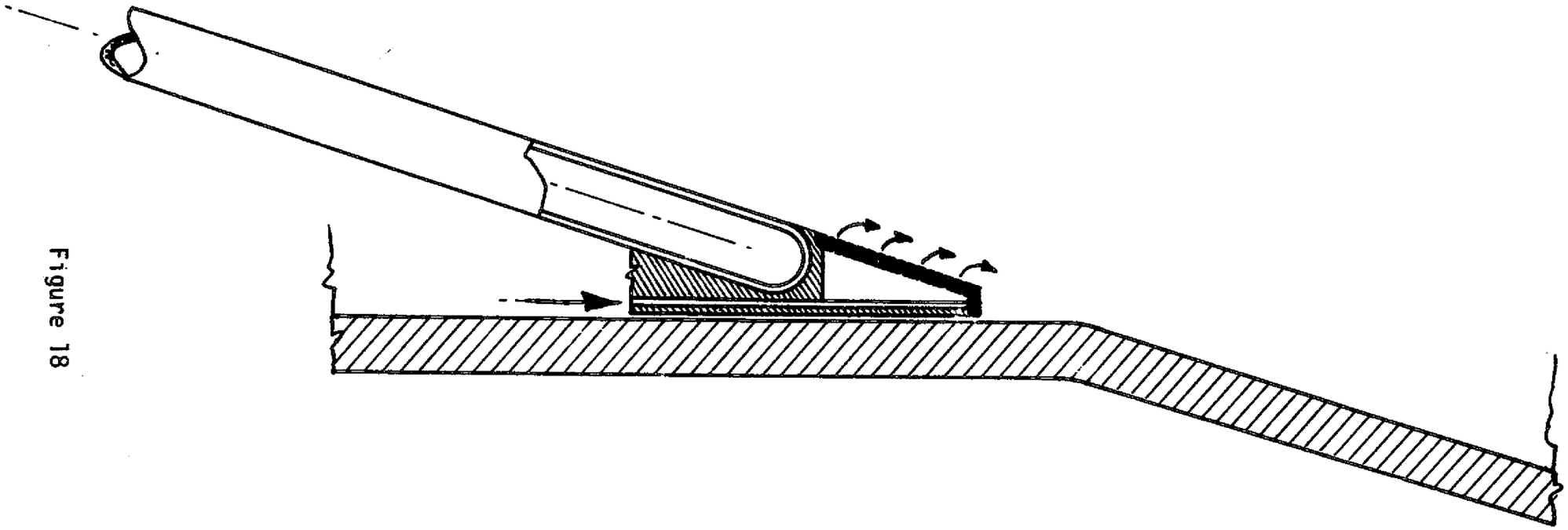
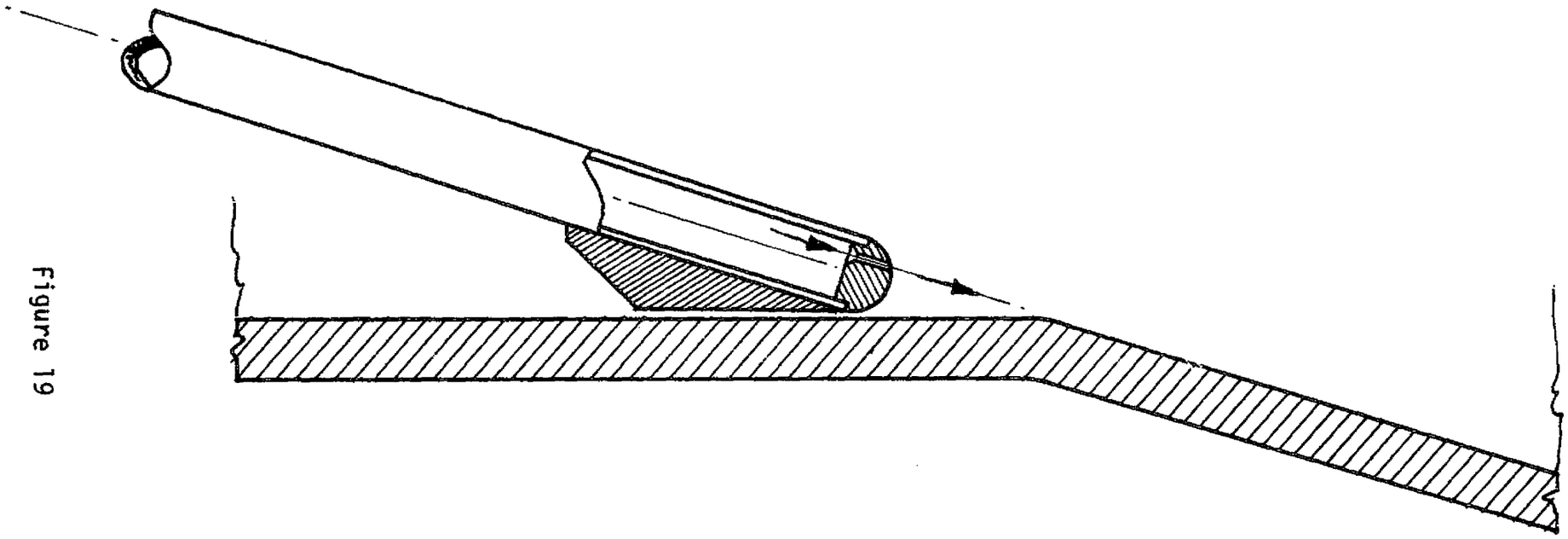


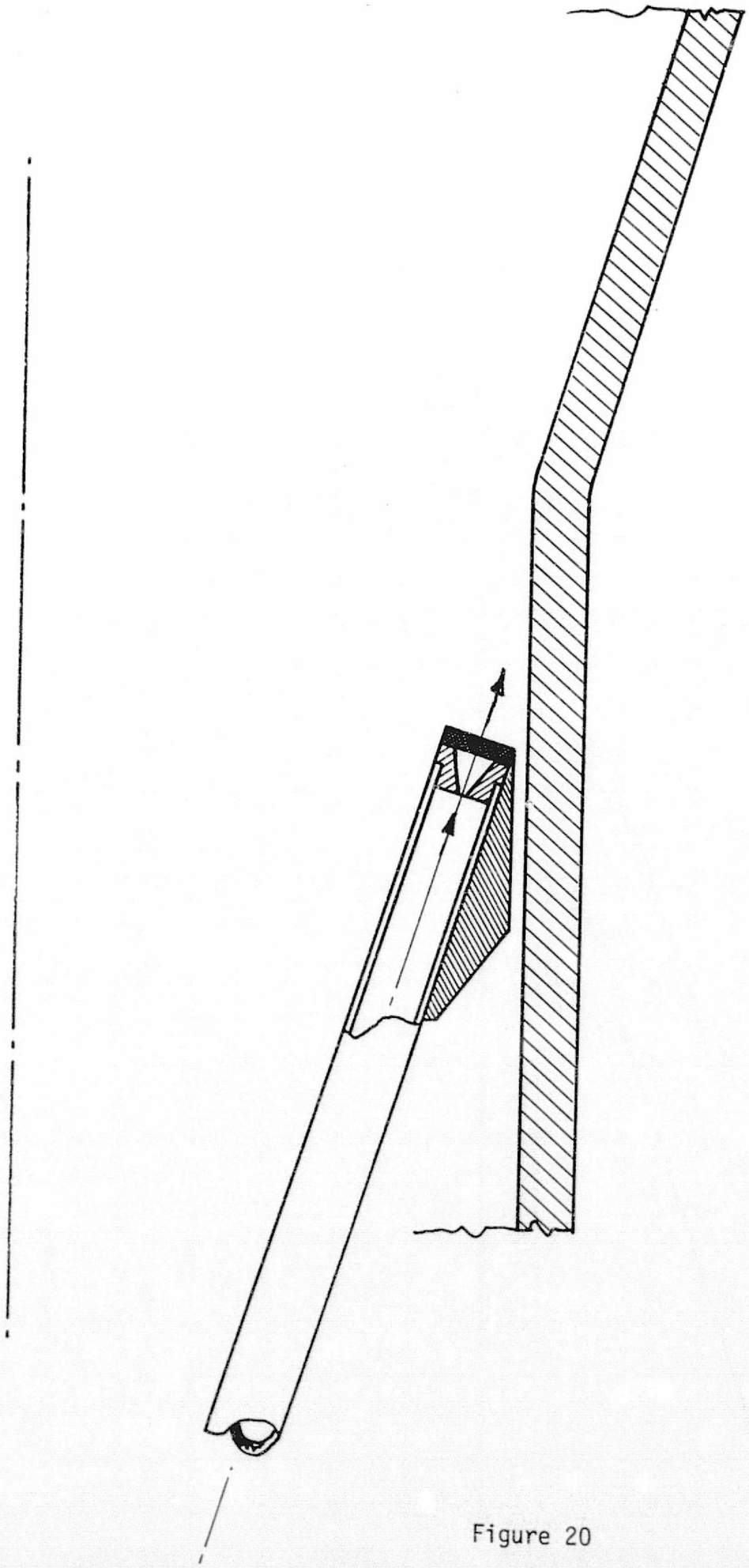
Figure 18

TIP COOLING BY INJECTING SECONDARY COOLANT THROUGH
RIGID MESH ALONE



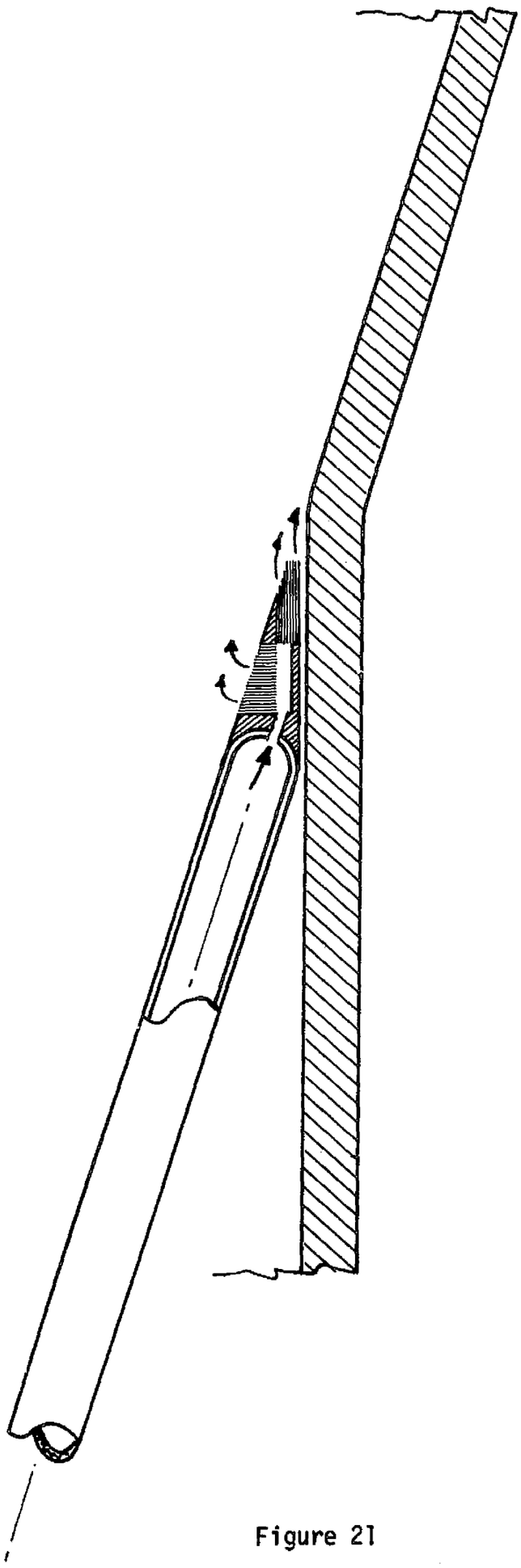
PROPELLANT INJECTED THROUGH SIMPLE ORIFICE

Figure 19



PROPELLANT INJECTED THROUGH RIGID MESH

Figure 20



PROPELLANT INJECTED THROUGH PLATELETS

Figure 21

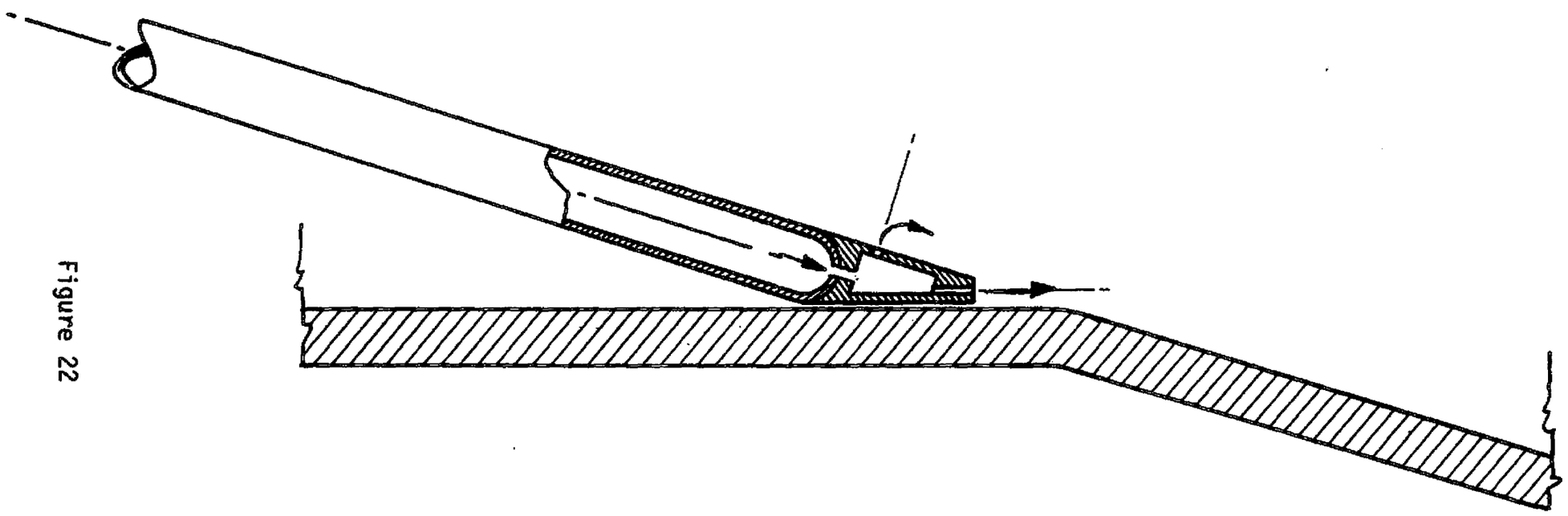
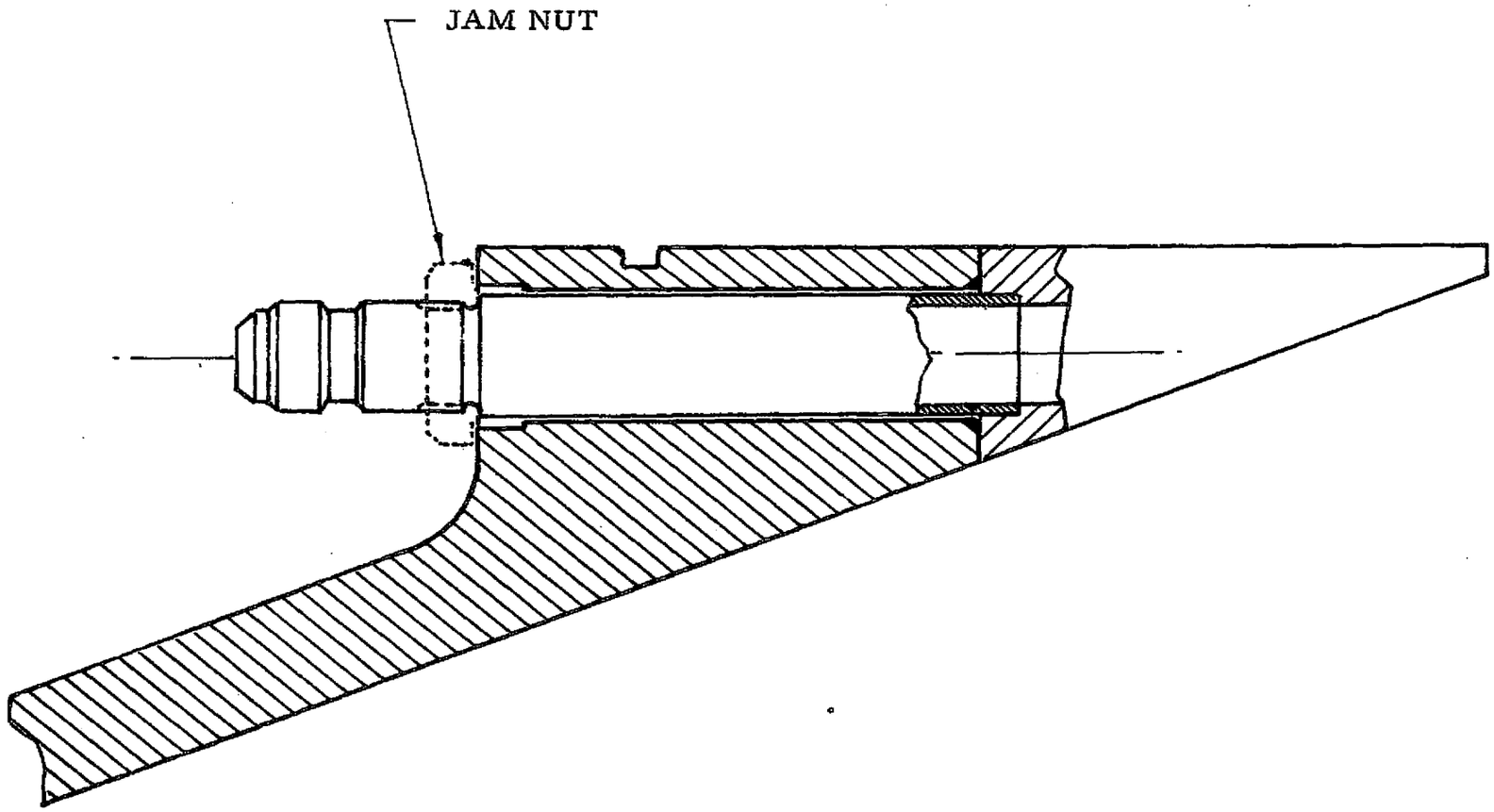
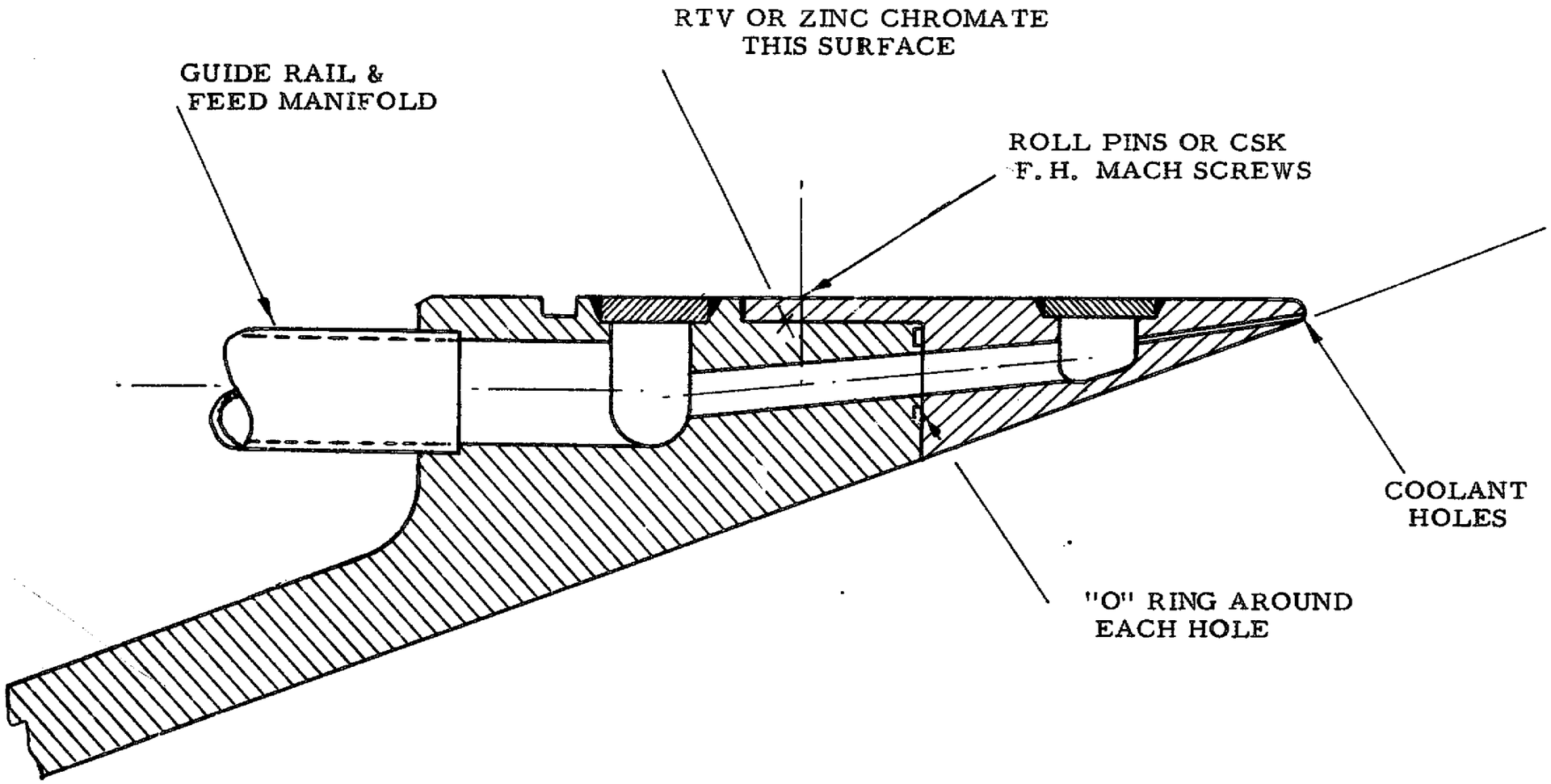


Figure 22

PROPELLANT INJECTED THROUGH BI-DIRECTIONAL ORIFICES



REPLACE ABLE TIP CONCEPT NO. 1



REPLACEABLE TIP CONCEPT NO. 2

Figure 24

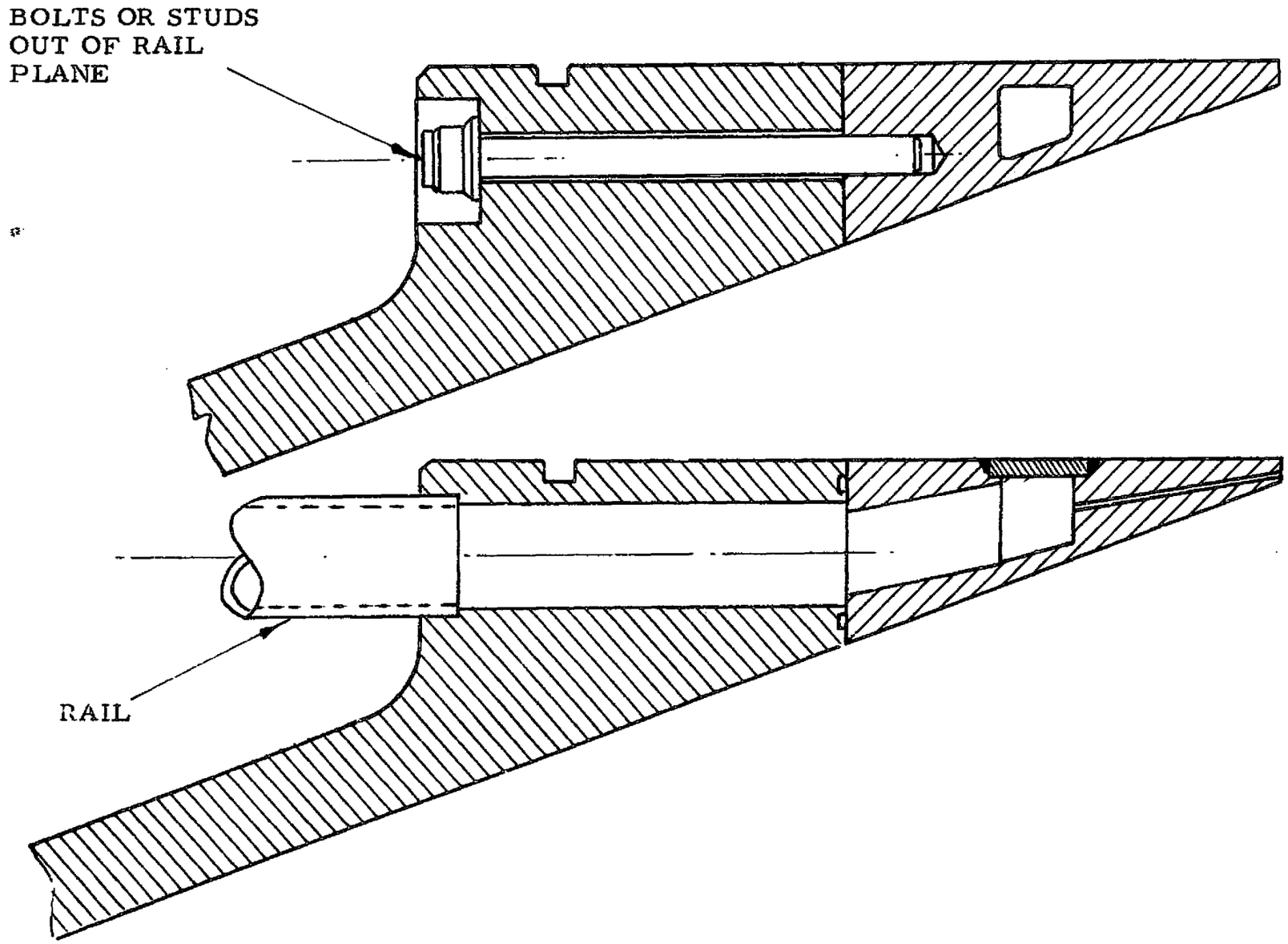
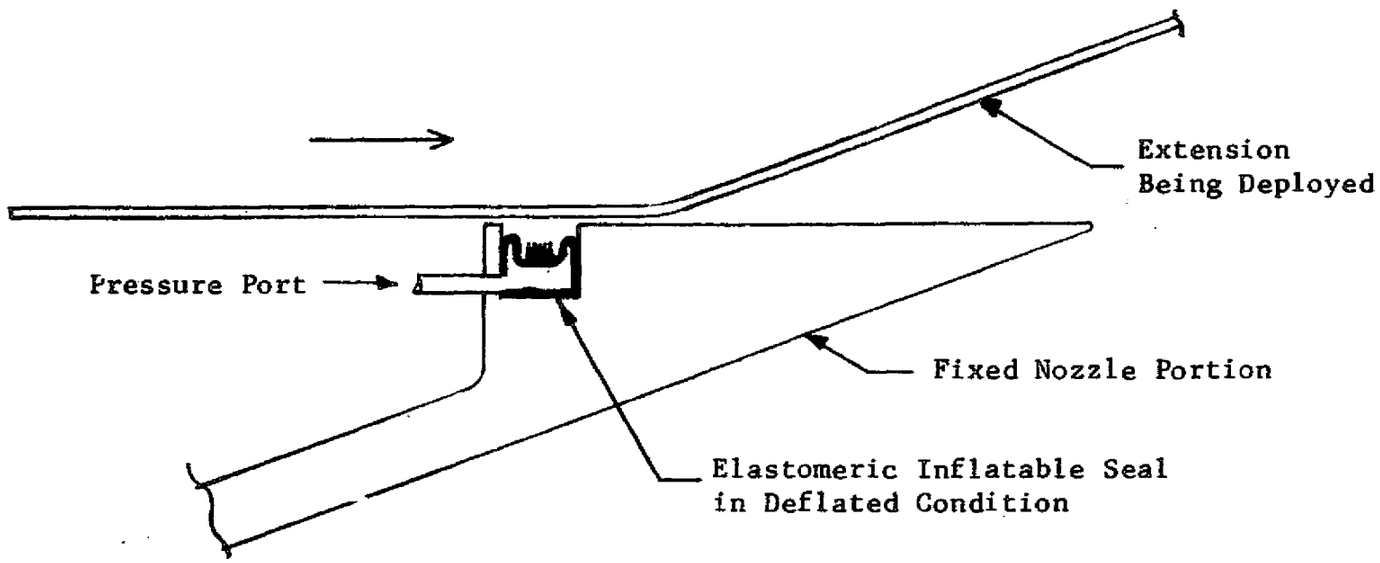


Figure 25

REPLACEABLE TIP CONCEPT NO. 3



INFLATABLE ELASTOMERIC SEAL CONCEPT

Figure 26

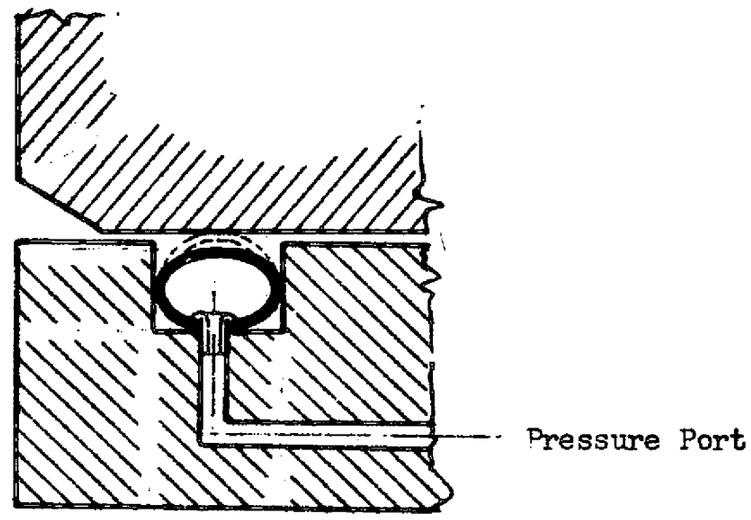
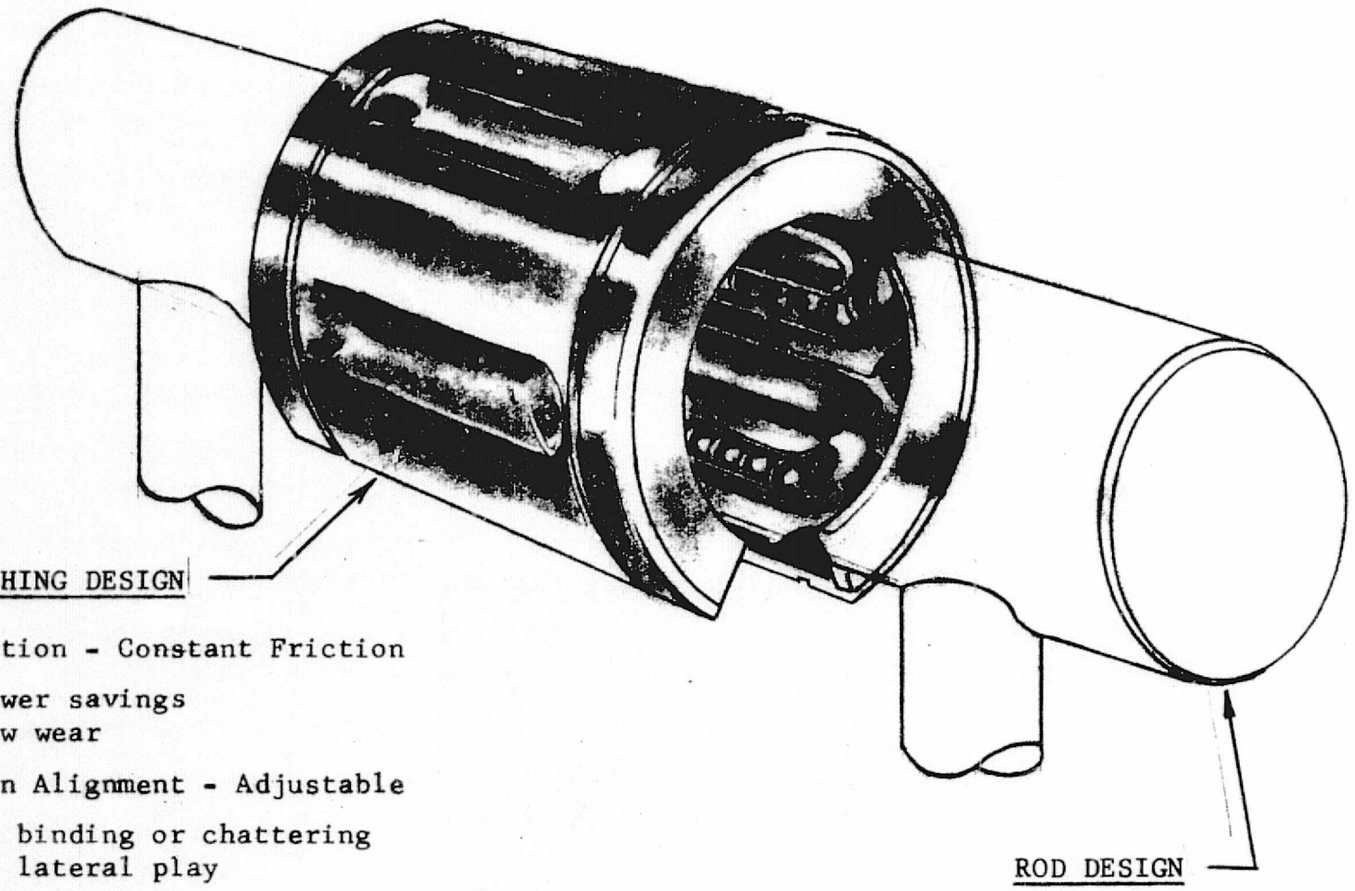


Figure 27

INFLATABLE METALLIC SEAL CONCEPT



BALL BUSHING DESIGN

Low Friction - Constant Friction

a. Power savings
b. Low wear

Precision Alignment - Adjustable

a. No binding or chattering
b. No lateral play

Lightweight (2.7 oz)

Good High Speed Operation

High Reliability

Four-Ball Circuit.

Static Load = 165 lb

Dynamic Load = 109 lb

ROD DESIGN

Centerless Ground

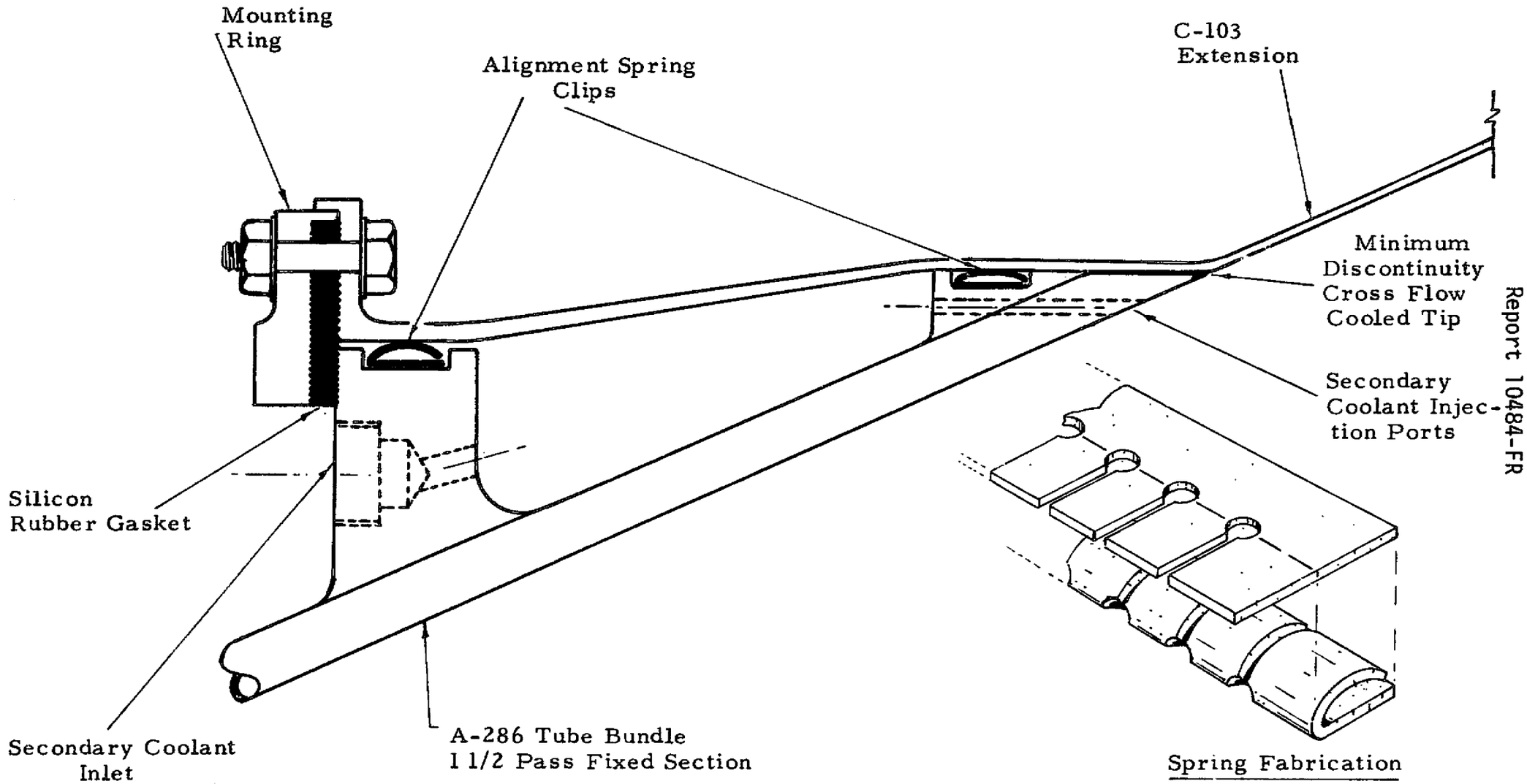
Straightness .001/.002/ft

Hardened (60 c)

Finish 12 → 24

Weight = .125 lb/in.

Figure 28. BALL BUSHING GUIDE SYSTEM



EXTENSION ALIGNMENT SPRINGS

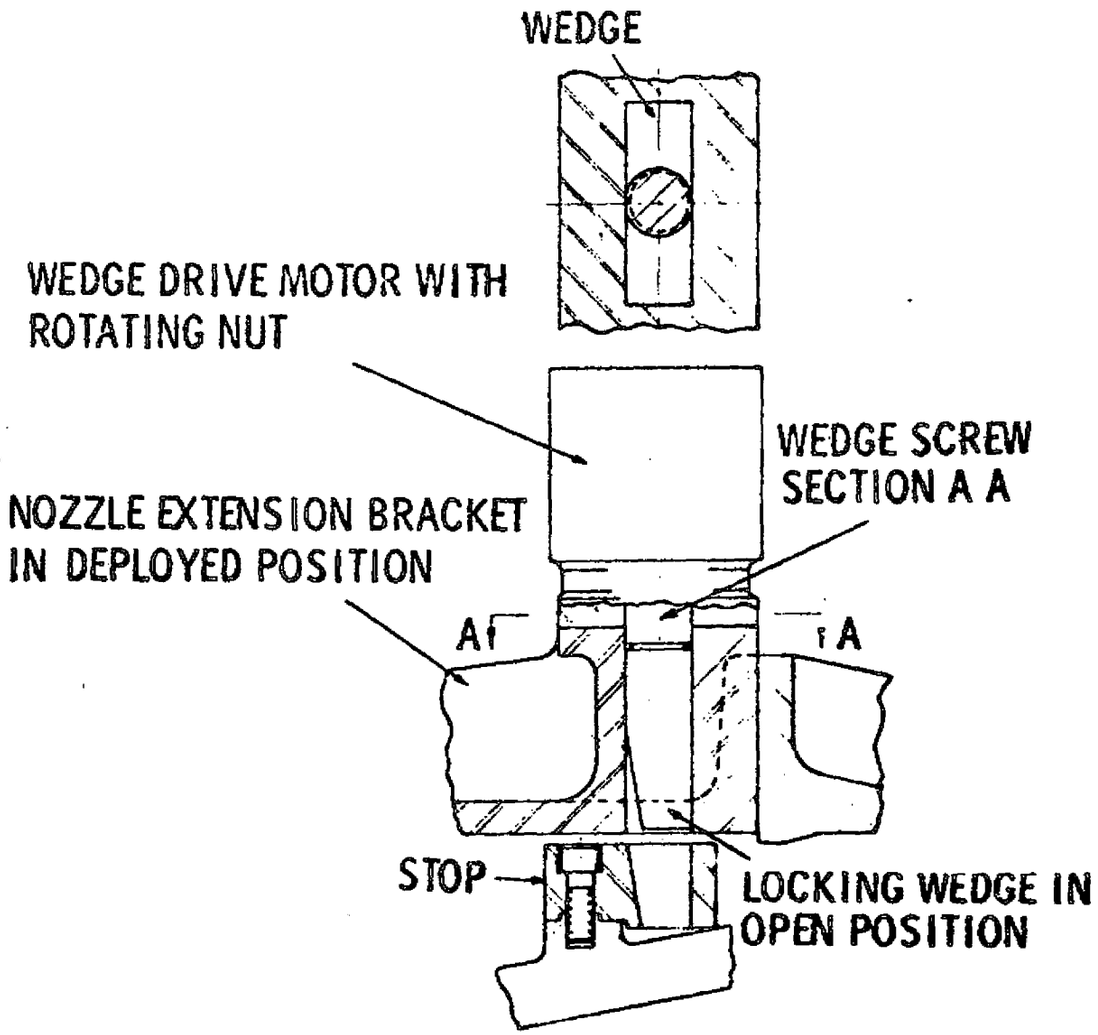


Figure 30 NOZZLE EXTENSION LOCKING DEVICE

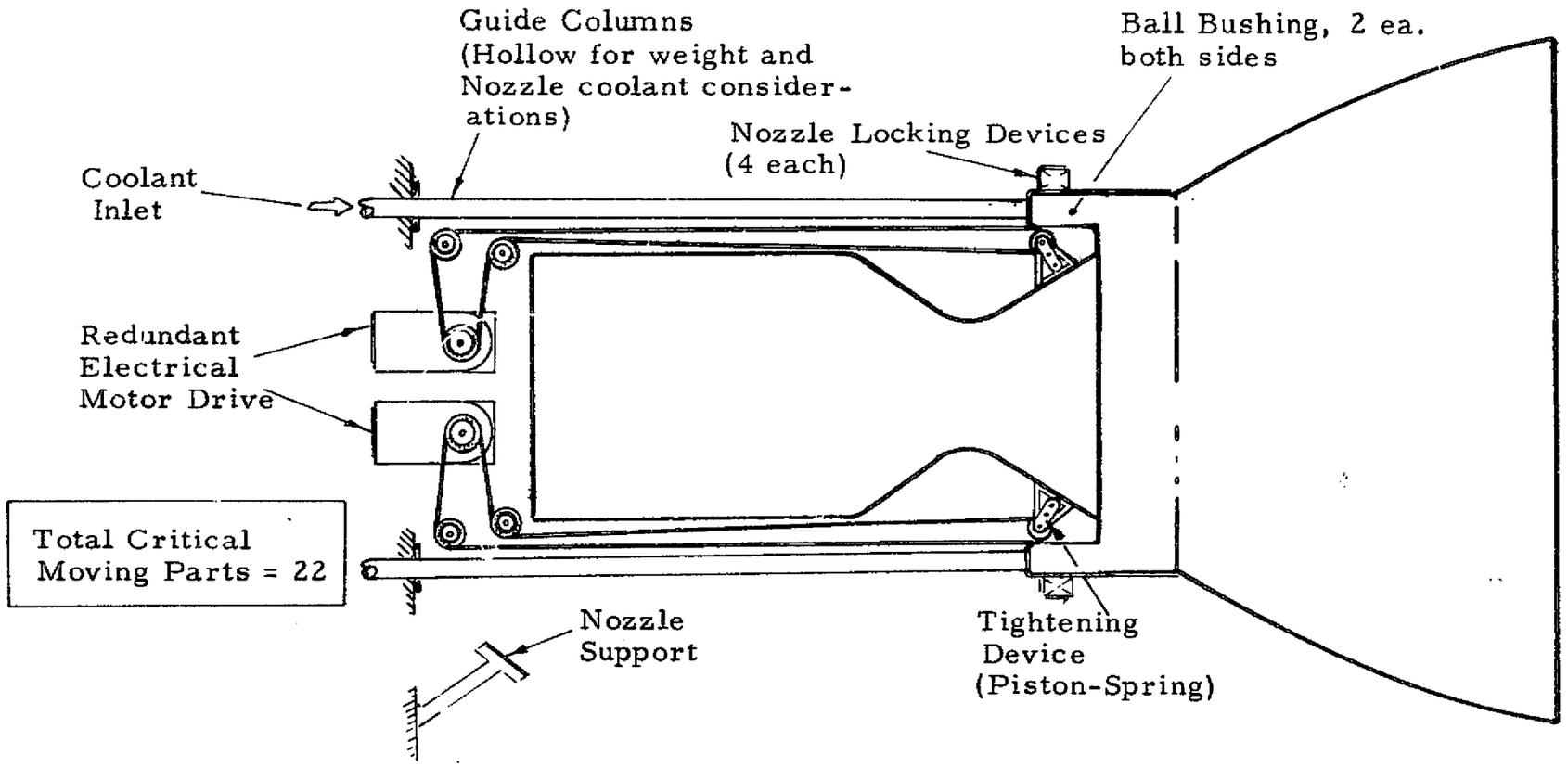


Figure 31

Report 10484-FR

MINIMUM CRITICAL COMPONENTS

ESTIMATE OF WEIGHT (lbs)

	Cable	Chain	Tape
2 ea. Extension Guide Columns (35 ft. long)	6.0	6.0	6.0
2 ea. Steel Tape, Cable or Chains (8 ft. ea.)	2.2	5.0	1.5
8 ea. Pullys and/or Sprockets (.8 lb ea.)	6.4	6.4	6.4
2 ea. Electrical Motors (5 lb ea.)	10.0	10.0	10.0
Drive Motor Support Bracketing	1.0	1.0	1.0
4 ea. Ball Bushings (2.7 oz. ea.)	0.6	0.6	0.6
Nozzle Supports -(Vibration & Shock) - Retracted Position (3 ea.)	2.0	2.0	2.0
2 ea. Tension (Spring) Devices	2.0	2.0	2.0
4 ea. nozzle Locking Devices (1 lb ea.)	4.0	4.0	4.0
Misc. Shafts, Nuts, Washers & Guide Column Supports	4.0	4.0	4.0
Total	38.2	41.0	37.5

DESIGN PROBLEMS

1. Pully Bind - Greater Problem with Chain Drive than with Cable or Tape.
2. Tightening Device Failure.
3. Should be designed so single system has ability to translate nozzle extension.
4. This design requires nozzle locking devices.

ELECTRICAL DRIVE - CABLE, TAPE OR CHAIN POWER TRANSMISSION

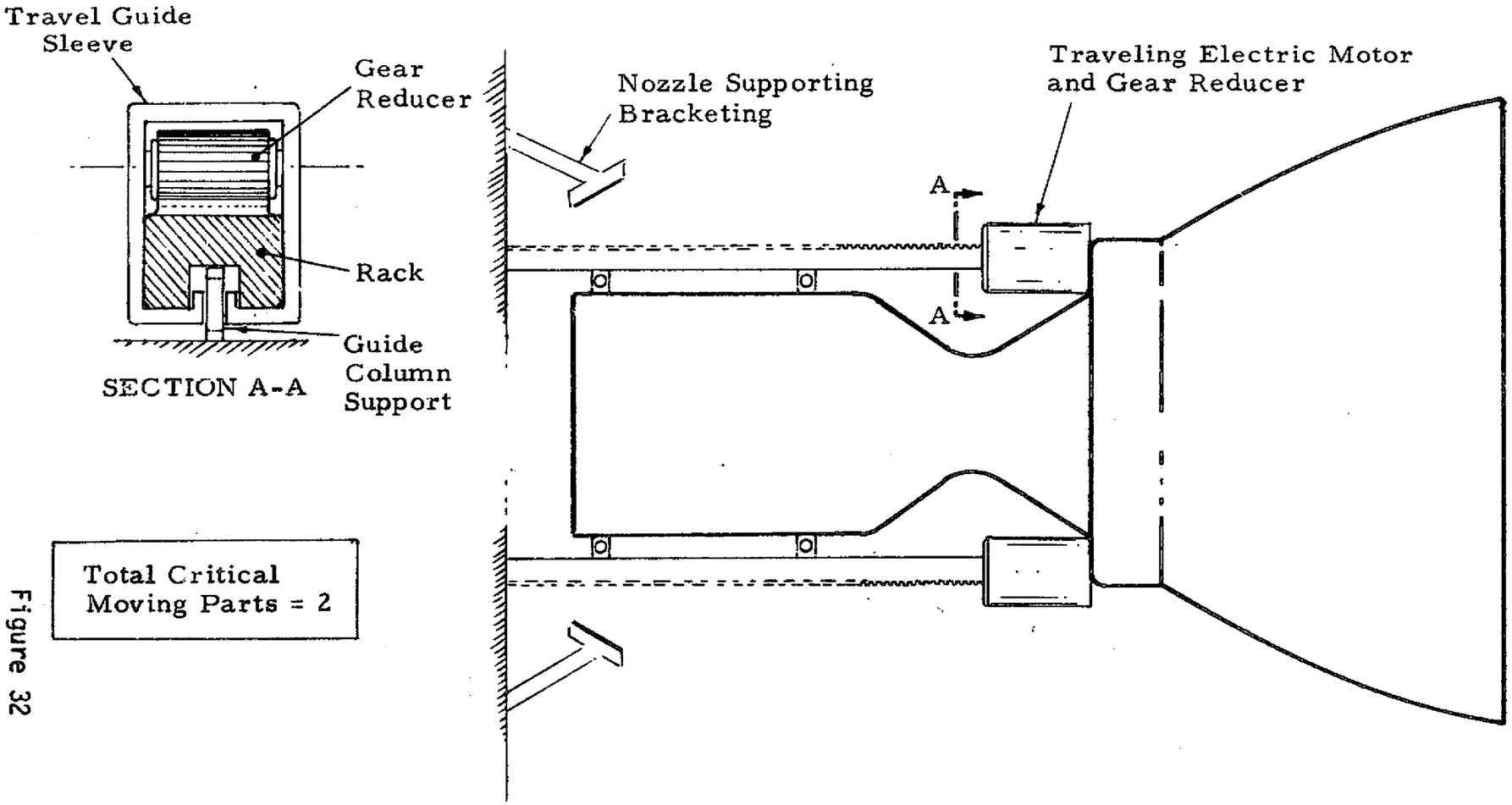


Figure 32

Minimum Critical Components	Estimate of Weights (lbs)
2 ea. Gear Racks - used as Guide columns	15.1
2 ea. Motor and Gear Reducer	12.0
3 ea. Nozzle Supporting Brackets (vibration and shock-retracted position)	2.0
Misc., column supports, nuts and washer	4.0
	33.1 lb.

Design Problems

1. Supply of electrical power to motors - traveling wires with traveling motors.
2. Nozzle locking devices are possibly not required with gear drive. Must be investigated.
3. Should be designed so single system has ability to translate nozzle extension.

ELECTRICAL DRIVE-BACK AND PINION OR WORM GEAR POWER TRANSMISSION

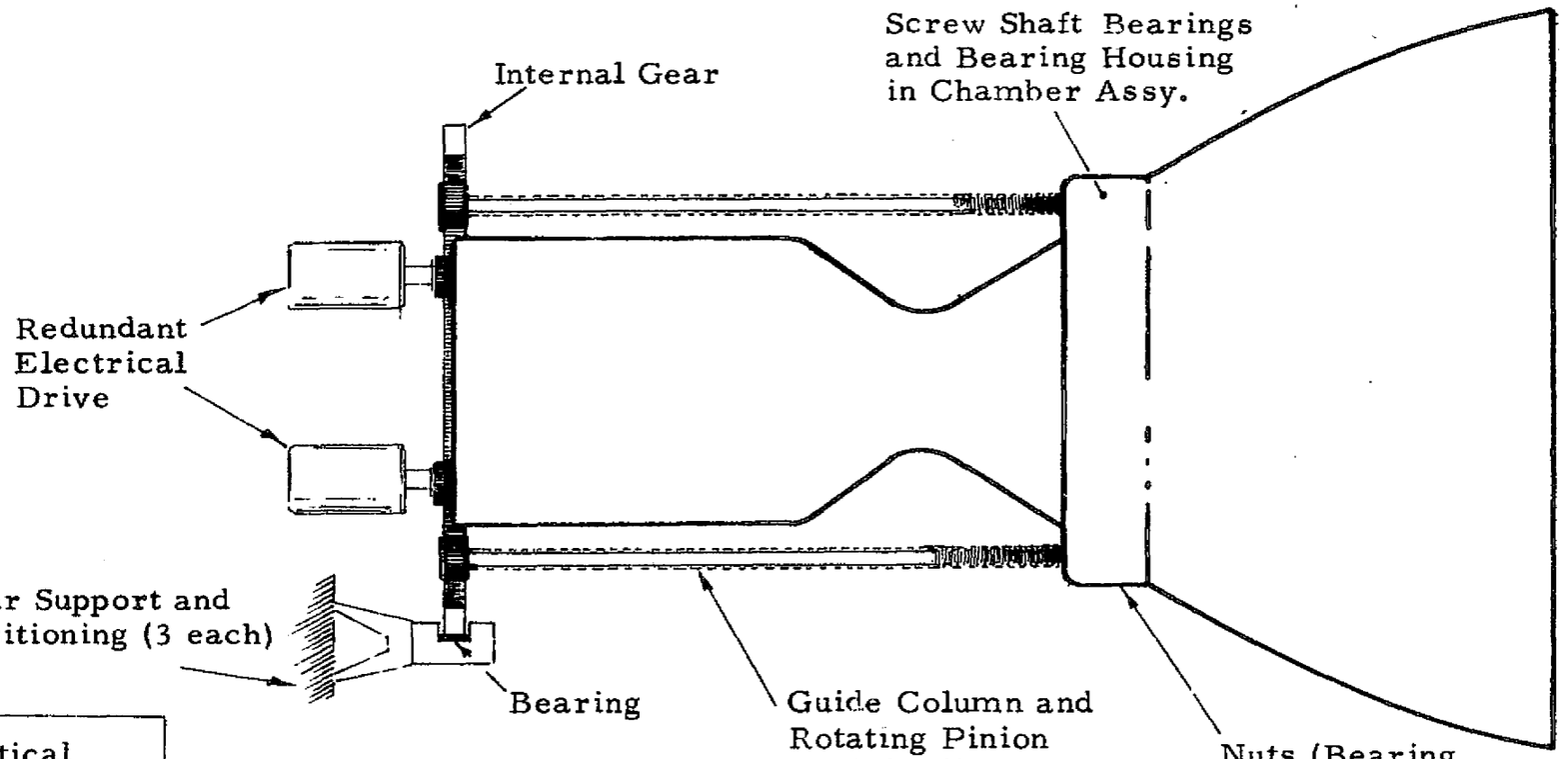


Figure 33

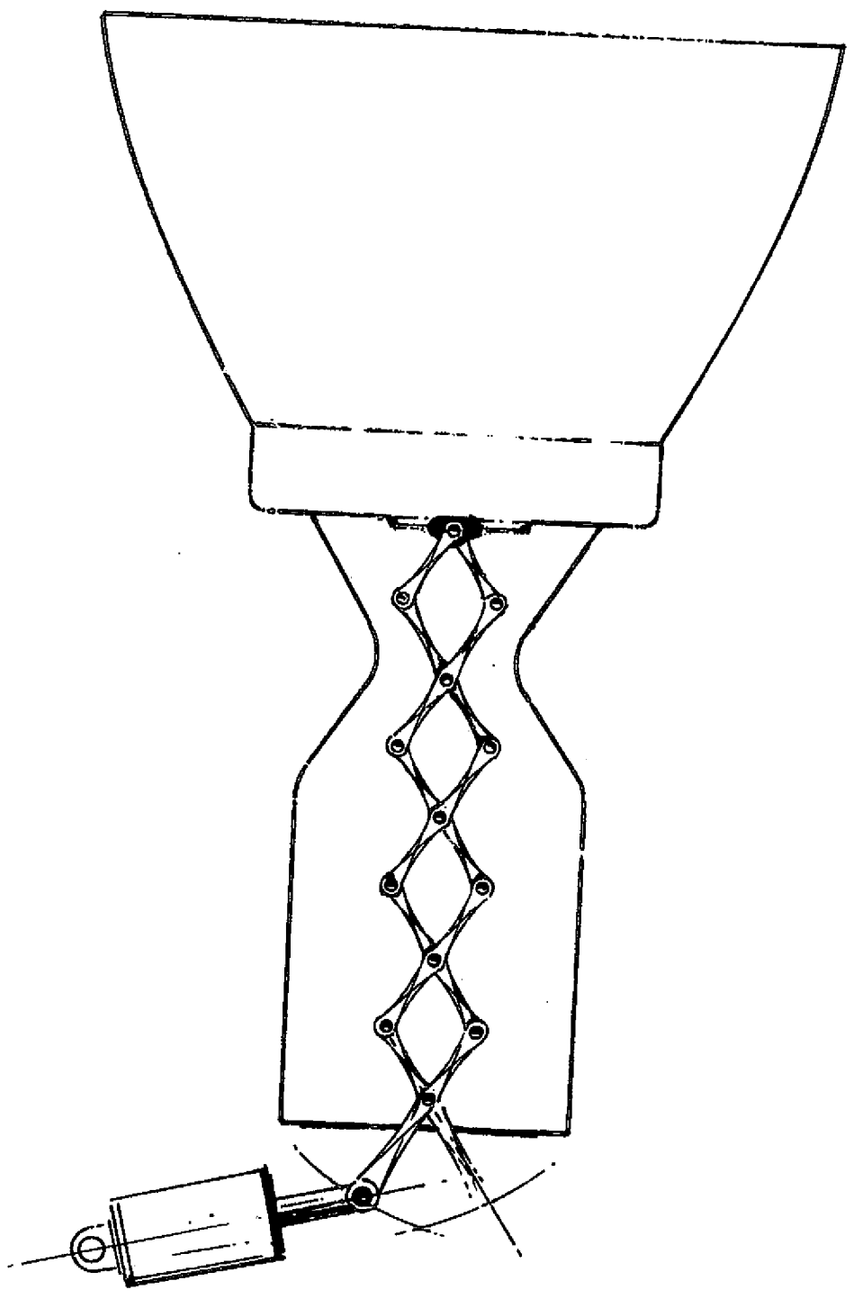
Total Critical Moving Parts = 9

MINIMUM CRITICAL COMPONENTS	ESTIMATE OF WEIGHT (lbs)
1 ea. Internal Gear	10.0
2 ea. Pinion Screw Shafts	6.0
2 ea. Electrical Motors	10.0
4 ea. Nuts (Bearing Retainers) (8 oz. ea.)	2.0
3 ea. Gear Supports and Positioning (120° apart)	3.0
3 ea. Nozzle Supporting Brackets (Vibration and Shock Retractor Position	2.0
Misc. Nuts, Bolts & Washers	2.0
Drive Motor Support Bracketing	1.0
Total	36.0 lbs.

DESIGN PROBLEMS

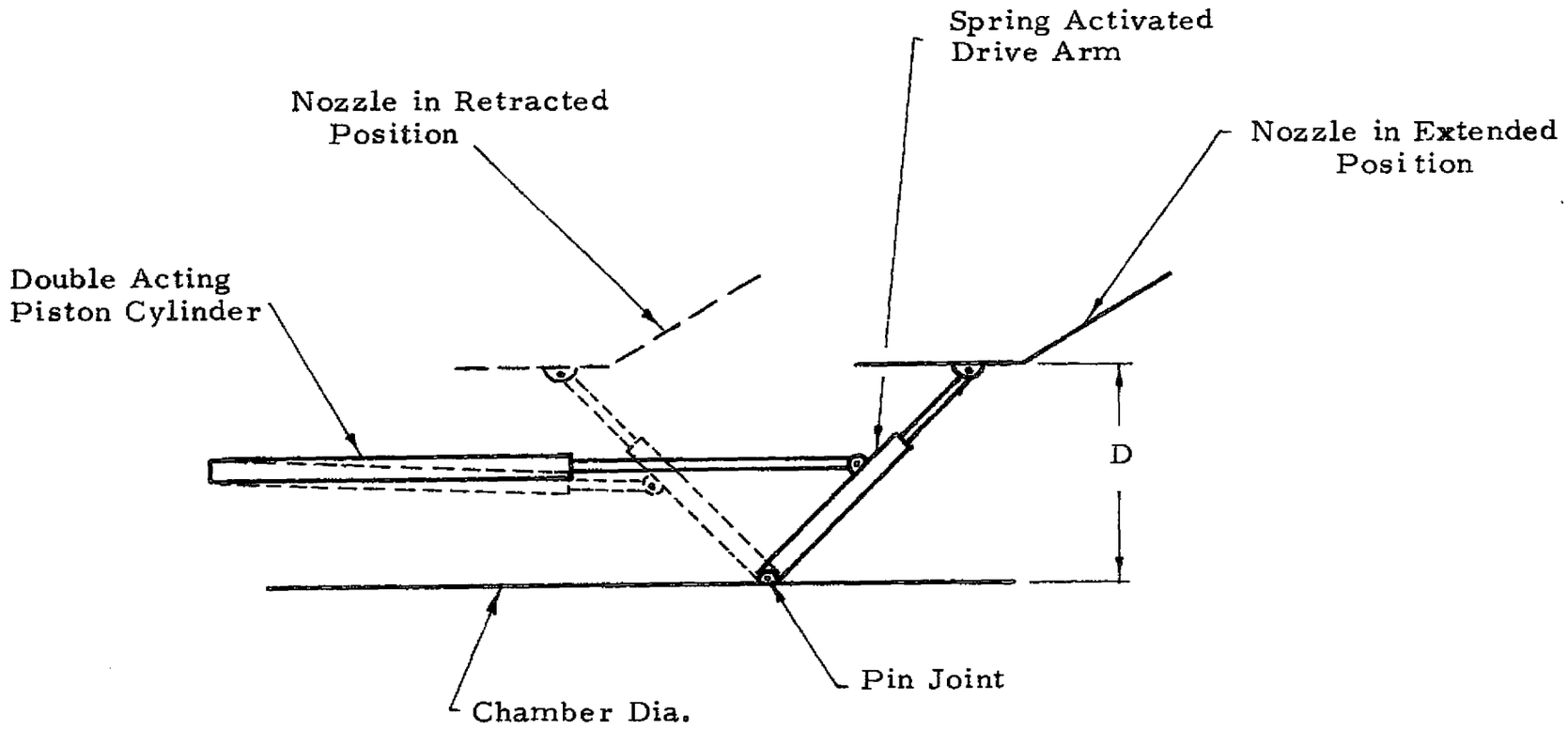
1. With Ball Screw Design, Guide Column Support, if required, is difficult.
2. Nozzle Locking Devices are probably not required with Ball screw concept must be investigated.
3. Should be designed so single Motor has ability to translate System.
4. Failure of bearing or ball screw could cause nozzle to become locked in fixed position. Must be investigated.

ELECTRICAL DRIVE - INTERNAL GEAR AND PINION - BALL SCREW POWER TRANSMISSION



PISTON-CYLINDER SCISSORS DRIVE

Figure 34



NOTES:

1. Distance "D" must be 1/2 stroke of nozzle otherwise, use 3 segment activating arm.
2. Stroke of piston-cylinder is 1/2 total nozzle travel from stowed to firing position.

PISTON - CYLINDER, SPRING DRIVE DEPLOYMENT SYSTEM

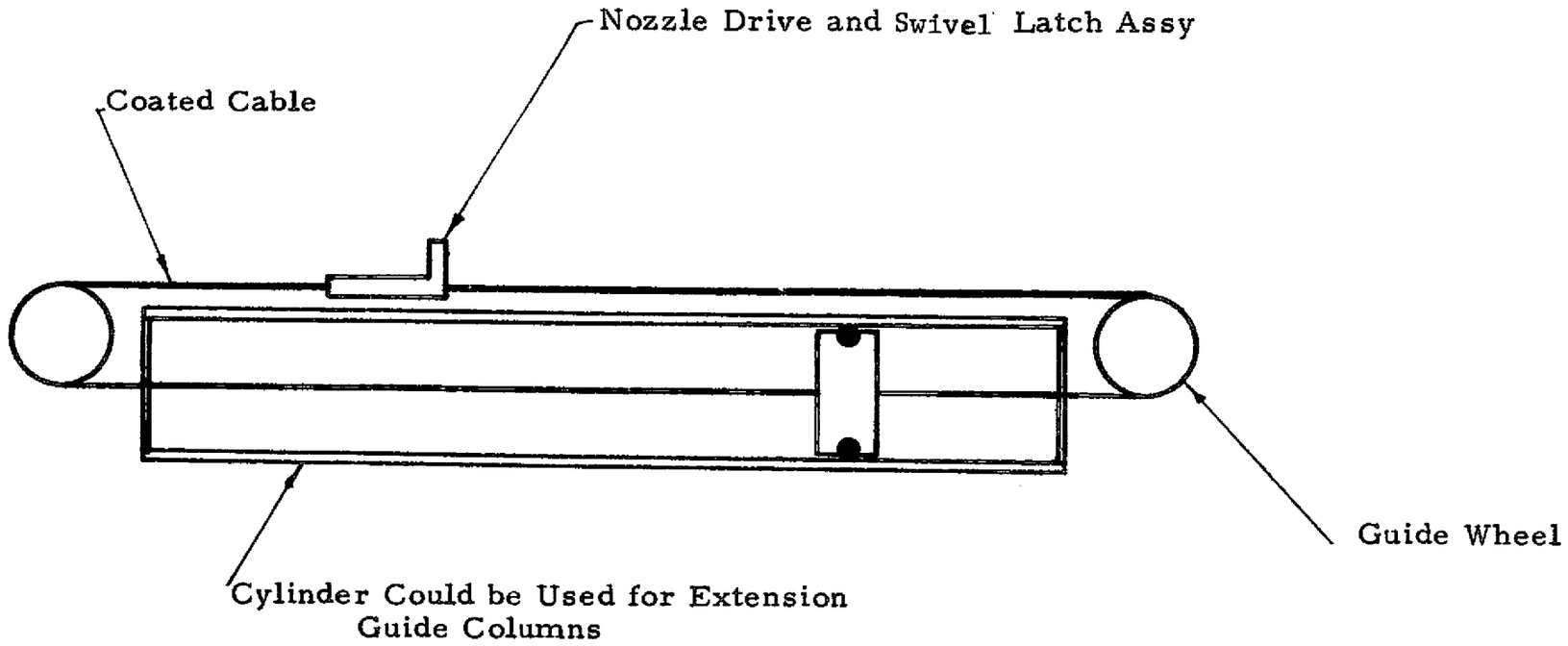
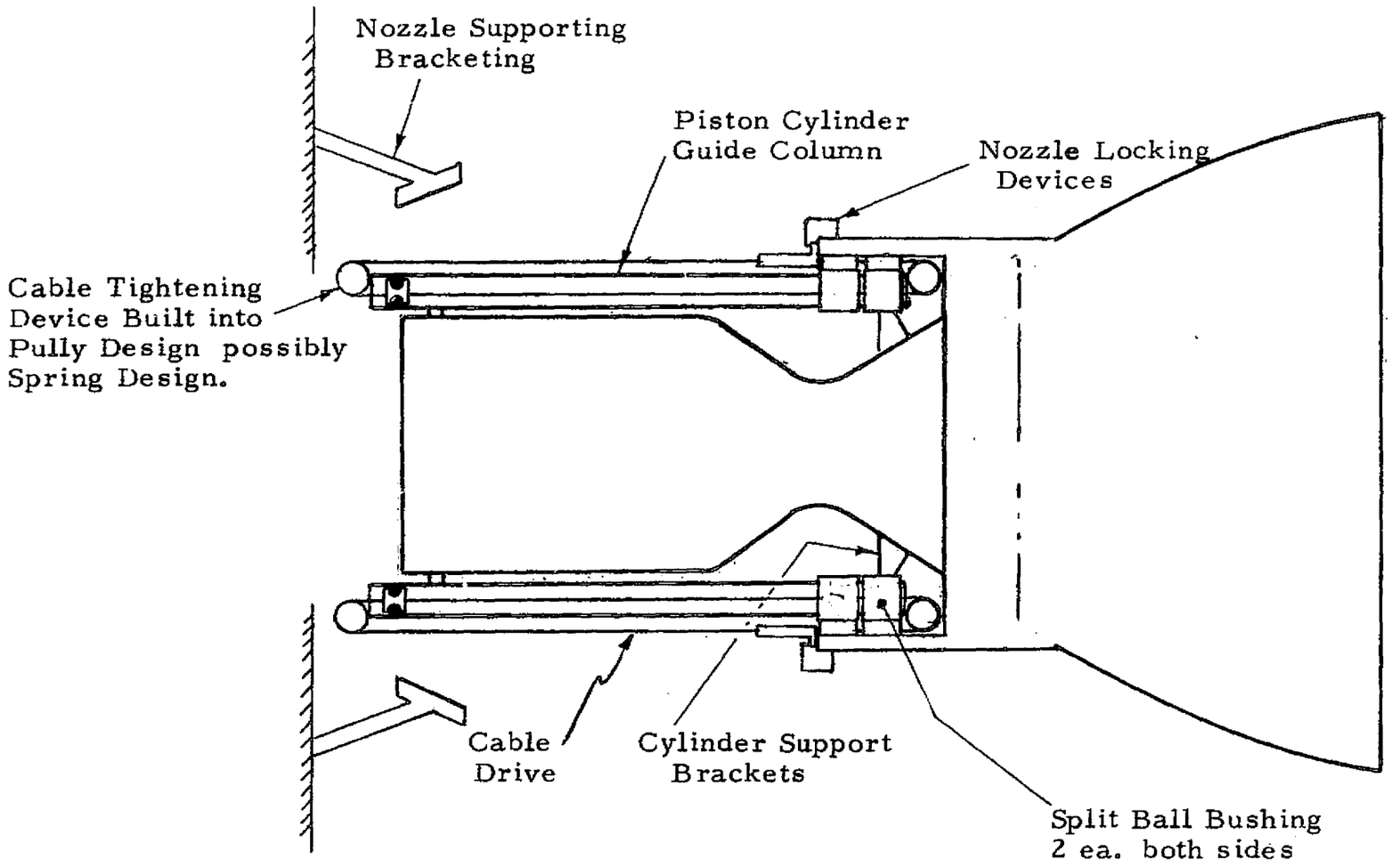


Figure 36

System Requirements:

1. Min. of 2 actuators to translate the nozzle extension.
2. Designed so single actuator could translate the nozzle extension if others failed.
3. Mechanical swival latch (See Figure 21) is required in case of piston or wire rope travel failure. This device allows nozzle extension to travel past the failed actuator.

GAS DRIVE PISTON - CYLINDER



MINIMUM CRITICAL COMPONENTS	ESTIMATE OF WEIGHT
2 ea. Piston-Cylinder (Guide Columns)	22.0
4 ea. Pullys	3.2
6 ft. Steel Cable (2 ea. 6 ft. long)	2.0
4 ea. Ball Bushings	0.6
4 ea. Nozzle Locking Devices	4.0
Misc. Nuts, Washers & Guide Column Supports	4.0
Total Weight	35.8 lb.

DESIGN PROBLEMS

1. Cylinder drive system possibly requires mechanical lock & unlock device to free nozzle extension in case of piston-cylinder or pully failure.

PISTON - CYLINDER - CABLE DRIVE

Figure 37

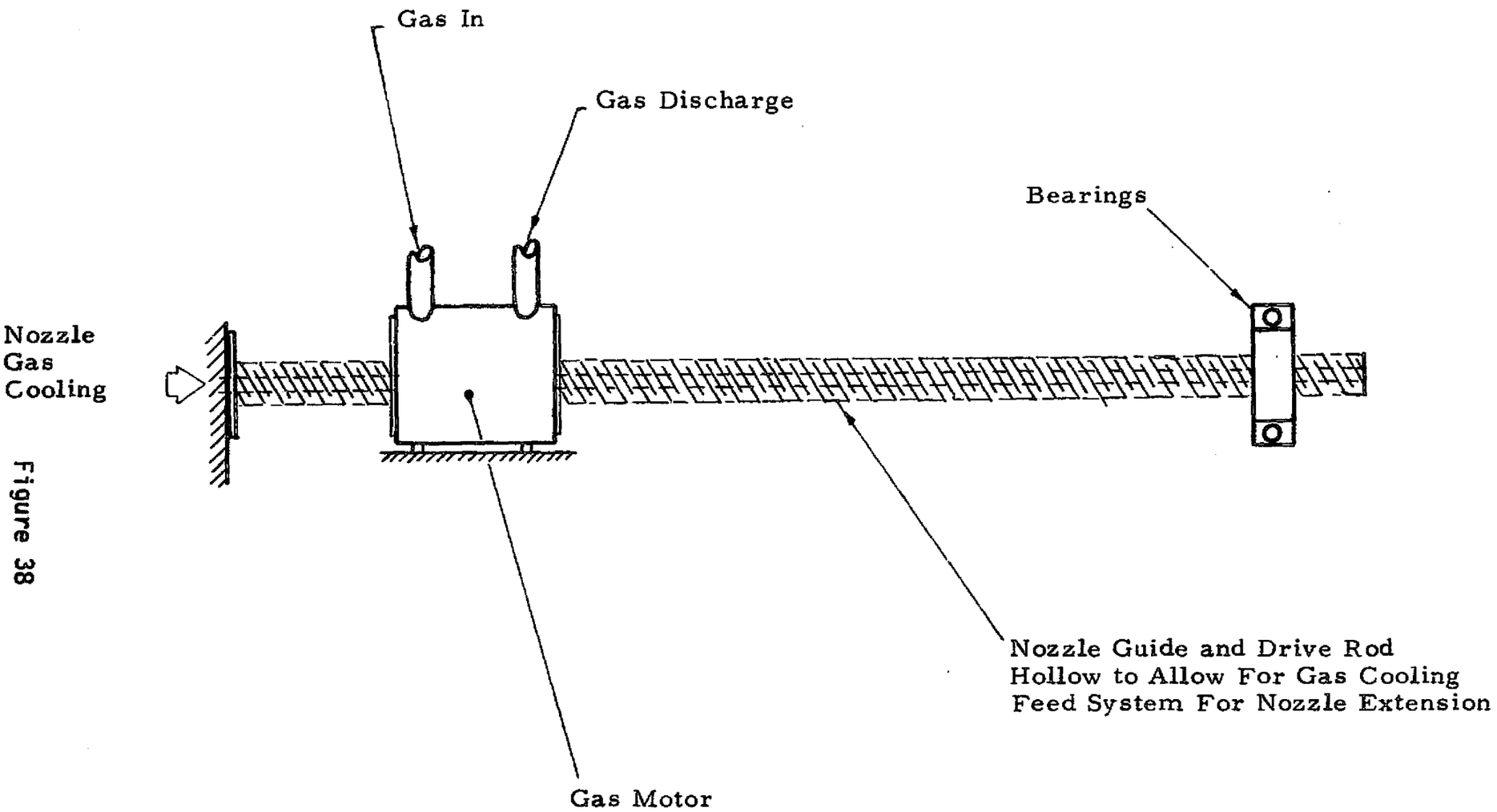


Figure 38

GAS DRIVE - ROTARY MOTOR

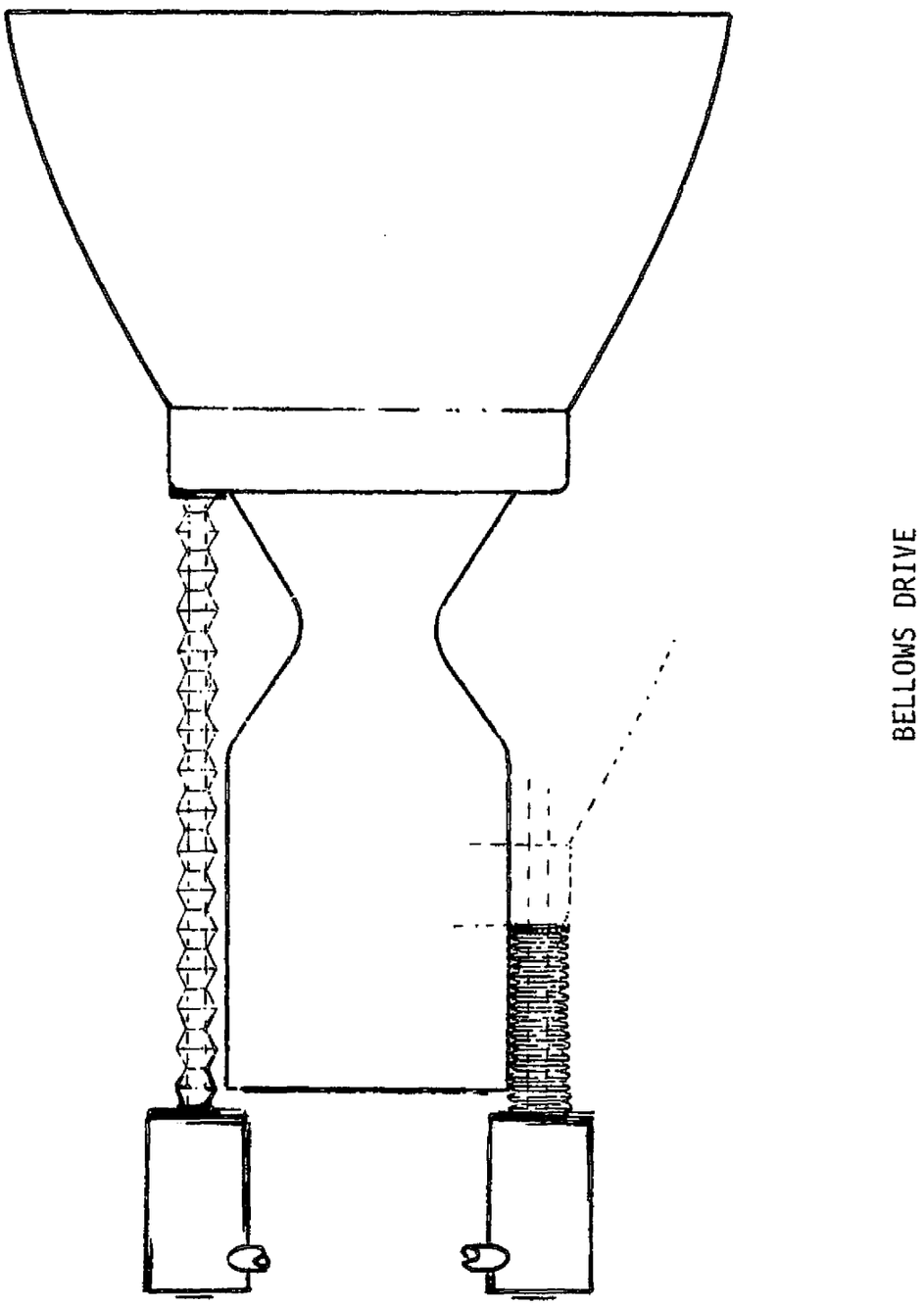
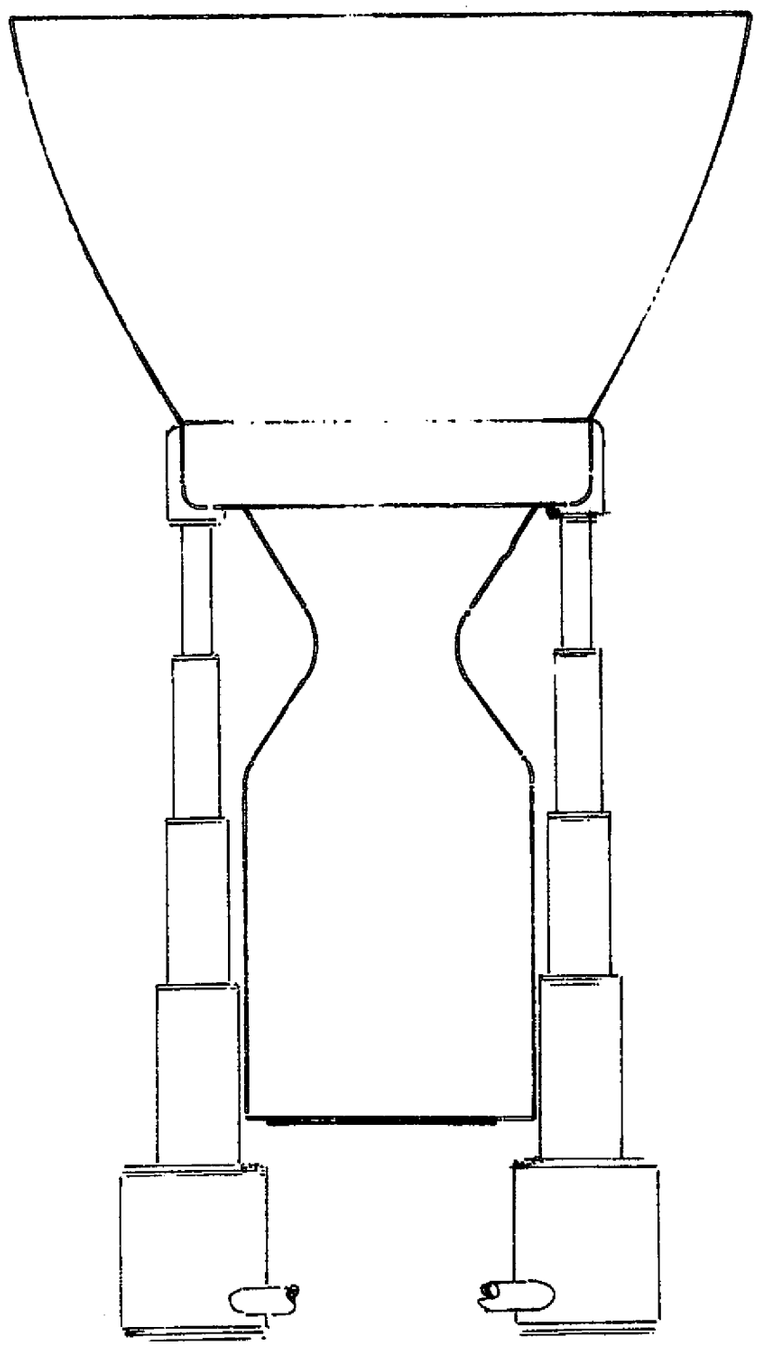


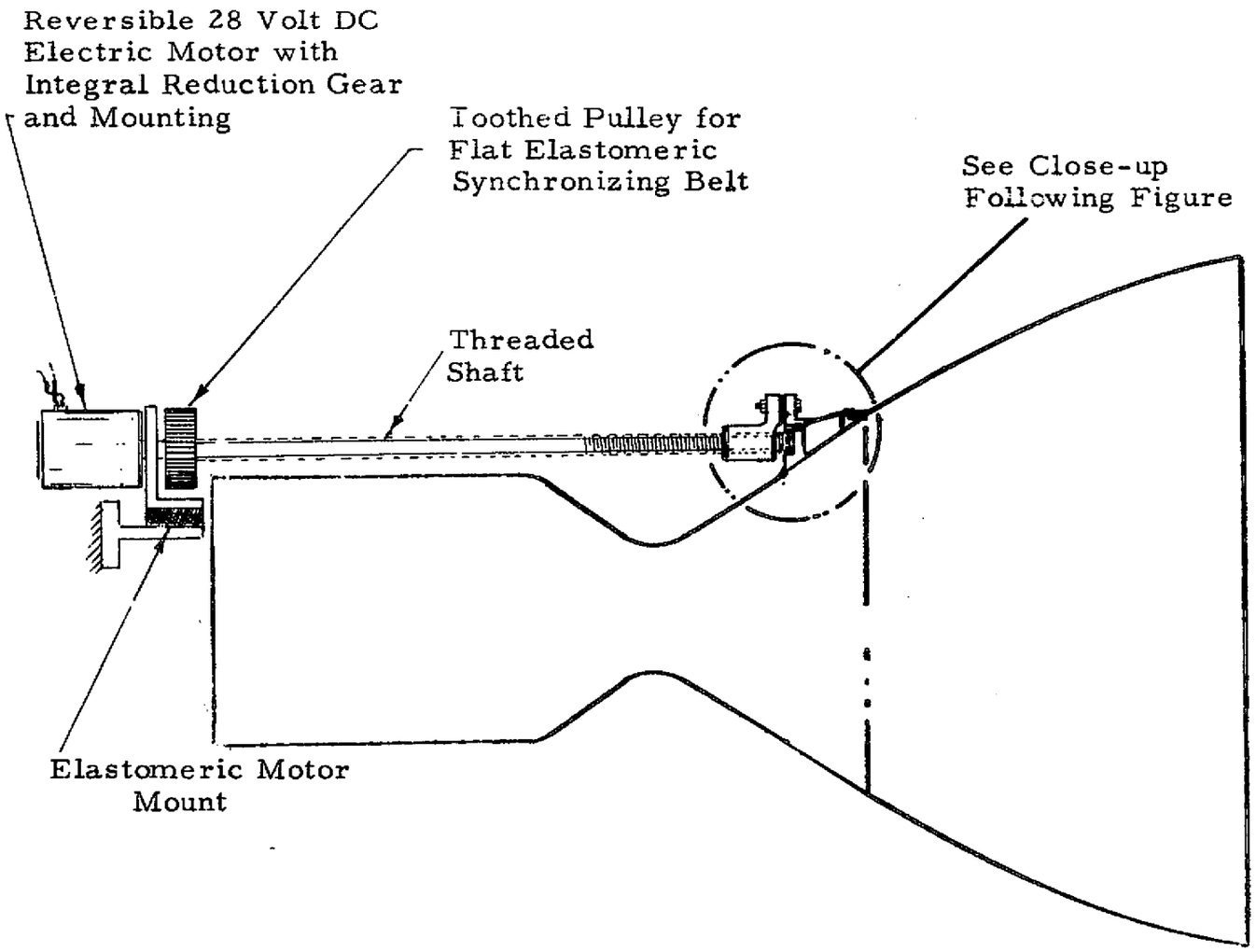
Figure 39

Report 10484-FR



TLLESCOPING ACTUATOR DRIVE

Figure 40



RECOMMENDED EXTENSION TRANSLATION SYSTEM

Figure 41

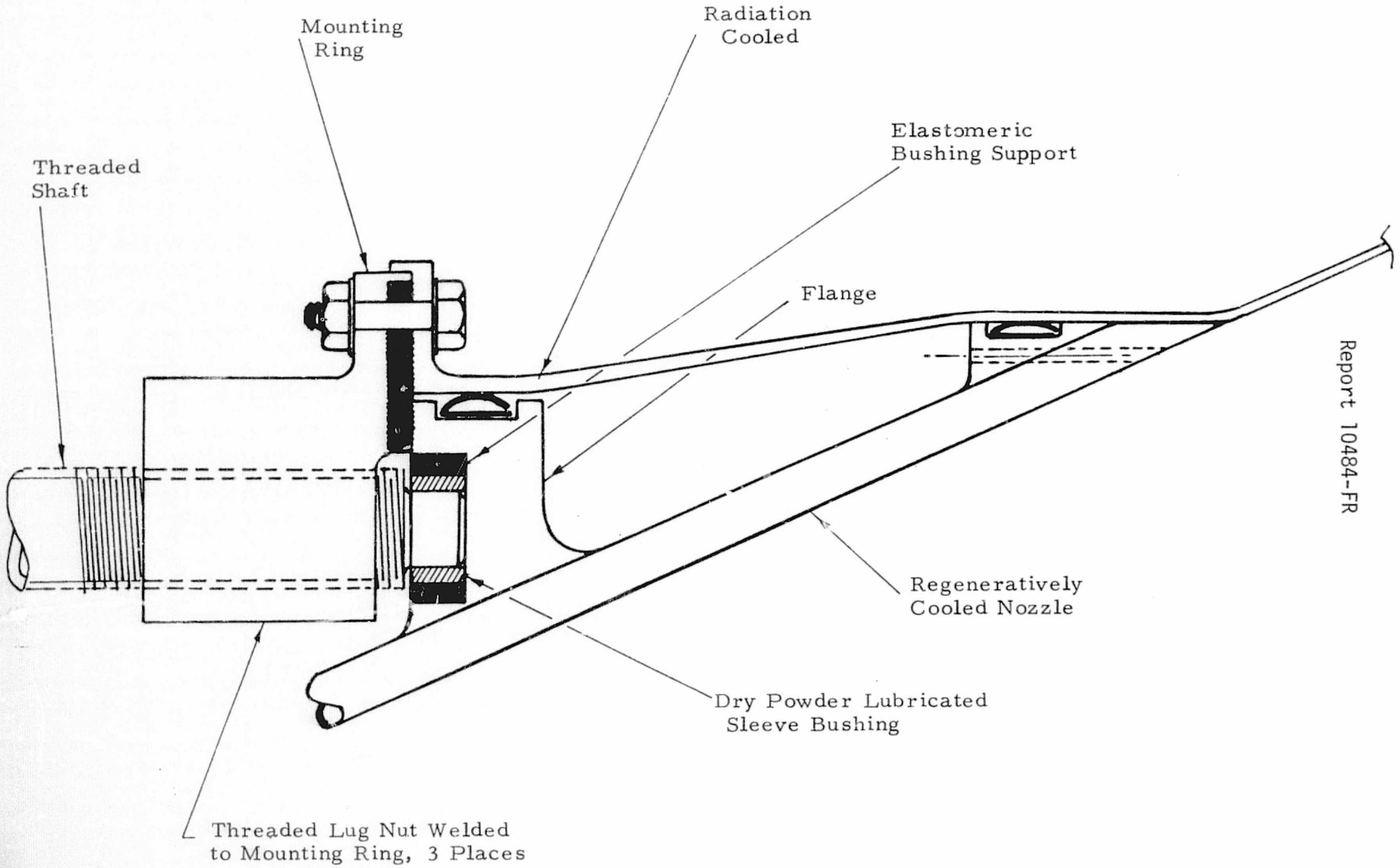
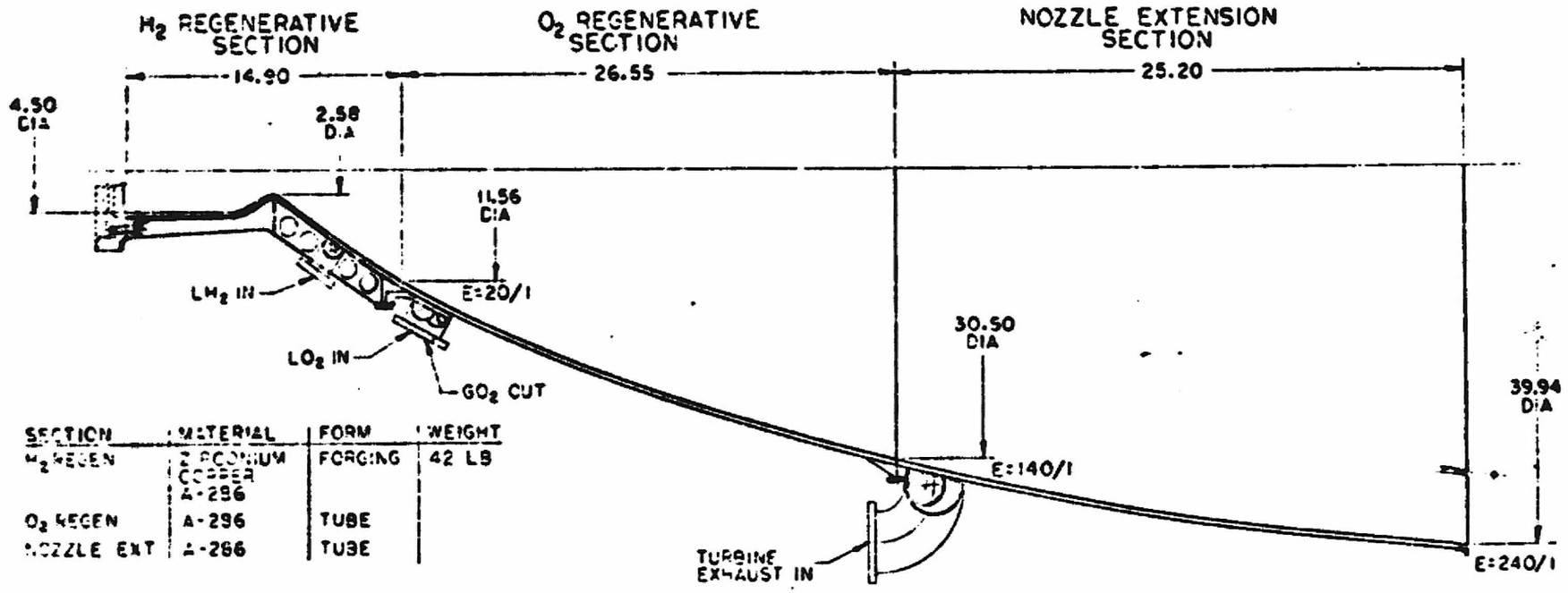


Figure 42

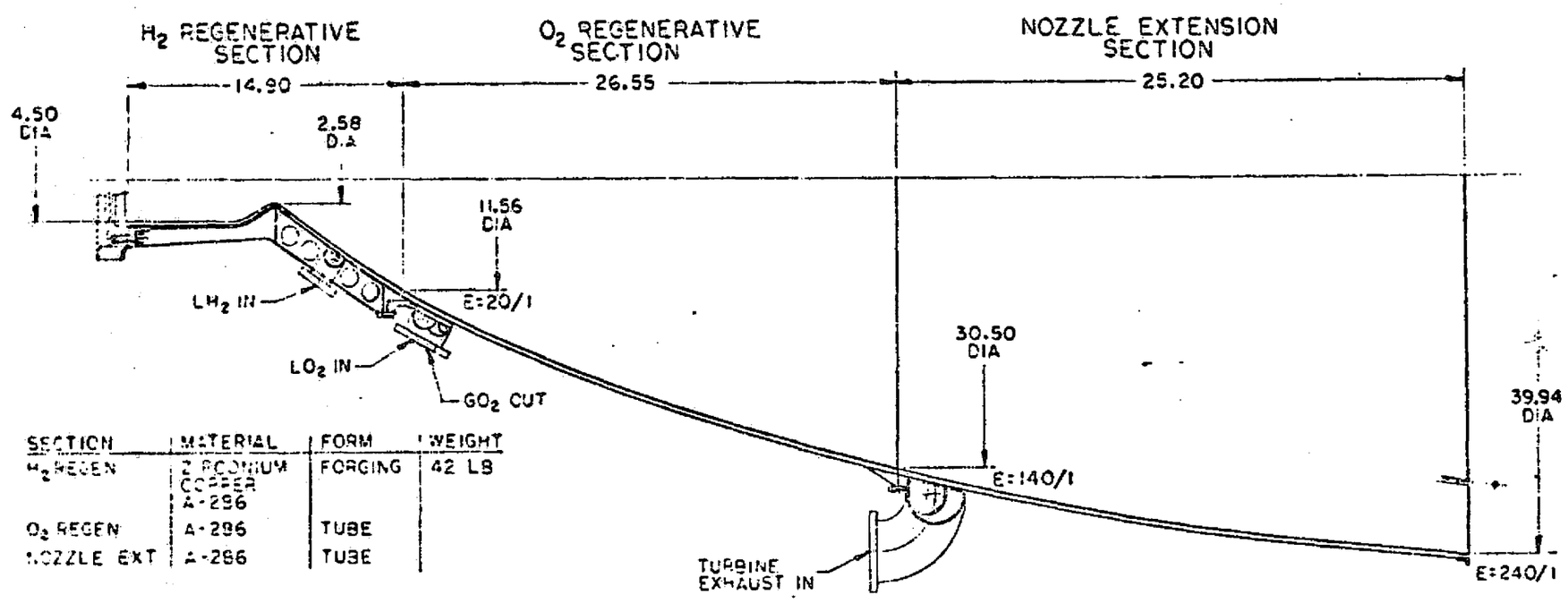
RECOMMENDED TRANSLATION SYSTEM DETAIL



SECTION	MATERIAL	FORM	WEIGHT
H_2 REGEN	ZIRCONIUM COPPER A-286	FORGING	42 LB
O_2 REGEN	A-286	TUBE	
NOZZLE EXT	A-286	TUBE	

Figure 43

Performance Study Base Case Design



SECTION	MATERIAL	FORM	WEIGHT
H_2 REGEN	ZIRCONIUM COPPER A-286	FORGING	42 LB
O_2 REGEN	A-286	TUBE	
NOZZLE EXT	A-286	TUBE	

Figure 43 Performance Study Base Case Design

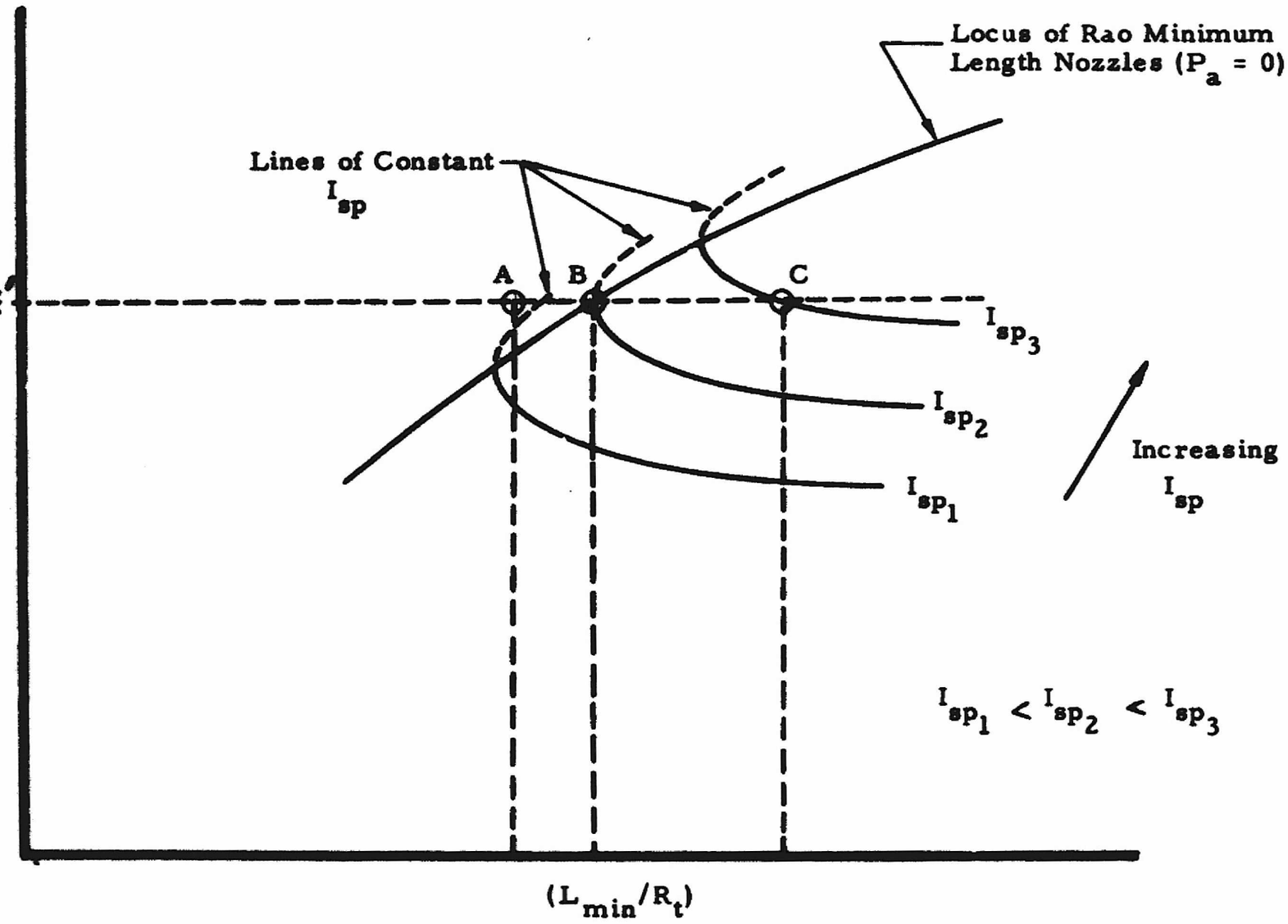


Figure 44

SCHEMATIC PLOT OF RAO NOZZLE DESIGN PARAMETERS

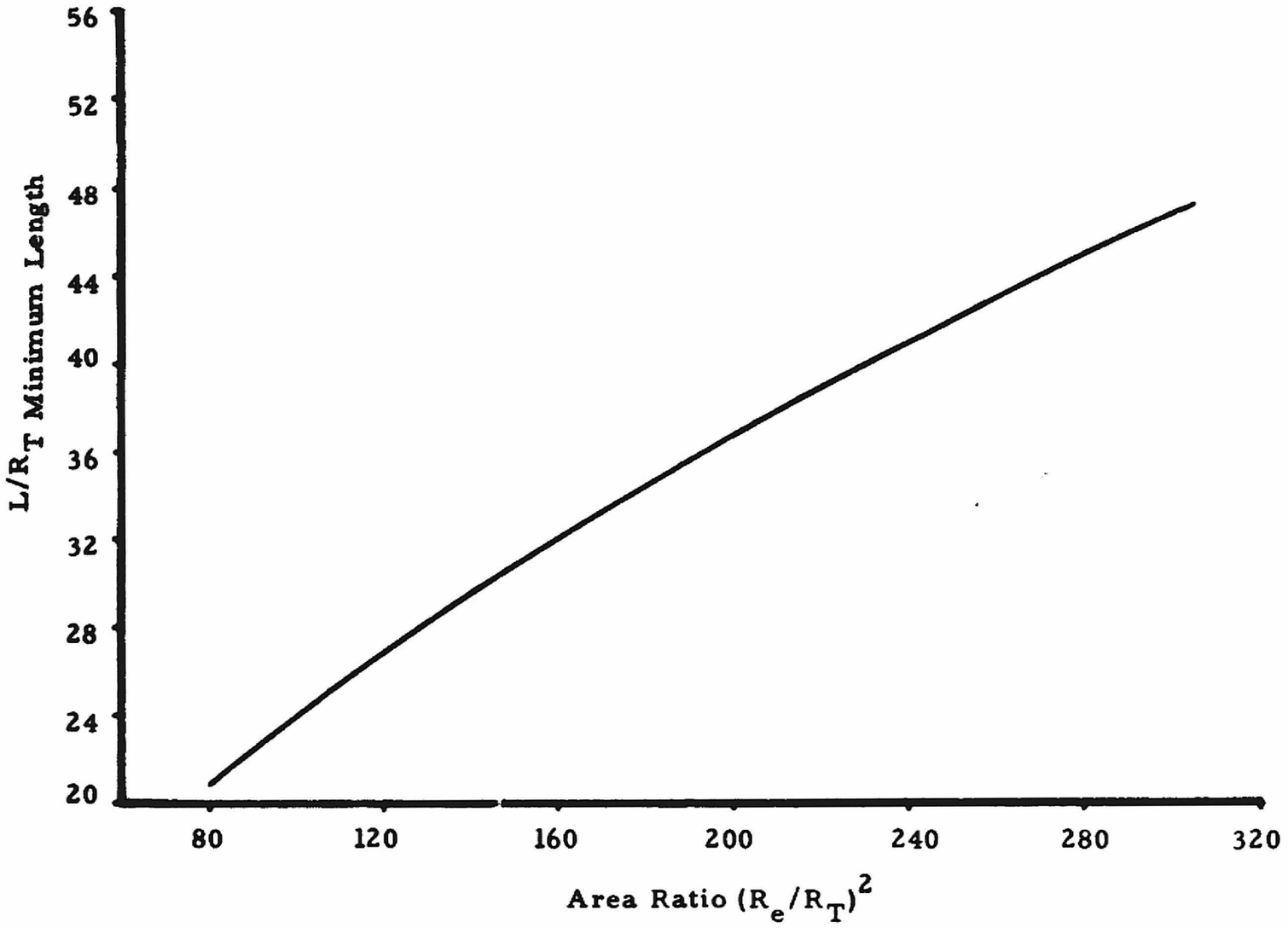


Figure 45

MINIMUM LENGTH RAO VERSUS EXPANSION RATIO (γ = 1.22)

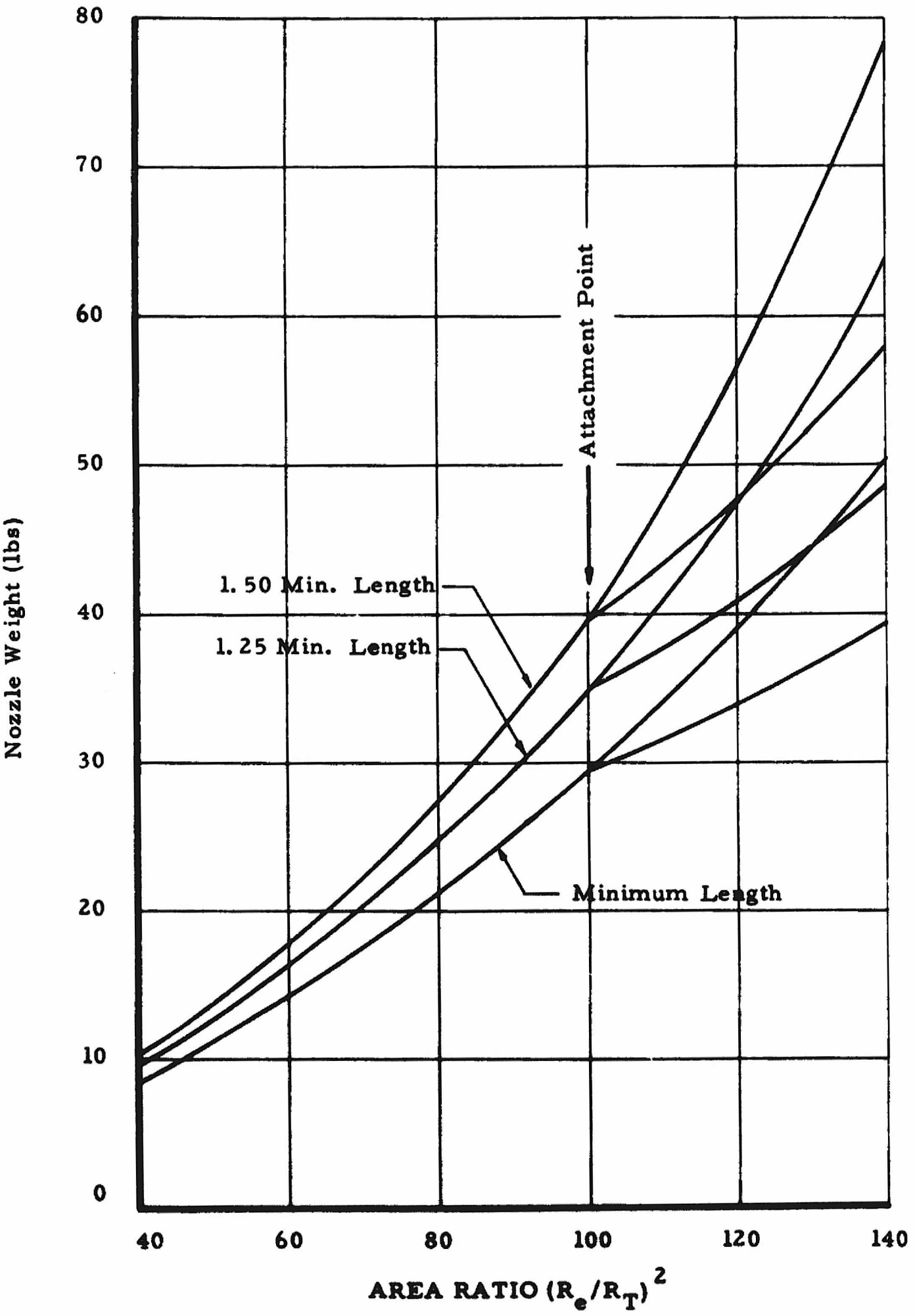


FIGURE 46 NOZZLE WEIGHT VS. AREA RATIO
(RADIATION-FILM COOLED EXTENSION, EXIT AREA RATIO = 140)

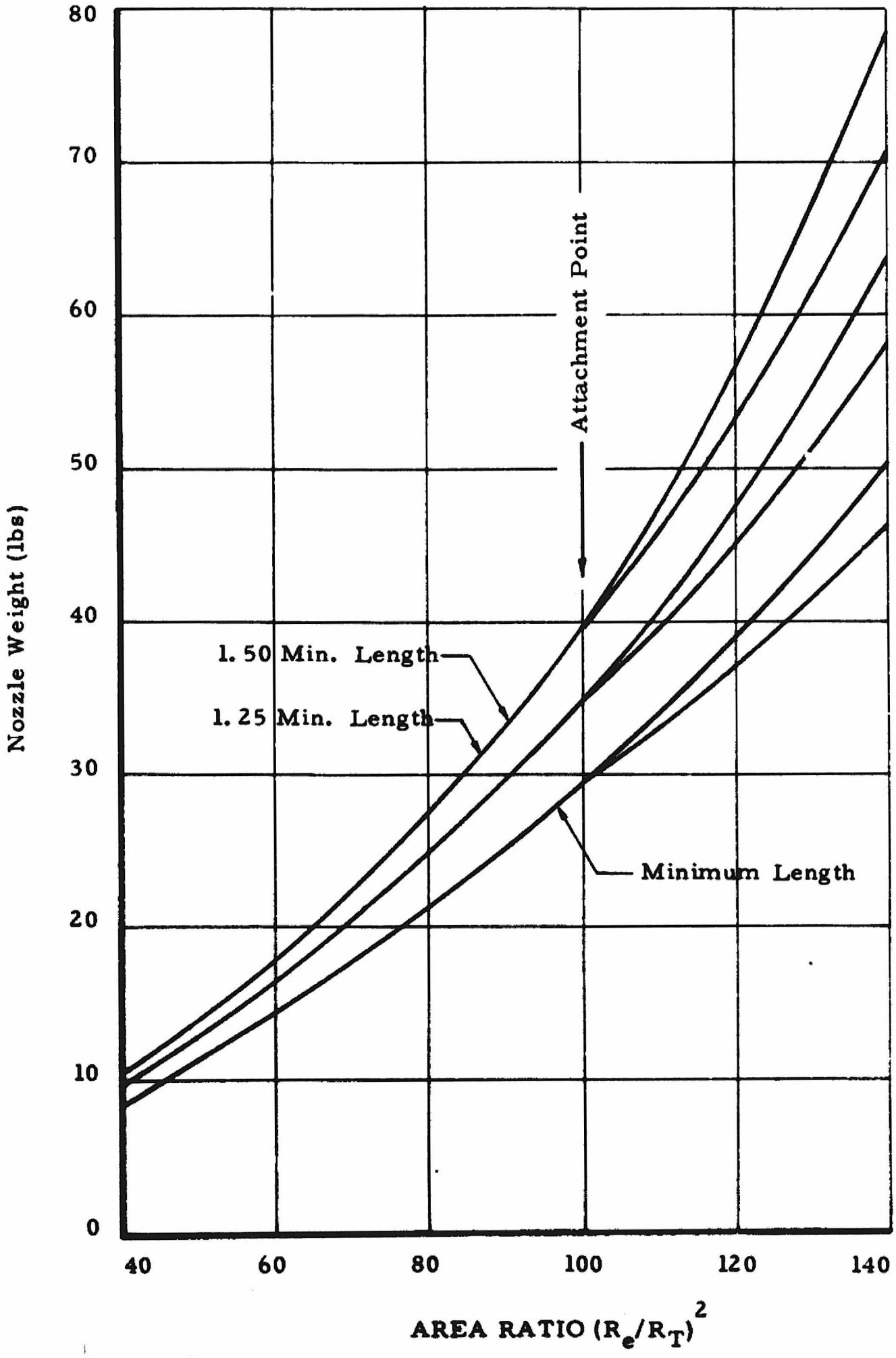


FIGURE 47 NOZZLE WEIGHT VS. AREA RATIO
(TUBE BUNDLE EXTENSION, EXIT AREA RATIO = 140)

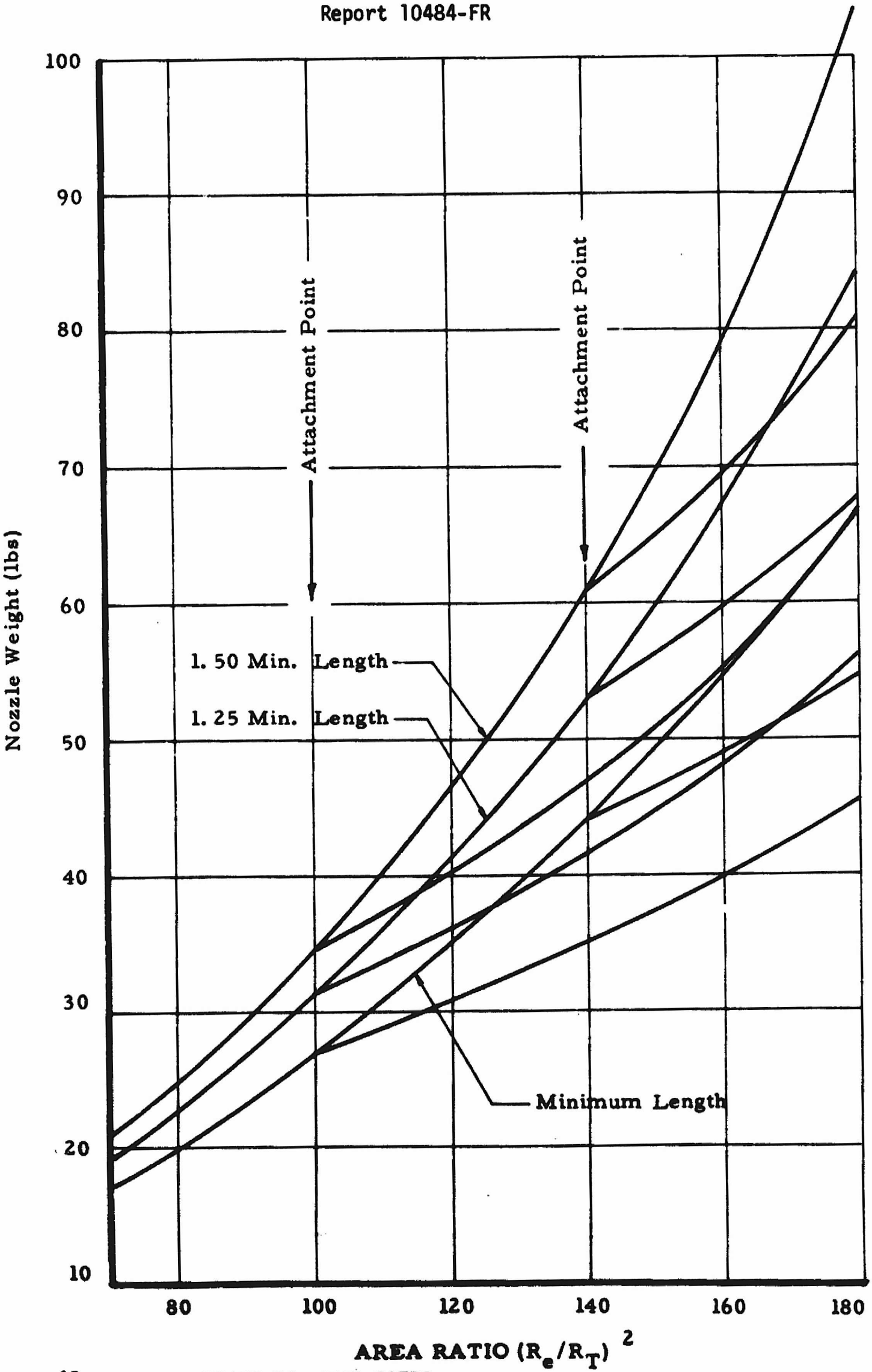


FIGURE 48 NOZZLE WEIGHT VS. AREA RATIO
(RADIATION-FILM COOLED EXTENSION, EXIT AREA RATIO = 180)

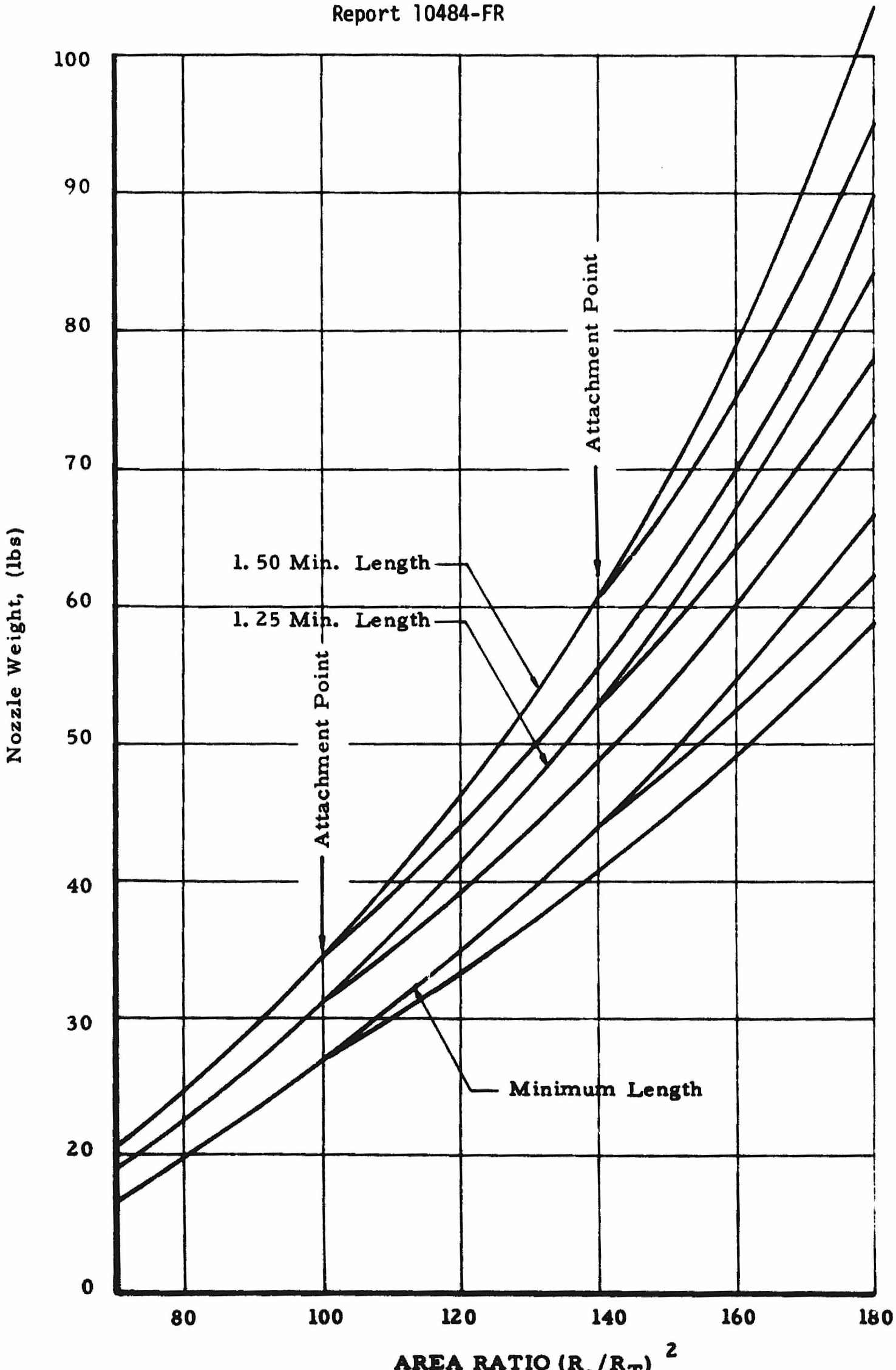


FIGURE 49 NOZZLE WEIGHT VS. AREA RATIO
(TUBE NOZZLE EXTENSION, EXIT AREA RATIO = 180)

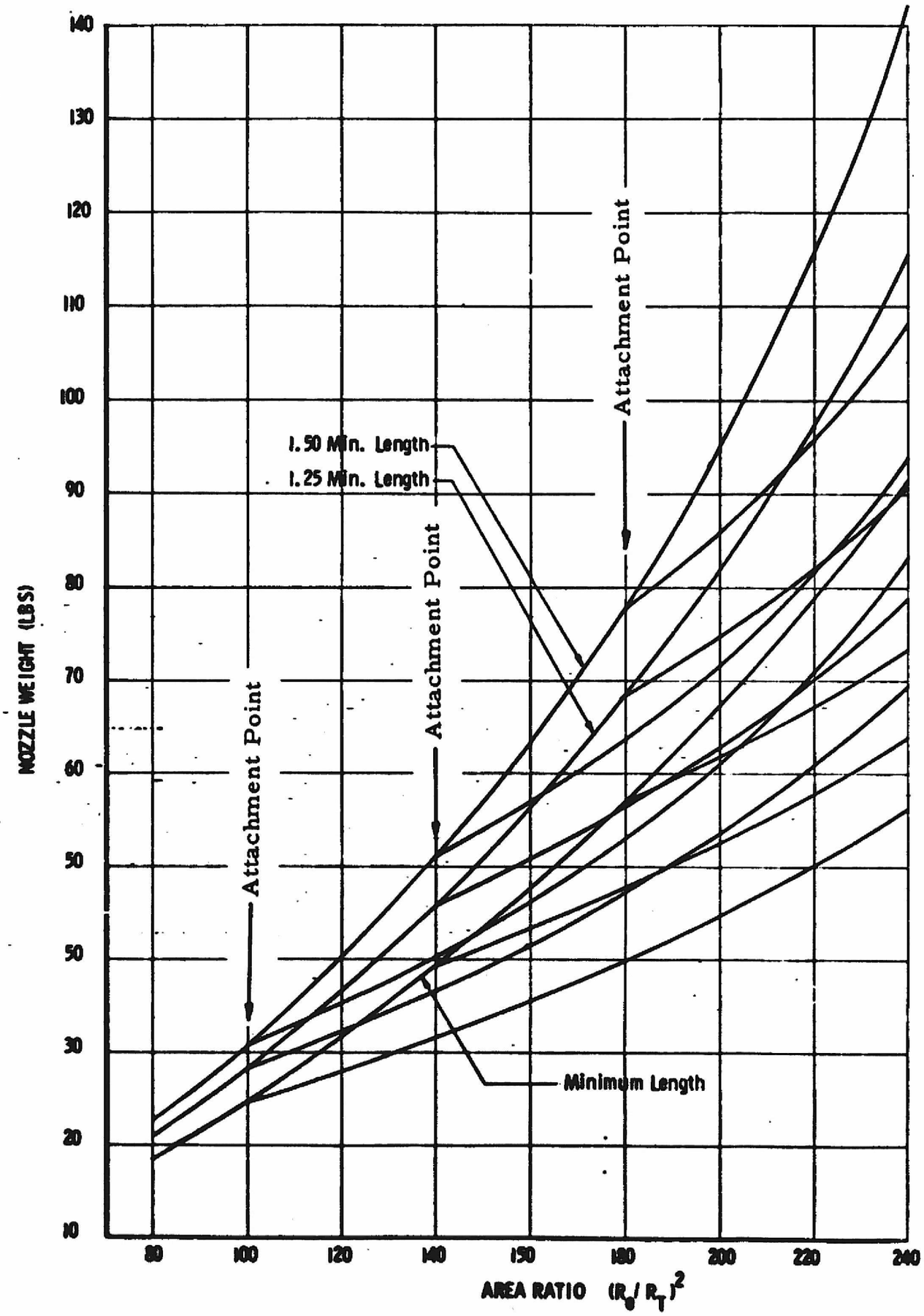


FIGURE 50 NOZZLE WEIGHT VS. AREA RATIO (RADIATION-FILM COOLED EXTENSION, EXIT AREA RATIO = 240)

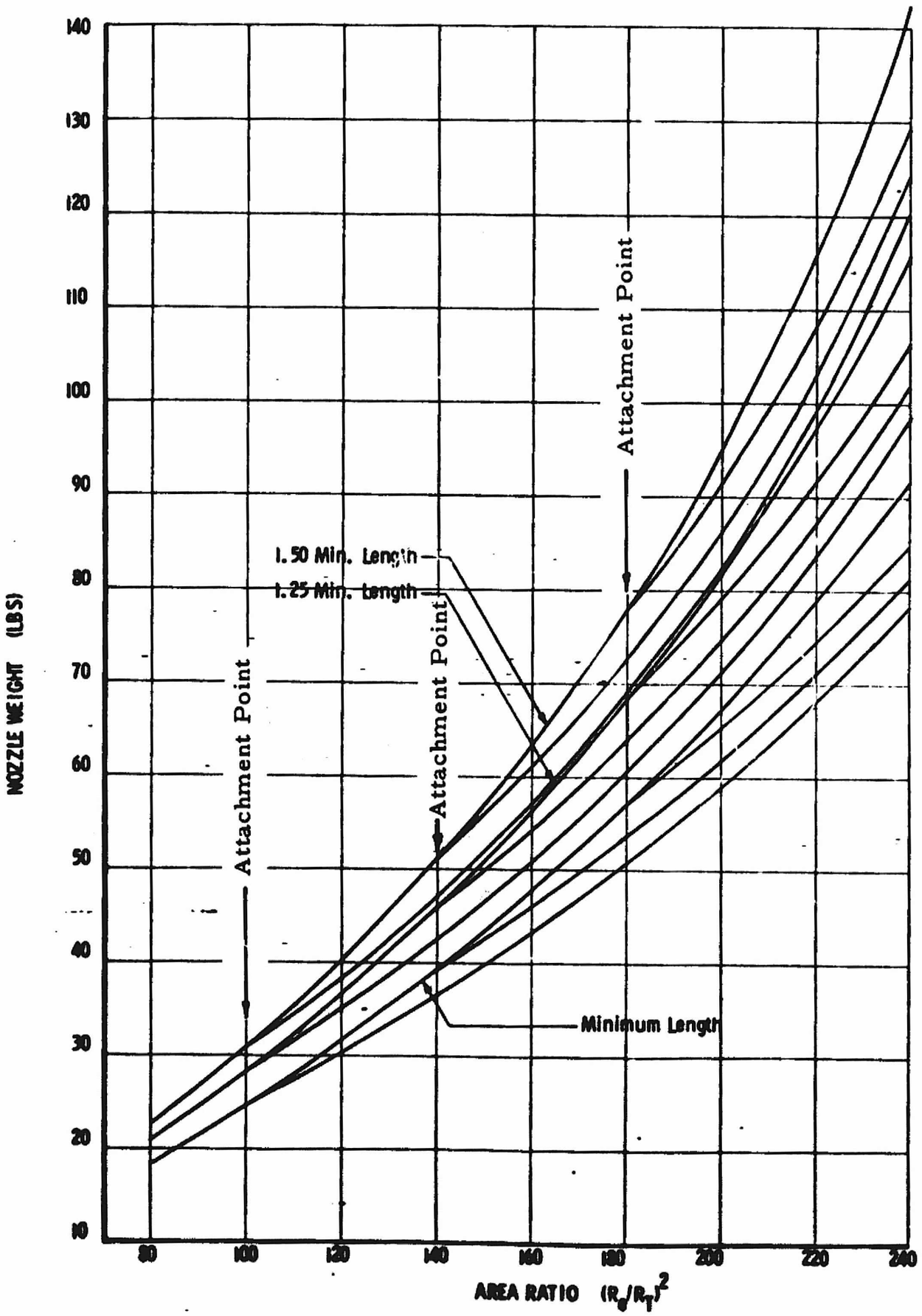


FIGURE 51 NOZZLE WEIGHT VS. AREA RATIO
(TUBE BUNDLE EXTENSION, EXIT AREA RATIO = 240)

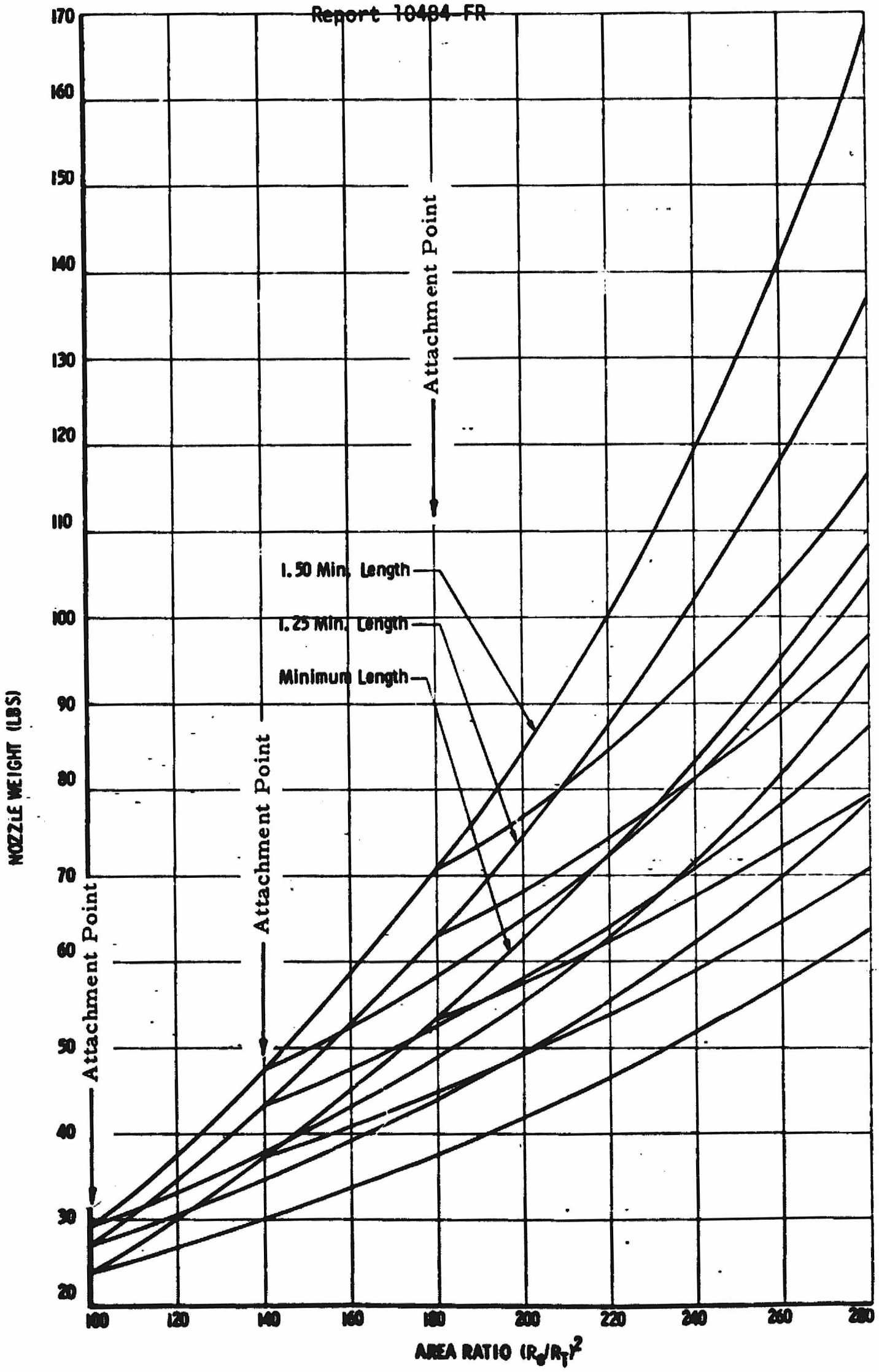


FIGURE 52 NOZZLE WEIGHT VS. AREA RATIO (RADIATION-FILM COOLED EXTENSION, EXIT AREA RATIO = 280)

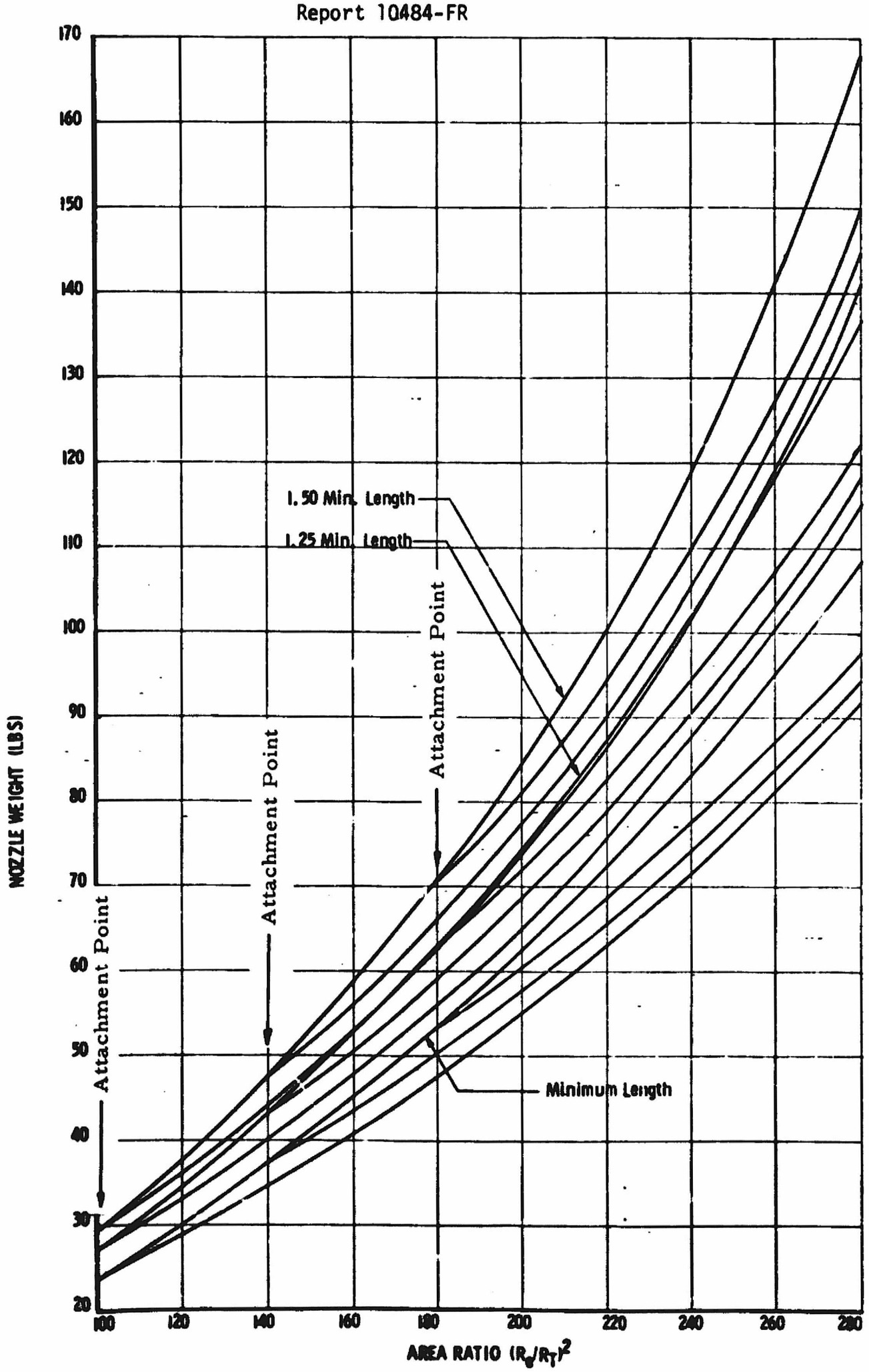


FIGURE 53 NOZZLE WEIGHT VS. AREA RATIO
(TUBE BUNDLE EXTENSION, EXIT AREA RATIO = 280)

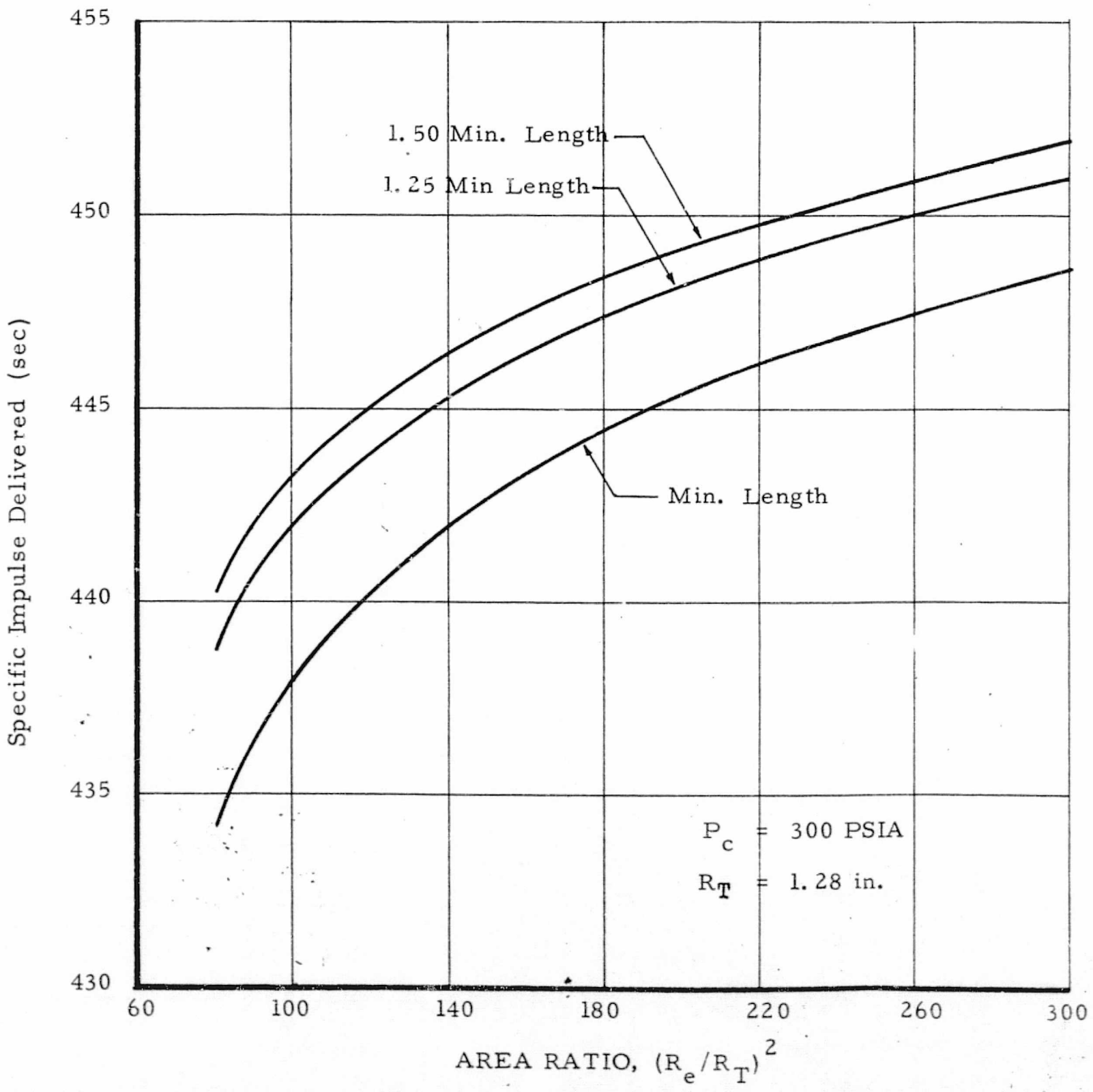


FIGURE 54 DELIVERED SPECIFIC IMPULSE VS. AREA RATIO
(R_t = 1.28, P_c = 300 PSIA)

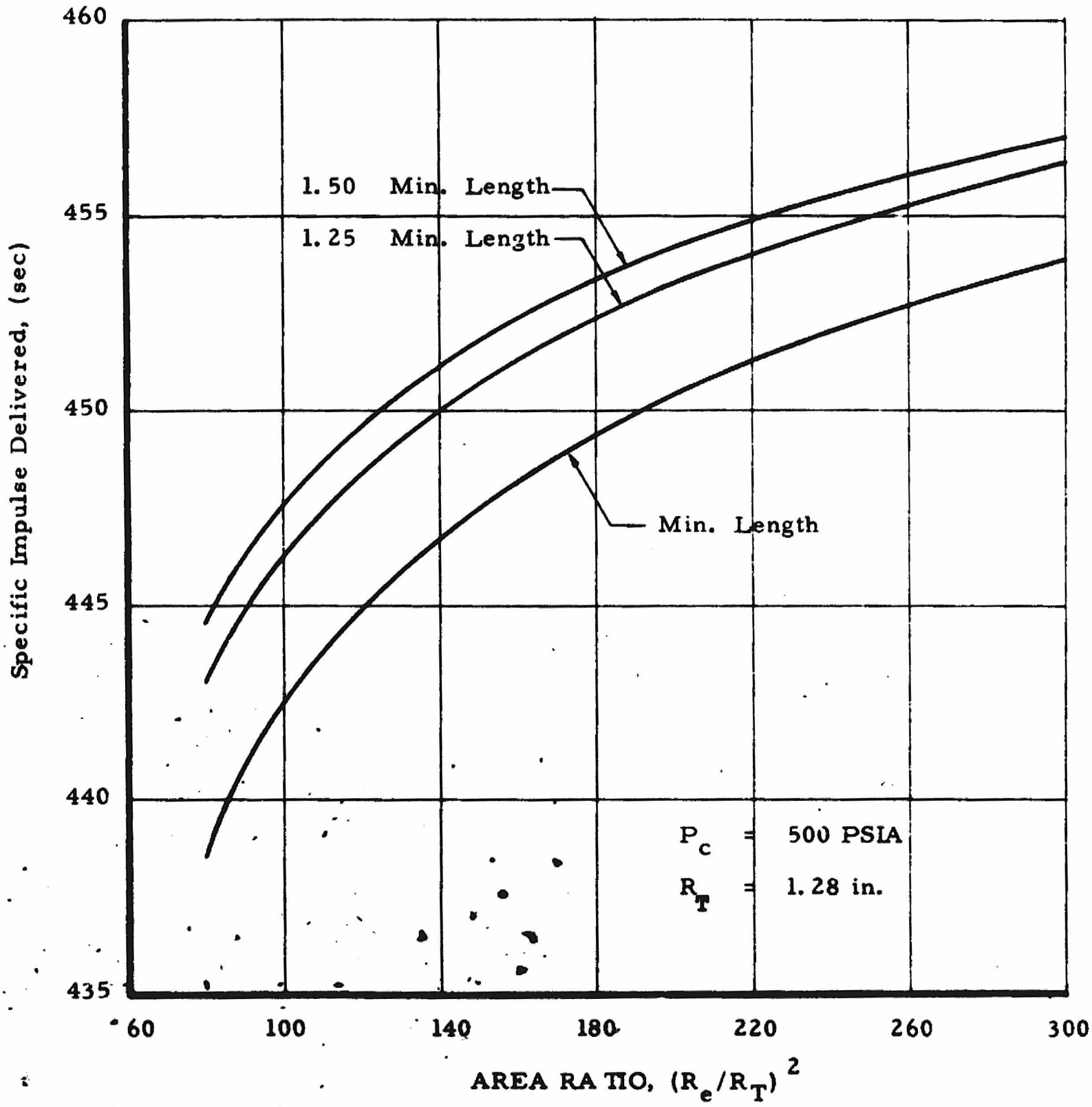


FIGURE 55 DELIVERED SPECIFIC IMPULSE VS. AREA RATIO
(R_t = 1.28, P_c = 500 PSIA)

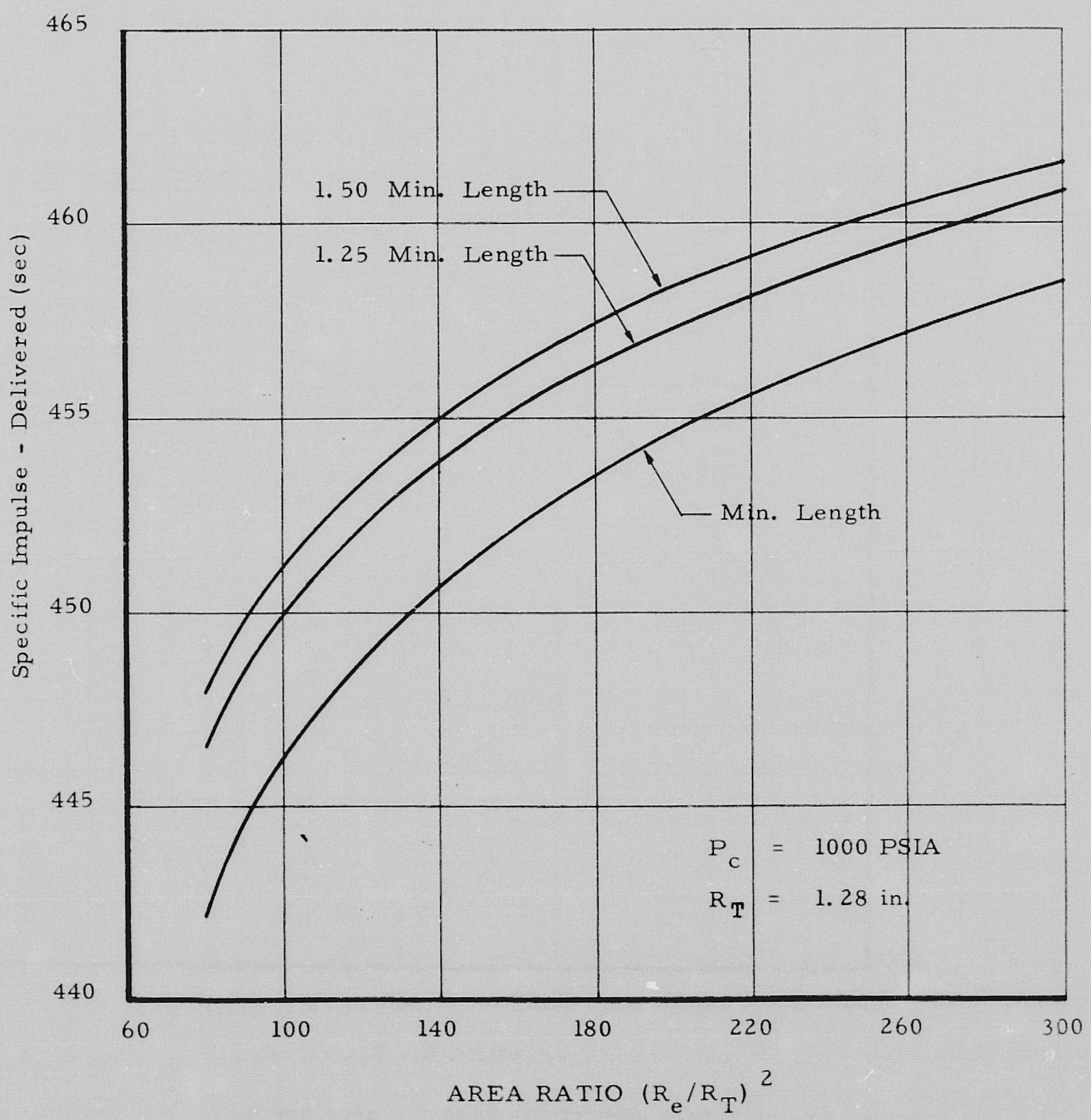


FIGURE 56 DELIVERED SPECIFIC IMPULSE VS. AREA RATIO (R_t = 1.28, P_c = 1000 PSIA)

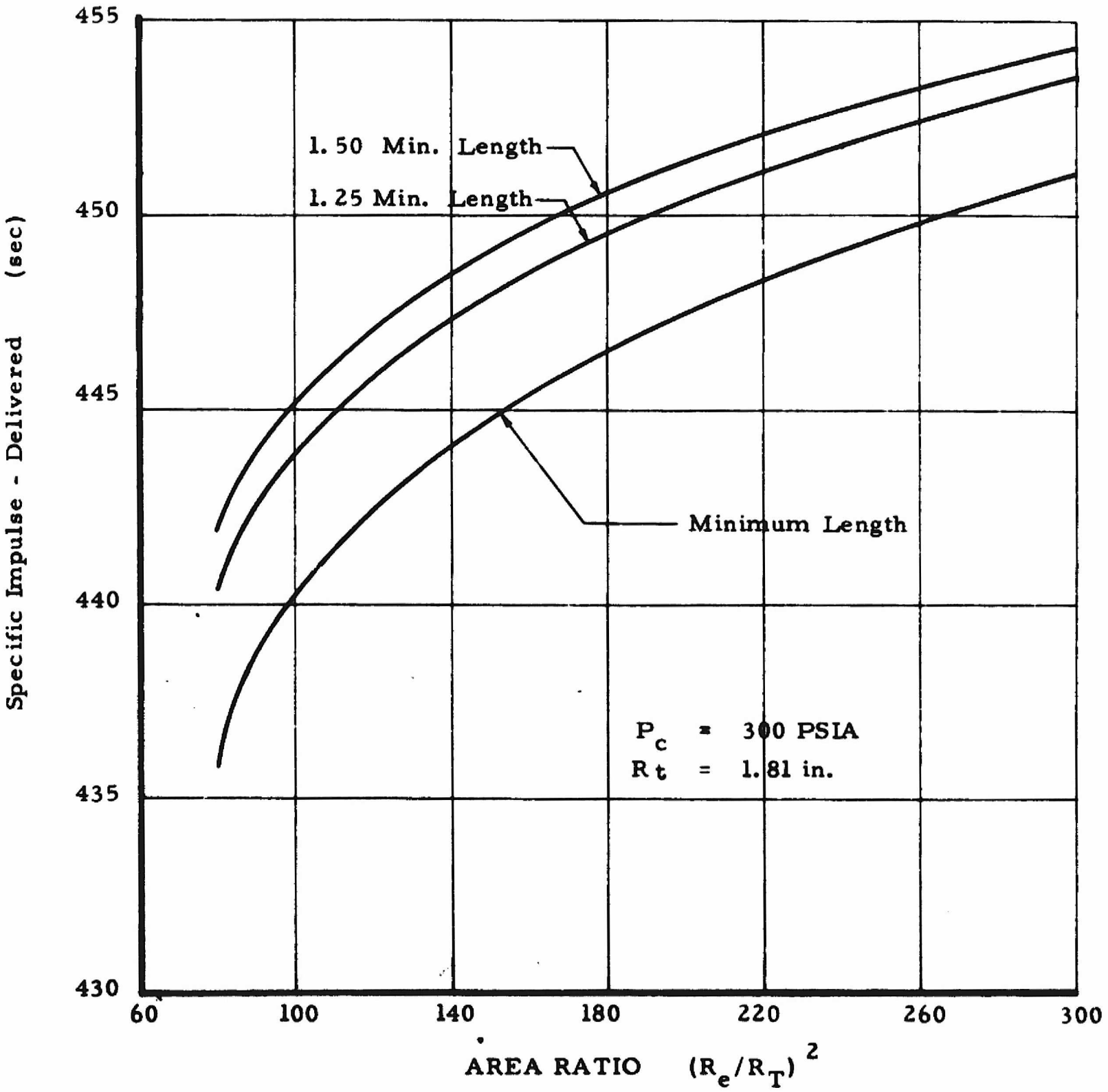


FIGURE 57 DELIVERED SPECIFIC IMPULSE VS. AREA RATIO
(R_t = 1.81, P_c = 300 PSIA)

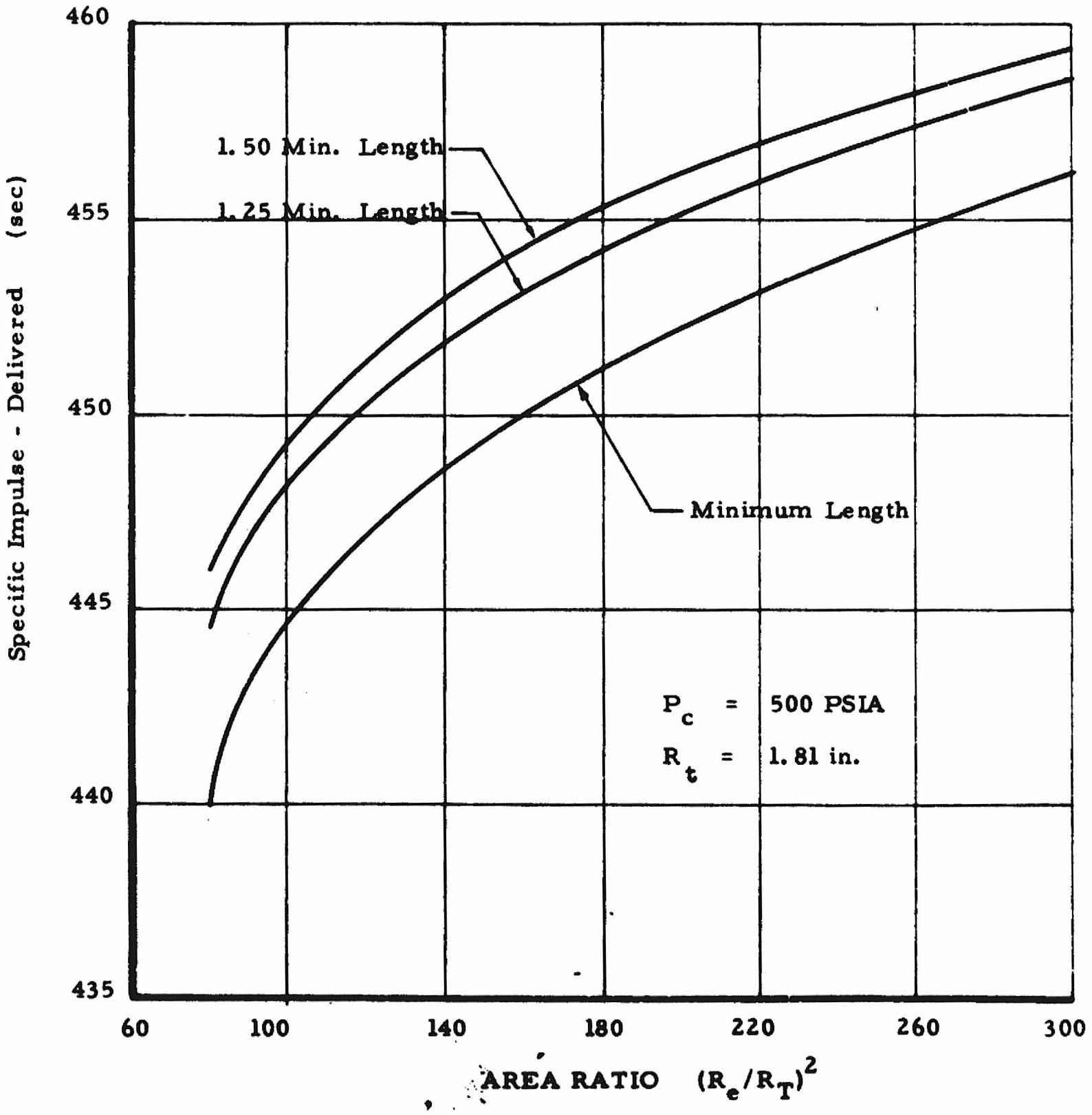


FIGURE 58 DELIVERED SPECIFIC IMPULSE VS. AREA RATIO (R_t = 1.81, P_c = 500 PSIA)

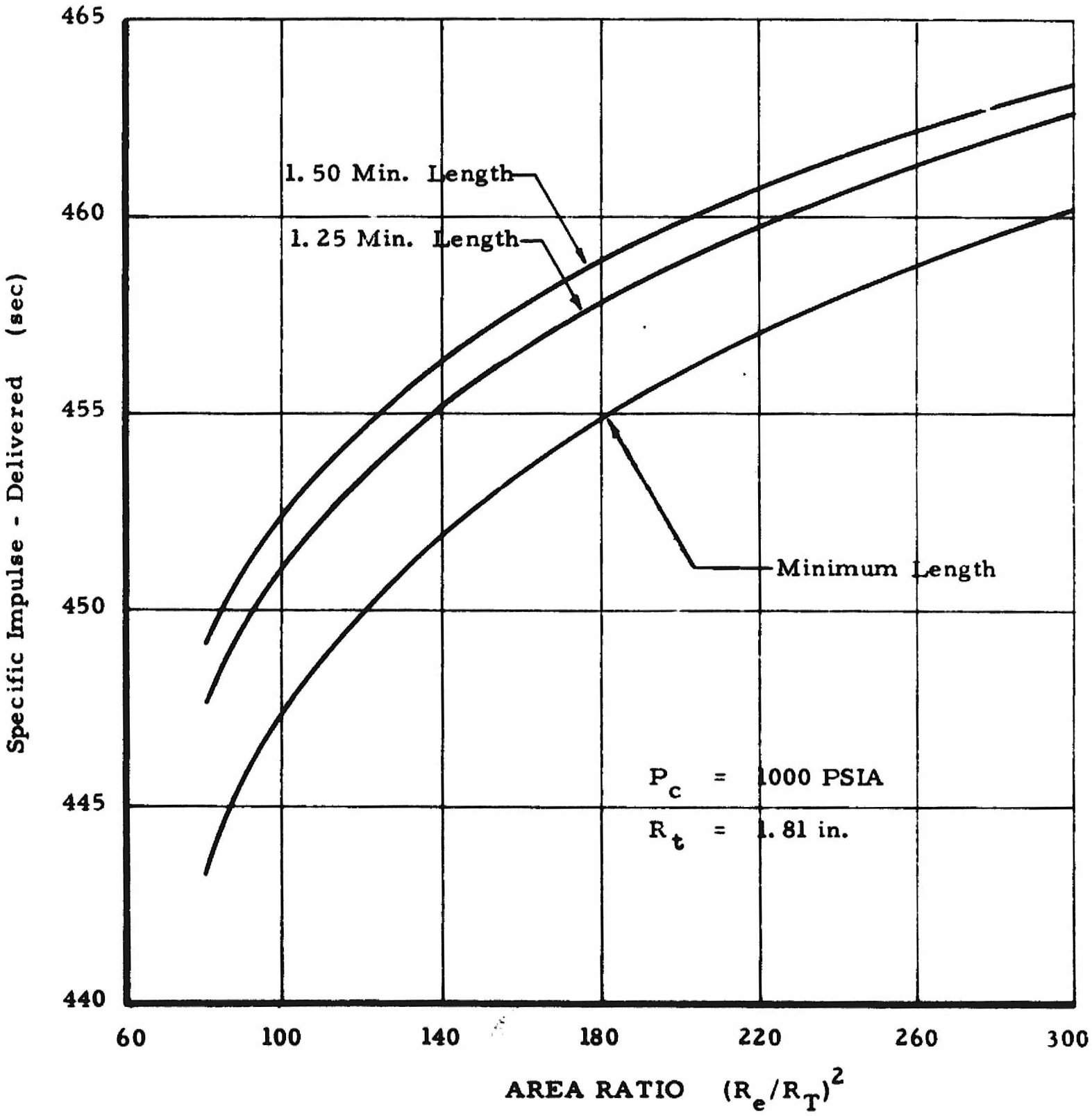


FIGURE 59 DELIVERED SPECIFIC IMPULSE VS. AREA RATIO (R_t = 1.81, P_c = 1000 PSIA)

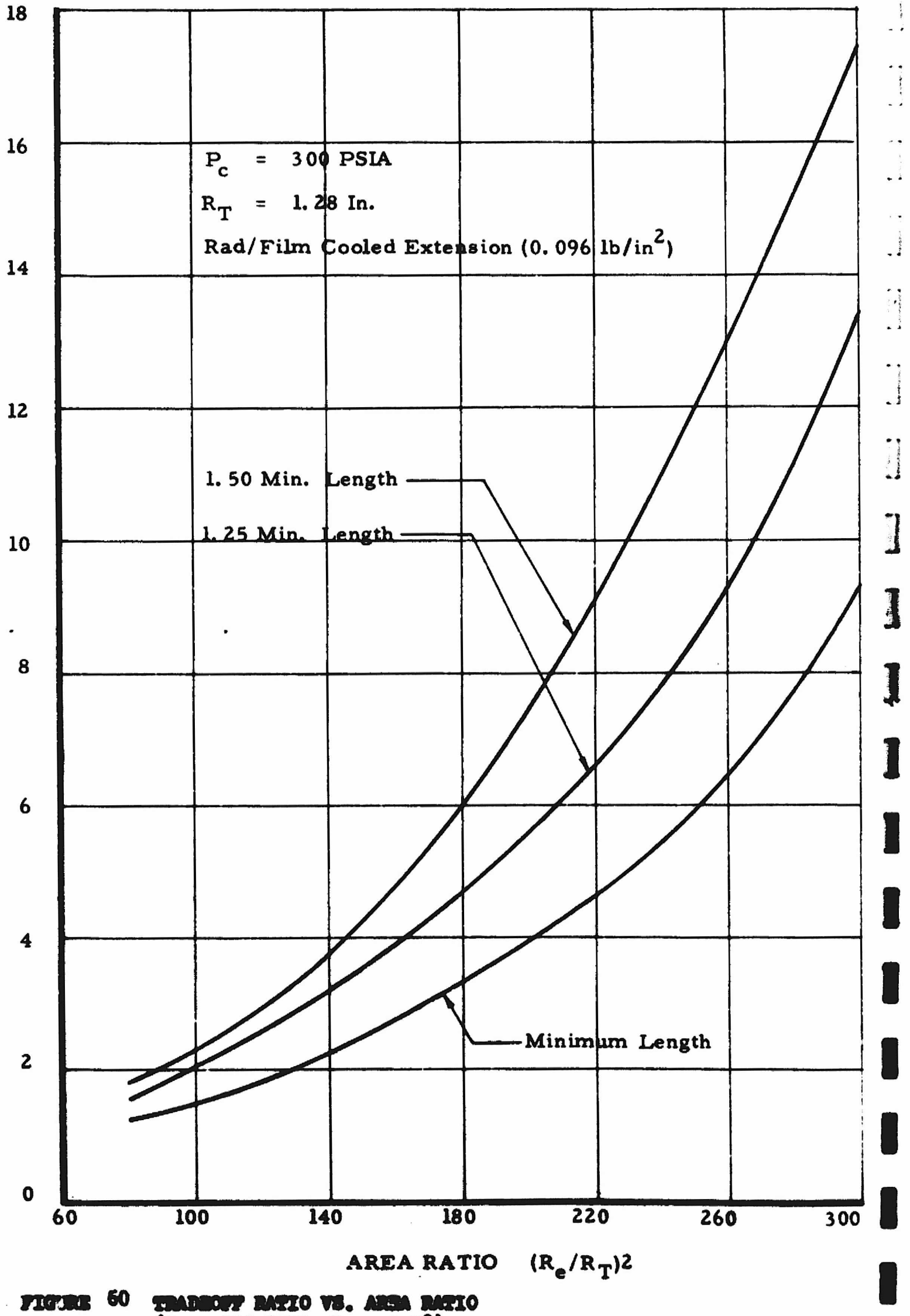


FIGURE 60 TRADEOFF RATIO VS. AREA RATIO
(P_c = 300 PSIA, R_T = 1.28)

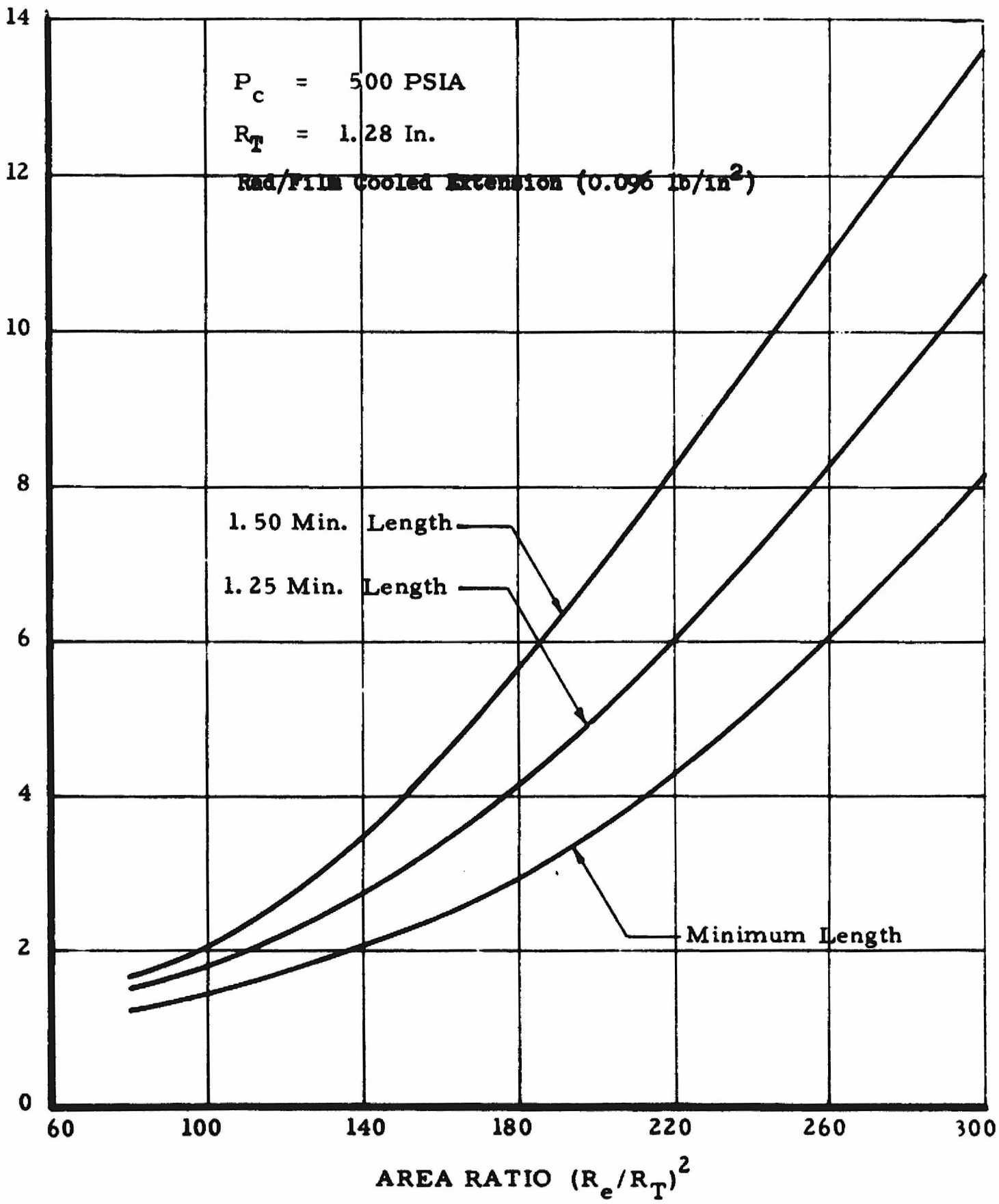


FIGURE 61 TRADE-OFF RATIO VS. AREA RATIO
(P_c = 500 PSIA, R_T = 1.28)

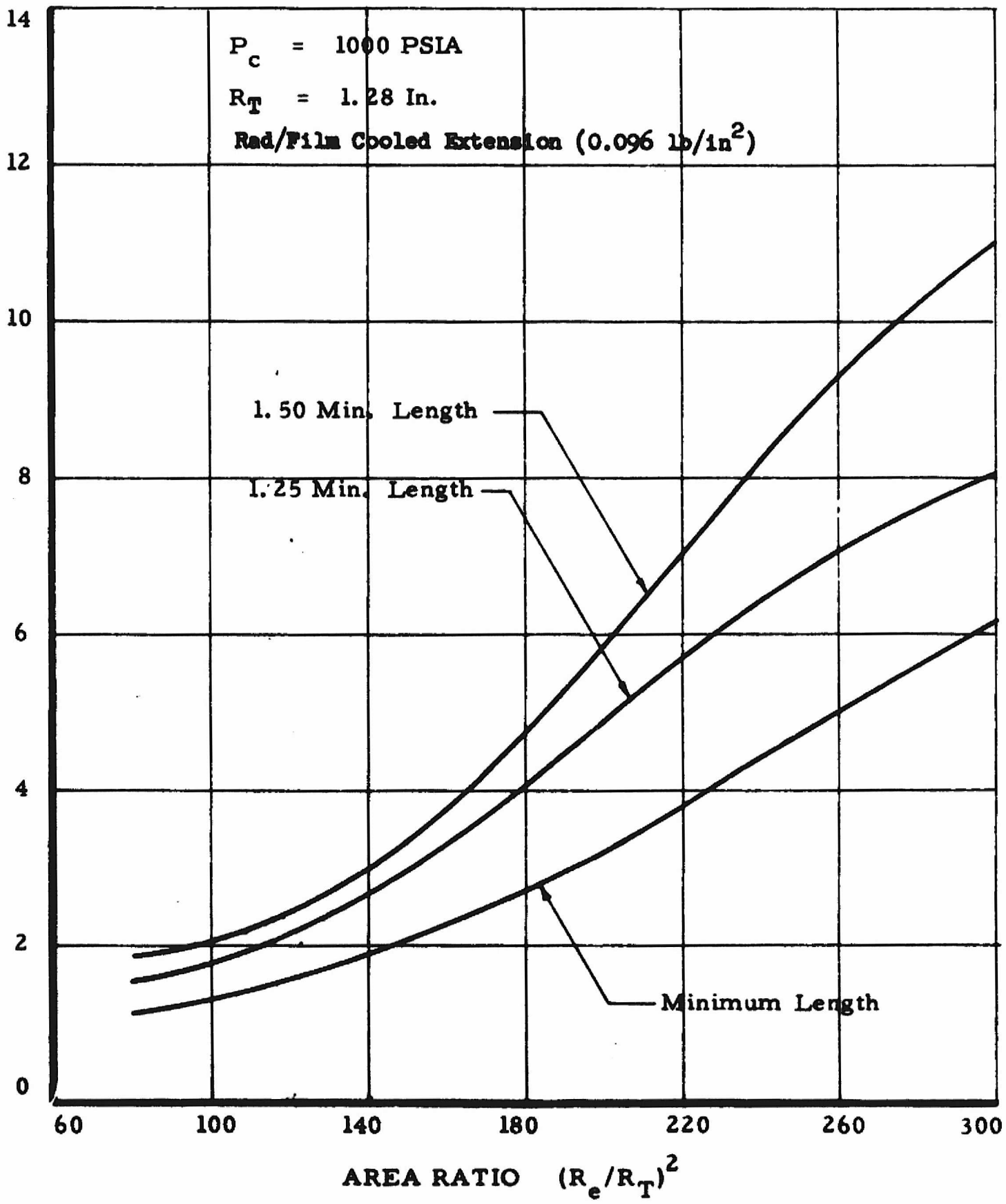


FIGURE 62 TRADE-OFF RATIO VS. AREA RATIO
(P_c = 1000 PSIA, R_T = 1.28)

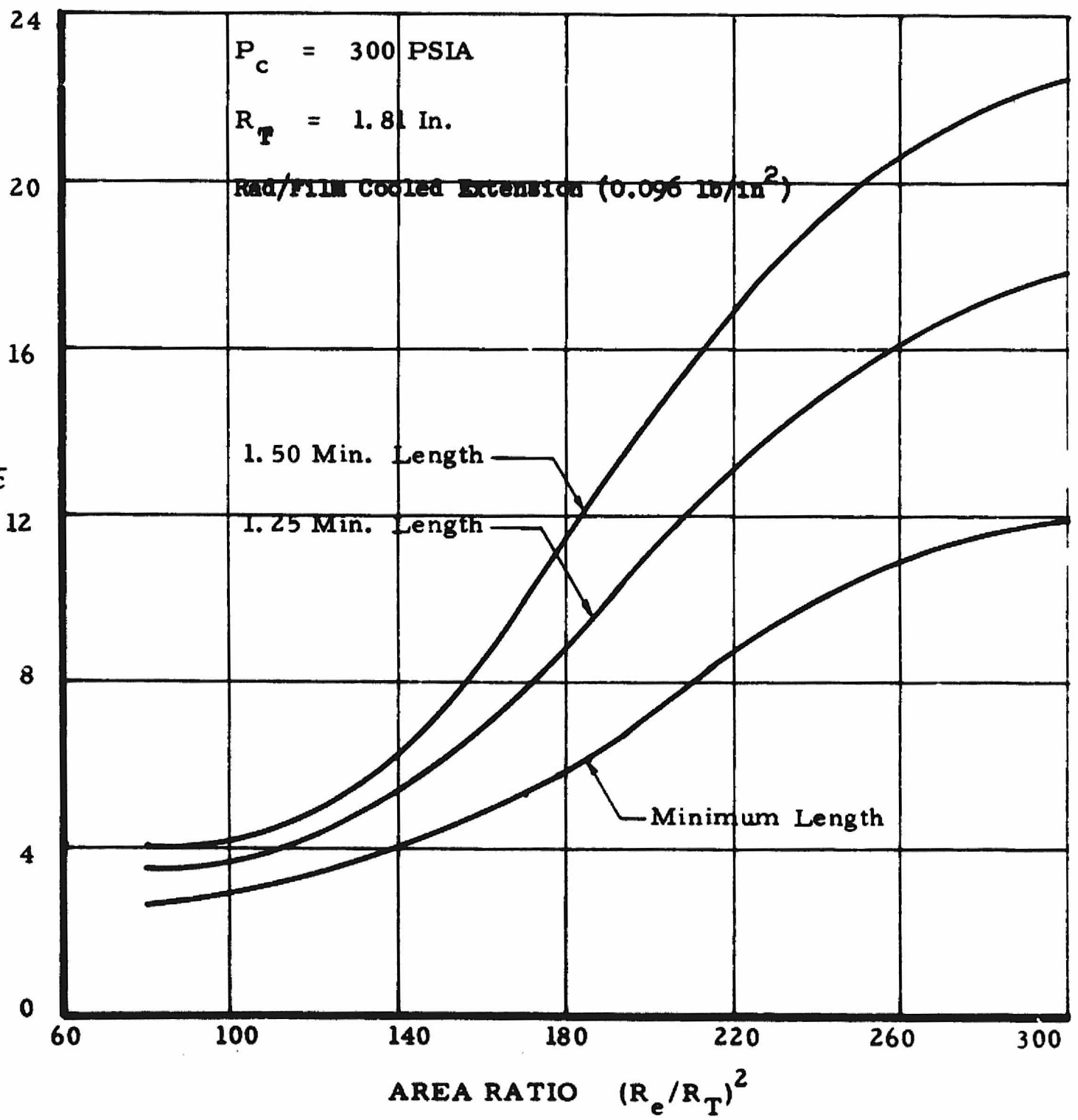


FIGURE 63 TRADE-OFF RATIO VS. AREA RATIO
(P_c = 300 PSIA, R_T = 1.81)

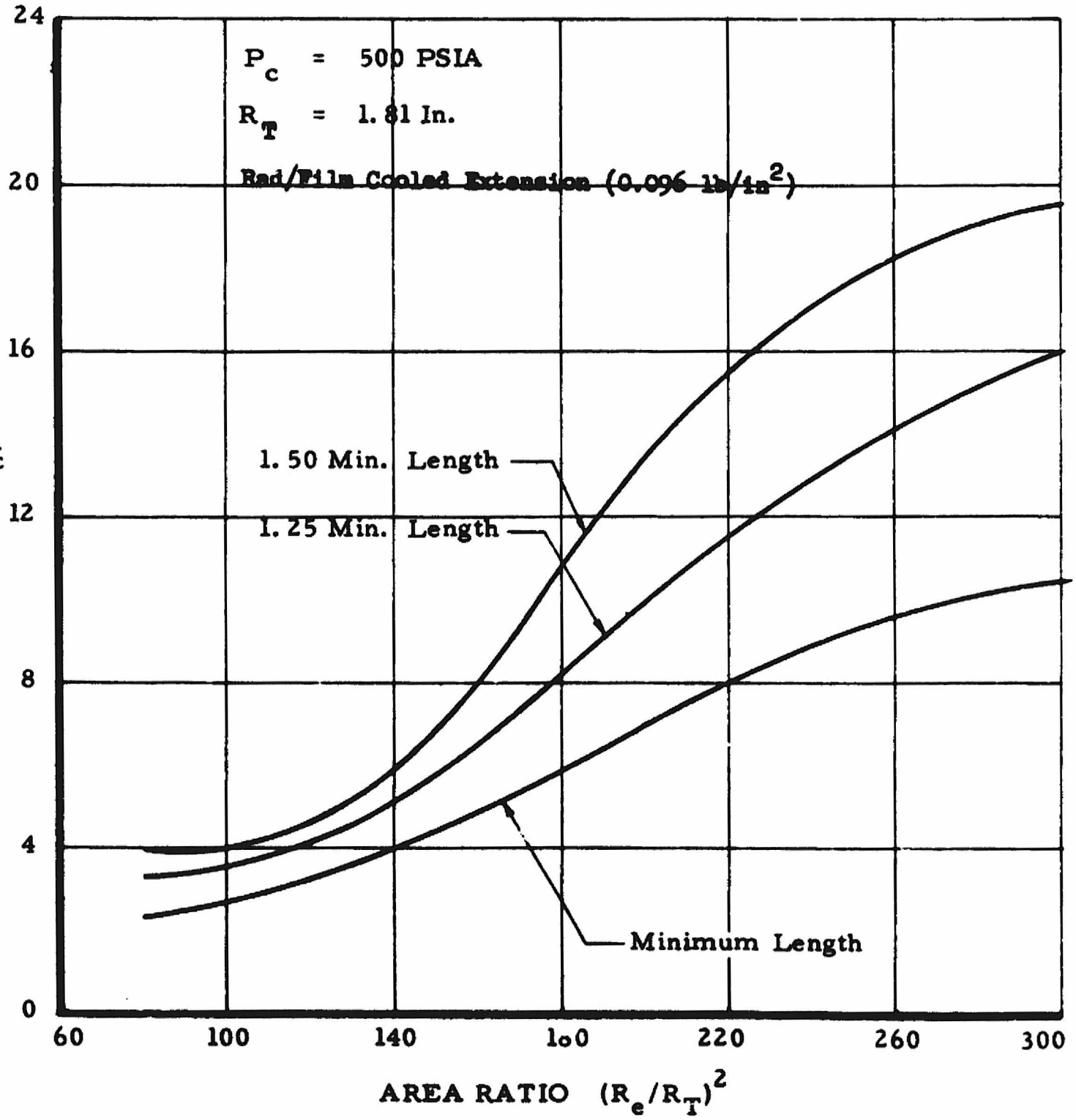


FIGURE 64 TRADE-OFF RATIO VS. AREA RATIO
(P_c = 500 PSIA, R_T = 1.81)

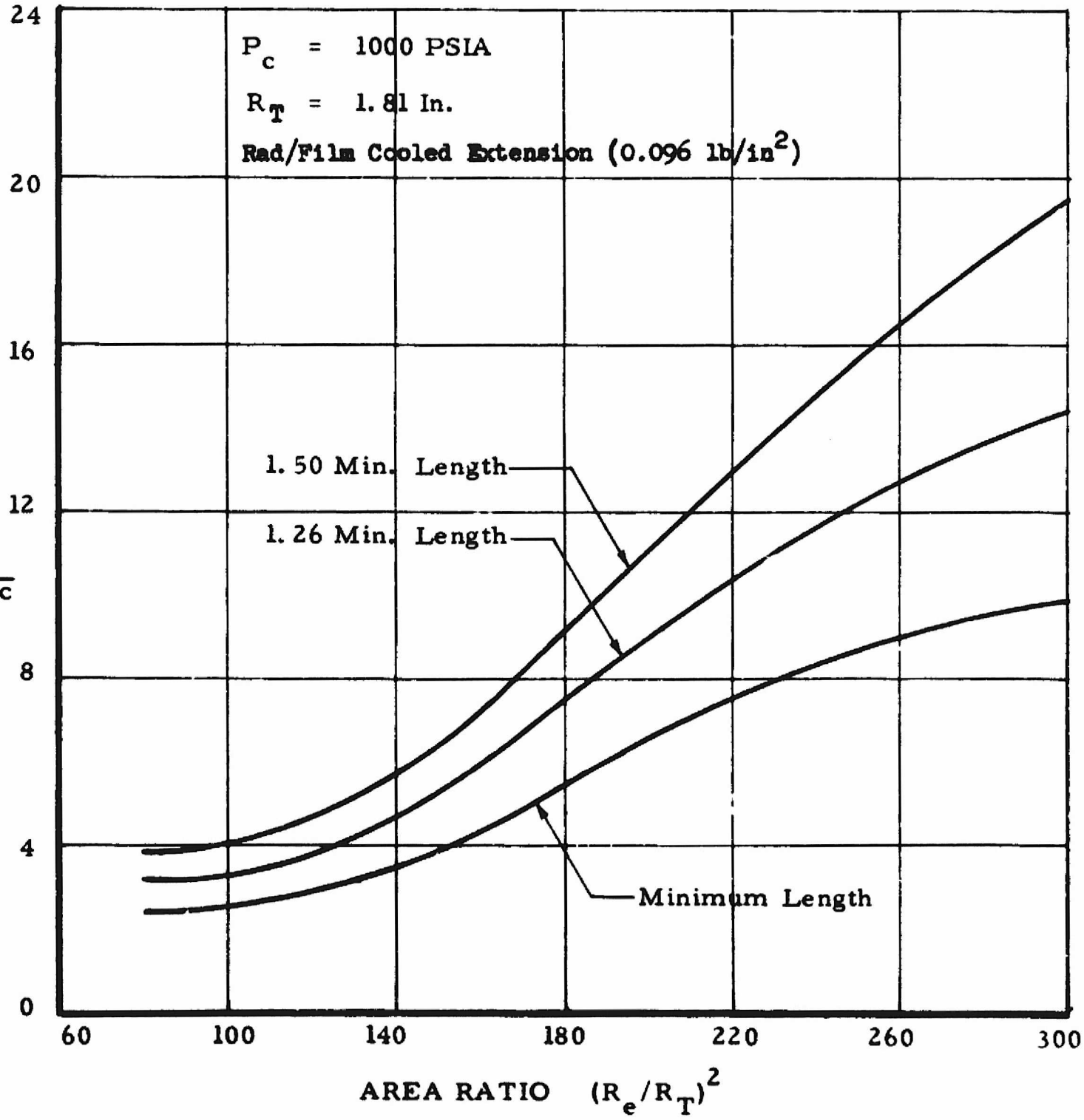


FIGURE 65 TRADE-OFF RATIO VS. AREA RATIO
(P_c = 1000 PSIA, R_T = 1.81)

NO. 341-10 DIETZGEN GRAPH PAPER
10 X 10 PER HALF INCH
EUGENE DIETZGEN CO.
MADE IN U. S. A.

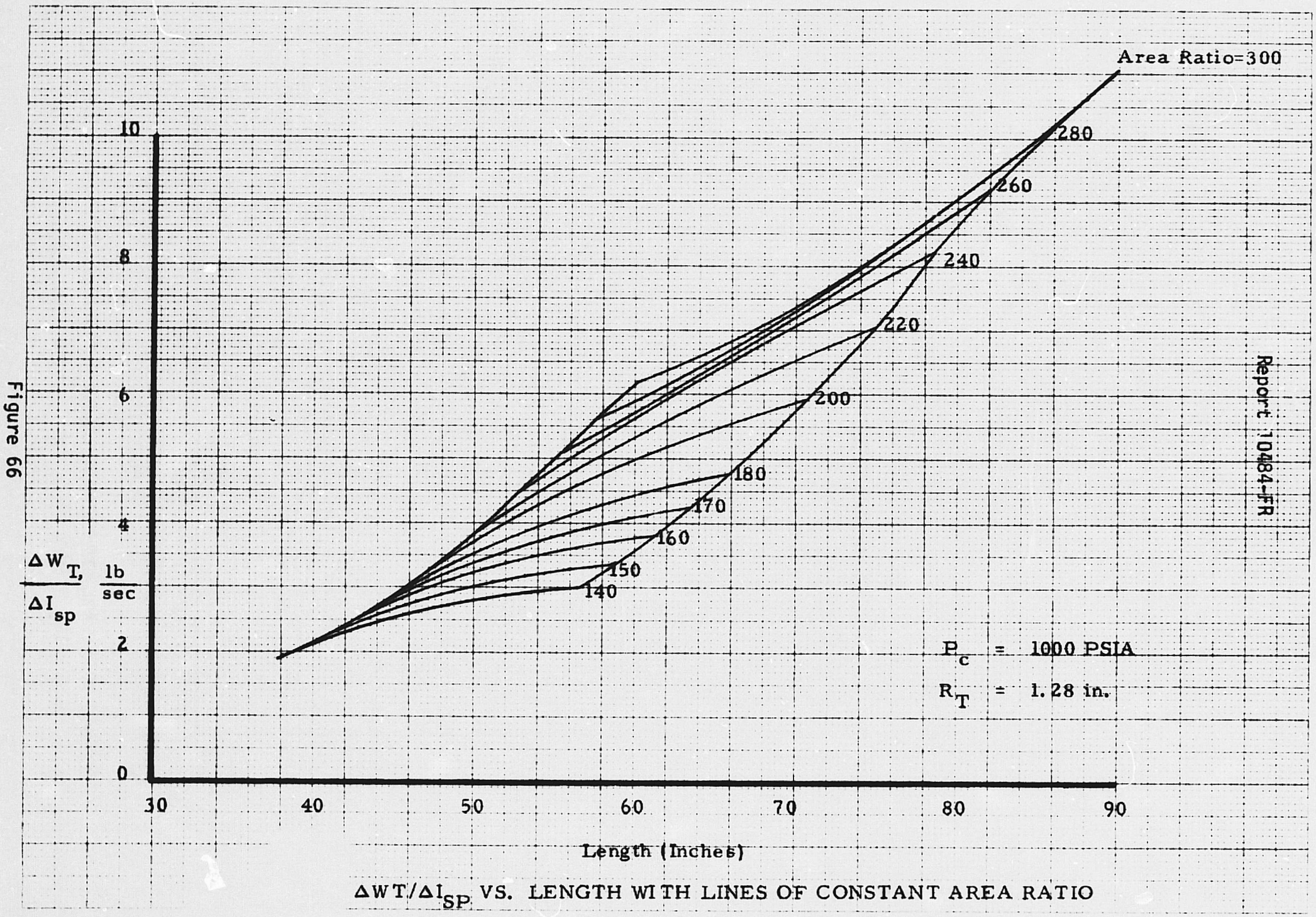


Figure 66 $\Delta W_T/\Delta I_{SP}$ VS. LENGTH WITH LINES OF CONSTANT AREA RATIO

Report 10484-FR

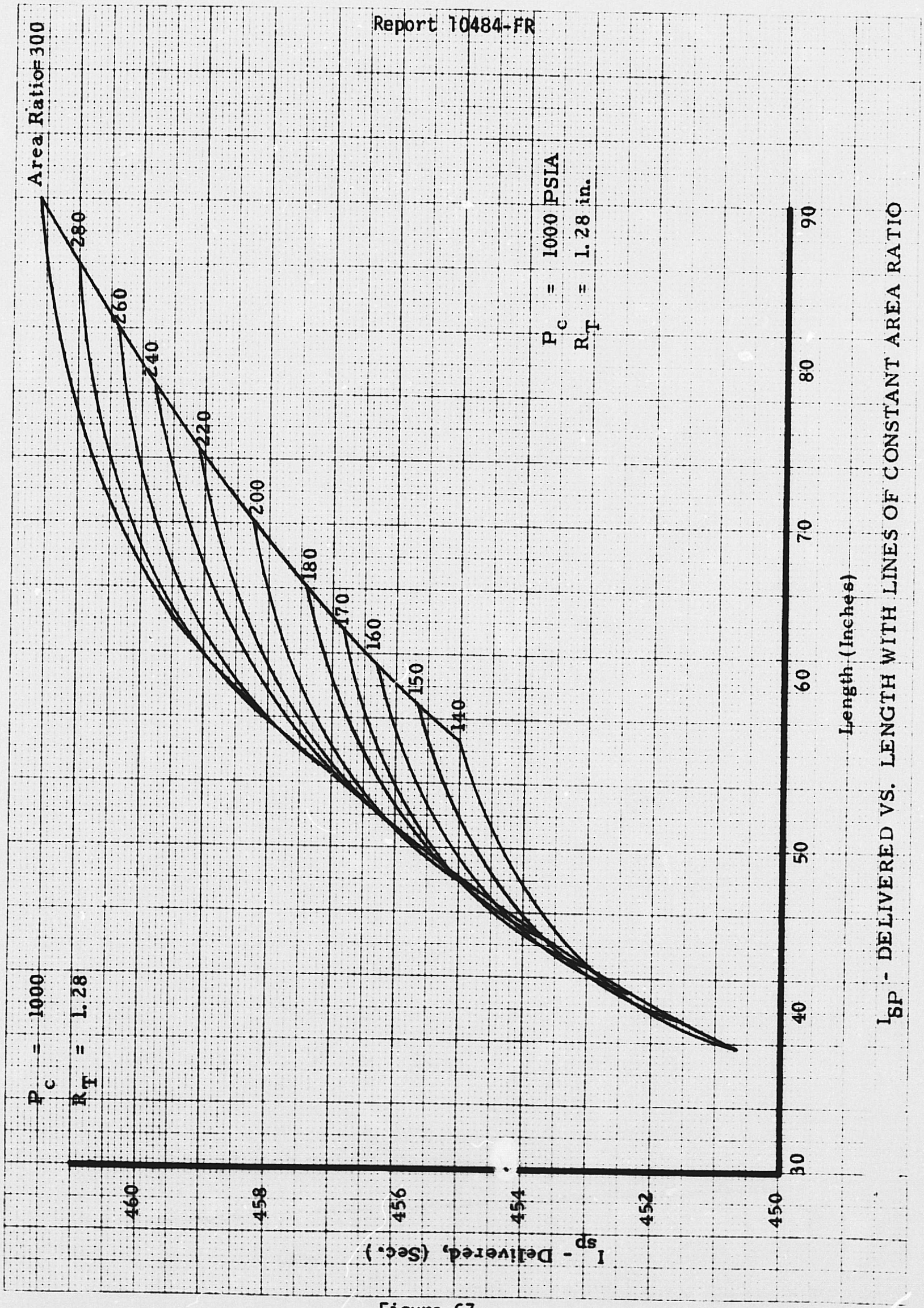
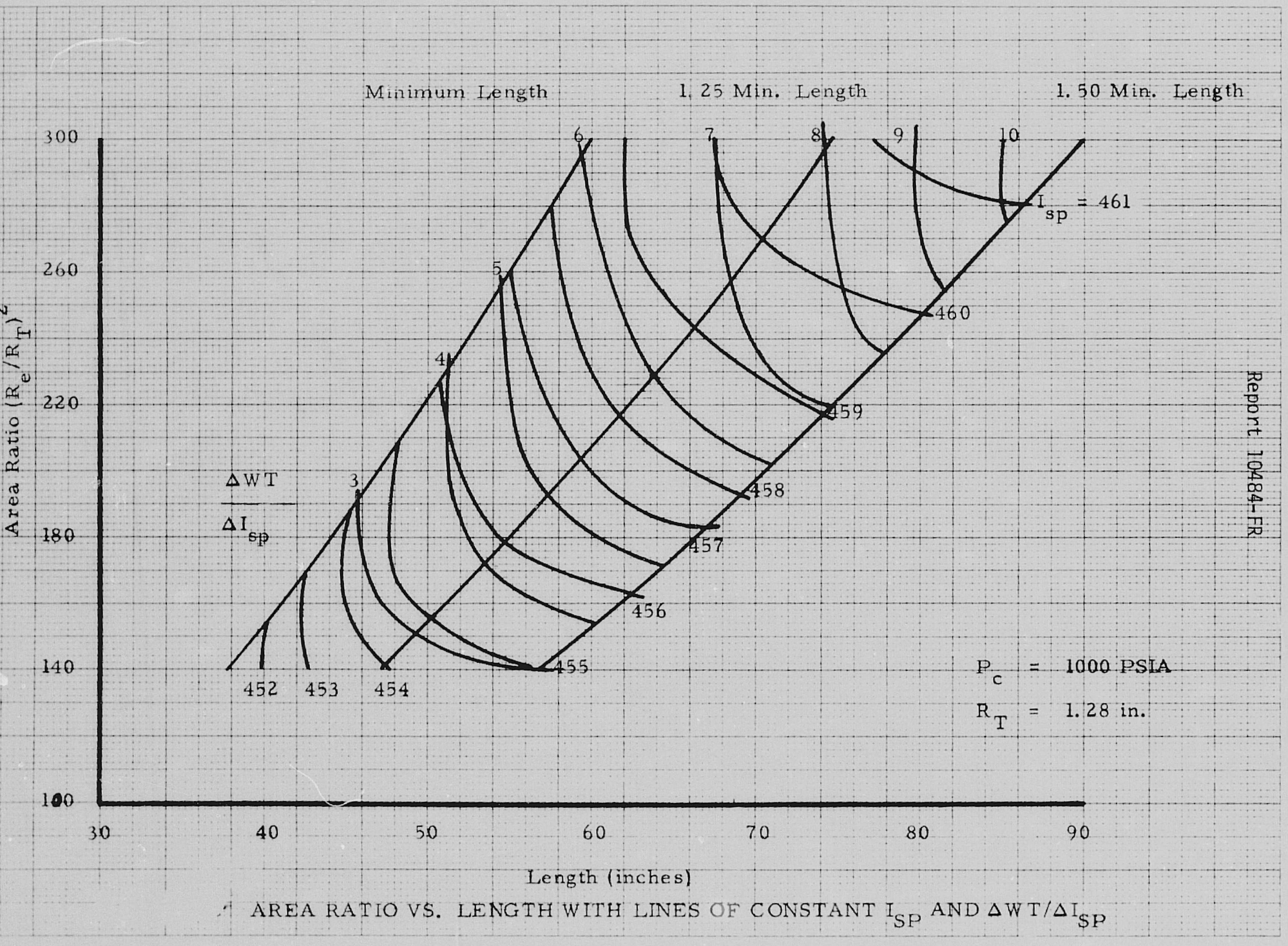

Area Ratio=300
280
260
240
220
200
180
170
160
150
140
P_c = 1000 PSIA
R_T = 1.28 in.
P_c = 1000
R_T = 1.28
460
458
456
454
452
450
I_{sp} - Delivered, (Sec.)
30
40
50
60
70
80
90
Length (Inches)
L_{SP} - DELIVERED VS. LENGTH WITH LINES OF CONSTANT AREA RATIO

Figure 67



AREA RATIO VS. LENGTH WITH LINES OF CONSTANT I_{SP} AND $\Delta WT/\Delta I_{SP}$

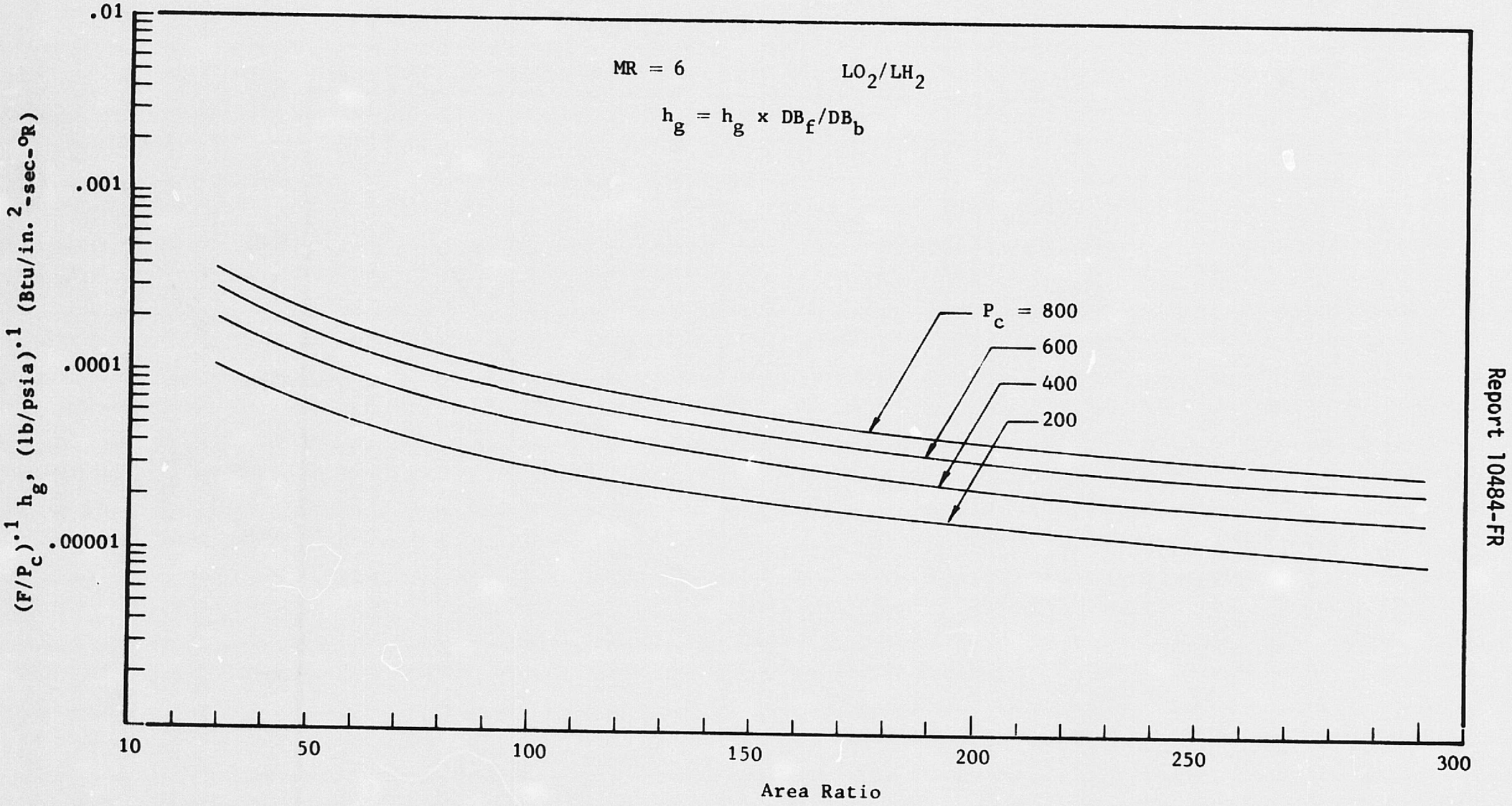


Figure 69 GAS-SIDE BULK FILM COEFFICIENT

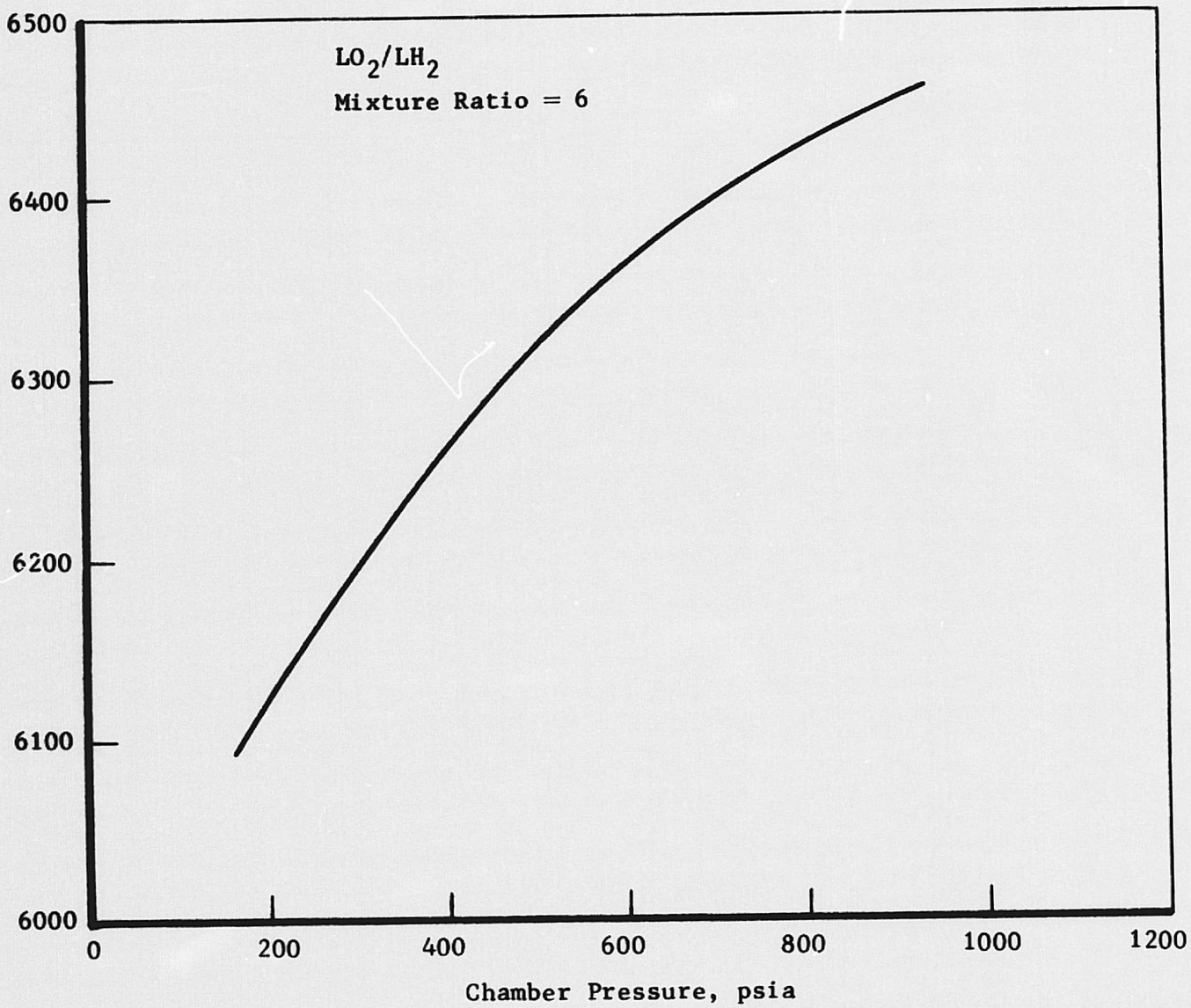
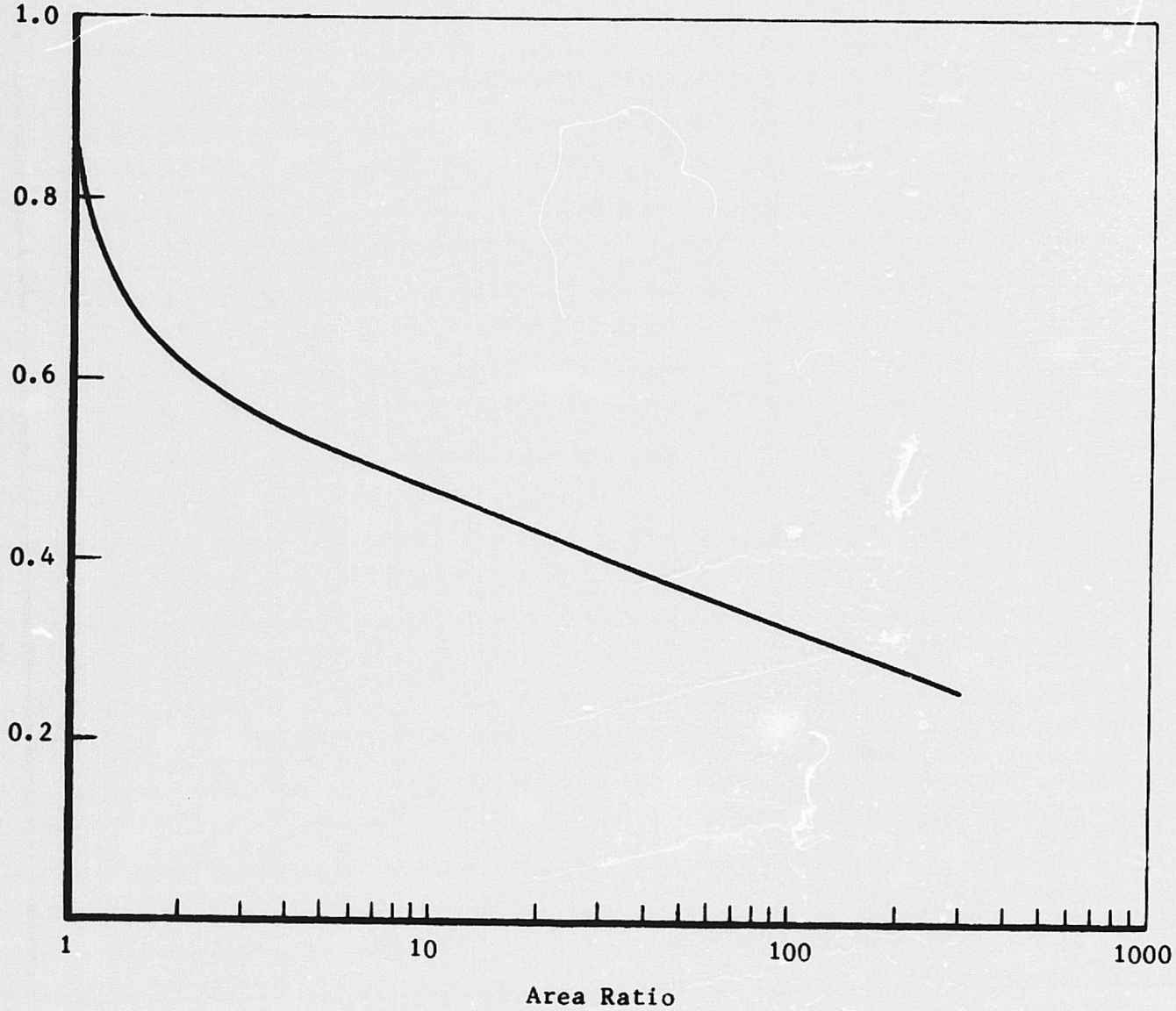


Figure 70 STAGNATION TEMPERATURE FOR O_2/H_2

MR = 6.0



T_s/T_c

Figure 71

T_s/T_c vs AREA RATIO FOR O_2/H_2, MIXTURE RATIO = 6.0

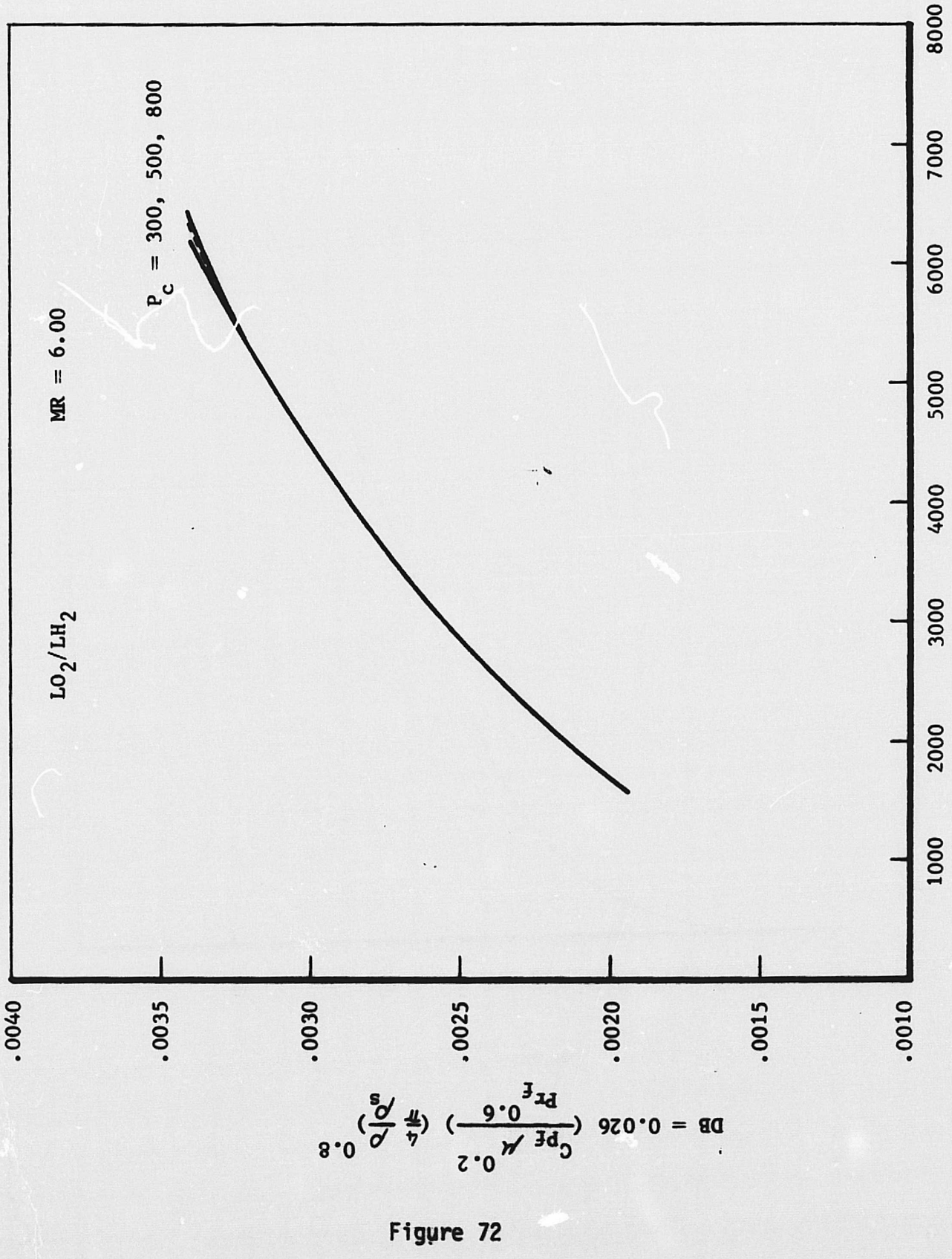
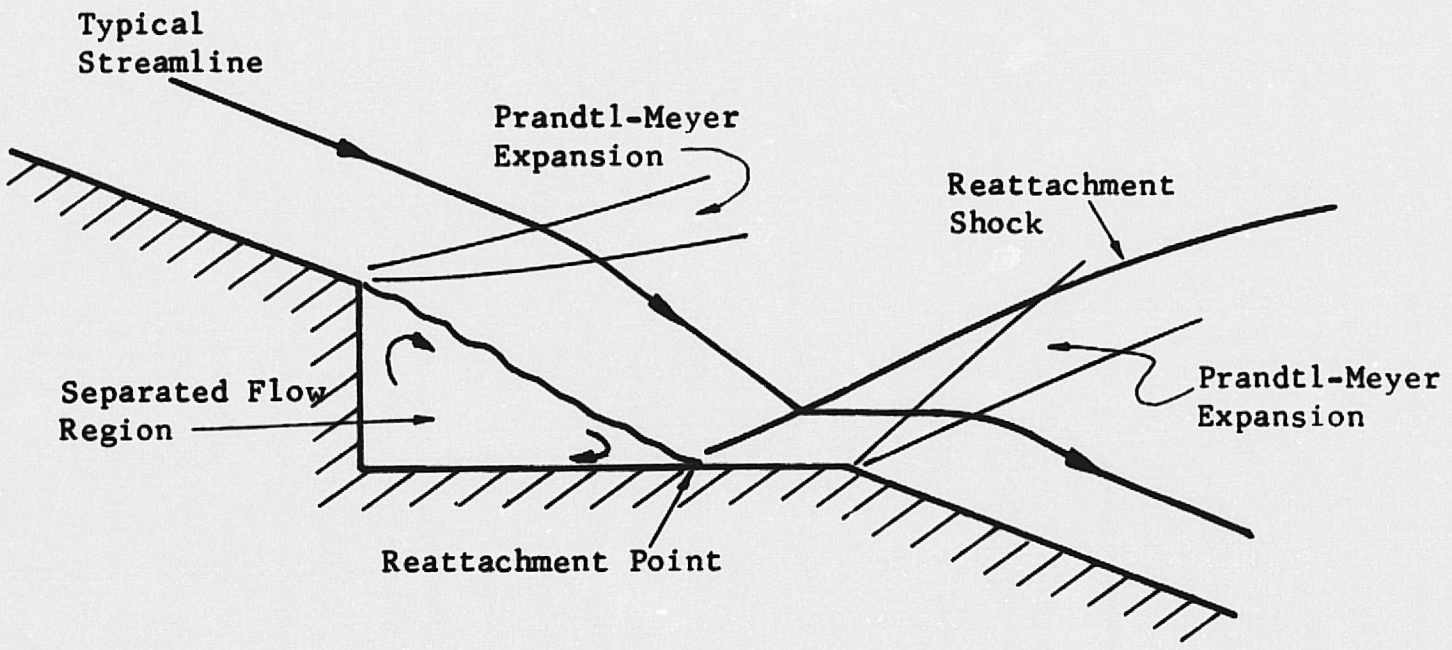
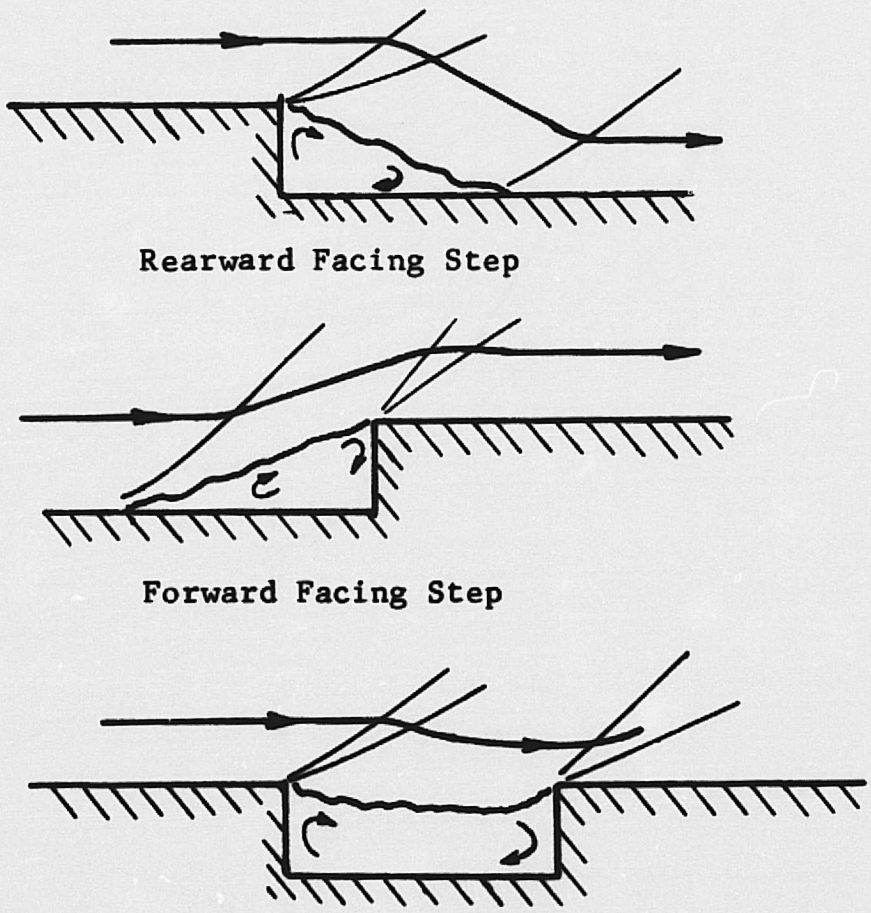

LO_2/LH_2
MR = 6.00
P_c = 300, 500, 800
$DB = 0.026 \left(\frac{C_{PE}\,\mu_E^{0.2}}{Pr_E^{0.6}}\right)\left(\frac{\dot{m}_4}{\rho_s}\right)^{0.8}$
.0040
.0035
.0030
.0025
.0020
.0015
.0010
1000
2000
3000
4000
5000
6000
7000
8000
Gas Temperature, °R
DB FACTOR FOR O_2/H_2

Figure 72



a. Extendable Nozzle attachment Joint Wall Discontinuity



b. Typical Wall Discontinuities

WALL DISCONTINUITIES
FIGURE 73

Report 10434-FR

RELATIVE HEAT TRANSFER COEFFICIENT ON THE DOWNSTREAM FACE OF A RECTANGULAR CAVITY, L/H=5

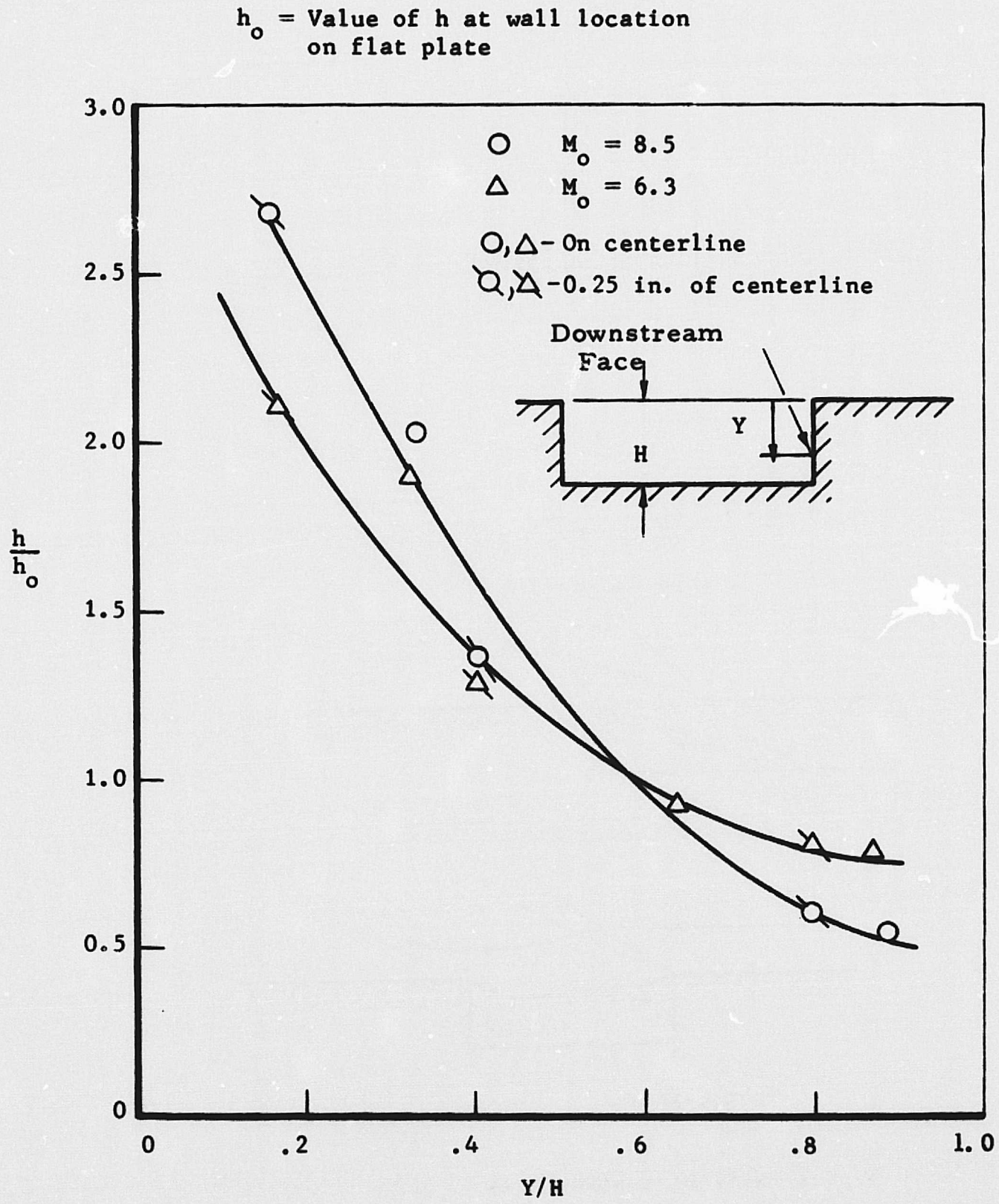


Figure 74

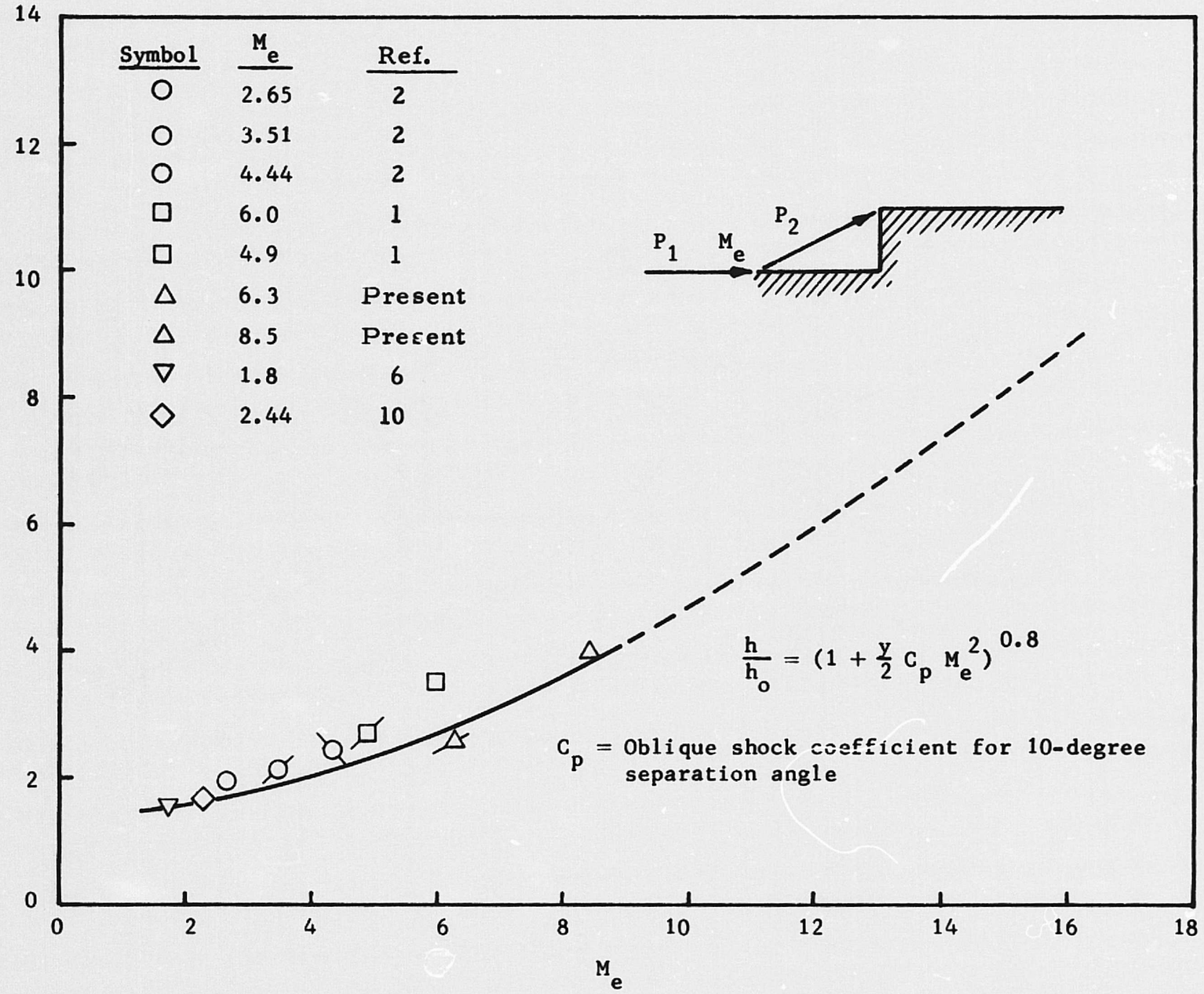


Figure 75 CORRELATION OF MAXIMUM HEAT FLUX UPSTREAM OF FORWARD FACING STEPS

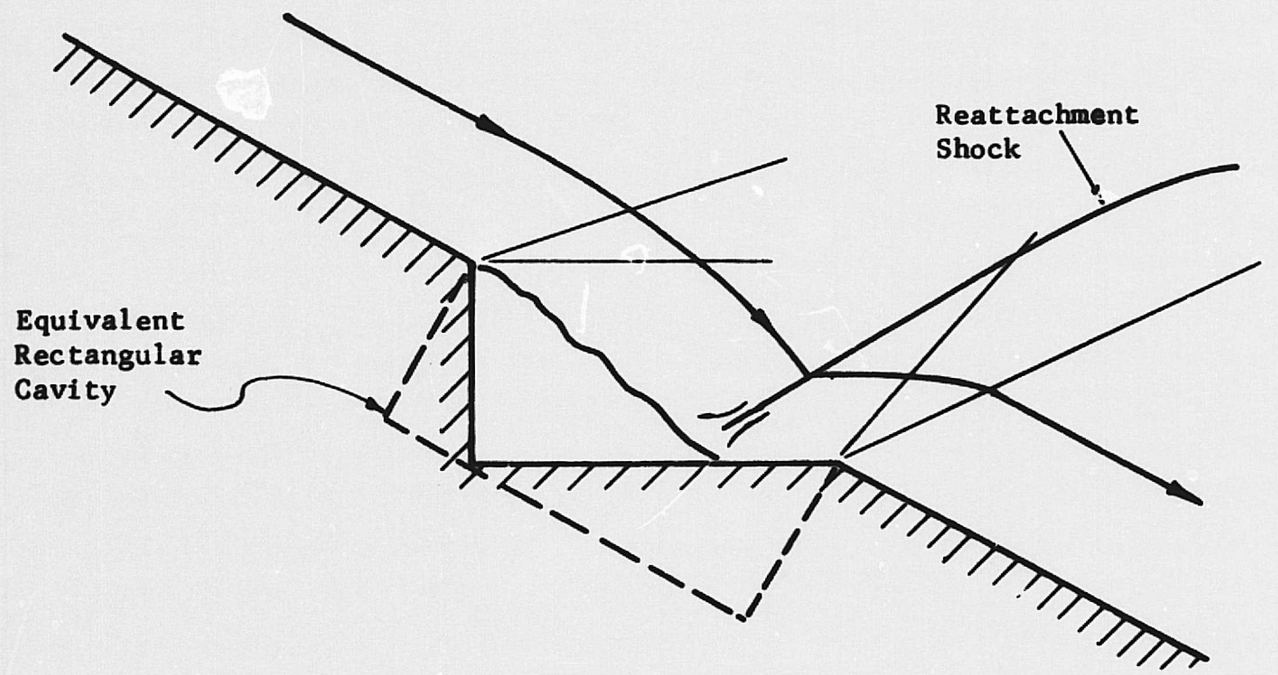


Figure 76 EQUIVALENT RECTANGULAR CAVITY

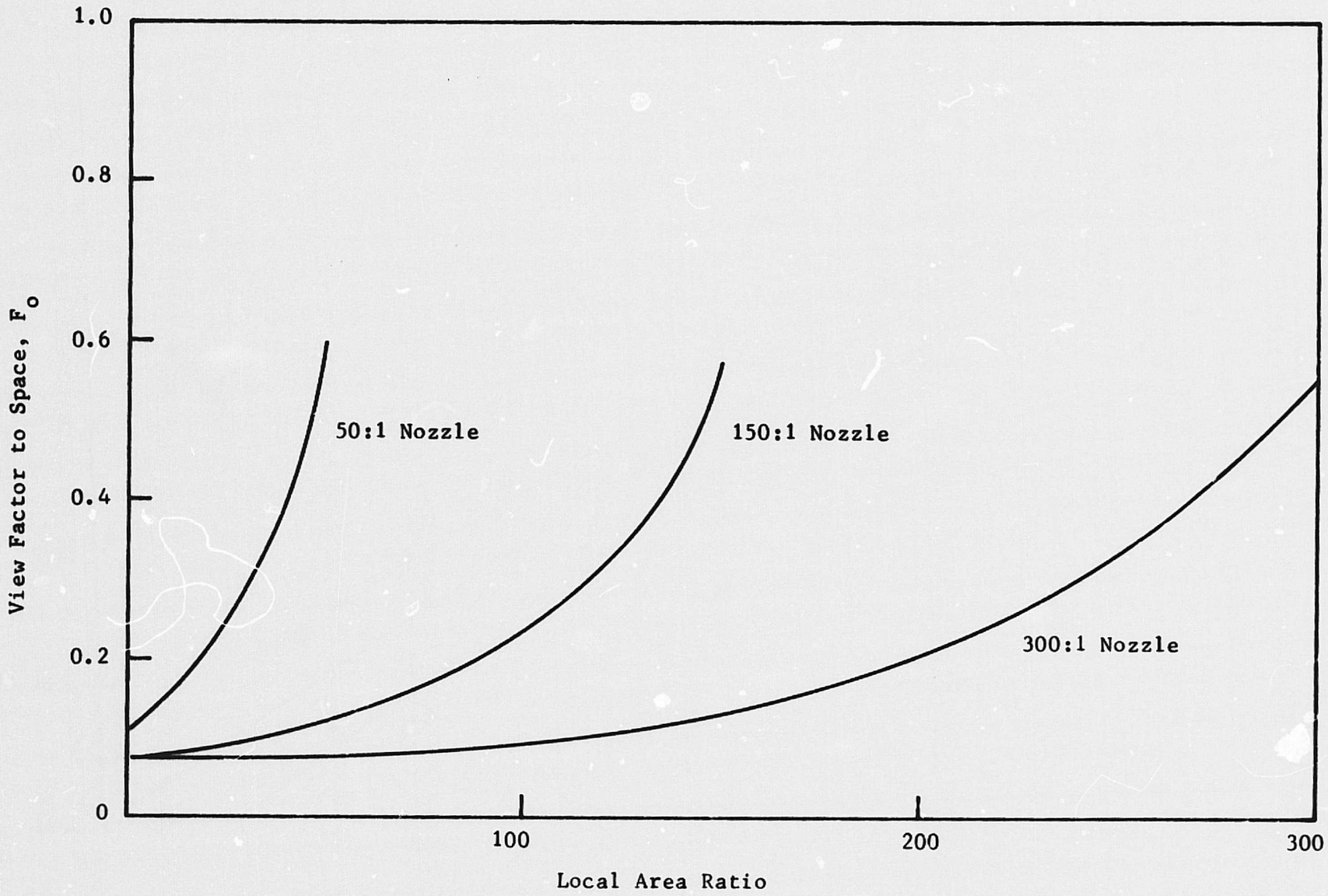


Figure 77

RADIATION VIEW FACTORS FROM INTERIOR NOZZLE SURFACE TO SPACE

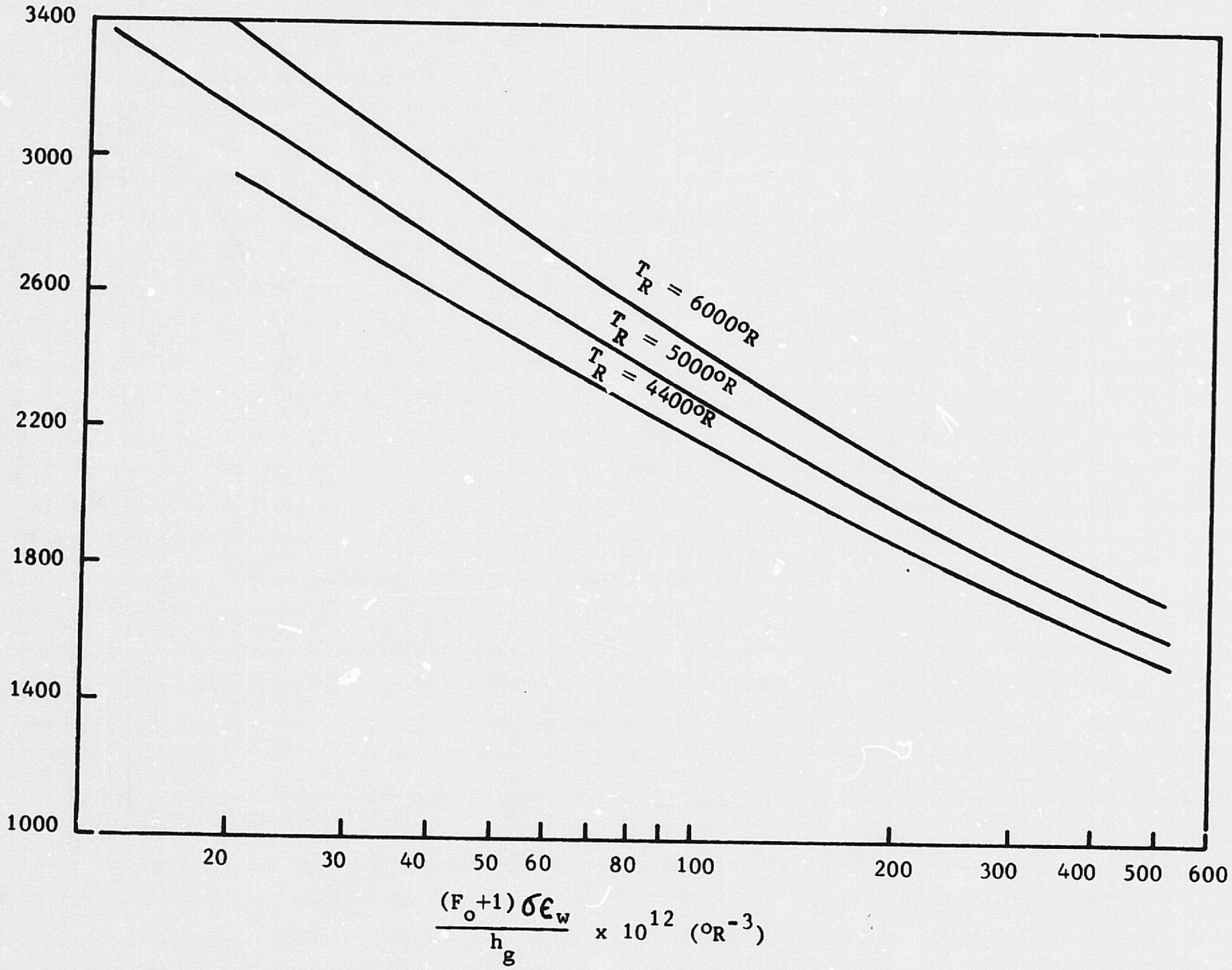


Figure 78

RADIATION EQUILIBRIUM TEMPERATURE FOR A THIN WALL NOZZLE

ENTRAINMENT MODEL COMPARISON WITH
HATCH AND PAPELL MODEL AND DATA

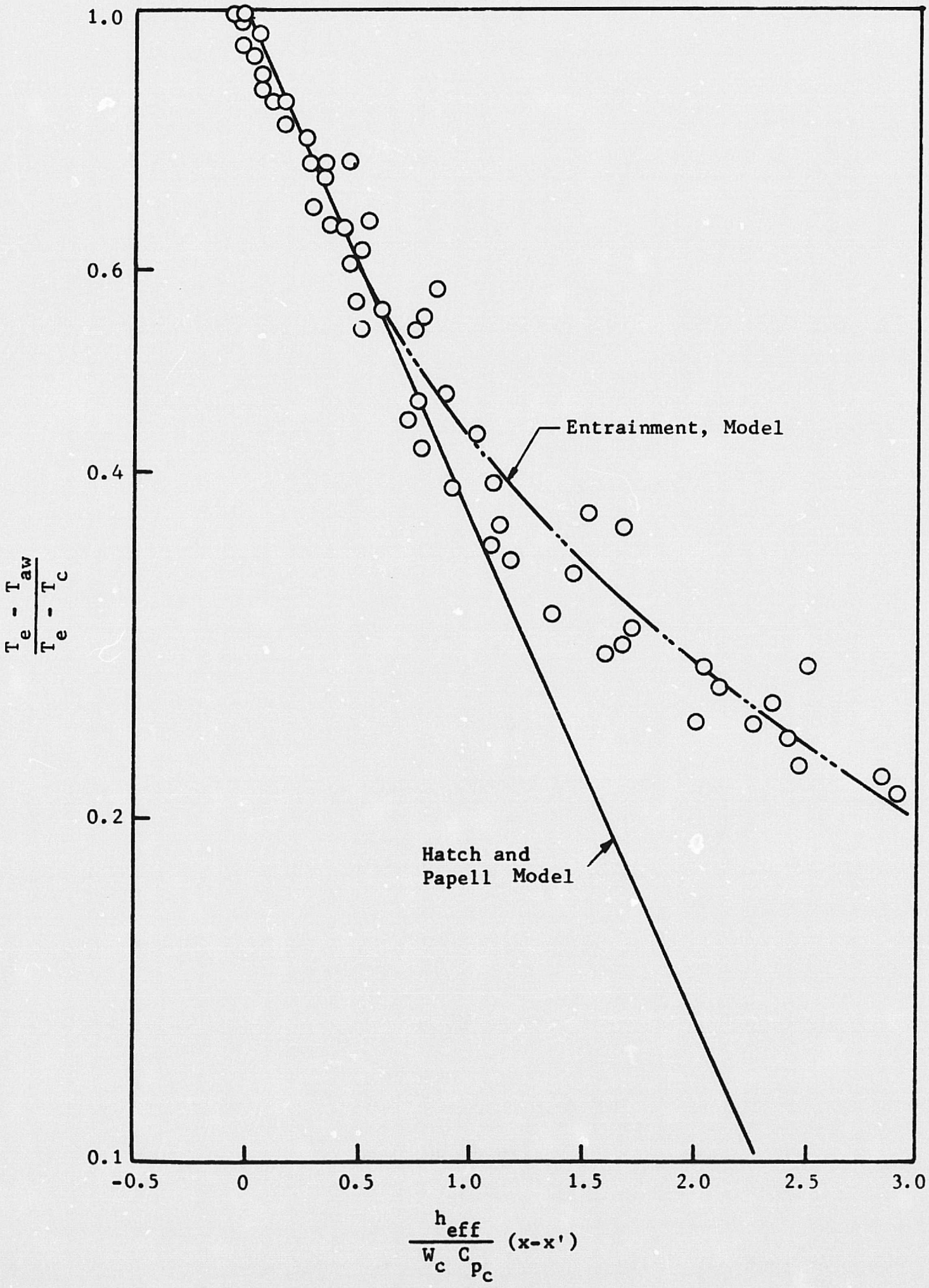


Figure 79

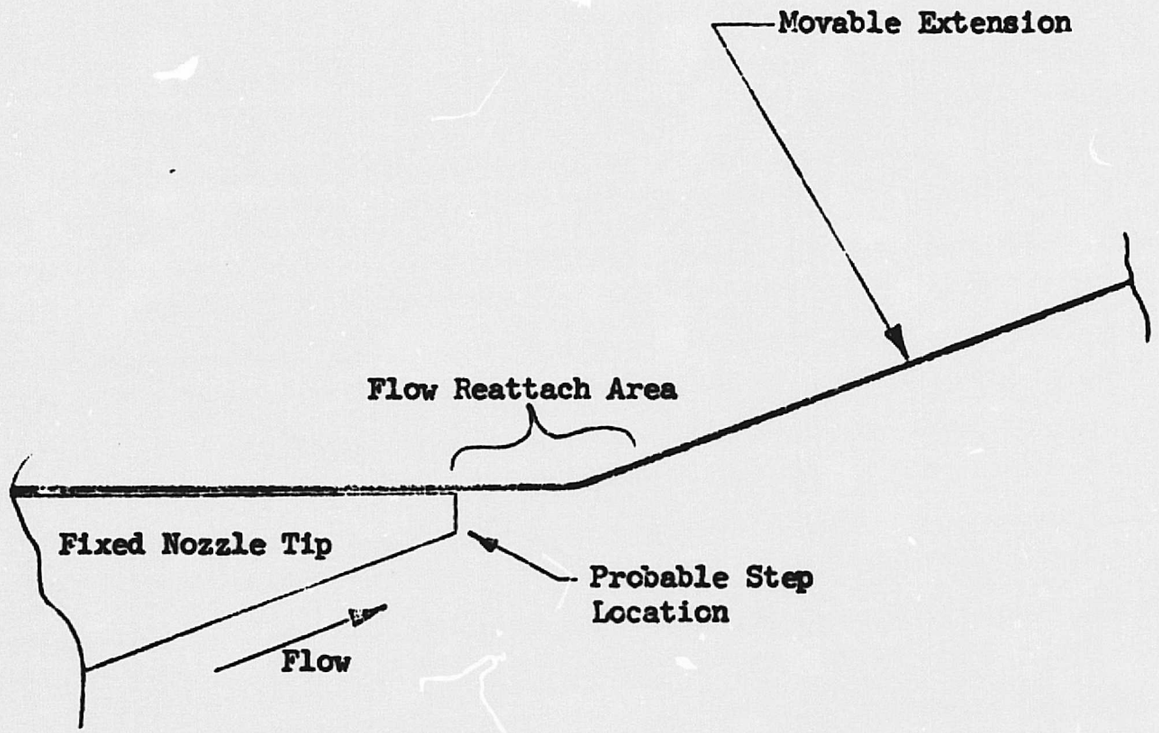
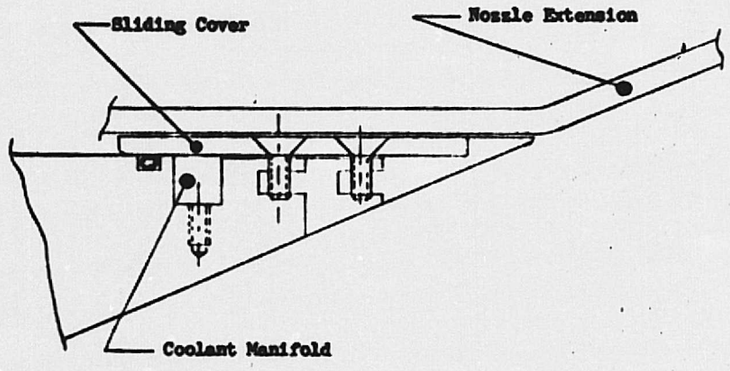
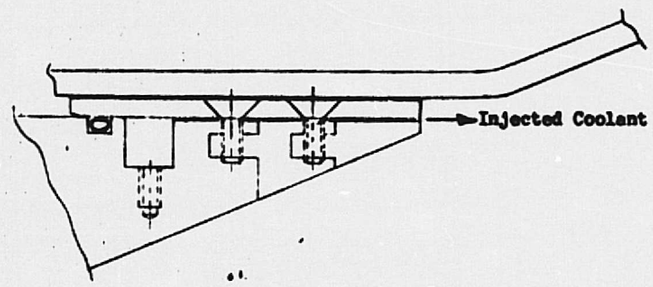


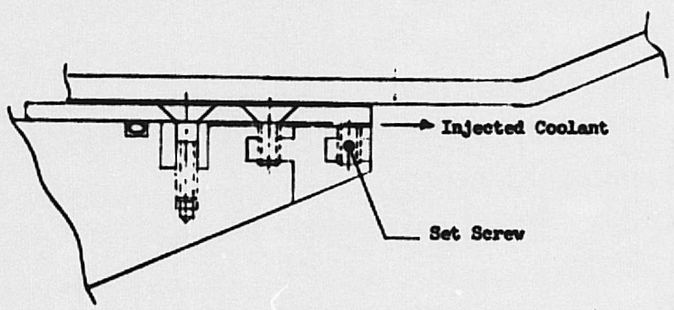
Figure 80 Fixed to Movable Transition Region



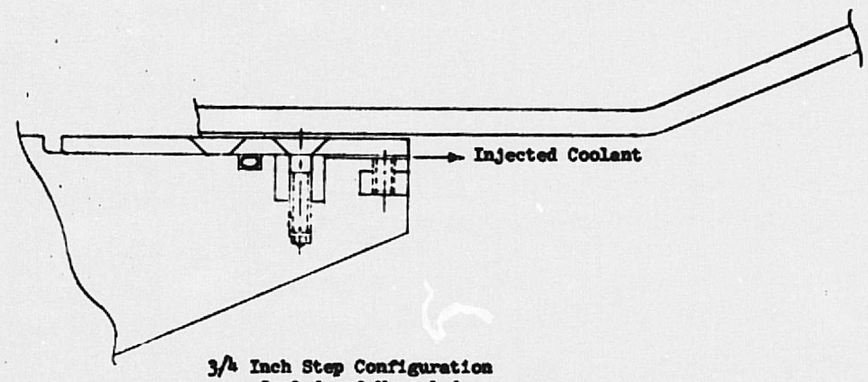
Zero Step Configuration
Uncooled



1/4 Inch Step Configuration
Cooled and Uncooled

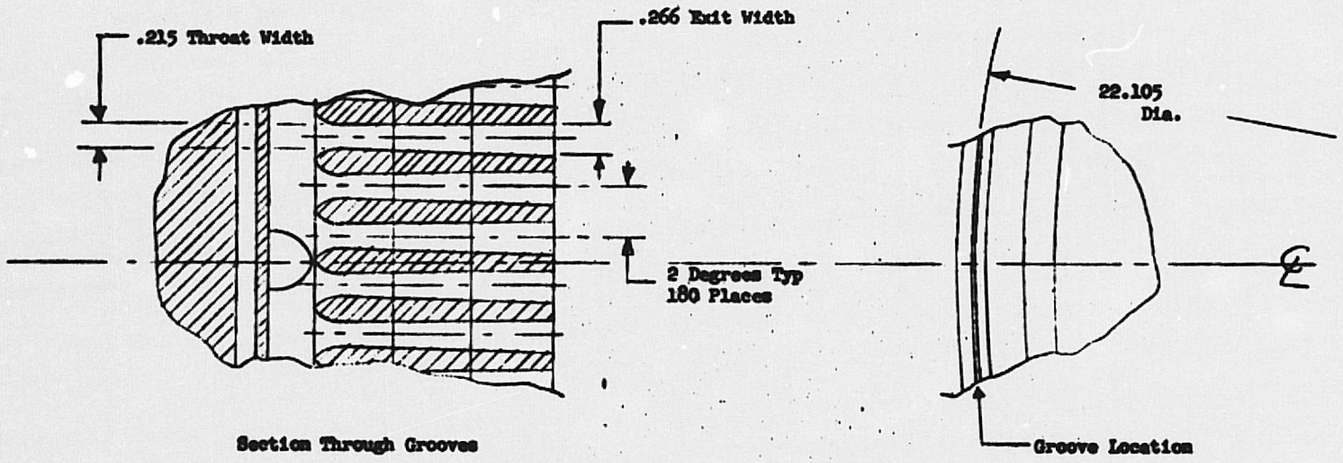


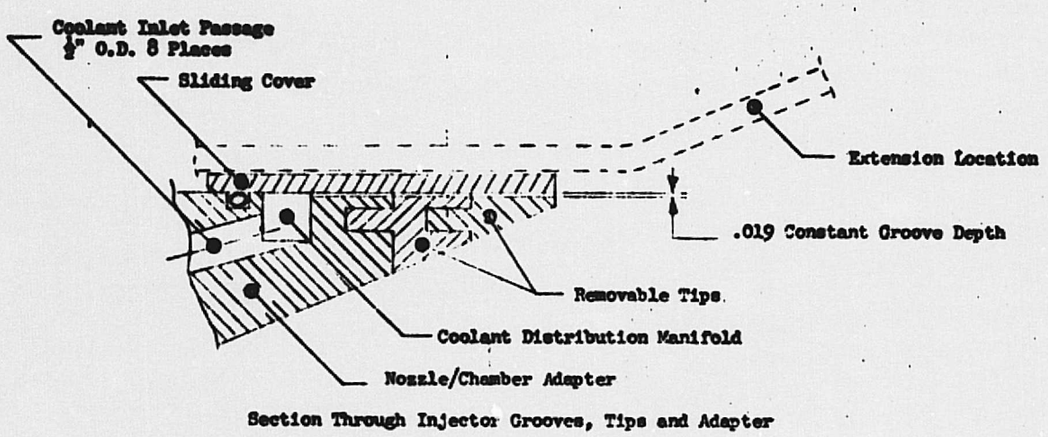
1/2 Inch Step Configuration
Cooled and Uncooled



3/4 Inch Step Configuration
Cooled and Uncooled

Figure 81 Variable Step Removable Tip Concept





Supersonic Coolant Injector Grooves

Figure 82

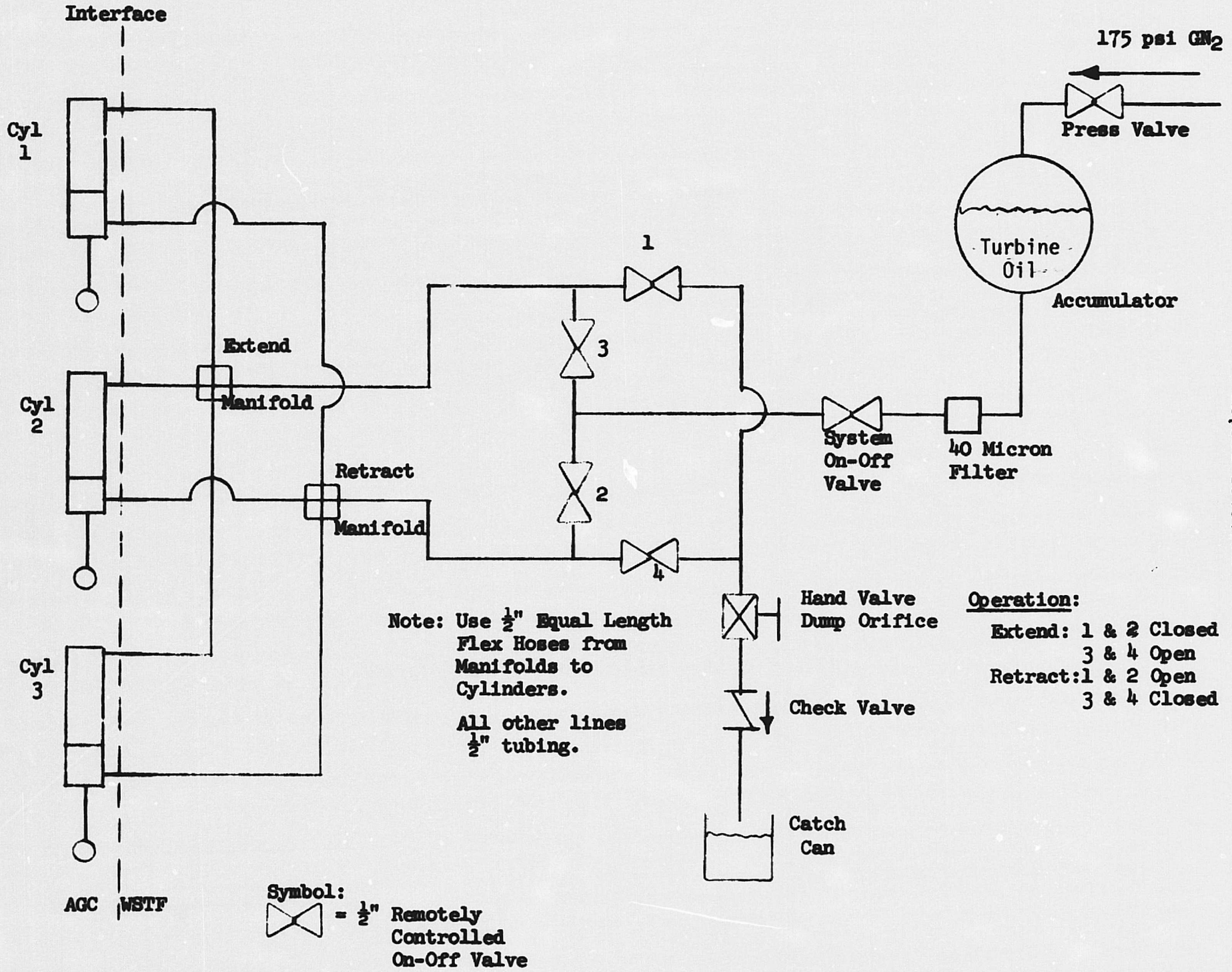
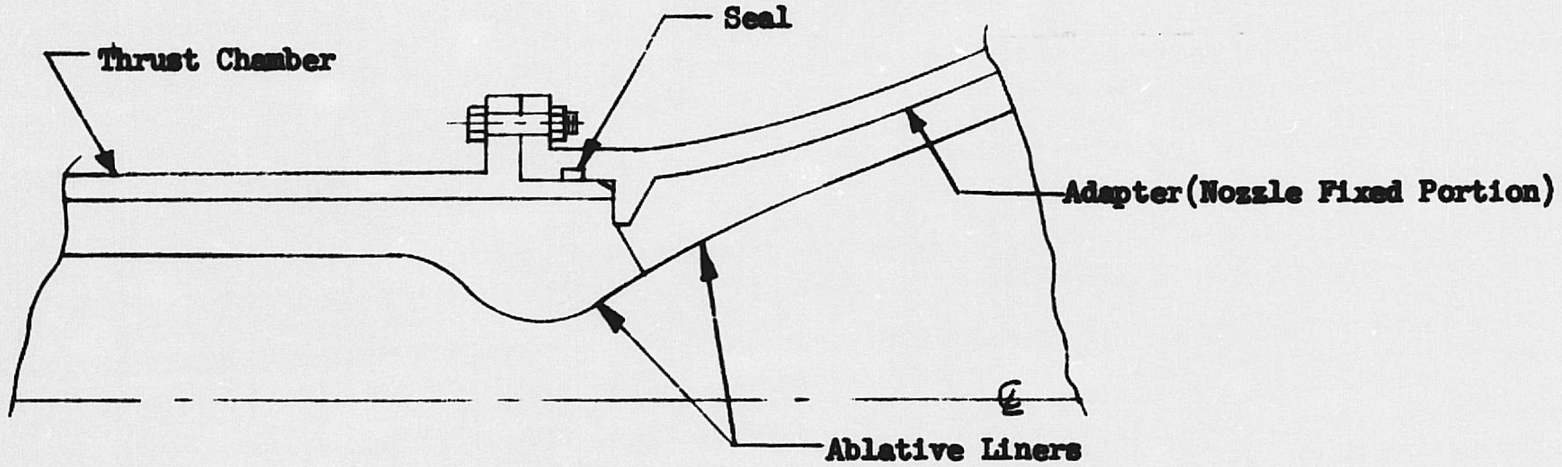
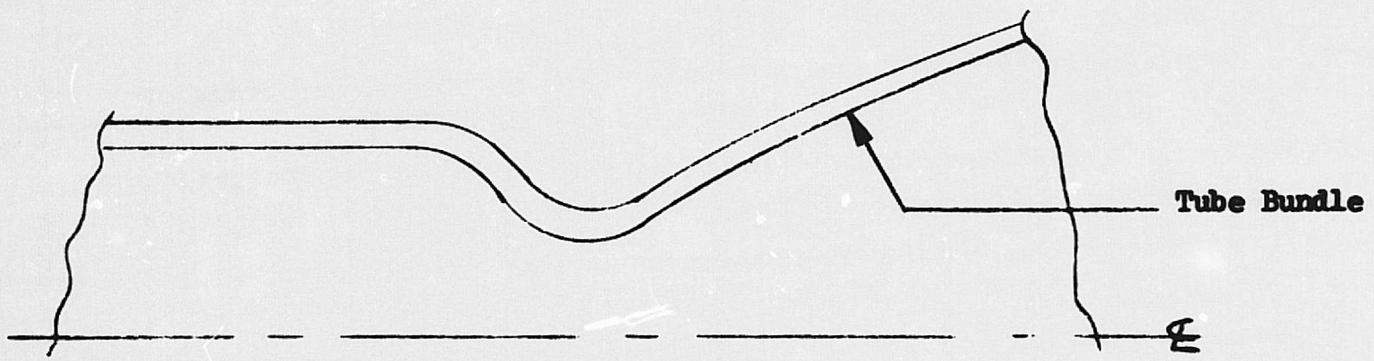


Figure 83 Suggested Actuation System for Extendable Nozzle Tests at White Sands Test Facility

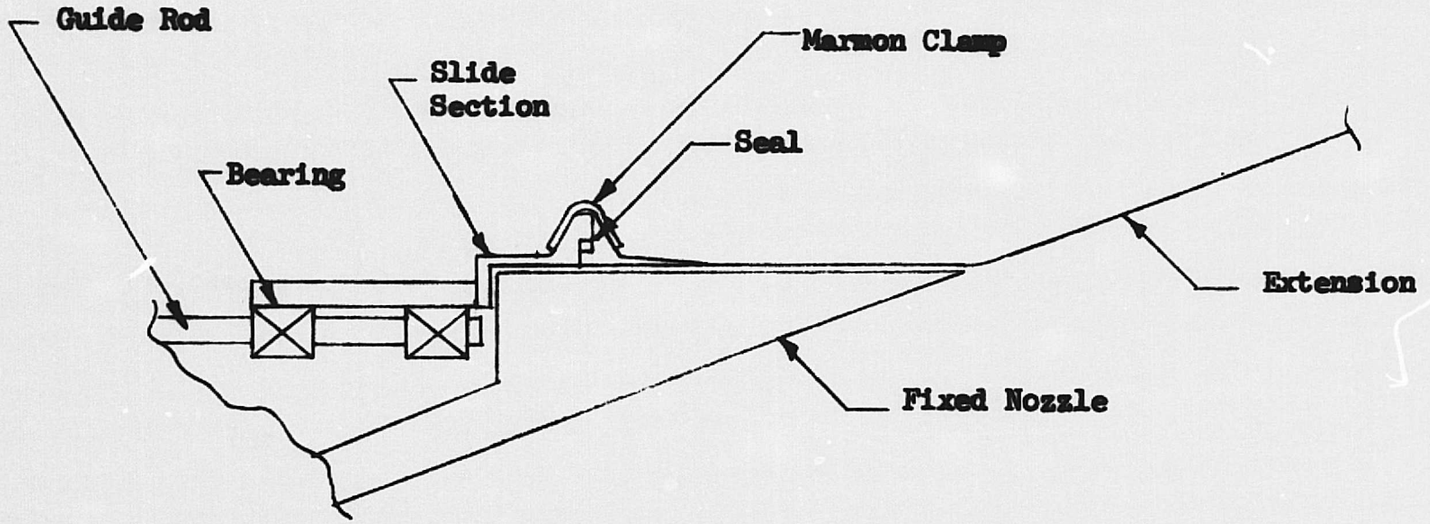


Ablative Chamber and Nozzle Requiring Seal

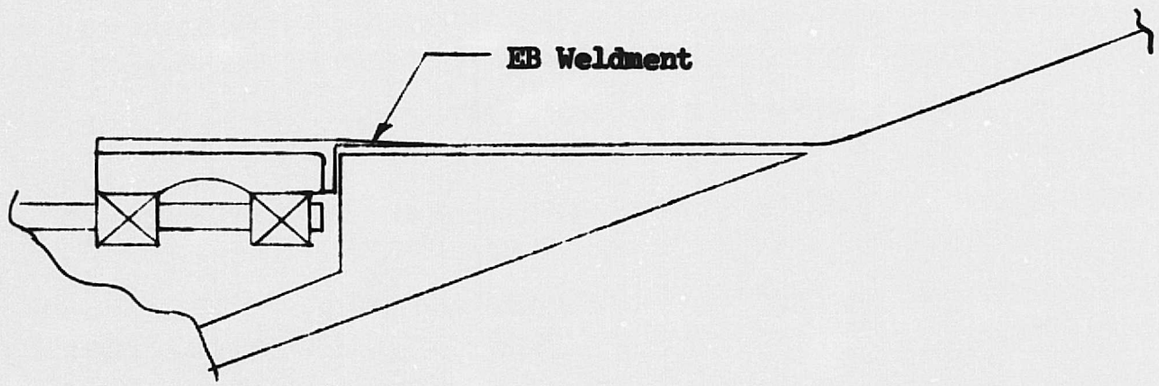


Integral Regeneratively Cooled Chamber and Nozzle
(No Seal Required)

Figure 84 Typical Ablative and Regeneratively Cooled Chamber - Nozzle Interfaces



Separate Slide and Extension Sections Requiring Seal



Integral Slide and Extension
(No seal required)

Separate and Integral Slide/Extension Interfaces

Figure 85

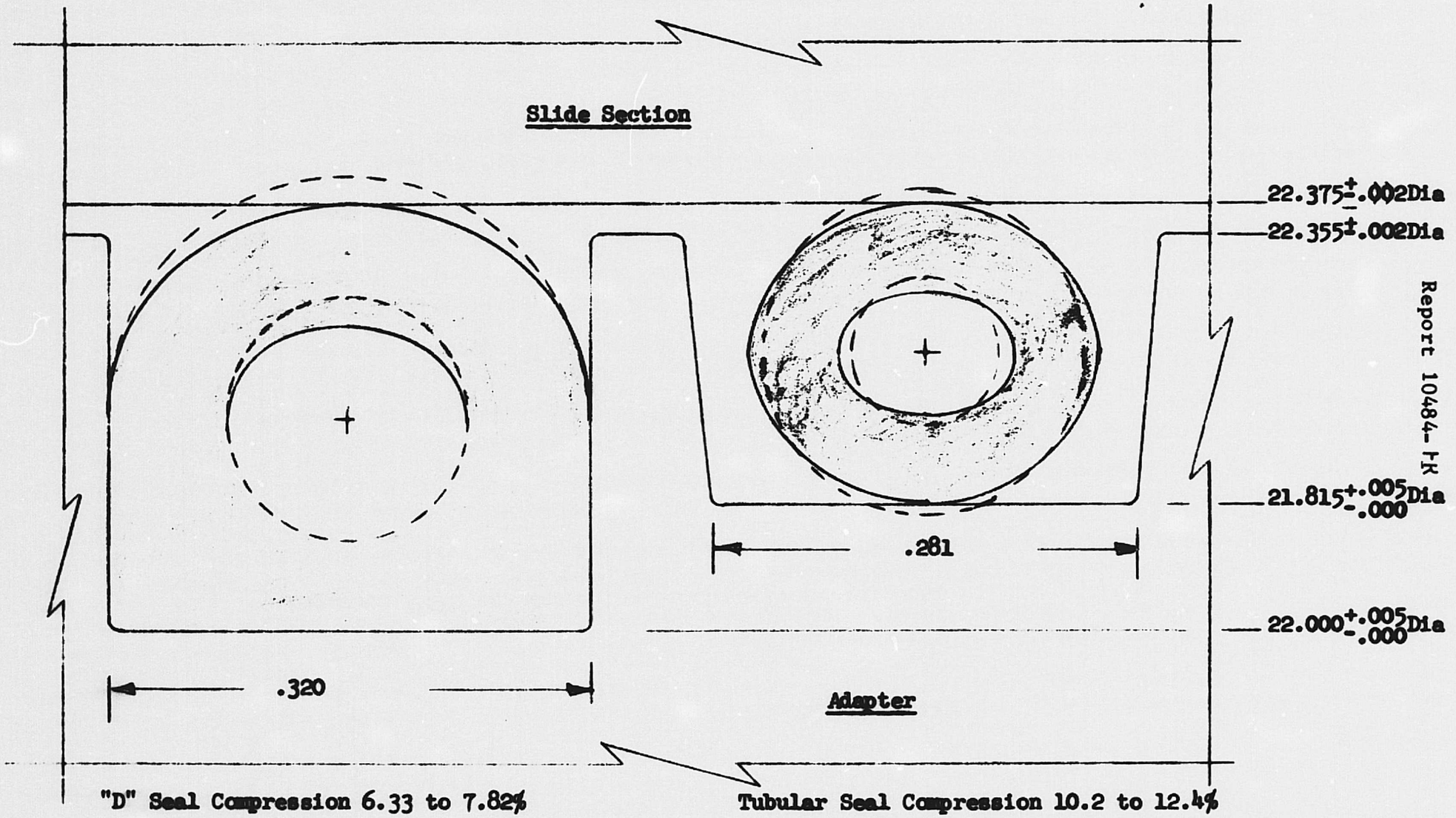
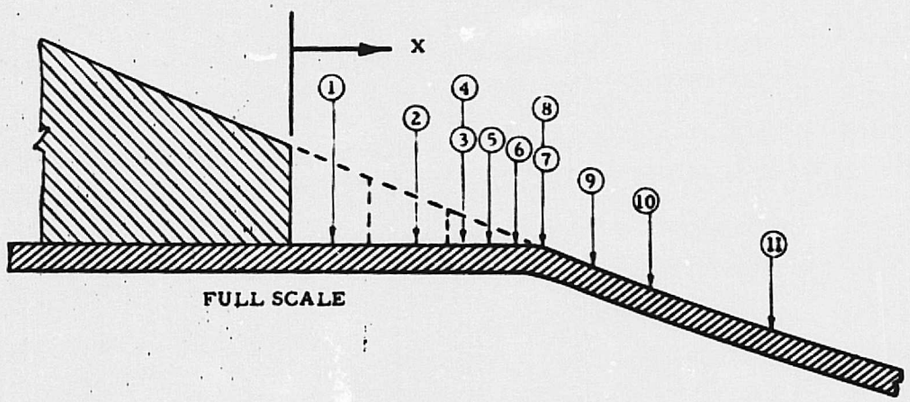
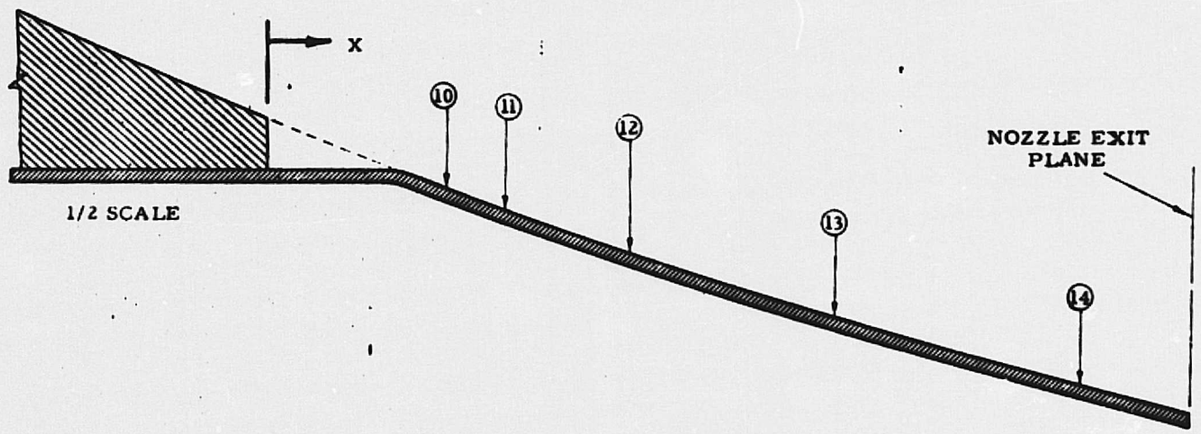


Figure 86 "D" and Tubular Seals as Used in the Extendable Nozzle Test Engine

PRESSURE TAP NO.	X INCHES
1	.35
2	1.00
3	1.38*
4	1.38
5	1.58
6	1.79
7	2.00*
8	2.00
9	2.39
10	2.85
11	3.80
12	5.75
13	9.00
14	12.90

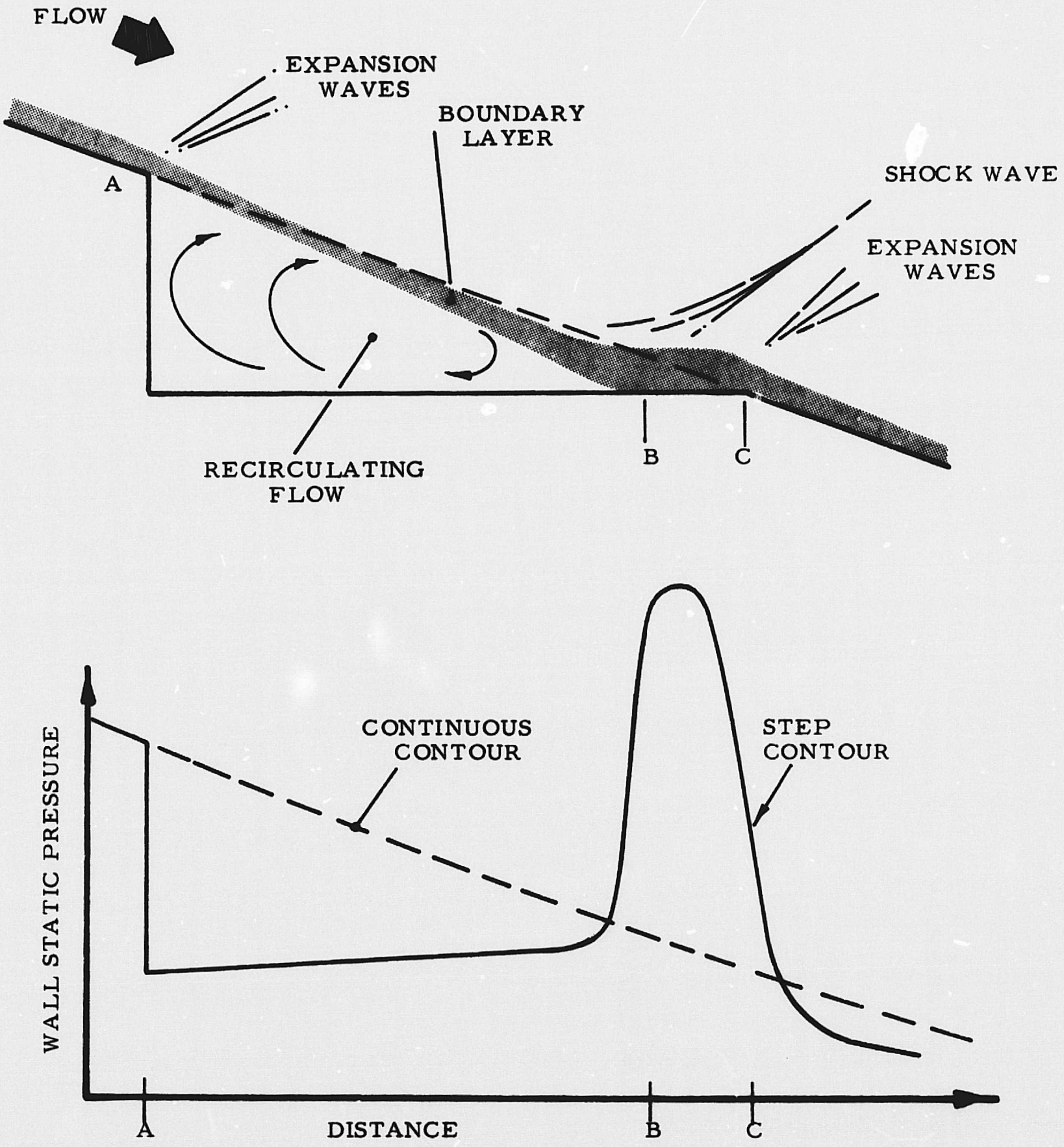
* NOTE: All pressure taps are in line with coolant passages except PT #3 and #7.





Nozzle Wall Pressure Taps for Test Engine

NOTE: ASSUMES NO FILM COOLING



Schematic of Flow Field and Pressure Profiles

Figure 88

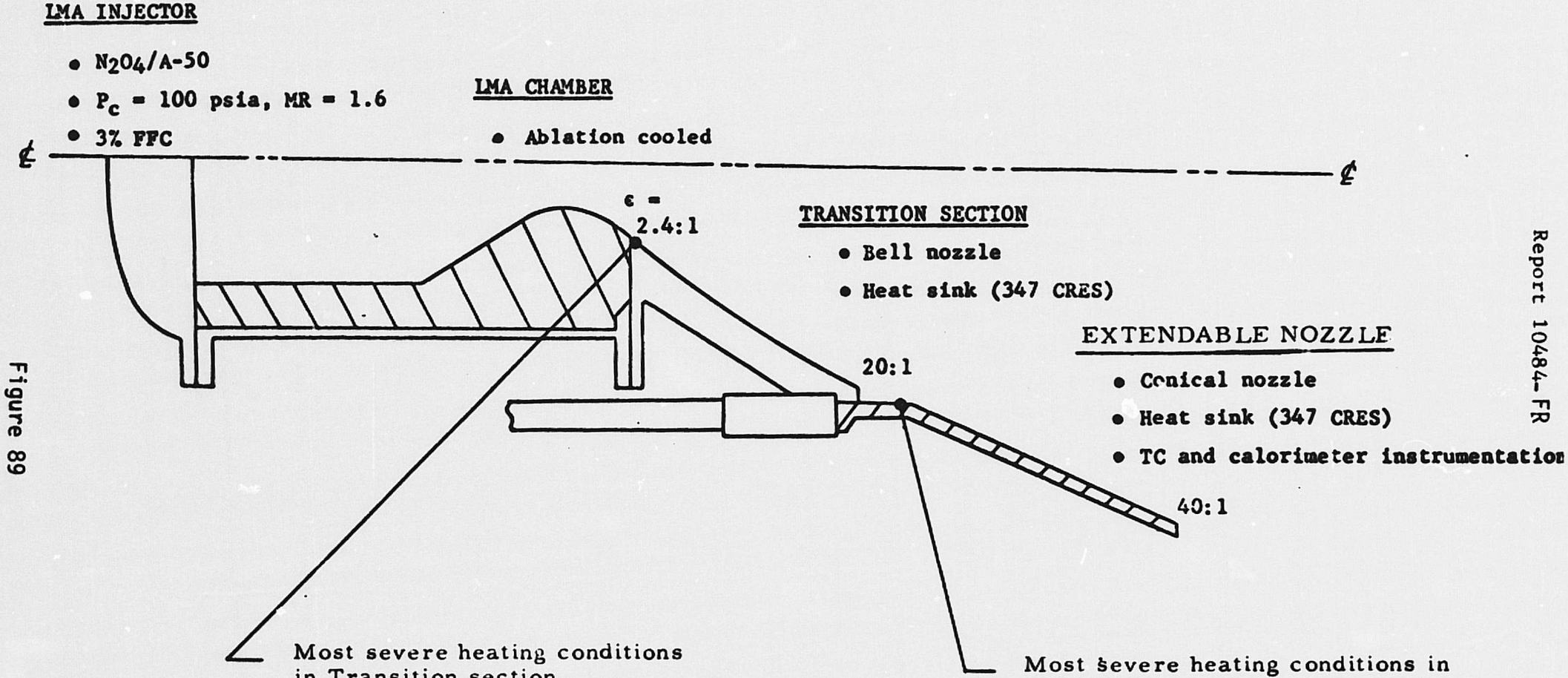
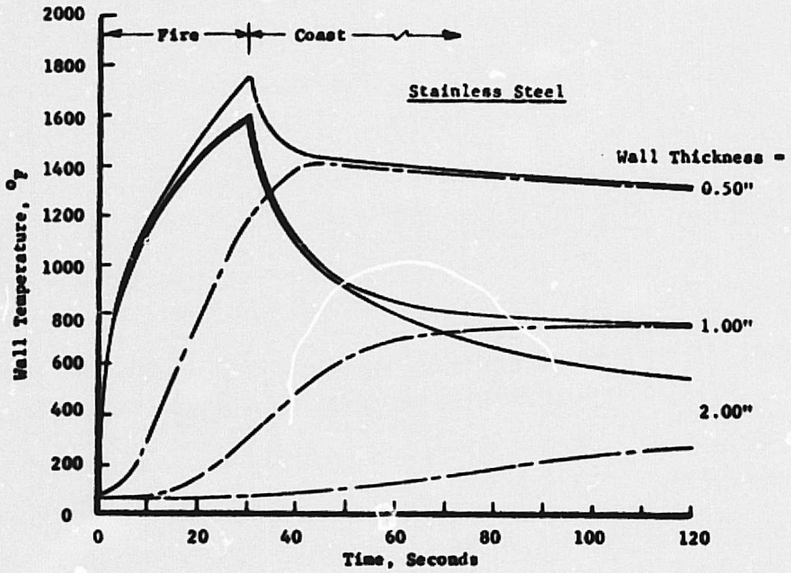


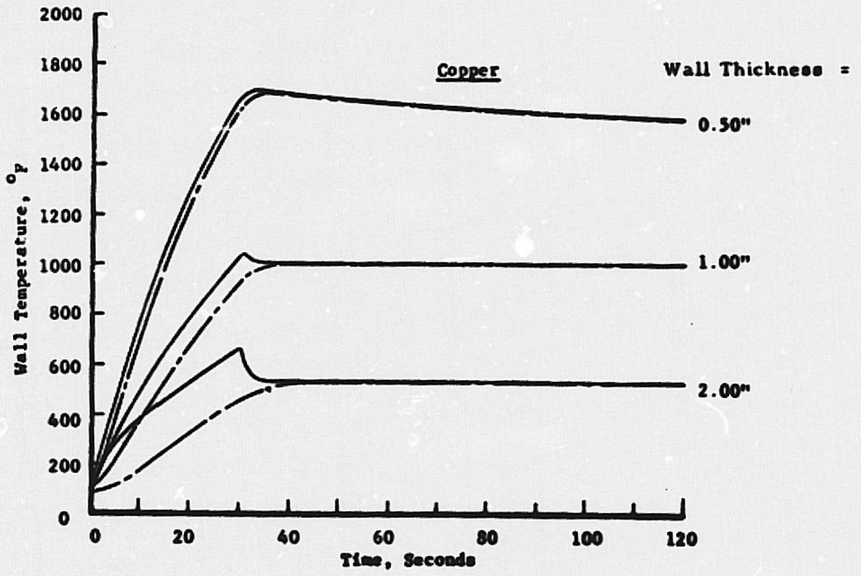
Figure 89

Report 10484-FR

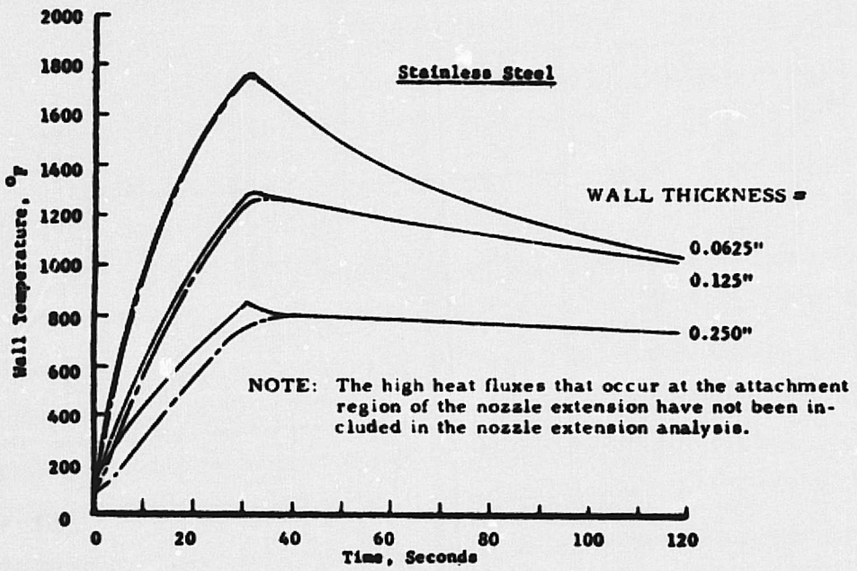
Extendable Nozzle Test Engine Cooling

TRANSITION SECTION TEMPERATURES (ϵ = 2.4:1)





NOZZLE EXTENSION TEMPERATURES (ϵ = 20:1)



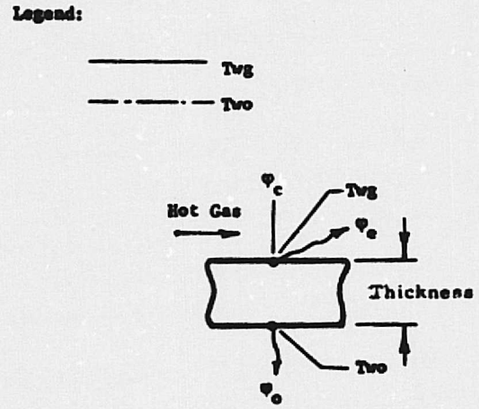
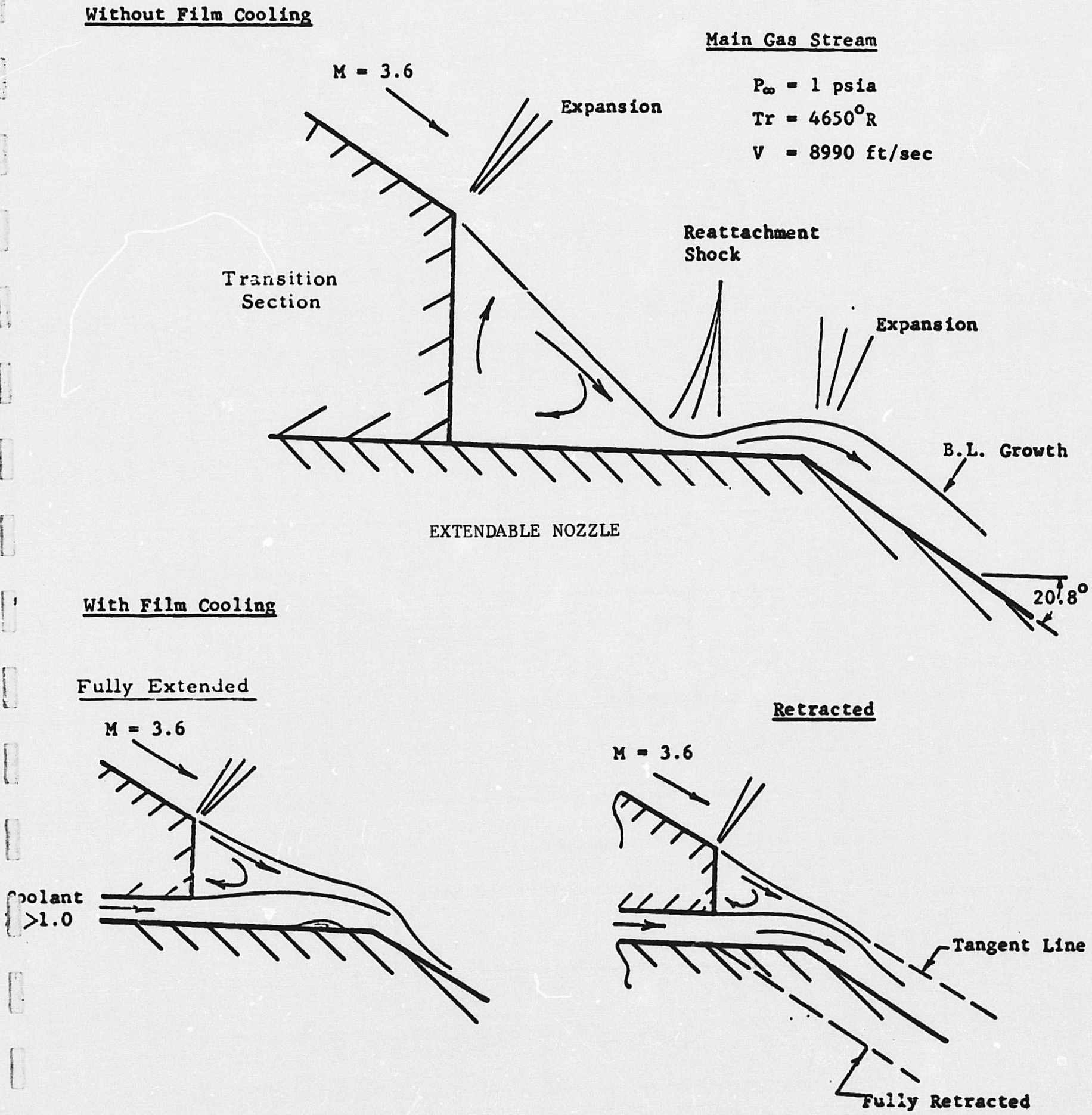


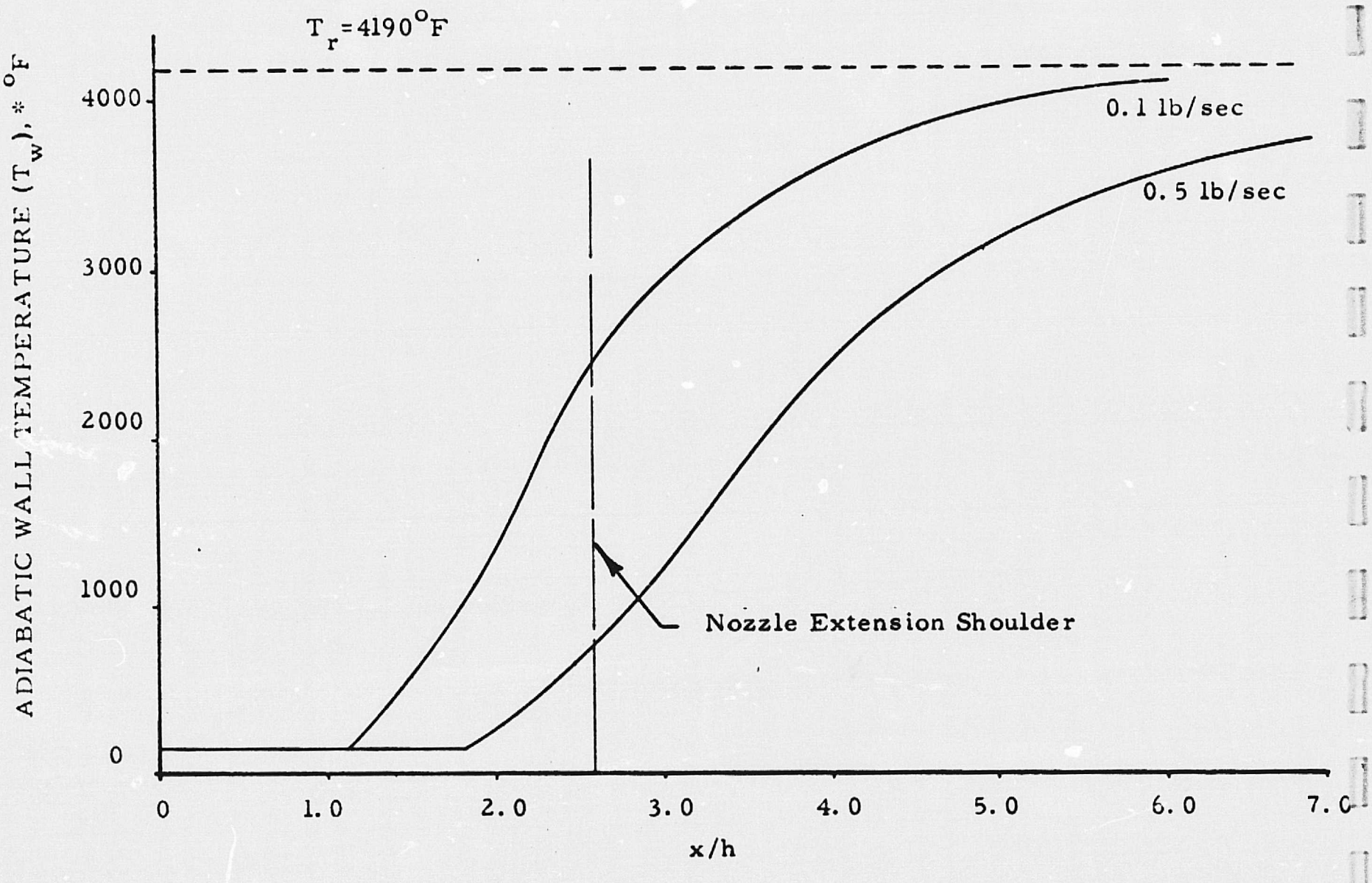
Figure 90

Heat Sink Design Transition Sections and Extendable Nozzle Temperature Response for a 30-sec Firing

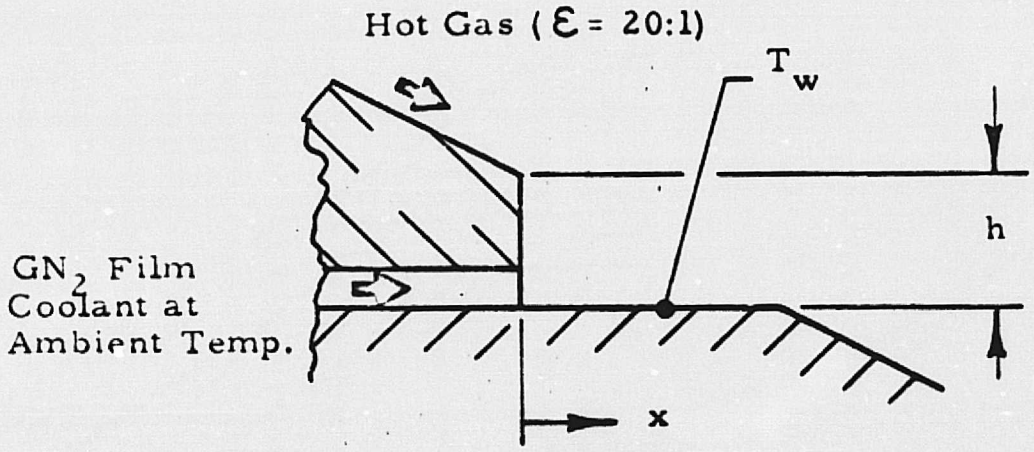


Extendable Nozzle Attachment Region Flow Characteristics

Figure 91



NOTE: The high heat fluxes that occur at the attachment region of the nozzle extension have not been included in the film cooling analysis.



* Adiabatic wall temperature includes the effect of film cooling

Adiabatic Wall Temperature at the Attachment Region

Figure 92

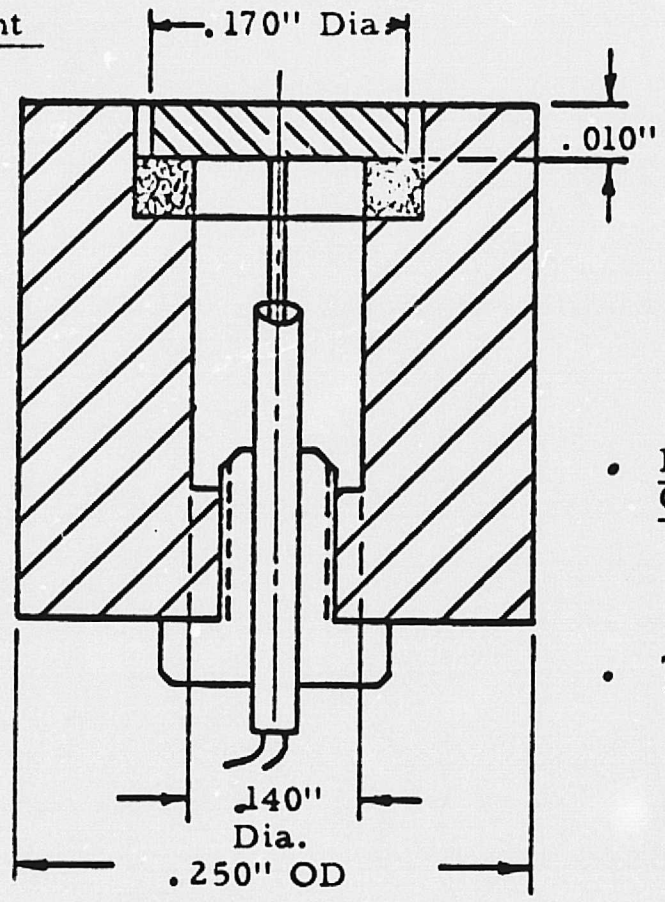
- Radiation Cooled Calorimeter For High Temperature (3000°F +) Service

- Calorimeter Element

  Tantalum or Tantalum alloy

- Calorimeter Body

  347 CRES



- Element Insulation

  (1) Air gap or low conductivity insulation

  (2) Low conductivity insulation

- Emissivity/Oxidation Resistant Coating

  Coat cavity and all calorimeter surfaces.

- Thermocouple Assembly

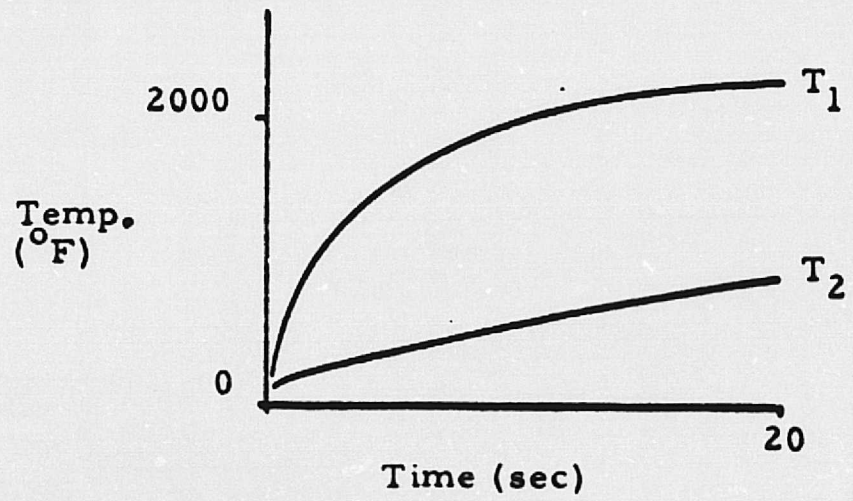
  0.020" OD tantalum sheathed w-Rh (Type I) thermocouple with swagelok fitting.

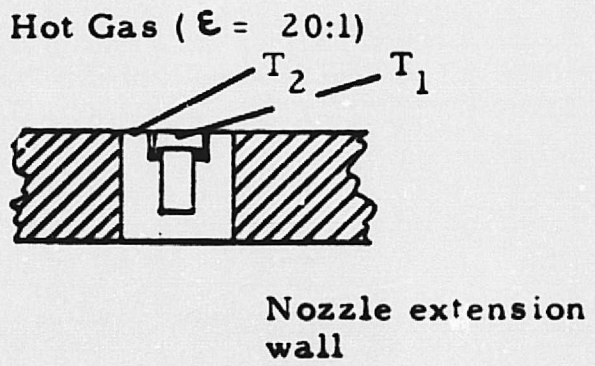
- Radiation Cooled Calorimeter For Low Temperature (2300°F max.) Service

  The low temp. calorimeter design is the same as the high temp. calorimeter design shown above except:

  - 200 series Nickel element required
  - 0.020" OD Stainless sheathed CA (Type K) thermocouple required

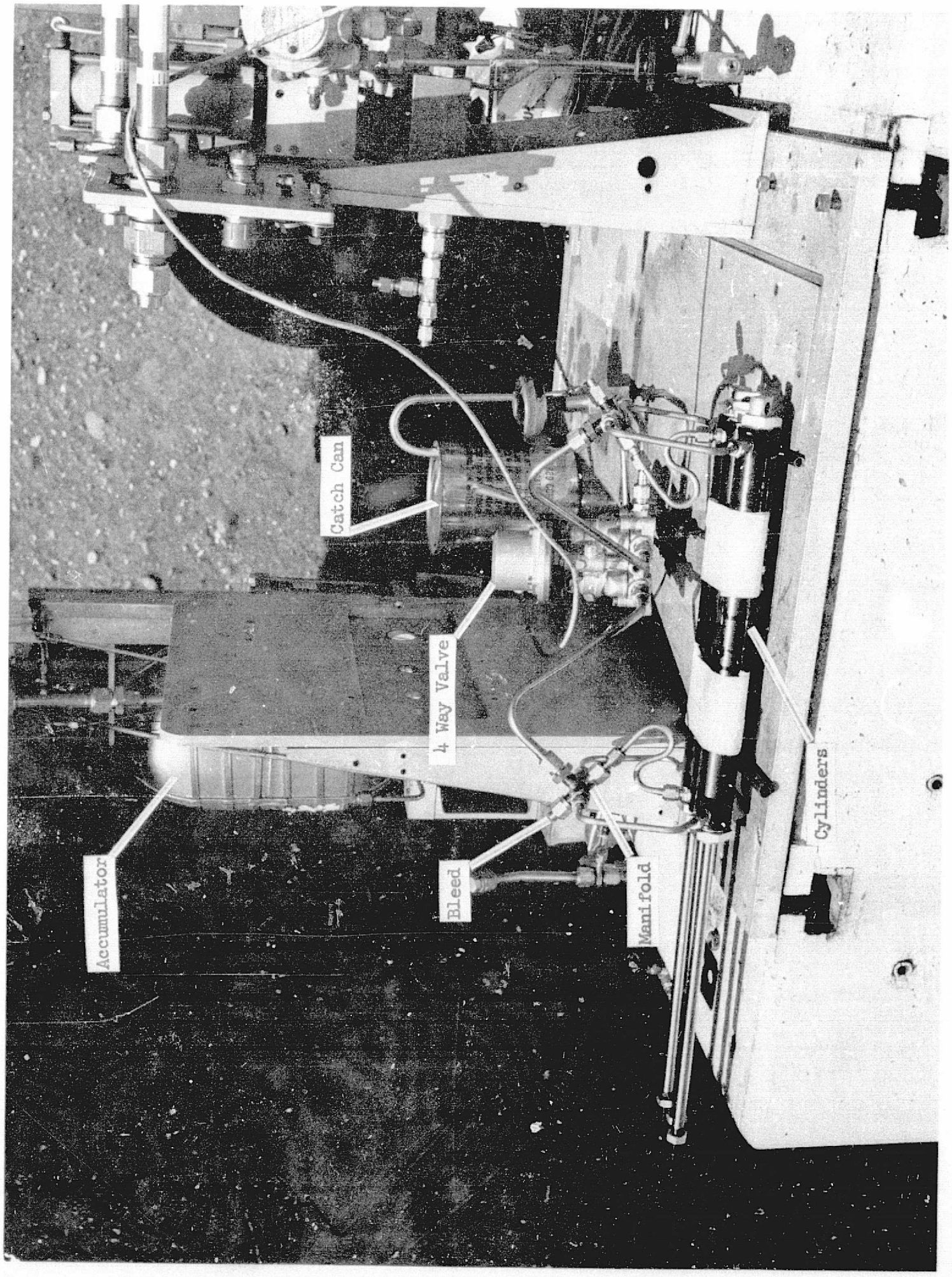
- Temperature Response Characteristics of Radiation Cooled Calorimeters





Radiation-Cooled Calorimeters for Use at the Nozzle Extension Attachment Region

Figure 93



Front View - Actuator Checkout System

Figure 94

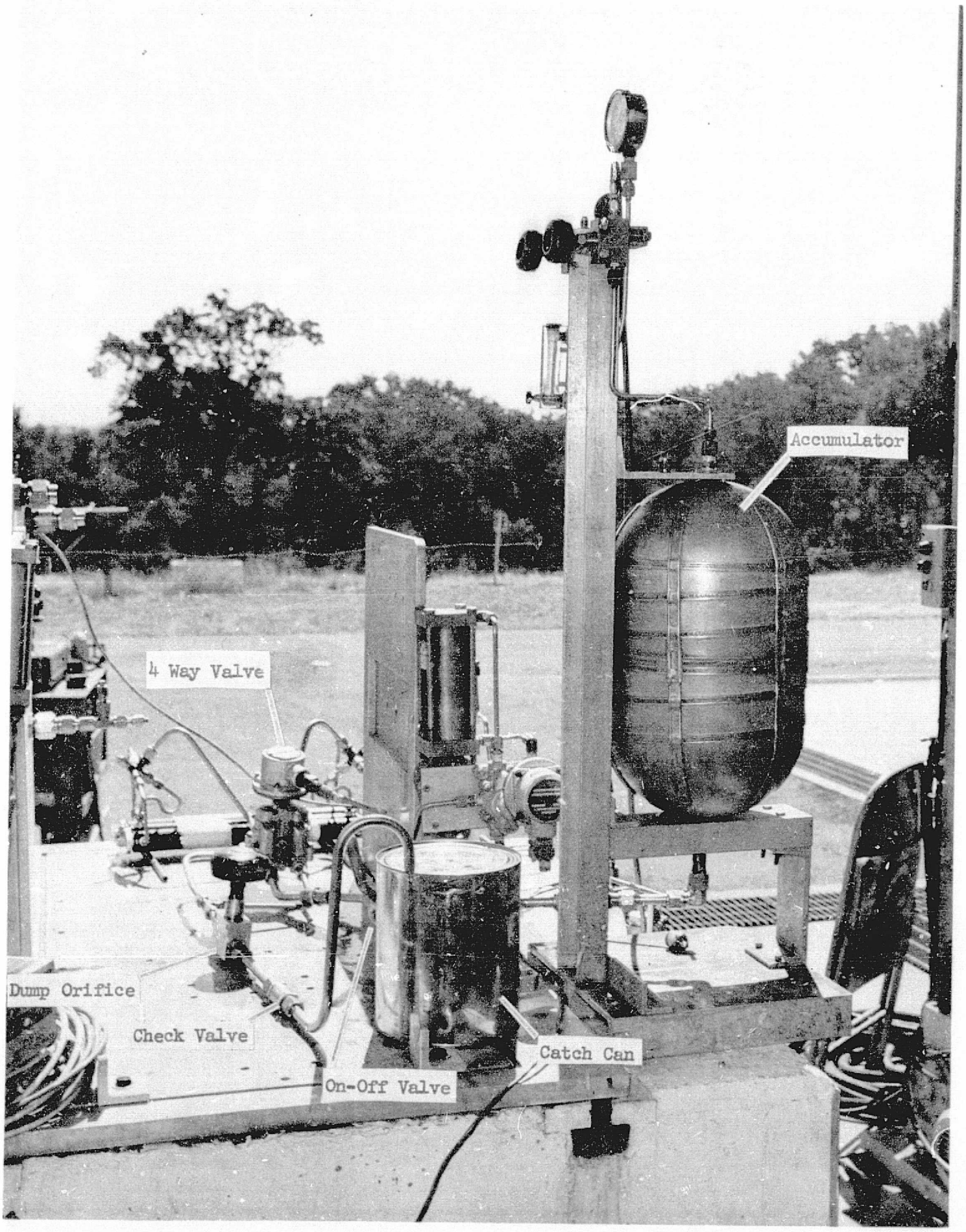
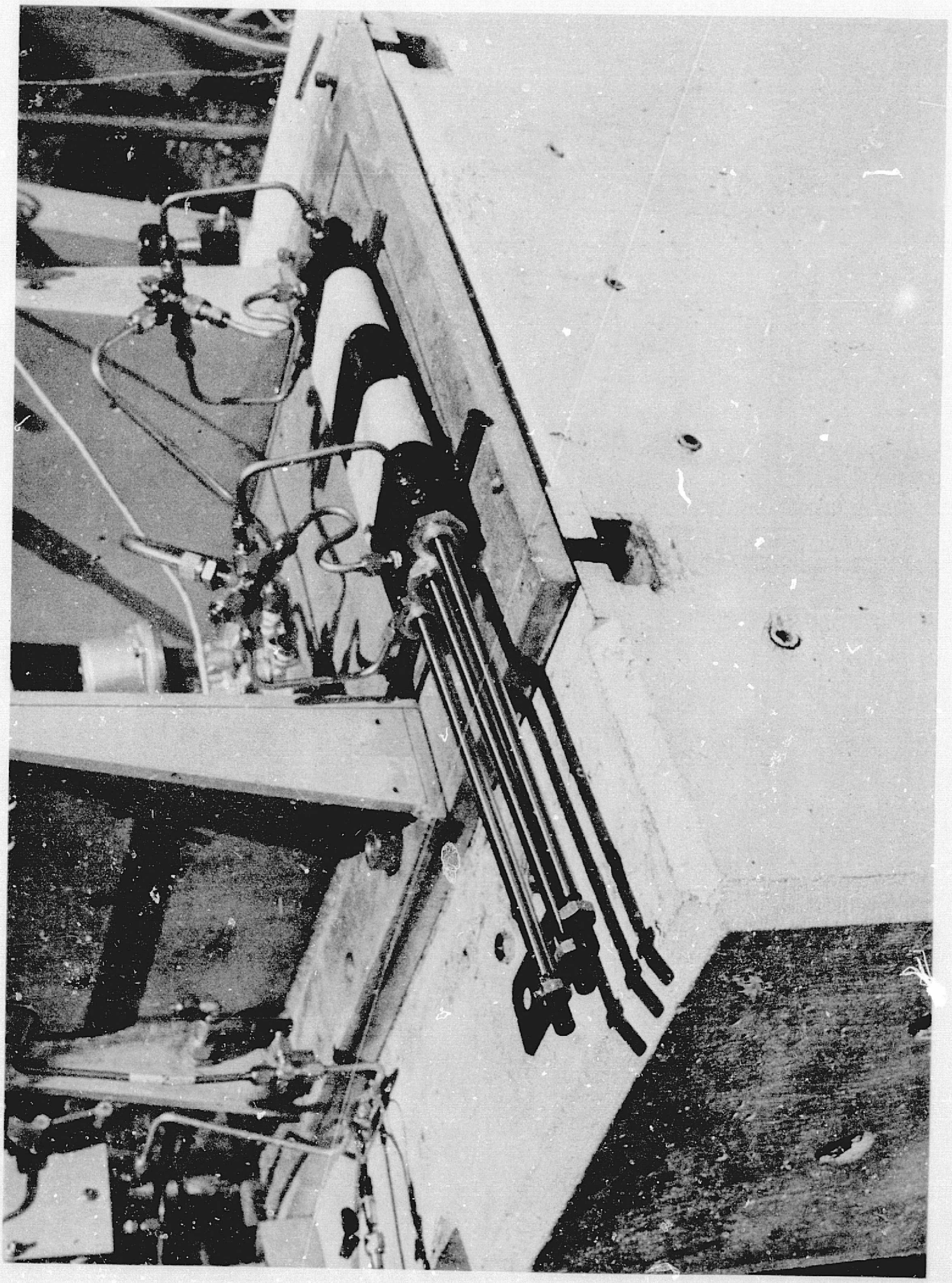
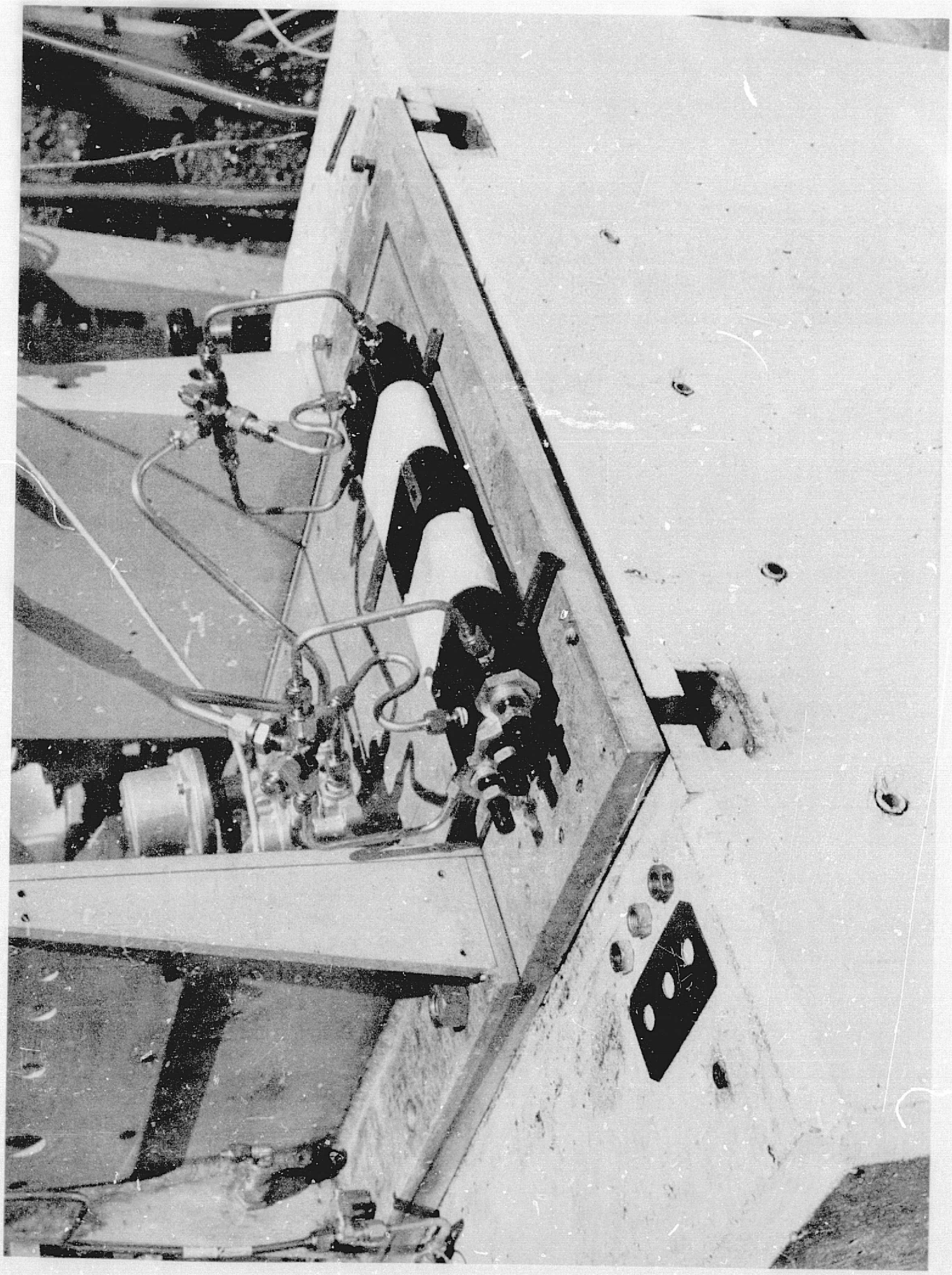


Figure 95. Rear View - Actuator Checkout System



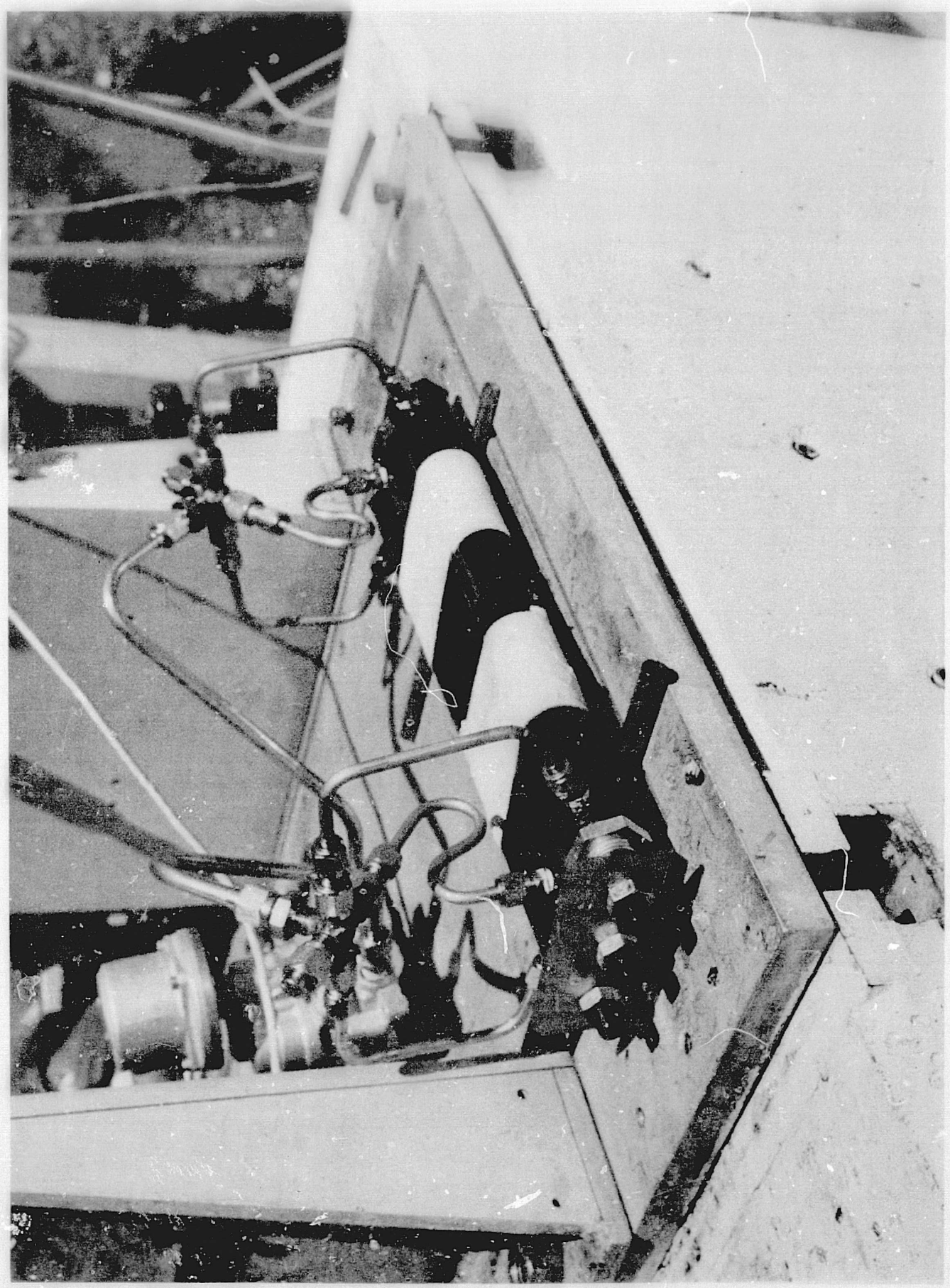
Actuators Extended

Figure 96



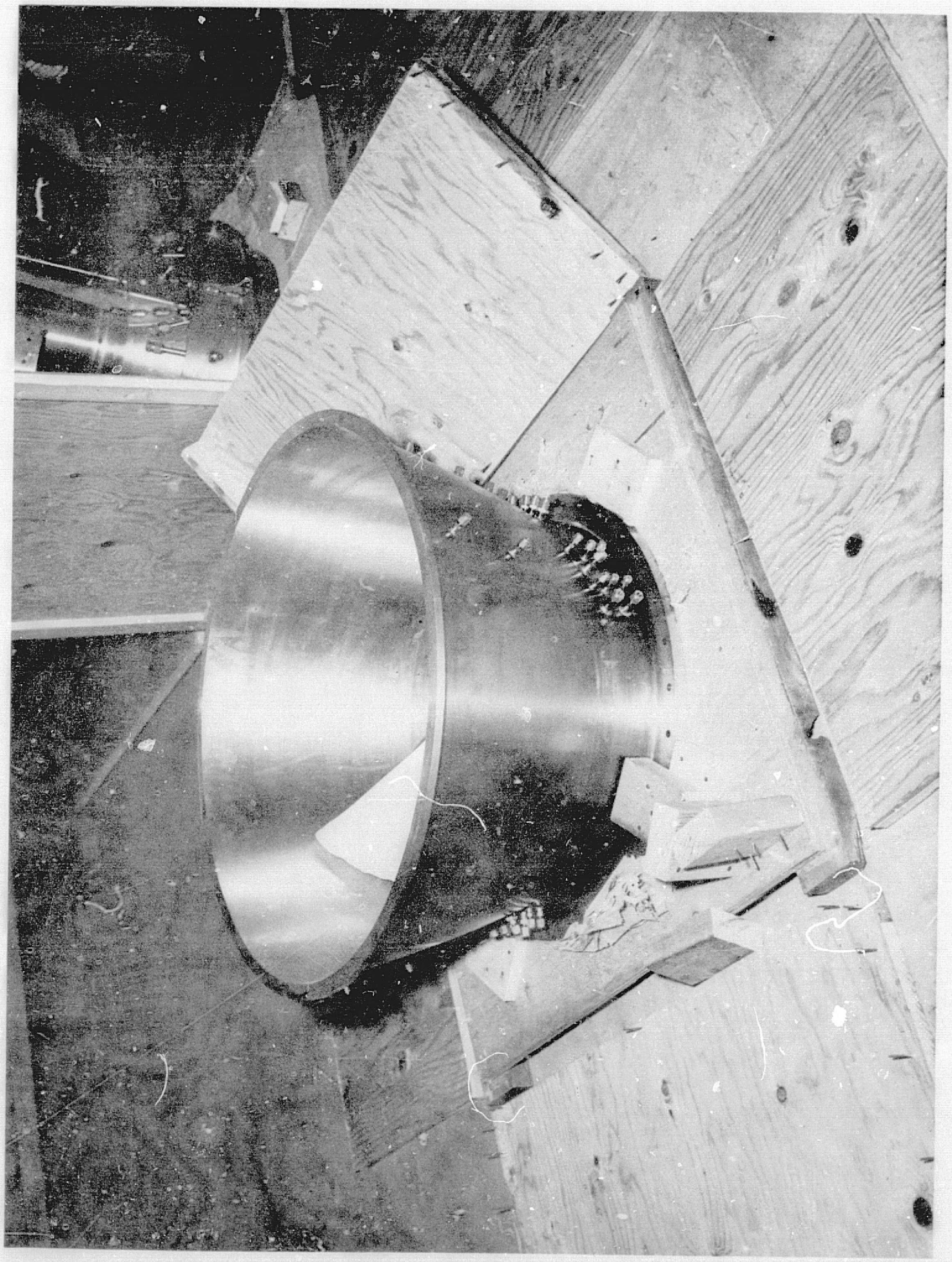
Actuators Retracted

Figure 97



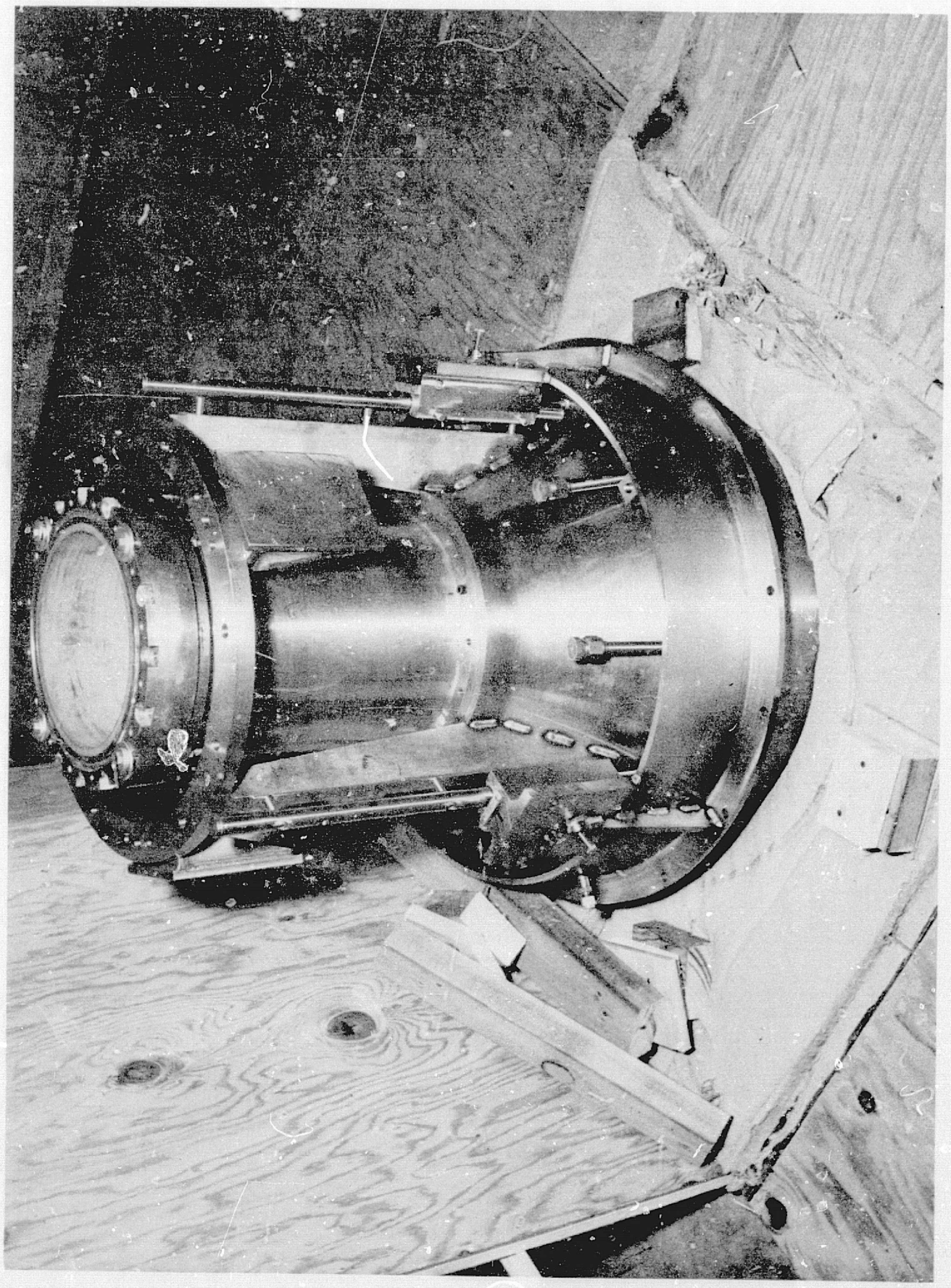
Actuator Rods Constrained with Thin Aluminum Strip

Figure 98



Nozzle Extension as Received at White Sands Test Facility

Figure 99



Basic Engine Assembly as Received at White Sands Test Facility

Figure 100

Report 10484-FR, Volume I

APPENDIX A

BIBLIOGRAPHY

Adamczack, R. L., Benzing, R. J., and Schwenker, H., Lubrication in Space Environments, Air Force Systems Command, Aeronautical Systems Div., Wright-Patterson AFB, Ohio, Proj. No. 3044, Task Nos. 03, 04, 05, Report ASD-TDR-62-541, June 1962.

Advanced Cryogenic Rocket Engine Program; Staged Combustion Concept, Quarterly Technical Report No. 6, Pratt & Whitney Aircraft Report PWA-FR-2572, AFRPL-TR-67-259, September 1967 (Conf.).

Aerospace Fluid Component Designer's Handbook, TRW Systems Group, Report No. RPL-TDR-64-25, February 1970.

Air Force Reusable Rocket Engine Program; SLR129-P-1, Pratt & Whitney Aircraft Report PWA-FR-2972, AFRPL-TR-69-3, January 1969 (Conf.).

Air Force Reusable Rocket Engine Program; XLR129-P-1 Engine Performance, Pratt & Whitney Aircraft Report PWA-FR-3108, AFRPL-TR-69-19, April 1969 (Conf.).

Altitude Performance Evaluation of a Rocketdyne Extendable Nozzle, Arnold Engineering Development Center Report AEDC-TR-67-160, September 1967 (Conf.).

Analytical and Experimental Investigations of High Expansion Area Ratio Nozzles, "Volume I: Analytical and Model Cold Flow Investigations," Rocketdyne Report No. R5708, Vol. I, RPL-TDR-64-3, December 1964 (Conf.).

Bauer, P., Investigation of Leakage and Sealing Parameters, Illinois Institute of Technology, Chicago, Contract AF 04(611)-9704, Proj. No. 6753, Report AFRPL-TR-65-153, August 1965.

"The Bearings Book, A Basic Reference Manual for Design Engineers," Machine Design, 13 June 1969.

Bowman, R. E., "How Radiation Affects Engineering Materials," Materials in Design Engr., Vol. 52, No. 1, July 1960, pp 119-134.

Boyd, W. K., and White, E. L., Compatibility of Rocket Propellants with Materials of Construction, Battalle Memorial Institute, Defense Metals Information Center, Columbus, Ohio, DMIC Memo 65, OTS PB 161215, 15 September 1960.

Boyd, W. K., et al., Compatibility of Materials with Rocket Propellants and Oxidizers, Battalle Memorial Institute, Defense Metals Information Center, Columbus, Ohio, Contract AF 33(615)-1121, Proj. No. 8975, 29 January 1965.

Bouguet, F. L., Jr., "The Radiation Hazard of Space," Space/Aeronautics, Vol. 39, No. 5, May 1963, pp 72-77.

Buckley, D. H., Swikert, M., and Johnson, R. L., "Friction, Wear, and Evaporation Rates of Various Materials in Vacuum to 10^{-7} mm Hg," Am. Soc. Lubrication Engrs. Trans., Vol. 5, No. 1, April 1962, pp 8-23.

Cannon, C. H., "Hot Pneumatic Systems," Control Eng., Vol. 6, No. 4, April 1959, pp 97-101.

Chace, R. A., "Locking Mechanisms for Hydraulic Actuators," Prod. Eng., Vol. 27, No. 6, June 1956, pp 164-166.

Chamay, A. J., and Sederquist, R. A., "An Experimental Investigation of Shock Vector Control with Gaseous Secondary Injection," American Rocket Society Space Flight Report to the Nation, New York, N.Y., 9-15 October 1961.

Cheney, A. J., Happoldt, W. G., and Swayne, K. G., "Designing Bearings with Nylon and Teflon Plastics," Machine Design, Vol. 28, No. 12, 14 June 1956, pp 143-146, 148, 150, 152.

Cloth Extendable Nozzle Firing Demonstration Program, Rocketdyne Report R-7232, AFRPL-TR-68-15, March 1968 (Conf.).

Demonstration of Expandable Nozzles, Aerojet-General Report No. LRP 199, November 1960.

Development, Design, Fabrication, and Demonstration of Packageable, High-Expansion-Ratio Nozzles for Solid Propellant Rocket Motors, Aerojet-General Corp. Report 0874-82-1Q, August 1964 (Conf.).

"Development of Storable High Performance Variable Thrust Liquid Rocket Engines for Space Applications," Packaged Liquid Propulsion Symposium (P. R. Scannell and T. D. Meyers), United Technology Corp., CPIA Publication No. 13, March 1963, pp 229-246 (Conf.).

DiSadio, A., "For High Pressure, Low Velocities--Bonded Coatings Lubricate Metal Parts," Prod. Eng., Vol. 31, No. 36, 5 September 1960, pp 48-53.

Durability and Performance Evaluation of Aerojet-General Corporation Expandable Nozzle Extensions and Nonrigid Conical Nozzle Extensions at Simulated Altitude, ARO, Inc. Report AEDC-TR-65-26, February 1965 (Conf.).

Evaluation Tests of Packageable High-Expansion Ratio Nozzle Extensions for Solid-Propellant Rocket Motors, Arnold Engineering Development Center Report AEDC-TR-68-113, July 1968 (Conf.).

Evans, H. E., Flately, T. W., and Federline, M. F., "Mechanical Elements for Vacuum Operation," ARS Paper No. 2711-62, presented at the ARS 17th Annual Meeting and Space Flight Exposition, Los Angeles, California, 13-18 November 1962.

Expandable-Nozzle Rocket Engine Design Concept, Aerojet-General Corp. Report 8290-4S, June 1964.

Expandable Nozzle Program Theoretical Studies, Space-General Corp. Report SGC 160-SR-1, March 1963.

Flexible Exit Cone Nozzle Development Program, Phase I Report, Thiokol Chemical Corp. Report AFRPL-TR-68-66, April 1968.

"Fluid Power Book," Machine Design, Vol. 32, No. 7, 22 March 1962.

Fragmentable Nozzle Final Report, Hercules Report ABL-TR-68-14, May 1968.

Hammel, R. L., Comments on Cold Welding, Space Technology Laboratories, Inc., Material Sciences Dept., Redondo Beach, California, Report No. 9869-6002-KU-000, 31 December 1962.

Hanson, F. M., Shore, J. J., and Greenwood, J. D., Static Seal Design and Practices, Aerojet-General Corp., Sacramento, California, February 1965.

Hyde, G. F., and Fuchsluger, J. H., "Materials for High Temperature Seals," Machine Design, Vol. 33, No. 26, December 1966, pp 154, 156, 158, 1 figure, 3 tables.

Investigation of Rigid and Expandable Rocket Nozzles at Mach Numbers from 1.8 to 3.0, ARO Inc. Report AEDC-TR-66-124, August 1966 (Conf.).

Jaffe, L. D., "Effects of Space Environment Upon Plastics and Elastomers," Chem. Engr. Progr., Symp. Ser., Vol. 59, No. 40, 1963.

Jaffe, L. D., and Rittenhouse, J. B., "How Materials Behave in Space," Materials in Design Eng., Vol. 56, No. 3, September 1962.

Jaffe, L. D., and Rittenhouse, J. B., "Behavior of Materials in Space Environments," ARS J., Vol. 32, No. 3, March 1962, pp 320-346.

Lewis, J. W., Coatings for Advanced Thrust Chambers, Aerojet Liquid Rocket Company, Sacramento, California, Contract NAS 3-11185.

Mayhew, W. E., "Hot Hydraulic Systems," Control Eng., Vol. 6, No. 4, April 1959, pp 92-97.

McConnell, B. D., "How Good Are Solid-Film Lubricants for Extreme Environments?," Prod. Eng., Vol. 32, No. 24, 12 June 1961, pp 70-73.

Menton, A. F., "Lubricants and Bearing Surfaces: Space Vehicle Applications Pose Special Problems," Missiles and Space, Vol. 7, No. 9, September 1961, pp 4-17.

Noonan, J. W., "Materials in the Design of Seals for Extreme Environments" Machine Design, Vol. 34, No. 19, 16 August 1962, pp 186, 188, 190, 192, 194, 196.

Packageable High Expansion Ratio Nozzles for Solid Propellant Motors, Aerojet-General Corp. Report AFRPL-TR-66-321, November 1966.

Packageable High Expansion Ratio Nozzles for Solid Propellant Motors, Aerojet-General Corp. Report AFRPL-TR-67-233, August 1967.

Packageable High Expansion Ratio Nozzles for Solid Propellant Motors, Aerojet-General Corp. Report AFRPL-TR-68-83, July 1968 (Conf.).

Palmer, E. B., "Solid-Film Molybdenum Disulfide Lubricants," Materials in Design Engr., Vol. 54, No. 2, August 1962, pp 122-126.

Performance Evaluation of an Aerojet-General Corp. Expandable Nozzle Extension and a Nonrigid Conical Nozzle Extension at Simulated Altitudes, Arnold Engineering Development Center Report AEDC-TDR-63-159, October 1963 (Conf.).

Peterson, M. B., and Johnson, R. L., "Solid Lubricants for Temperatures to 1000°F," Vol. 13, No. 4, April 1957, pp 203-207.

Radiant Cooling of Thin-Walled Metal Exhaust Cones, Aerojet-General Corp. Report TM 155SRP, December 1960.

Rathbon, F. O., Jr., "Metal-to-Metal and Metal-to Gasketed Seals for Extreme Environment Applications," Machine Design, Vol. 37, No. 18, 5 August 1965, pp 158-169.

Rathbon, F. O., Jr., "Metal-to-Metal and Metal Gasketed Seals," paper presented at SAE National Aerospace Fluid Power Systems and Equip. Conf., Los Angeles, 18-20 May 1965, pp 156-169, 175.

Rentschler, L. M., "How to Design Plastic Bearings," Machine Design, Vol. 34, No. 23, 27 September 1962, pp 156-162.

Saelman, B., "Hydraulic Actuation Systems," Machine Design, Vol. 29, No. 10, 16 May 1957, pp 131-134.

Schwerdtfeger, L. H., "New Ideas for Designing Rotary Hydraulic Actuators," Machine Design, Vol. 31, No. 6, 6 August 1959, pp 134-137.

"The Seals Book: A Basic Reference Manual for Design Engineers," Machine Design, 19 June 1969.

Spreading of Rocket Exhaust Jets at High Altitudes, ARO Inc. Report AEDC-TR-59-11, June 1959.

Structural Synthesis of Composite Materials for Ablative Nozzle Extensions, Aerospace Corp. Report TR-0066 (5122-20)-1, SAMSO TR-69-201, July 1969.

Stephens, W. T., "Points to Consider in Selecting Hydraulic Systems Components," Machine Design, Vol. 28, No. 4, 23 February 1965, pp 108-115.

"Ten Commandments for Design Reliability," SAE Journal, Vol. 67, No. 11, November 1959, pp 35-37.

Thrust-Vectoring Methods, U.S. Naval Ordnance Test Station Report TP 2123, NAVORD Report 6423, December 1958 (Conf.).

Titan Product Engineering; Expandable Nozzle Program, Aerojet-General Corp. Report BSD-TR-66-363, February 1967 (Conf.).

Weapon System 107 A-2 Product Engineering Program; Expandable Nozzles and Ablative Thrust Chamber, Monthly Report No. 1, Aerojet-General Corp., August 1964.

"Which is Best for Aerospace Control Power," Machine Design, Vol. 34, No. 27, 22 November 1962, pp 349-141.

APPENDIX B

TEST PLAN

Report 10484-FR, Volume 1, Appendix B

TEST PLAN

A. OBJECTIVE

1. To demonstrate the operation of an extendable and retractable nozzle.
2. Evaluate the effect of contour mismatch at the nozzle attach interface on heat transfer and gas dynamics.
3. Evaluate the feasibility of film cooling at the nozzle attach interface and nozzle sealing.

B. PLANNED TESTS (See Pages 8 and 9)

C. MATERIAL FURNISHED

1. Nozzle Assy - Extendable
   Dwg. No. 1159360
2. Thrust Chamber Valves
   P/N AG-41245
3. Plumbing, Thrust Chamber
   Valves to Injector (See Page 10)

D. GENERAL OPERATING REQUIREMENTS

1. All tests are to be conducted with N_2O_4 as the oxidizer and A-50 as the fuel.
2. Nominal Altitude - Steady-state operating conditions are as follows:
   P_c = 100 psia
   W_t = 11.02 lb/sec
   W_o = 6.89 lb/sec
   W_f = 4.13 lb/sec
   MR = 1.6
   F = 3200 lb
3. Any test over 5 sec in duration is to be terminated if the following operating conditions are exceeded:
   P_c = 125 psia
   MR = 1.5 to 1.7
   T_A-1, -2 & -3 = 300°F (temperature at any one of the 3 C.A. thermocouples located in the chamber-nozzle adapter)

4. All pressure transducer line lengths other than on the nozzle extensions are to be as short as possible.
5. All pressure transducer line lengths on the nozzle extension are to be greater than three inches.

E. INSTRUMENTATION REQUIREMENTS

1. Specific parameter requirements (See Pages 11 and 12).
2. Tabor (or equivalent) pressure transducers to be supplied by White Sands Testing Facility.
3. Heat Transfer Instrumentation will be supplied by AGC. This instrumentation will be as displayed on Page 13. Installation and adjustment will be accomplished in the presence of the AGC representative.

F. TEST PREPARATION

1. Valve Timing

	Open (sec)	Close (sec)
Injector Fuel Valve (TCFV)	0.180	0.060
Injector Oxidizer Valve (TCOV)	0.050	0.040

Injector Propellants Purge Valves -- Solenoid (On-Off)

Nozzle Extension Actuator Valves -- Solenoid (On-Off)

Note: The nozzle deployment and retraction actuators have built-in snubbing (flow control orifices) systems.

2. Switch Settings

TCOVS @ 75% TCOV opening

TCFVS @ 75% TCFV opening

3. Valve Actuation Pressure Settings

TCOV Actuation @

TCFV Actuation @

4. Injector Purge Pressure Settings

TCOPV = 150 psig regulator outlet

TCFPV = 150 psig regulator outlet

5. Malfunction Timer Settings

a. M-7 (TCOVS and TCFVS) $\frac{FS_1 + \text{sec}}{0.7 \pm .05}$

6. Malfunction Shutdown Signals

   a. TCOVS makes prior to TCFVS during engine start.

   b. M-7 timer times out prior to TCOVS and TCFVS make.

   c. TCOVS opens during run.

   d. TCFVS opens during run.

   Note: All malfunctions initiate normal engine shutdown sequence (FS_2).

G. ENGINE TEST SEQUENCE

The following engine start, steady state and shutdown sequence is to be used for all tests (see Page 14 - Electrical Sequence).

1. Engine Start Sequence

   a. Propellant feed systems filled, bleed and pressurized.

   b. Energize manually and simultaneously both fuel (A-50) and oxidizer (N_2O_4) injector manifold nitrogen purges (see Page 10).

   c. Arm switch on.

   d. Energize engine fireswitch (FS_1).

   e. FS_1 energizes TCOVPV and TCFVPV and starts timers M-1 and M-7 and de-energizes TCOPV and TCFPV.

   f. LTCOV begins to open.

   g. LTCFV begins to open.

   h. LTCOV opens 75% to 95% and makes TCOVS.

   i. LTCFV opens 75% to 95% and makes TCFVS. TCFVS and TCOVS must be set so that under normal operation, TCOVS makes first. If TCFVS makes before TCOVS, engine shutdown (FS_2) must be initiated.

   j. $FS_1 + 0.7 \pm .05$ sec M-7 timer times out. If both TCOVS and TCFVS have not made, FS_2 is initiated.

2. Steady State Engine Operation

3. Shutdown Sequence

   a. M-1 duration timer times out.

   b. FS_2 energized.

   c. FS_2 de-energizes TCOVPV and TCFVPV, starts M-5 and M-6 timers.

   Note: LTCOV and LTCFV closing time to be determined by valve operational characteristics vs. requirement for oxidizer lag in shutdown transient.

d. FS_2 + 0.5 sec (max) M-6 timer times out and TCFPV opens.

e. FS_2 + 1.0 to 1.5 sec M-5 timer times out, TCOPV opens.

Note: Both TCFPV and TCOPV to remain open following test. Purges are to be manually closed @ FS_2 + 2 minutes minimum, or as determined by the nozzle-chamber adapter temperature as monitored on the Brown Recorders.

4. Nozzle retraction and deployment (see Page 15).

H. PHOTOGRAPHIC COVERAGE

Following are the photographic coverage requirements for this test series.

1. Still Photographs

a. All photographs to be 8-1/2 x 11 black and white.

b. All newly installed test hardware to be photographed prior to testing.

c. All test hardware damage will be photographed before the hardware is removed from the test stand. Additional photographs may be required after removal from the test stand.

d. All photographs to have an identification card having the following particulars:

(1) Test number
(2) Date
(3) Item nomenclature
(4) P/N

Note: Identification card may be attached to or located near object being photographed.

e. Request four copies and negatives of all still photographs.

f. Photographs of component instrumentation will be taken prior to the first test. Any tests with different instrumentation than that used on the first test will be photographed prior to testing.

2. Movie Coverage

a. One 64 fps color film with flash bulb indication of FS_1 and FS_2 to be visible on film. Camera to be located to give optimum overall view of test hardware with some exhaust flame (if possible).

b. One 1000 fps color film to be used during the first 5 sec of each of the first four tests and Test Number 18.

I. DATA REQUIREMENTS

Following are the data requirements for this test series.

1. All test data to be available to Cog. AGC Engr. Rep. One copy of each record is requested.
2. The test engineer shall include on a Test Remarks Sheet pertinent comments relative to instrumentation, oscillograph records, test abnormalities, hardware damage, variation in test procedure from the proposed test plan, hardware disposition, and procedures used or existing not elsewhere mentioned. A complete posttest discussion is most important and cannot be overemphasized.
3. Six (6) equally spaced chamber throat and nozzle exit diameter readings are to be taken prior to Test No. 1 and following each test block.
4. Parameter and parameter sample rates are noted on Pages 11 and 12.

SYMBOLS LIST

NOMENCLATURE	PARAMETER
PoT	Pressure-Oxidizer Tank.
FMo-1	Flow Meter - Oxidizer Line
FMo-2	Flow Meter - Oxidizer Line
T_oFM	Temperature-Oxidizer Propellant
P_oTCV	Pressure-Oxidizer Thrust Chamber Valve Inlet
LTC_oV	Travel - Oxidizer Valve
PoL	Pressure - Oxidizer Line Injector Inlet
PoJ	Pressure - Injector Oxidizer Manifold
P_c	Pressure - Chamber
PfJ	Pressure - Injector Fuel Manifold
PfL	Pressure - Fuel Line Injector Inlet
LTC_fV	Travel - Fuel Valve
P_fTCV	Pressure - Fuel Thrust Chamber Valve Inlet
T_fFM	Temperature - Fuel Propellants
FMF-1	Flow Meter - Fuel Line
FMF-2	Flow Meter - Fuel Line
PfT	Pressure - Fuel Tank
FCV	Film Coolant Valve
TCV	Thrust Chamber Valve
FS_1	Engine Start Fireswitch
FS_2	Engine Shutdown Fireswitch
Duration	Time from FS_1 to FS_2 (M-1 time out)
Arm	Electrical power is supplied to the engine

SYMBOLS LIST (cont.)

NOMENCLATURE	PARAMETER
TCOVPV	Thrust Chamber Oxidizer Valve Pilot Valve
TCFVPV	Thrust Chamber Fuel Valve Pilot Valve
M-1	Timer #1 (M-6 is #6, etc.)
TCOPV	Thrust Chamber Oxidizer Purge Valve
TCFPV	Thrust Chamber Fuel Purge Valve
LTCOV	Thrust Chamber Oxidizer Valve Travel
LTCFV	Thrust Chamber Fuel Valve Travel

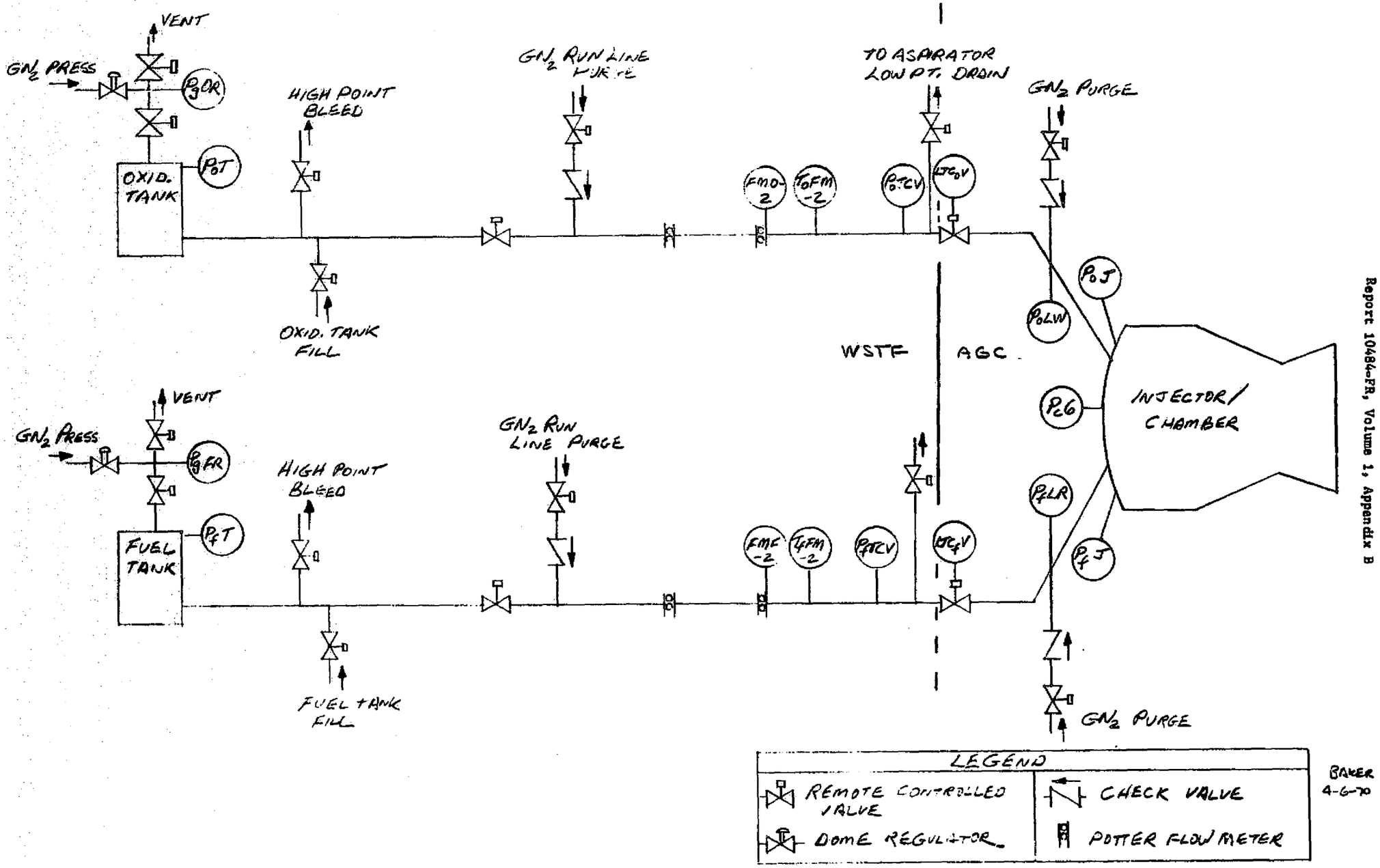
PLANNED TESTS

Test No.	Test Objective	Step Height	Nozzle Position	Test Duration	Comments
1 & 2	1. Engine base performance. 2. Nozzle heat and pressure loads uncooled. 3. Checkout and balance.	None	Fully extended.	3 & 5 sec	1. Altitude environment. 2. Continuous nozzle contour. 3. Pot .250 step height. 4. Fully instrumented. 5. Uncooled test.
3	1. Engine base performance 2. Nozzle heat and pressure loads uncooled.	.250	Fully extended.	5 sec	1. Altitude environment. 2. Fully instrumented. 3. Uncooled test.
4	1. Engine performance @ $\dot{M}_c$= Low. 2. Nozzle heat and pressure loads cooled. 3. Coolant system performance.	.250	Fully extended.	15 sec	1. Altitude environment. 2. Fully instrumented. 3. Velocity of injection = High. 4. Coolant $\dot{M}$ = Low.
5	1. Engine performance @ $\dot{M}_c$= Medium. 2. Nozzle heat and pressure loads cooled. 3. Coolant system performance.	.250	Fully extended.	15 sec	1. Altitude environment. 2. Fully instrumented. 3. Velocity of injection = High. 4. Coolant $\dot{M}$ = Medium.
6	1. Engine performance @ $\dot{M}_c$= High. 2. Nozzle heat and pressure loads cooled. 3. Coolant system performance	.250	Fully extended.	15 sec	1. Altitude environment. 2. Fully instrumented. 3. Velocity of injection = High. 4. Coolant $\dot{M}$ = High.
7	1. Engine base performance. 2. Nozzle heat and pressure loads uncooled.	.500	Fully extended.	5 sec	1. Altitude environment. 2. Fully instrumented. 3. Uncooled test.
8	1. Engine base performance @ $\dot{M}_c$ = Low. 2. Nozzle heat and pressure loads film cooled. 3. Coolant system performance.	.500	Fully extended.	15 sec	1. Altitude environment. 2. Fully instrumented. 3. Velocity of injection = Med. 4. Coolant $\dot{M}$ = Low.
9	1. Engine performance @ $\dot{M}_c$= Medium. 2. Nozzle heat and pressure loads cooled. 3. Coolant system performance.	.500	Fully extended.	15 sec	1. Altitude environment. 2. Fully instrumented. 3. Velocity of injection = Med. 4. Coolant $\dot{M}$ = Medium.
10	1. Engine performance @ $\dot{M}_c$= High 2. Nozzle heat and pressure loads cooled. 3. Coolant system performance.	.500	Fully extended.	15 sec	1. Altitude environment. 2. Fully instrumented. 3. Velocity of injection = Med. 4. Coolant $\dot{M}$ = High.
11	1. Engine base performance. 2. Nozzle heat and pressure loads uncooled.	.750	Fully extended.	5 sec	1. Altitude environment. 2. Fully instrumented. 3. Uncooled test. 4. Retract and extend before and after test.

PLANNED TESTS

Test No.	Test Objective	Stop Height	Nozzle Position	Test Duration	Comments
12	1. Engine performance @ $\dot{M}_c$ = Low. 2. Nozzle heat and pressure loads. 3. Coolant system performance.	.750	Fully extended.	15 sec	1. Altitude environment. 2. Fully instrumented. 3. Velocity of injection = Low. 4. Coolant $\dot{M}$ = Low. 5. Retract and extend before and after test.
13	1. Engine performance @ $\dot{M}_c$ = Medium. 2. Nozzle heat and pressure loads. 3. Coolant system performance.	.750	Fully extended.	15 sec	1. Altitude environment. 2. Fully instrumented. 3. Velocity of injection = Low. 4. Coolant $\dot{M}$ = Medium. 5. Retract and extend before and after test.
14	1. Engine performance @ $\dot{M}_c$ = High. 2. Nozzle heat and pressure loads.	.750	Fully extended.	15 sec	1. Altitude environment. 2. Fully instrumented. 3. Velocity of injection = Low. 4. Coolant $\dot{M}$ = High. 5. Retract and extend before and after test.
15	1. Engine base performance. 2. Nozzle heat and pressure loads uncooled.	.250	Partially extended.	5 sec	1. Altitude environment. 2. Fully instrumented. 3. Uncooled test.
16	1. Engine performance @ $\dot{M}_c$ = High. 2. Nozzle heat and pressure loads film cooled. 3. Coolant system performance.	.250	Partially extended.	15 sec	1. Altitude environment. 2. Fully instrumented. 3. Velocity of coolant injection = High. 4. Coolant $\dot{M}$ = High.
17	1. Engine performance @ $\dot{M}_c$ = Medium. 2. Nozzle heat and pressure loads film cooled. 3. Coolant system performance.	.250	Partially extended.	15 sec	1. Altitude environment. 2. Fully instrumented. 3. Velocity of coolant injection = High. 4. Coolant $\dot{M}$ = Medium.
18	1. Extension and retraction during test.	.250	-	10 sec	1. Altitude environment. 2. Fully instrumented. 3. Velocity of coolant injection = High. 4. Coolant $\dot{M}$ = High.
19 & 20	CONTINGENCY TESTS				

PROPOSED WATER FLOW SCHEMATIC
EXTENDABLE NOZZLE PROGRAM

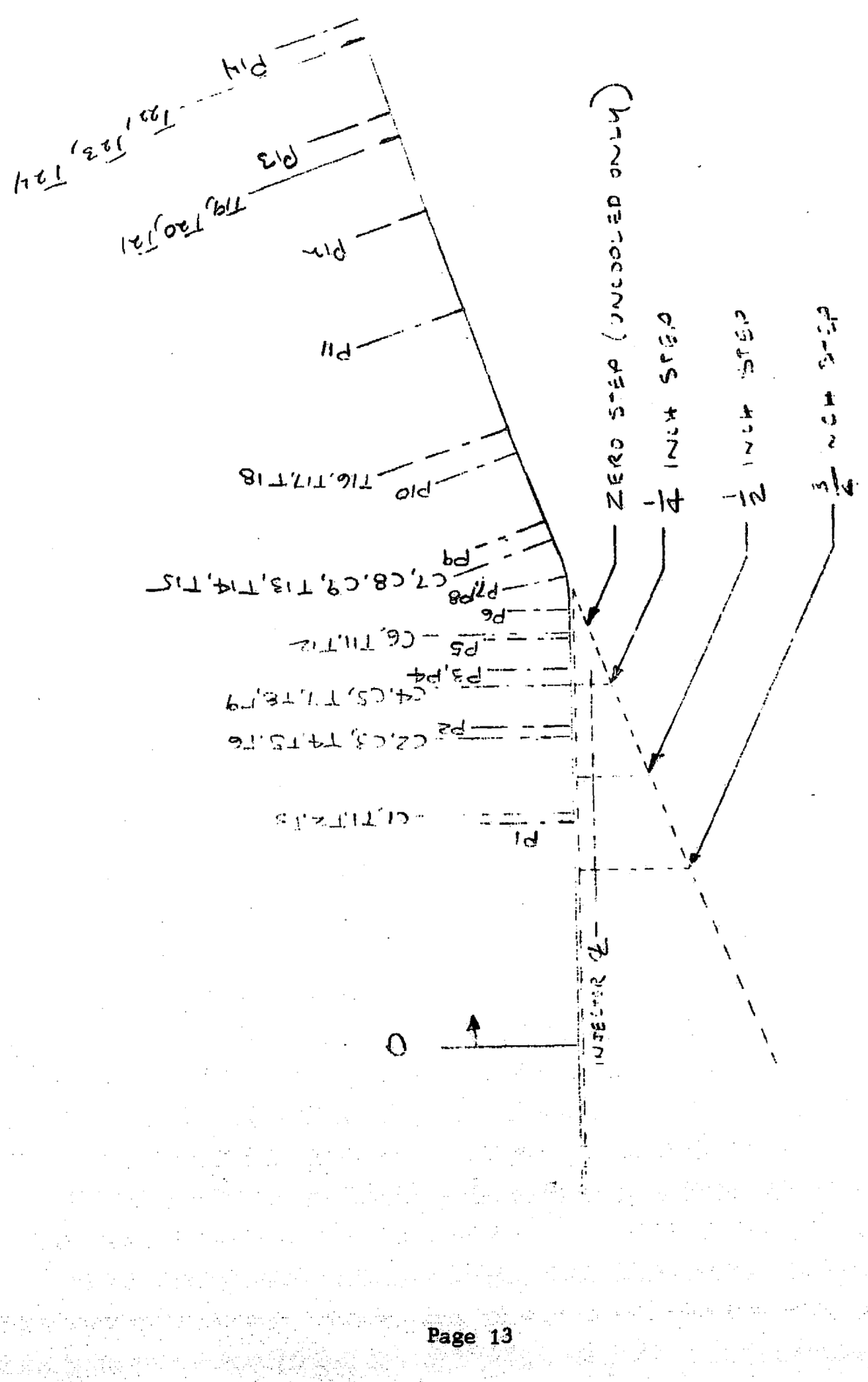


INSTRUMENTATION REQUIREMENTS

FUNCTION	RANGE	ADC	STRIP CHART	OSCILLOGRAPH	REMARKS
PgOR	0-200	L	X		
PoT	0-200	M	X	X	
PgFR	0-200	L	X		
PfT	0-200	M	X	X	
PoTCV	0-200	M	X	X	
PfTCV	0-200	M	X	X	
FMO-2	0-10 lb/sec	M	X	X	
FMF-2	0-10 lb/sec	M	X	X	
ToFM-2	0-10 mv	LL	X		
TfFM-2	0-10 mv	LL	X		
LTCoV	Valve Trace			X	
TCVPV	Current Trace			X	
TCoVS	Switch Trace			X	
LTCfV	Valve Trace			X	
TCfVS	Switch Trace			X	
TCoPV	Switch Trace			X	
FS_1 & FS_2	Switch Trace	X	X	X	

INSTRUMENTATION REQUIREMENTS (cont.)

FUNCTION	RANGE	ADC	STRIP CHART	OSCILLOGRAPH	REMARKS
FA	0-5K	X	X	X	
FB	0-5K	X		X	
PoJ	0-200 psi	M	X	X	
PfJ	0-200 psi	M	X	X	
P_c	0-200 psi	M	X	X	
PoL	0-500 psi	M			
PfL	0-500 psi	M			
TN_2	0-100°F	N		X	C A Thermocouple Film Coolant Manifold Temp.
Chamber-Nozzle Adapter					
TA-1	0-500°F		X		
TA-2	0-500°F		X		
TA-3	0-500°F		X		
P_{FCM}-1	0-50 psia		X		
P_{FCM}-2	0-50 psia		X		
Nozzle Extension					
TN-1 thru -24	0-2400°F	N		X	C A Thermocouples
TNC-1 thru -9	0-3600°F	N		X	Tungsten Rhenium Thermocouples
P_N-1 thru -14	0-5 psia	N		X	Nozzle Pressures



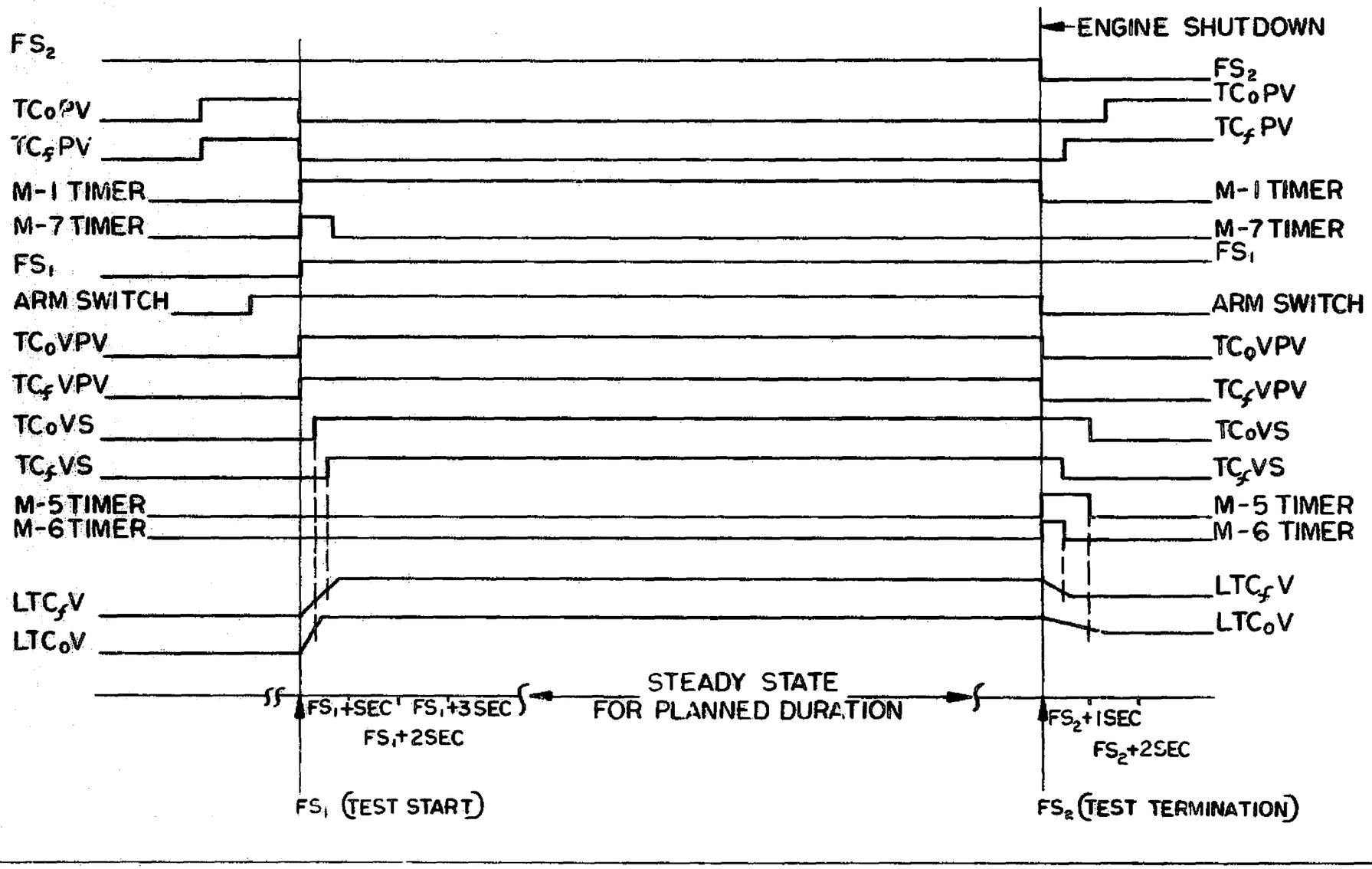
T = Thermocouple

C = Calorimeter

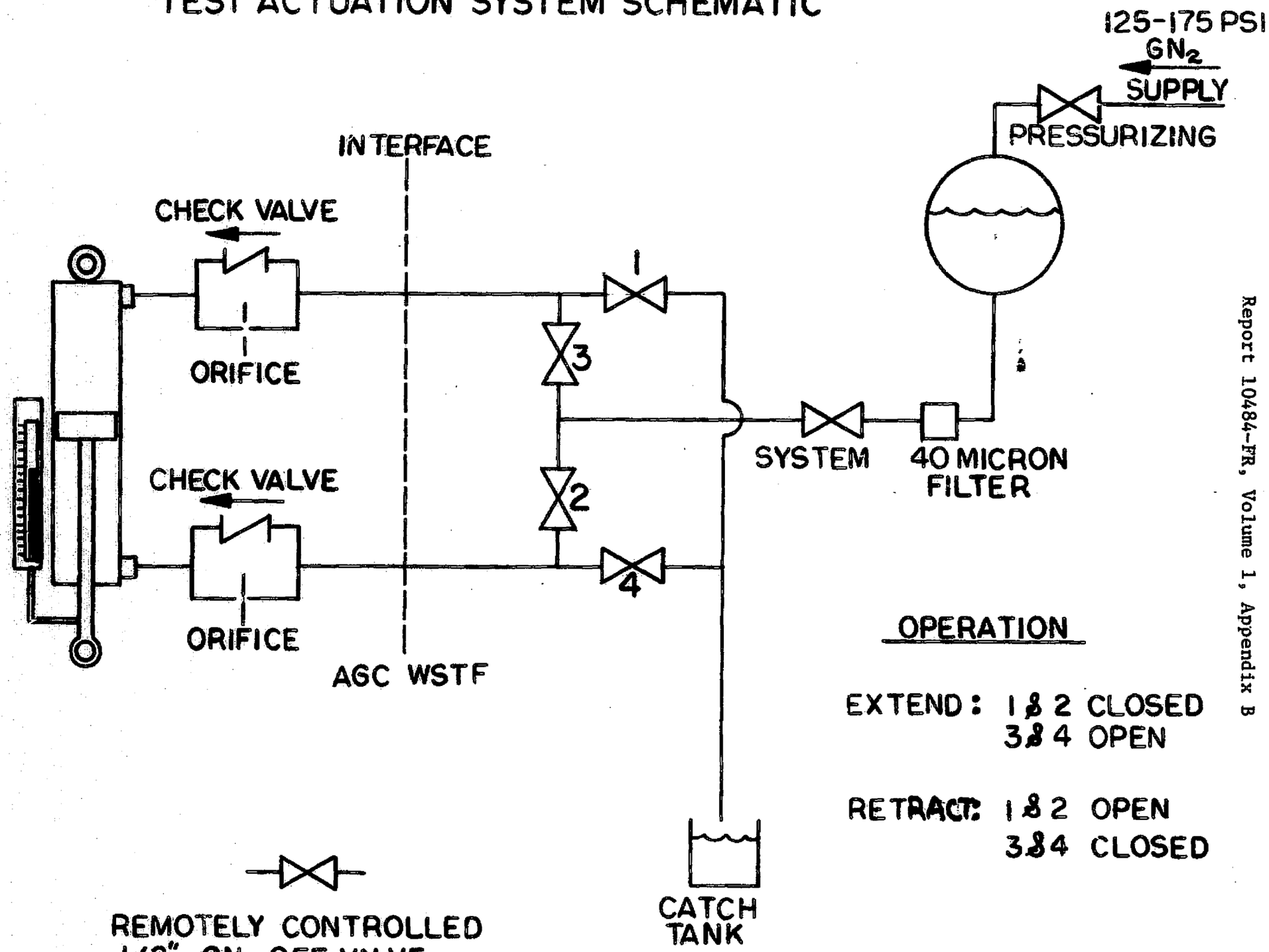
P = Pressure Tap

INSTRUMENTATION IN REGION OF REMOVABLE TIPS

PROPOSED ELECTRICAL SEQUENCE FOR ENGINE START AND SHUTDOWN



PROPOSED EXTENDABLE NOZZLE TEST ACTUATION SYSTEM SCHEMATIC



OPERATION

EXTEND: 1 & 2 CLOSED
3 & 4 OPEN

RETRACT: 1 & 2 OPEN
3 & 4 CLOSED

APPENDIX C

PREDICTED WHITE SANDS DIFFUSER PERFORMANCE

INTER-OFFICE MEMO

TO: E. Schmauderer 24 April 1970

FROM: W. H. Baker, Jr.

SUBJECT: Predicted White Sands Test Facility Diffuser Performance During Test of Extendable Nozzle

Reference: (a) White Sands Test Facility Diffuser Hand Book, Publication 0724-M1

Enclosure: (1) Analysis Sheets prepared by H. M. Hudson, Dept. 9550, 21 April 1970

DISCUSSION:

This memorandum summarizes the results of a brief analysis made by H. M. Hobart as to the predicted operation of the ascent and descent diffusers at White Sands Test Facility while testing the extendable nozzle, AGC P/N 1159360. The work sheets are presented as Enclosure (1). Reference (a) was used in conjunction with tab runs of similar Aerojet motors run under similar conditions to predict diffuser performance.

Since it is probable that the nozzle will be tested in the LEM descent diffuser (77-inch inlet) and that, if the performance is satisfactory for this case, it would also be satisfactory for the smaller 36-inch inlet ascent diffuser , since both use the same steam-driven two-stage ejector, only the large diffuser was analyzed for operation.

Referring to Enclosure (1), the extendable nozzle has the following operating characteristics:

Propellants	N_2O_4/A-50
Mixture Ratio	1.6
Mass Flow	11.3 lb/sec
Throat Diameter	4.944 in.
Chamber Pressure	100 psia

E. Schmauderer 24 April 1970

For the extendable nozzle/descent diffuser combination, the over-all area ratio is 242.5. The contraction ratio of the diffuser is 1.5.

From Aerojet tab runs of similar engines predicting diffuser operation, it appears that a contraction ratio of more than 1.89 cannot be tolerated. $1.5 < 1.89$ so this indicates satisfactory operation.

Secondly, the over-all area ratio in the contraction zone is 161. Again, from Aerojet performance runs and motor chamber pressure, this corresponds to a discharge pressure of 0.91 psia and a required dry air equivalent of 4.4 lbs air/lb propellant or 49.7 lbs/sec. If the diffuser is capable of providing a suction pressure less than .91 psia at an air flow of 49.7 lbs/sec, it should operate satisfactorily.

Figure 6-5, Ref. (a), indicates a suction of about .75 psia at 50 lbs/sec air flow, therefore the diffuser should work. (If this air flow were scaled using our J-4 facility parameters, we would expect a suction pressure of .90, or marginal operation.)

Next, using Aerojet predicted performance runs, an inlet pressure of .02178 psia (147,000 ft altitude) would be expected. Figure 6-2, Ref (a), predicts 142,000 to 145,000 ft for extendable nozzle motor sizes so this indicates satisfactory agreement.

Thirdly, even if the diffuser can be expected to operate satisfactorily during steady state operation, will it handle motor start-up? Ref. (a) states that diffuser starts are smooth with no hysteresis effects. It can therefore be anticipated that the diffuser will start and continue operation smoothly with motor start-up.

Fourth, predicted satisfactory operation in the larger descent diffuser would also predict satisfactory operation in the smaller ascent diffuser since both are driven by the same ejector system.

E. Schmauderer 24 April 1970

Once satisfactory operation of the engine/diffuser combination has been established, the only other area of concern is what may happen when the nozzle is fully retracted and the fixed portion of the nozzle continues to exhaust toward the diffuser entrance plane which is now 5.5 inches aft of the exhaust plane of the nozzle.

In other words, does the exhaust plume still enter the diffuser or partially flow into the test chamber?

Referring to Enclosure (1), it can be calculated that the physical angle between the 77-inch diffuser and the nozzle exit is about 78 degrees. Similarly, by taking the difference between the Prandtl-Meyer expansion angle at full expansion (ϵ = 242) and at the nozzle exit plane (ϵ = 20), it can be calculated that the plume can only expand outward 33 degrees in addition to the 20 degree half angle or 53 degrees total. This indicates that, even if no turning of the flow downstream were to occur, the plume would impinge the diffuser wall 15 inches aft of the inlet.

Similar calculations for the smaller 36-inch diffuser show that the flow still impinges 4 inches aft of the inlet. This indicates that no diffuser extension section is necessary for operation in the retracted position.

In conclusion, on the basis of available information, it appears that the combination of the extendable nozzle assembly and either the 36-inch or 77-inch diffuser will operate satisfactorily.

W. H. Baker, Jr.

W. H. Baker, Jr.
Advanced Development
Engine Components Department

10

Report 10484-FR, Volume 1, Appendix C

AGCS 1900-8 (REV 5/69) GBF

TEST EQUIPMENT SKETCH

PAGE 1 OF 3 PAGES

AEROJET-GENERAL CORPORATION SACRAMENTO • CALIFORNIA	DRAWN	ENGINEER	TEO/WO	TEST EQUIPMENT SKETCH OR CALCULATION NUMBER
	CHECKED	APPROVED	DATE 21 APR 70	
			TEST AREA APPROVED	

DESCENT DIFFUSER

$\frac{A}{A_*} = 242.5$

$N_2O_4/460$ MR = 1.6 $\dot{w}$ = 11.3

$$\frac{1}{\phi} = \frac{77^2 - 44.5^2}{77^2} = \frac{3948.75}{5924} = \frac{1}{1.501}$$

ϕ = 1.89 MAX

$$\frac{A_2}{A_*} = \frac{242.5}{1.50} = 161.$$

@ 70 PSIA P_{DISCH} = 0.64 PSIA

@ 100 psia $P_{disch.}$ = 0.91 PSIA

air load = 4.4 LB air/LB prop

49.7 LB/SEC DAE OR

178,920 LB/HR

97,900 LB/HR SCALED TO J-2

(1.83 "H_2 = 0.90 PSIA)

WSTF CHART SAYS ~0.75 PSIA (SEEMS OK)

INCET PRESSURE $\frac{10}{7}(0.01525) = 0.02178$ PSIA

= 0.001482 ATM = 1.482×10^{-3}

Page 4

147,500 ~~ft~~ alt simulation

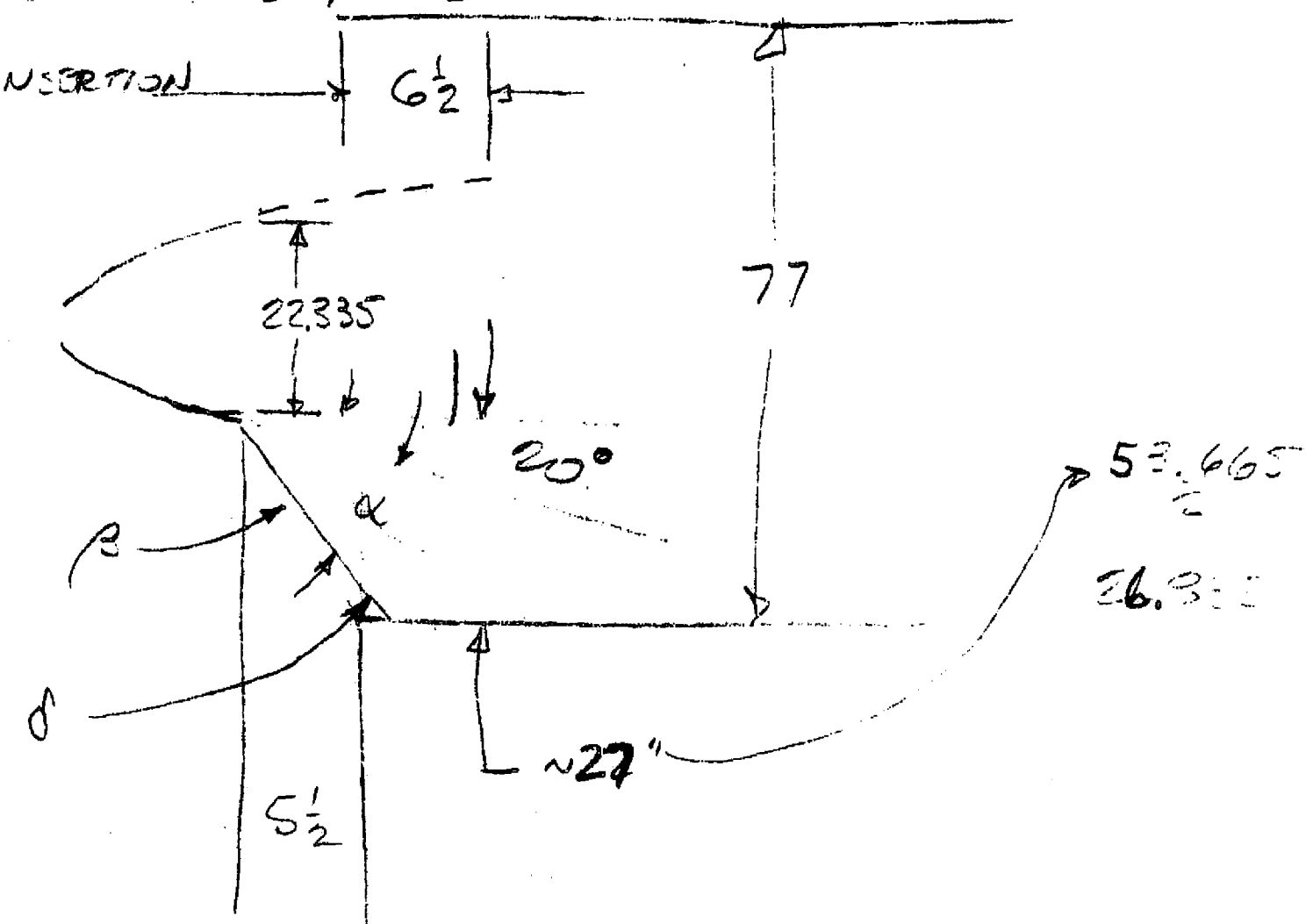
WSTF CHART SAYS 142 - 165 ~~ft~~ (agree)

AGCS 1900-8 (REV 5/69) GBF

TEST EQUIPMENT SKETCH

AEROJET-GENERAL CORPORATION SACRAMENTO • CALIFORNIA	DRAWN	ENGINEER	TEO/WO	TEST EQUIPMENT SKETCH OR CALCULATION NUMBER
	CHECKED	APPROVED	DATE	
			TEST AREA APPROVED	

DESCENT DIFFUSER



$\tan\beta = \frac{26.832}{5.5} = \frac{4.87}{3.969} \simeq \frac{78.4°}{75.9°}$

$\frac{A_{NE}}{A_*} = 20.00 \quad \nu = 82°$

$\frac{A_{IN}}{A_*} = 242.5 \quad \nu = 115°$

$\Delta\nu = 33° = \alpha$

$\delta = \alpha + 20° = 33 + 20 = 53° < 78.4$

OK

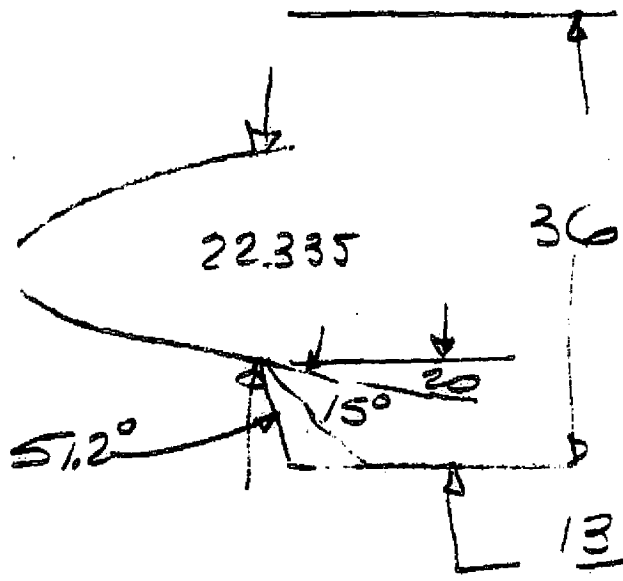
AGCS 1900-8 (REV 5/69) GBF

TEST EQUIPMENT SKETCH

AEROJET-GENERAL CORPORATION SACRAMENTO • CALIFORNIA	DRAWN	ENGINEER	TEO/WO	TEST EQUIPMENT SKETCH OR CALCULATION NUMBER
	CHECKED	APPROVED	DATE	
			TEST AREA APPROVED	

ASCENT DIFFUSER

Assume Spike 6 1/2 reused



$$\frac{13.665}{2} = 6.835$$

$$\tan\beta = \frac{6.835}{5.5} = 1.243 = 51.2°$$

$$\frac{A_{NE}}{A^*} = 20.00 \quad \nu = 82°$$

$$\frac{A_N}{A^*} = \left(\frac{36.00}{4.044}\right)^2 \cong 53.0 \quad \nu = 97°$$

$$\alpha = \Delta\nu = 15°$$

$$\delta = 20° + \Delta\nu$$

$$= 20 + 15 = 35°$$

$$< 51.2°$$

OK

APPENDIX D

FILM COOLANT INJECTOR DESIGN CALCULATIONS

FILM COOLANT INJECTOR DESIGN CALCULATIONS

The purpose of the film coolant injector for the extendable nozzle test engine is to inject cooling nitrogen supersonically into the flow attach region at the fixed-movable nozzle joint. It was to be an integral part of the adapter section and meet the following desired requirements:

(a) Capable of supersonic injection.

(b) Integral with removable step rings in adapter tip.

(c) Provide slightly different injection velocity at each step for the same manifold pressure.

(d) Provide nitrogen mass flows from 0.1 to 0.5 lb/sec.

(e) Provide uniform peripheral nitrogen flow around injector diameter. (Groove width to be at least two times web width if discrete nozzles are used.)

A sixth requirement is that the exit pressure of the nitrogen from the groove be equal to or greater than the static pressure of the exhuast gas in the nozzle at the point of injection. It was also decided to inject aft parallel to the nozzle centerline.

Initially, an annulus was considered that would give the full peripheral coverage desired. Preliminary calculations, however, showed that the distribution could not be guaranteed to be evenly distributed simply based on machining and concentricity tolerances. It was therefore decided to make the injector of a number of discrete supersonic nozzles or grooves, satisfying the conditions listed above.

Several different numbers of grooves were investigated from 120 to 240. One hundred eighty grooves were decided upon as best satisfying the above conditions, having physical dimensions that could be more easily machined and still not representing too large a number to machine.

The following represents the design calculations for the grooves as finally decided upon:

1. Known or assumed information for nitrogen, γ = 1.4 MW = 28

   min manifold pressure = P_T = 5 psia

   manifold temp = T_T = 530°R.

   Highest main nozzle pressure in region equal 1.14 psia, therefore, assume groove exit pressure no lower than 1.2 psia or $\frac{P \text{ exit}}{P_T} \times P_T = 1.2$.

   $\dot{W}_{min}$ = .1 lb/sec at P_T = 5 psia

   (Very low total pressures were considered since high pressures made the grooves entirely too small for accurate machining.)

   $\frac{\text{Groove Width}}{\text{Web Width}} \doteq 2/1$ with web width approximately 1/8".

2. Calculations

   a. $R_{NIT} = \frac{R}{MW} = \frac{1545}{28} = 55.3 \ \frac{\text{ft} \cdot \text{lb-f}}{\text{lb-m} \ °R}$

   b. $\dot{w} = \frac{P^* A^*}{\sqrt{\frac{R \times T^*}{\gamma g}}} = \frac{P_T \times \frac{P^*}{P_T} A^*}{\sqrt{\frac{R \times T^*/T_T \times T_T}{\gamma g}}}$

   at M = 1 P^*/P_T = .634 T^*/T_T = .833
   γ = 1.4

   $\dot{w} = \frac{P_T \times .634 \ A^*}{\sqrt{\frac{55.3 \times 530 \times .833}{1.4 \times 32.2}}} = .0272 \ P_T \ A^* \text{ lb/sec}$

   c. For P_T of 5 psia and $\dot{w}$ of .1 lb/sec, then

   $A^* = \frac{\dot{w}}{.0272 \ P_T} = \frac{.1}{.0272 \times 5} = .735 \text{ in.}^2$

   or total throat area of all grooves - .735 in.^2

   d. For P_{EX} = 1.2 psia at $\dot{w}$ = .1 lb/sec and P_T = 5 psia

   $\frac{P_{EXIT}}{P_T} = \frac{1.2}{5} = .24$

   For γ = 1.4 and P_{EXIT}/P_T = .24

   $M_{EXIT} = 1.585 \quad \frac{A_{EXIT}}{A^*} = 1.239$

and $\frac{V}{C^*} = 1.4175 = \frac{\text{Local Vel}}{\text{Vel of Sound at Throat}}$

e. Area Exit = $\frac{A_{EXIT}}{A^*} \times A^* = 1.239 \times .735 = .910$ in.^{2}

or total exit area of all grooves = .910 in.^{2}

f. Assume constant groove depth of .020 in.

Assume mean groove diameter of 22.315 in. or a circumference of 71 in.

g. For 180 grooves, the width of 1 groove + 1 web on that circumference

$= \frac{\text{circumference}}{N} = \frac{71}{180} = .3945$ in.

h. For a 2:1 slot to web ratio the web width

$= \frac{.3945}{3} = .1315$ in.

and the groove width = .1315 x 2 = .263 in.

i. For final dimensions use Depth = .019 inches.

j. Exit groove width = $\frac{A_{EXIT}}{.019 \times 180} = .266$ in.

k. Web width final for final design mean dia of 22.086 in

$= \frac{\text{Dia} \times \pi - N \times \text{Groove Width}}{N}$

$= \frac{22.086 \times \pi - 180 \times .266}{180} = .120$ in.

l. Throat width = $\frac{A^*}{\text{Depth} \times N} = \frac{.735}{.019 \times 180} = .215$ in.

m. C* = vel of sound at throat

$$= \sqrt{\gamma R T_T \times \left(\frac{T^*}{T_T}\right) g}$$

= 1050 ft/sec

$V_{exit} = C^* \times \frac{V}{C^*} = 1050 \times 1.4175 = 1485$ ft/sec.

Other calculations were made to determine the exit conditions as the removable tips were removed. All pertinent data is given in the following table and the injector configuration is shown in Figure G1.

CHAMBER NOZZLE AND COOLANT INJECTOR DATA

CHAMBER NOZZLE DATA

Step height, in.	0.25	0.50	0.75
Nozzle radius at tip, in.	10.90	10.66	10.42
Nozzle Area ratio	19.4:1	18.6:1	17.8:1
Nozzle wall pressure, psia	1.04	1.09	1.14
Nozzle Mach number	3.548	3.521	3.493

COOLANT RING INJECTION GROOVE DATA

Number of grooves	180			
*Groove depth, in.	0.019			
Groove exit width, in.		0.266	0.248	0.229
*Groove throat width, in.	0.215			
Area ratio		1.238	1.153	1.065
Mach number		1.585	1.465	1.300
Velocity, exit, ft/sec		1485	1410	1251
Exit pressure for 5 psia and $\dot{w}$ - 0.1 lb/sec		1.20	1.435	1.752

*At 5 psia, groove dimensional tolerances of ±0.001 can produce mass flows of 0.0944 to 0.1055 lb/sec and exit pressures at 0.25 in. step height of 0.94 to 1.635 psia.

APPENDIX E

ACTUATOR ANALYSIS

Report 10484-FR, Volume 1, Appendix E

EXTENDABLE NOZZLE

Preliminary analysis of actuator loads and action times and velocities.

1. All calculations based on the following input:
   a. Actuation, 3 ea flairline F-1-1/8-12 HC air/oil cylinders.
   b. Fluid used, any acceptable hydraulic fluid.
   c. Working System Pressure, 175 psi.
   d. Aerodynamic load on nozzle tending to retract.
   e. Weight of moving parts, 163.91 lbs.
   f. No system losses or orificing assumed in analysis.
   g. Nozzle fired vertically down.
2. Summation of forces, nozzle firing down.
   a. Actuator forces available.
      Retract piston area = $3\ (1.25^2 - .5^2)\ .785 - 3.09\ in.^2$
      Retract force available = $3.09\ in.^2 \times 175\ psi = 538\ lbs$
      Extend piston area = $3\ (1.25^2) \times .785 = 3.66\ in.^2$
      Extend force available = $3.66\ in.^2 \times 175\ psi = 640\ lbs$
   b. Dead weight reacting force = 163.91 lbs down or in extend direction.
   c. Aerodynamic force of exhaust gas.
      Projected area of exit cone = $(D_1^2 - D_2^2)\ .785 \doteq (30^2 - 22^2)\ .785 = (415)\ .785 = 325\ in.^2$.
      Assume that during translation, until seal is broken, full 1.2 psia at ε = 20:1 could act on area.
      Areo Force = $325 \times 1.2 \doteq 400$ lbs constant.
   d. Summation of Forces
      Total force = available force + dead weight + aero force
      Total force retract = 538 - 163.91 + 400 = 774 lbs
      Total force extend = 640 + 163.91 - 400 = 404 lbs

      Note: If aero forces were neglected entirely, total force extend and retract would be 374 and 803 lbs respectively or approximately equal and opposite to those above for purposes of analysis.
3. Resulting Accelerations
   a. Mass of moving wt = $\frac{wt}{g} = \frac{163.91}{32.2} = 5.1$ slugs
   b. $Acc._{retract} = \frac{Force\ Ret}{Mass} = \frac{774}{5.1} = 15.2\ ft/sec^2$
   c. $Acc._{ext} = \frac{404}{5.1} = 7.8\ ft/sec^2$

4. Actuation Times

a. S = distance traveled = 12 in. = 1 ft.

b. $S = 1/2\ \alpha t^2 + V_{int}t \quad (V_{in}t = 0)$

$S = 1/2\ \alpha t^2$

$t = \sqrt{\frac{2}{\alpha}}$

$t_{retract} = \sqrt{\frac{2}{15.2}} = 0.363$ sec

$t_{extend} = \sqrt{\frac{2}{7.8}} = 0.506$ sec

5. Resulting velocities

a. Vel near end of stroke

$V_{ret} = \alpha t = 15.2 \times .363 = 5.5$ ft/sec = 66 in/sec

$V_{ext} = 7.8 \times .506 = 3.95$ ft/sec = 47.5 in/sec

b. Average velocities

$V_{ret\ ave} = S/t = \frac{12}{.363} = 33$ in/sec

$V_{ext\ ave} = \frac{12}{.506} = 23.8$ in/sec

6. Minimum flow requirement to satisfy even 23.8 in/sec = V x Piston Area

= 23.8 x 3.66 = 87 in^3/sec

= 22.5 gpm

This is obviously a flow rate that we cannot meet.

7. Actual required flows and losses.

a. If we desire to move at 6 in/sec Vel = 6 in/sec x 3.66 = 22 in^3/sec

= 5.7 gal/min

b. In a 1/2" line of .622 ID and .324 area this amounts to a flow vel of $\frac{22}{.324 \times 12} \doteq 5$ ft/sec

From Parker-Hannifin Hydraulic Cylinder book Page 29, this amounts to a pressure loss per ft of .24 lbs for 100 ft of lines, this would be a loss of 25 lbs of working pressure at the cylinder = 150 psi.

c. For 3 cyl having 1/8 npt fittings, the total flow area = .0825 $in.^2$.

5.7 gallons/min = 22 in^3/sec

for hyd fluid, ρ = .0312

22 in^3/sec = .69 lb/sec

7.c. (cont.)

For standard flow

$$\dot{w} = C_D\ A\ \sqrt{2g\rho\Delta P}$$

$$\sqrt{2g\rho\Delta P} = \frac{\dot{w}}{C_D A}$$

$$\Delta P = \frac{\left(\frac{\dot{w}}{C_D A}\right)^2}{2g\rho}$$

Given $A = 0.825$ in.^{2} $\rho = .0312$ lb/in.^{3} $g = 388$ in/sec^2

$\dot{w} = .69$ lb/sec and assume $C_D = .6$

Then $\Delta P = \frac{\left(\frac{.69}{.6 \times .0825}\right)^2}{2 \times 388 \times .0312} = \frac{196}{24} = 8.1$ psi

8. Assume working pressure of system - line loss - orifice loss
= 175 - 25 - 8 = 142 psi
Then repeating all steps of 2 thru 5 above, we get for extending valves.

2'.a Extend force available = 3.66 x 142 - 520 lbs

2'.d Total force exit = 520 + 163.91 - 400 = 284 lbs

3'.c Acc ext = $\frac{284}{5.1}$ = 5.6 ft/sec^2

4'.b $t_{ext} = \sqrt{\frac{2}{5.6}}$ = .598 sec

5'.a V_{ext} = 5.6 x .598 = 3.35 ft/sec = 40 in/sec

5'.b Ave Vel ext = $\frac{12}{.598}$ = 20 in/sec

9. This indicates that system will have to be orificed down to obtain 6 in/sec and that pressure losses are not a governing factor.

10. G loads to stop
Actuators have cushions which act during approximately the last 1/2 in. of travel. Assuming velocity to be as high as 20 in/sec for a conservative analysis

20 in/sec = 200 ft/min

Assuming no aero force to help slow the nozzle in the extend mode, from Page 66 of the above referenced catalog the total load on the actuators, F

$= W_g + W$

where g for S = 1/2" and 100 ft/sec

= 1

10 (cont.)

then F = 164 + 164 = 328 lbs or 110 lbs/actuator

Report 10484-FR, Volume 1, Appendix F

STRUCTURAL ANALYSIS

OF

EXTENDABLE NOZZLE

TEST PROGRAM

April 1970

Prepared By:

R. A. Anderson
Engineering Supervisor
Structural Engineering Section

Approved By:

J. W. Starr, Supervisor
Technology Components
Structural Engineering Section
Engineering Operations

Report 10484-FR, Volume 1, Appendix F

APPENDIX F

THERMAL STRESS ANALYSIS

Report 10484-FR, Volume 1, Appendix F

TABLE OF CONTENTS

		Page
I.	Introduction	1
II.	Summary	2
III.	Margins of Safety	3
IV.	Criteria	4
V.	Method of Analysis	6
VI.	Results	6
	A. Nozzle Adapter Shell	7
	B. Exit Cone	7
	C. Support Structure	8
	D. Attachment Bolts	10
	E. Interface Ring	12
	F. Ball Bushings	12
	G. Propellant Coolant Tubes	15
	H. Engine Shutdown	16
VII.	References	17

LIST OF TABLES

No.	Title	Page
1	Extendible Nozzle Predicted Weights	18
2	Extendible Nozzle Thermal Gradients	19

LIST OF FIGURES

No.	Title	Page
1	Revised Geometry at Fwd Flange Interface	20
2	Static Wall Pressure Distribution	21
3	Extendible Nozzle Thermal Gradients	22
4	Extendible Nozzle Thermal Gradients at 8:1	23
5	Tensile Strength Properties CRES 347	24
6	Stress/Strain Relationship CRES 347	25
7	Coeff. of Thermal Expansion	26
8	Cyclic Life CRES 347	27
9	Finite Element Grid	28
10	Summary of Effective Stresses	29
11	Nozzle Fwd Flange eff. Strain Distribution	30

I. INTRODUCTION

An extendible nozzle design configuration was submitted by the thrust chamber design group for structural evaluation. The nozzle was designed to evaluate various concepts of partial and complete extension upon performance, seal configurations, etc.

The data supplied included a basic configuration drawing (SK 954-10 modified during analyses), pressure and thermal criteria and safety factor requirements.

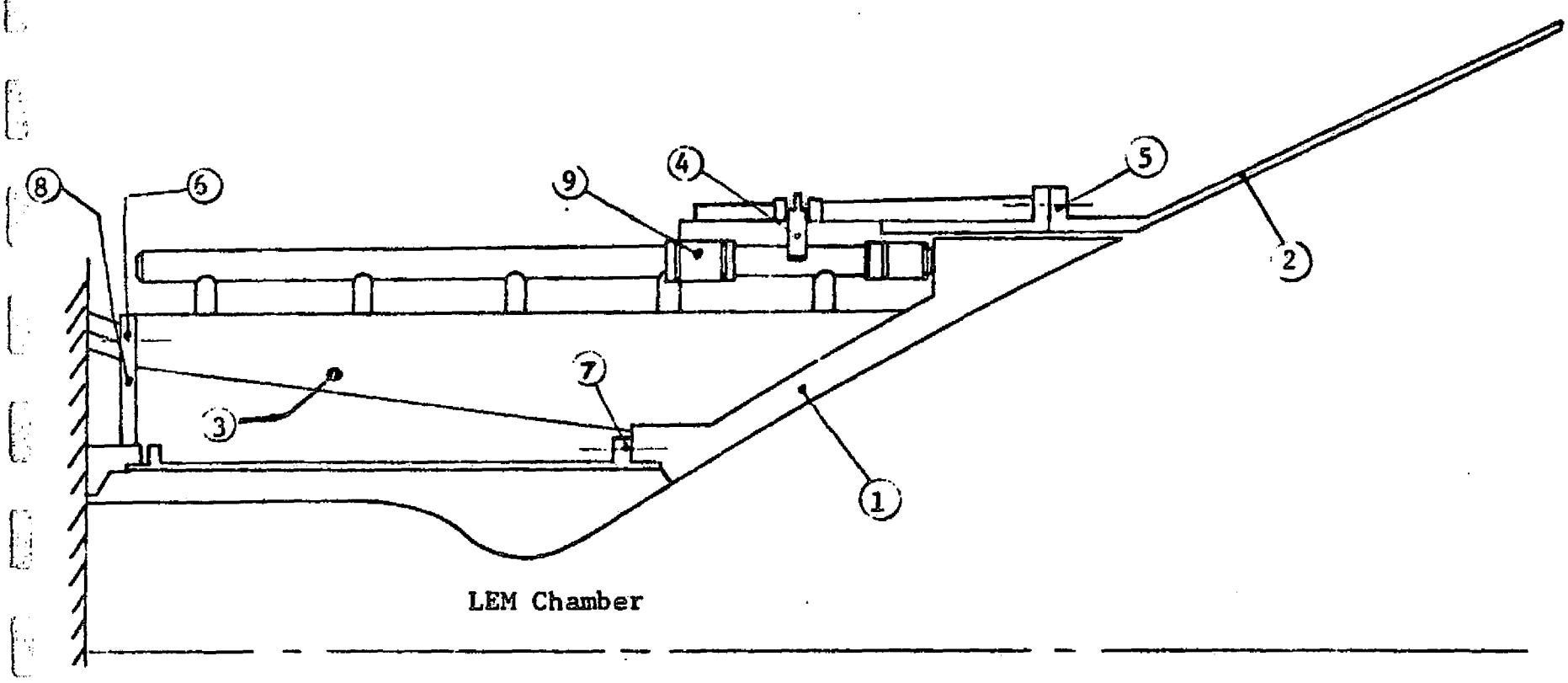
The purpose of the analysis was to identify any critical areas, establish structural adequacy, and provide a brief report of the results.

II. SUMMARY

The analysis of the nozzle was conducted in two phases. First a mechanical load evaluation and second a combined mechanical-thermal evaluation was performed. The mechanical load evaluation was conducted using conventional structural theory. The combined thermal mechanical solution was conducted on the basis of the finite element method of analysis. The time period chosen for evaluation was the maximum expected operating time of 15 seconds from an ambient temperature condition. Less firing time provides lower thermal gradients and reduced strains.

The pressure/thrust loads do not subject the nozzle itself to any significant stress levels. The major source of stresses are those thermally induced by the operating conditions. The largest strain level is near the forward flange where the CRES 347 chamber adjoins the LEM chamber. The design was modified after preliminary analyses revealed that very high stresses would be developed at this location. The modification consisted of extending the ablative chamber aft which resulted in a decrease in maximum temperatures and gradient. The maximum effective strain at the forward flange was determined to be 1.43% with an effective stress of 27,000 psi at 1200°F resulting in a margin of safety of +0.65. A separation between the CRES 347 nozzle and the ablative liner at this location is desirable to preclude local crushing of the silica liner. The condition is satisfied by the nominal .010 $\pm$ .010 tolerance provided by the drawings.

III. MARGINS OF SAFETY



EXTENDIBLE NOZZLE

	Component	Stress Mode	Applied Stress	Allowable	M.S.
(1)	Nozzle Adapter ~~Shell~~	Thermal-EH Stress	27,000	45,000 (ult)	+ .65
(2)	Exit Cone	Thermal-EH Stress Stability-Buckling	27,500 -	64,000 (ult)	+1.3 -
(3)	Support Structure	Compression	20,000	33,000 psi	+ .65
(4)	Shear Pins	Shear-Limit	17,000 psi	20,000 psi	+ .16
(5)	Bolts, Exit Cone	Vibr./Accel.	161 lbs/in	710 lbs/in	+4.4
(6)	Bolts, Support Struc.	Vibr./Accel.	1400 lb/bolt	14,000 lb/bolt	+9.0
(7)	Bolts, Comb. Chmbr.	Shear	1260 lb/bolt	3700 lbs/bolt	+2.0
(8)	Interface Ring	Bending	<22,500	>50,000 psi	+1.2
(9)	Ball Bushings	Compression	135 lbs (static)	162 lbs	+ .20

IV. CRITERIA

A. CONFIGURATION

The basic design configuration evaluated is given by Drawing SK 954-10. The revised geometry at the forward flange interface of the adapter to the LEM chamber is depicted on Figure 1. The predicted weight distribution and center of gravity of the nozzle assembly is given in Table 1.

B. LOADS

1. Pressure

a. A safety factor of 1.5 was applied to pressure values.

b. The nozzle static wall pressure distribution used in the analysis is given in Figure 2.

2. Thermal

a. A safety factor of 1.0 was applied to temperature values.

b. The maximum operating time considered was 15 seconds. It is planned that there shall be sufficient coast time between cycles that an ambient or near ambient condition shall be achieved before restart.

c. The gas-side and back-face temperature transient for various nozzle stations is given in Figures 3 and 4. These data are for both 15 second and 30 second firing durations. The maximum thermal gradients developed for the 15 second duration shown in Table 2.

3. Shock

a. The actuator mechanism shall have a damper such that shock loads shall be less than 100 g's.

b. The maximum dynamic load to be considered is 100 g's any direction.

C. MATERIAL PROPERTIES

The structural material used for the nozzle adapter shell, exit cone and support structure is CRES 347 stainless steel.

1. Allowable Strength (Reference 1)

a. Tension

Tensile ultimate, yield and elongation at elevated temperatures is given in Figure 5.

b. Compression Yield

F_{CY} = 54.2 ksi @ 70°F

= 38.2 ksi @ 1000°F

c. Shear

F_{SH} = 75.3 ksi @ 70°F

= 39.9 ksi @ 1000°F

2. Modulus of Elasticity (Reference 2)

The modulus of elasticity at elevated temperature is defined by the stress-strain relationships shown in Figure 6. The moduli used in the computer solution were the bilinear moduli approximating the secant moduli over a 4% strain range as shown.

3. Thermal Coefficient of Expansion (Reference 3)

The thermal coefficient of expansion is defined in Figure 7.

4. Cyclic Life (Reference 4)

The low cyclic fatigue capability of the material for total elastic and plastic strain at temperature is depicted in Figure 8.

V. METHOD OF ANALYSIS

The analysis of the support structure and bolted joints was conducted on the basis of conventional structural theory. The analysis of the nozzle adapter shell and exit cone under combined thermal and mechanical loads was conducted on the basis of a finite element technique of Reference 5. The method replaces the continuous structure with a system of elastic quadrilateral rings (elements) interconnected at a finite number of nodal points (joints). The equilibrium equations, in terms of unknown nodal point displacements, are developed at each nodal point with the solution of these equations being the solution to the system. In the procedure displacements, loads or stresses subjected to the structure are replaced by equivalent values acting at the nodal points of the finite-element system. Since each element may have separate mechanical properties and loading, multi-material or orthotropic nozzle structures of arbitrary geometry can be evaluated. The effects of finite length, curved boundaries, variable boundary end conditions, linear and nonlinear variation of modulus of elasticity and coefficient of thermal expansion with temperatures are completely accounted for in the solution.

The finite element representation of the nozzle structure as an assembly is shown in Figure 9.

VI. RESULTS

The pressure/thrust loads do not subject the nozzle assembly to any significant stress levels. The major source of stresses are those thermally induced by the operating conditions. A summary of the finite element analysis of the nozzle structure under combined thermal-mechanical loads is depicted in Figure 10. The time period chosen for evaluation was the maximum expected operating time of 15 seconds. Less firing time provides lower thermal gradients

and reduced strains. All firings were assumed to initiate from an ambient temperature condition. These data show the overall effective stress distribution and the local critical stresses and strains.

A. CHAMBER - NOZZLE ADAPTER

1. Thermal-Mechanical Stresses

The largest strain level is near the forward flange where the CRES 347 chamber adjoins the LEM chamber. The strain distribution at this location is given in Figure 11. The maximum effective strain was determined to be 1.43% with an effective stress of 27,000 psi at 1200°F. The results are:

$\epsilon = 1.43\%$	strain
$F_{ty} = 27{,}000$ psi	stress-applied
$F_{tu} = 45{,}000$ psi	stress-allowable ultimate @ 1200°F

The margin of safety is

$$M.S. = \frac{45}{27} - 1 = +.65$$

Cyclic life = 80 minimum (Figure 8)

2. Adapter-Chamber Separation

A gap between the CRES 347 nozzle and the ablative liner is desirable to preclude local crushing of the silica liner. Drawings provide for a nominal .010 separation with a tolerance of $\pm$.010. The gap is to be filled with RTV which should satisfactorily protect the liner.

B. EXIT CONE

1. Thermal-Mechanical Stresses

The largest strain on the exit cone is .0143 in/in which provides a minimum fatigue life of 80 cycles. This is an adequate margin

to the less than 12 cycles planned. The maximum effective stress is 27.5 ksi with an associated allowable stress of 64,000 psi.

$$M.S._{OH} = \frac{64}{27.5} + = +1.3$$

2. Stability

$$q_{cr} = \frac{EI\ Cos^3\alpha(n^2-1)}{a^3(1-r^2)}$$

n = node
α = cone angle
a = radius
r = Poisson's ratio

$$I = \frac{(1)(.20^3)}{12}$$

$$= .67 \times 10^{-3}$$

a = 15 in
n = 2
$E = 29 \times 10^6$
$\alpha = 23°$

$$q_{cr} = \frac{(29 \times 10^6)(.67 \times 10^{-3})(.78)(3)}{(3400)(.91)}$$

$$= 14.7 \text{ psi}$$

This should be sufficient against buckling due to uniform overpressure. Maximum transient pressure expected in nozzle is .50 psi at exit and 2.0 psi at 20:1 area ratio. No reasonable flow distribution (axisymmetrical) should conceivably cause buckling of the nozzle extension.

C. SUPPORT STRUCTURE

1. Stability

Three webs .625 in. thick approximately 1.5 in. wide and 14 in. long. Critical buckling allowable load about minor axis:

$$P_{cr} = \frac{\pi^2 EI}{(L')^2}$$

For fixed ended beam $L' = .5\ L$

$$P_{cr} = \frac{(\pi^2)(30 \times 10)^6 (.030)}{50}$$

$$= 180{,}000 \text{ lbs}$$

Web is not buckling critical

Max Compressive load allowable:

$$P_{compr} = 33{,}000 \text{ lb/web}$$

Applied load < 20,000 lb/web (assuming 100 g's axial load at full thrust)

Minimum M.S. $\frac{33}{20} - 1 = +.65$

2. Local Support Web Effect on Shell

The bending stress as calculated in the report is

$$f_b < 6.4\ p$$

for 100 psi chamber pressure

$$f_{by} < 6400 \text{ psi}$$

$$< 10000 \text{ psi for 1.5 safety factor}$$

Allowable stress > 20,000 psi

3. Shear Pins Extendible Nozzle

The extendible portion of the nozzle weights approximately 100 lb

Assuming a 100 g factor

3 pins 1/2" diameter each

Shear stress

$$f_s = \frac{\frac{10{,}000}{3}}{\frac{\pi\ .50^2}{4}} = \frac{(3300)(4)}{\pi(.50^2)} = 17{,}000 \text{ psi}$$

Shear stress allowable for a 300 series stainless is approximately 20,000 psi.

A close tolerance fit is necessary unless pin material is better than 300 series stainless.

$$M.S._y = \frac{20}{17} - 1 = +.16$$

D. ATTACHMENT BOLTS

1. Exit Cone to Slide Section

Considering lateral g' load upon minimum section maximum load location

Wt = 87 lbs

Accel = 100 g's

Maximum tension load upon one side or lbs/in neglecting any appreciable thrust during this transient condition.

$$P = \frac{M}{\pi R^2} = \frac{(87)(100)(7)}{(\pi)(11.0)^2} = 161 \text{ lbs/inch}$$

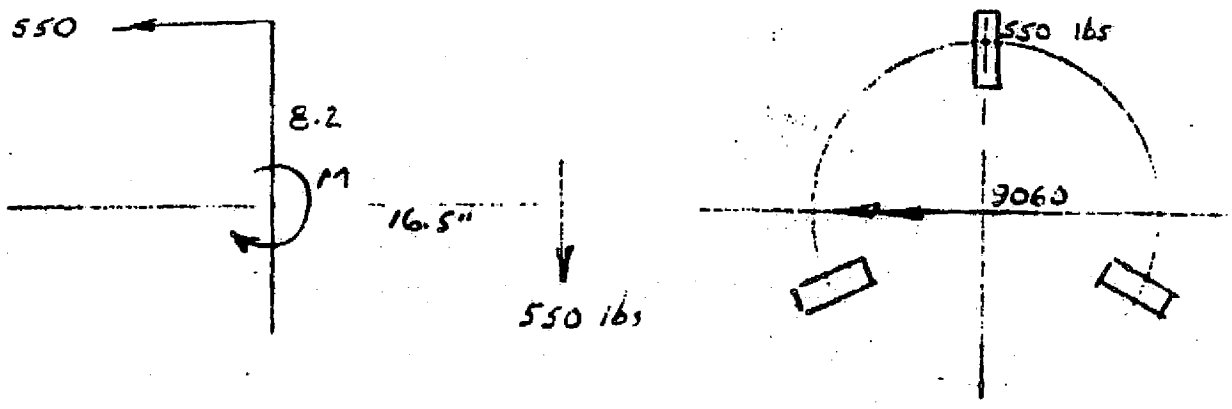
16 1/4" bolts would provide an allowable load

P = 710 lb/inch

$$\text{Min M.S.} = \frac{710}{161} - 1 + 4.4$$

2. Complete Nozzle to External Support Structure

Considering a 10 g factor for the entire chamber nozzle assembly and 16 1/2" dia bolts



Moment about attach point per a 10g factor would impose 5500 lbs maximum load.

Considering 16 bolts

$$P_b = \frac{2\pi\ (8.2)}{16}\ \frac{550 \times 10}{\pi 8.2^2}$$

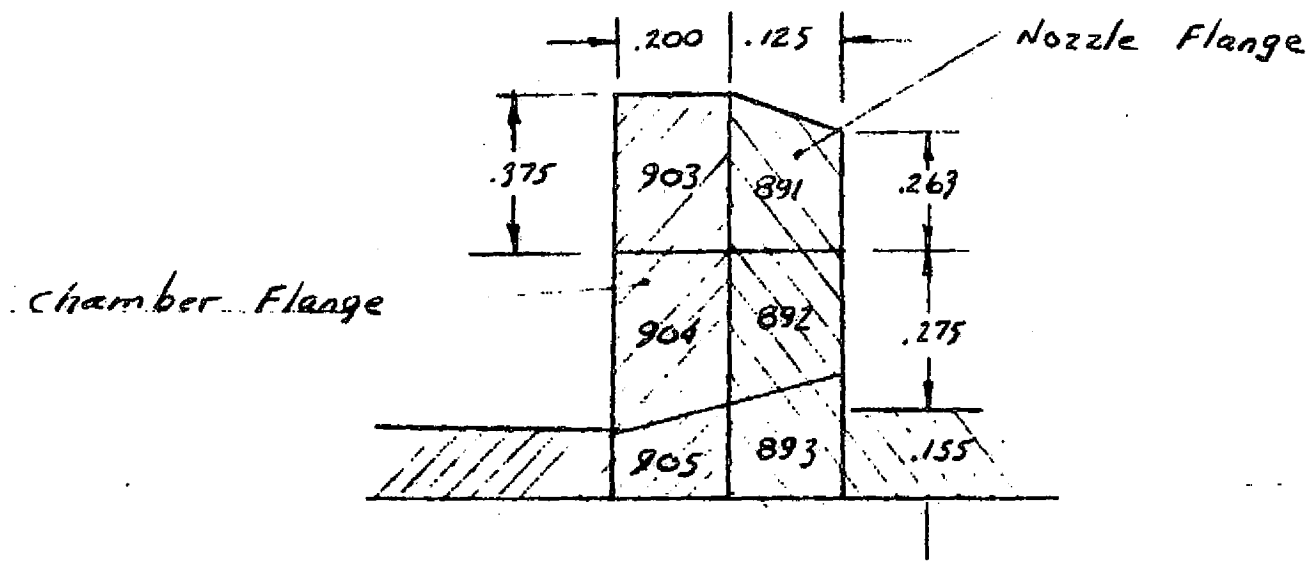
$$3.2\ (430) = 1400\ \text{lbs/bolt}$$

P_b = 14,200 lb/bolt yield allowable

M.S. = +9.0

3. Extendible Nozzle to Comb. Chamber

These bolts primarily react the shear between the two flange systems. The bolts are 1/4" and are 16 in total.



Element	Dimensions	Area	Stress (psi)		Load (lbs)		Σ	
			Rad.	Axial	Rad.	Axial	Rad.	Axial
891	≈.325 x .125	.041	-252	+8000	-	+330		
892	≈.275 x .125	.034	-3800	-4100	-130	-140	-330	+140
893	≈.24 x .125	.030	-6600	-1600	-200	-50		
903	≈.375 x .20	.047	+1950	+3700	+100	+170		
904	≈.275 x .20	.035	+4270	-1000	+150	-35	+300	-130
905	≈.155 x .20	.020	-2200	-14,000	-45	-280		

Bolt load requirements are negligible.

Max load is in shear = 330 + 300 = 630 lbs/inch

Considering 16 1/4" bolts on 5.22 in radius the load per bolt in shear is

$$P_s = 1260 \text{ lbs}$$

Allowable shear for An-4 bolts is 3700 lbs

$$M.S. = \frac{3700}{1260} - 1 = +2.0$$

(This load is thermally induced and therefore no S.F. required)

E. INTERFACE RING

A 5/8" thick ring welded to the three support webs is attached to a ground support ring of at least this equivalent thickness by 16 1/2" bolts. Assuming ground support columns are located inbetween nozzle columns (120° between supports) the bending stress

$$f_b = 22{,}500 \text{ psi}$$

Allowable $F_{by} > 50{,}000$ psi

$$M.S. > +1.2$$

F. BALL BUSHINGS

1. Thompson Ball Bushings OPN-122026

This is a 4 ball circuit with a rated load capacity of:

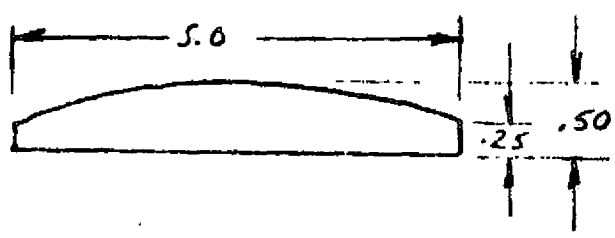
static	162 lbs
rolling	109 lbs

The adapter is supplied with three sets of these roller assemblies located 120° apart.

The axial load is reacted partially by a couple of which one of each double set reacts a compressive load.

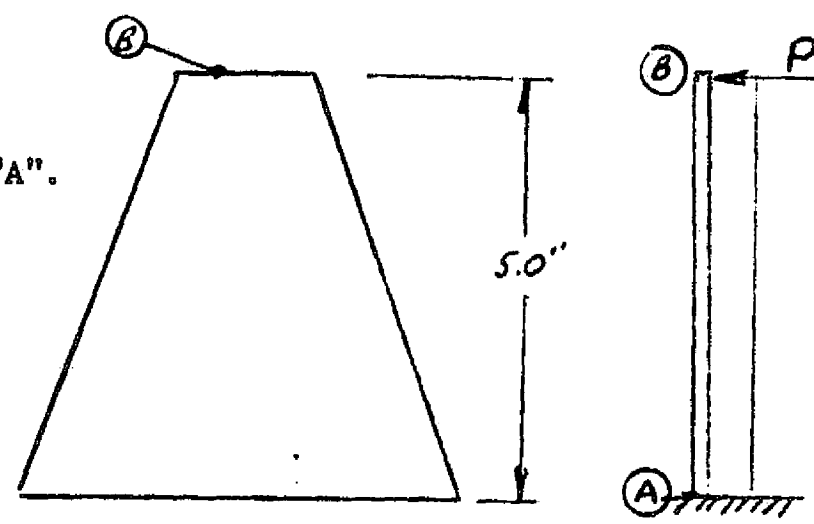
The normal load upon the bearing is approximately one lb due to operating pressures.

At 15 seconds of operating time the thermal expansion increases the load in the bearings to the following



Considering deflection of "B" where ball bushing is located as relative to position "A".

$$\Delta_B = \frac{PL^3}{3EI}$$



Conservatively

Assume t = .50 in

Width = 5.0 in.

for minimum deflection

$$K = \frac{P}{\Delta} = \frac{3EI}{L^3} = \frac{3(30 \times 10^6)(.052)}{125}$$

$$I = \frac{5 \times .5^3}{12} = .052 \text{ in}^4$$

$$= 37.50 \times 10^3$$

$$= 37{,}000 \text{ lbs/inch}$$

Radial deflection of the chamber (not including reaction of beam) would be

$$\Delta R_A = R \alpha \Delta T$$

$$< (7.0)(10 \times 10^{-6})(600)$$ Where bulk temp is less than 600°F

$$< .0420 \text{ in}$$

Considering deflection radially at B

$$\Delta R_A = (11)(9.5 \times 10^{-6})(300)$$

$$= .0310$$

differential radial expansion

$$\Delta_R = \Delta R_B - \Delta R_A$$

$$= .042 - .031 = .011 \text{ to be resisted}$$

by beam supporting ball bushings

$$P = (.011)(37000) = 400 \text{ lbs}$$

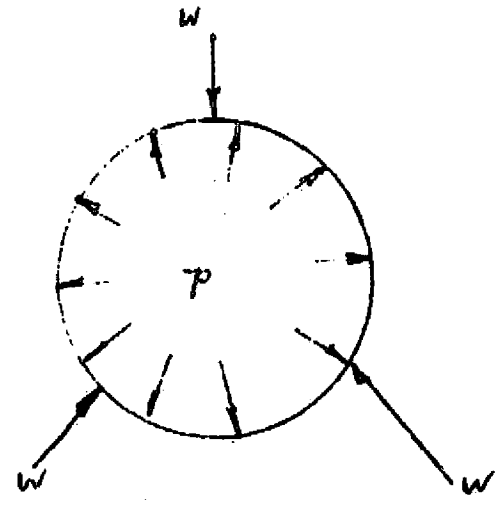
Considering effect of beam web

t = .625

W = 3.0 in

L = 15 in

= .056



$$\Delta_{A,B,C} = \frac{.875\ pR^2}{tE} \quad \frac{.137\ R^3}{2EI}$$

Stiffness of beam

$$K = \frac{12EI}{L^3}$$

$$I_{max} = \frac{(.625)(3.0^3)}{12} = 1.4$$

$$I \text{ are } \frac{(.625)(2.5^3)}{12} = .80$$

$$L = 15 \text{ in}$$

Considering the beam does not rotate where it is attached to shell

$$K = \frac{(12)(30 \times 10^6)(.80)}{(15)^3}$$

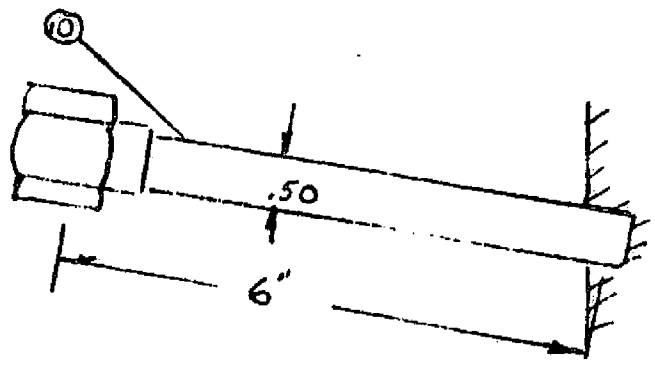
$$= 84{,}000 \text{ lbs/in}$$

The stiffness of the beam is approximately twice that of the rod bushing support. The resulting axial load upon the bushing therefore is

$$P_b = 1/3\ (400) = 135 \text{ lbs}$$

Considering the conservatism of the analysis the ball bushings should be satisfactory for static loads. However the nozzle should not be deployed after more than approximately 7-10 seconds of firing.

G. PROPELLANT COOLANT TUBES



Minimum t = .049

OD = .50

Some support should be provided to any long length of piping connected to this inlet.

Pressure induced stresses are negligible

No thermal stresses

Lateral loads that can be withstood

$$W = \frac{f_b(Z)}{L}$$

Z = section modulus = .007 in^3

$f_b > 35{,}000$ lb/in^2

L = 6 in

$$= \frac{(35000)(.007)}{6} = 41.0 \text{ lbs}$$

for a 100 g requirement

$W < 1/2$ lb

Lateral stability should be provided for attaching piping unless length is decreased to approximately 2 inches from present 6. Increasing the tube thickness is not a solution.

H. ENGINE SHUTDOWN

1. Thermal Loads

The only areas subject to larger stresses at ending shutdown would be where the bulk temperature would provide greater deflections than the operating, high gradient condition.

The maximum uniform temperature would be less than 500°F per the heat transfer evaluation. As no restart is to be attempted until the part has been cooled, no temperatures greater than those considered will exist.

VII. REFERENCES

1. AGC Materials and Fabrication Data Sheets, No. 3.2.2, dated 21 September 1965

2. Air Weapons Handbook, ARDC-TR-59-66, Ferrous Alloys, page 5 of 8

3. Solid Engine Design Handbook, Mechanical, Physical Thermal Properties, AISI 347 Stainless Steel, August 1957

4. Simplified Thermal Fatigue Analyses for Liquid Rocket Combustion Chambers, AIAA Journal of Spacecraft, January 1967, page 128

5. Campbell, D. M., "Finite Element Stress Analysis Computer Program for Axisymmetrical Bodies of Revolution and Plane Structures Applicable to Compressible Solids with Non-Linear Material Properties, dated 5 March 1970

TABLE 1

EXTENDIBLE NOZZLE PREDICTED WEIGHTS

Component/Item	Weight lbs.	Moment About Nozzle Attach Point in. lb
Engine		
Chamber	20.00	124.30
Chamber Liner	27.29	182.90
Injector/Valves (est.)	20.00	-60.00
Subtotal	67.29	240.20
Adapter		
Attach flange and main body	263.45	5,002.86
Gussets, brackets, misc. hdwe.	28.76	254.32
Rails and supports	12.00	120.00
Actuators	15.00	0.00
Subtotal	319.21	5,377.18
Slide Section	76.26	1,801.15
Exit Cone	87.65	2,641.28
Total	550.41 lbs	9,059.81 in. lb

Predicted CG 16.5 in. aft of flange

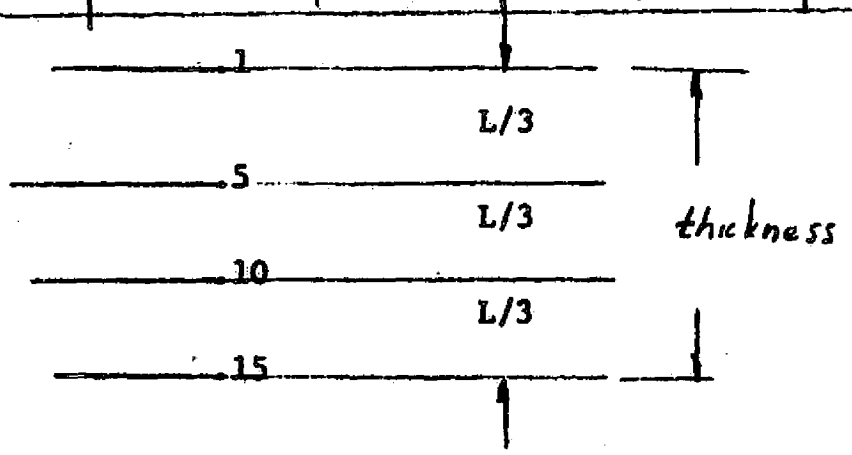
Total predicted wt moved by actuators = 163.91 lbs

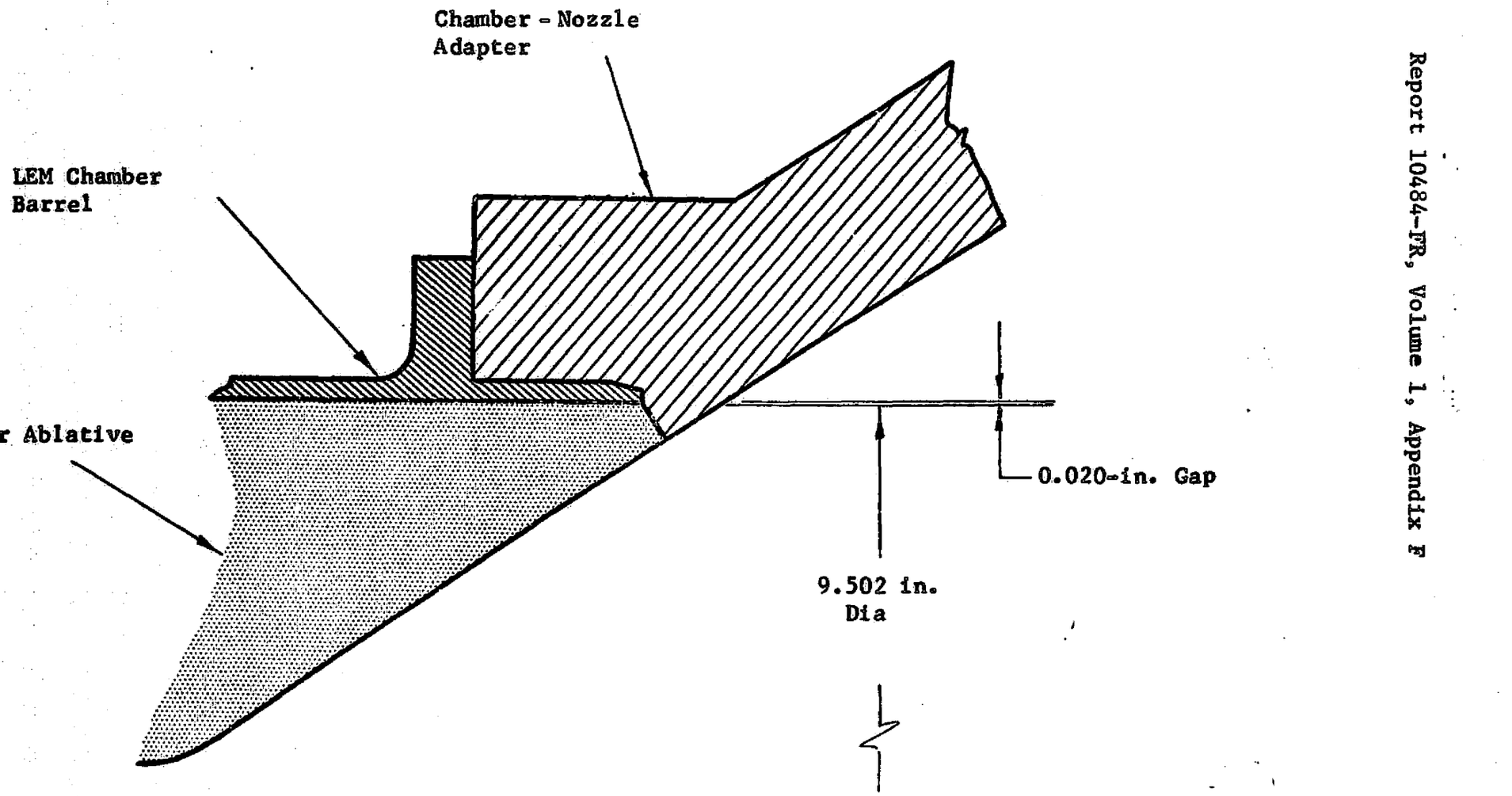
TABLE 2

THERMAL GRADIENTS

EXTENDIBLE NOZZLE

Nozzle Location	Wall Thick.	Duration	Node 1	5	10	15
2.4:1	2.0	15 sec	1306	253	72	70
8:1	.73	15	765	454	215	143
Seal Req.						
12.33:1	2.5 in	15	188	147	117	107
20:1	.125	15	808	785	767	761
	.200	15	644	601	567	555
	.250	15	538	479	433	418





Revised Geometry at Forward Flange Interface
of Adapter to LEM Chamber

Figure 1

G. HURR
26 FEB 70

RETRACTIBLE - EXTENDIBLE NOZZLE PROGRAM

R_t = 2.472 IN.
DRAD = .704 IN.
URAD = 3.522 IN.
γ = 1.24
P_c = 120 PSIA.
T_c = 5506 °R
R_g = 73.0 ft/°R

RAO NOZZLE TO ϵ = 20
CONICAL FROM ϵ = 20 TO 40

		X (in)	R (in)	M	θ (°)	P_w (psia)	T (°R)	∫PdA	ρ (lb/ft³)	V (fps)	ρV	(ρV)^.8	Drag (lb.)
TANGENCY →	33	0.2990	2.5870	2.2150	33.0000	19.96	3464.66	0.0	5.2390E-03	7.0390 03	4.3720 01	2.0615 01	2.6870 00
	34	0.9230	2.6470	2.3150	34.2000	9.22	3151.01	101.0	5.4100E-03	7.2320 03	3.9220 01	1.8850 01	4.8380 00
	35	1.6350	2.7220	2.4053	34.6000	7.04	3055.33	160.1	4.9133E-03	7.3013 03	3.5577 01	1.7415 01	6.9970 00
	36	1.9470	2.6530	2.4700	34.6000	6.01	3166.14	217.2	4.3940E-03	7.5315 03	3.2419 01	1.6160 01	9.0620 00
	37	2.4604	2.8070	2.5520	34.6000	5.32	3290.56	272.5	3.8781E-03	7.6580 03	2.9659 01	1.5050 01	1.1070 01
	38	2.9200	2.8720	2.6220	34.6000	4.95	3316.03	326.4	3.5013E-03	7.7780 03	2.7225 01	1.4065 01	1.3070 01
	39	3.5050	2.9270	2.6916	34.6000	4.71	3343.72	380.1	3.1583E-03	7.8885 03	2.4919 01	1.3183 01	1.4770 01
	40	4.0820	2.9630	2.7506	34.8000	4.56	3354.18	433.0	2.8983E-03	7.9775 03	2.3115 01	1.2365 01	1.7720 01
	41	4.6570	3.0130	2.8150	34.8000	4.51	3334.08	485.0	2.6643E-03	8.0670 03	2.1493 01	1.1535 01	1.9650 01
	42	5.1950	3.0500	2.8721	34.8000	4.44	3326.21	536.1	2.4630E-03	8.1500 03	1.9983 01	1.0745 01	2.1550 01
	43	5.7140	3.1040	2.9304	34.8000	4.35	3317.05	586.3	2.2760E-03	8.2270 03	1.8643 01	1.0125 01	2.3430 01
	44	6.2960	3.1470	2.9971	34.8000	4.26	3269.17	635.5	2.1010E-03	8.2980 03	1.7445 01	9.5440 00	2.5300 01
	45	6.8800	3.1980	3.0650	34.8000	4.18	3242.39	683.8	1.9533E-03	8.3660 03	1.6350 01	8.9370 00	2.7160 01
	46	7.4990	3.2360	3.1356	34.8000	4.10	3219.75	731.3	1.8230E-03	8.4300 03	1.5370 01	8.4270 00	2.9010 01
	47	8.1200	3.2810	3.2033	34.8000	4.03	3197.54	778.0	1.7053E-03	8.4940 03	1.4475 01	8.0320 00	3.0850 01
	48	8.7560	3.3260	3.2794	34.8000	3.96	3178.34	824.0	1.5983E-03	8.5440 03	1.3650 01	7.6980 00	3.2680 01
	49	9.4035	3.3720	3.3517	34.8000	3.87	3160.46	869.5	1.4999E-03	8.5970 03	1.2900 01	7.3980 00	3.4505 01
	50	10.0660	3.4160	3.4256	34.8000	3.79	3144.44	914.4	1.4100E-03	8.6480 03	1.2190 01	7.1245 00	3.6325 01
	51	10.7445	3.4600	3.5020	34.8000	3.71	3129.19	958.8	1.3275E-03	8.6960 03	1.1550 01	7.0435 00	3.8136 01
	52	11.4370	3.5060	3.5792	34.8000	3.63	3114.38	1002.7	1.2540E-03	8.7420 03	1.0961 01	6.7320 00	3.9900 01
	53	12.1455	3.5520	3.6576	34.8000	3.60	3100.13	1046.2	1.1840E-03	8.7860 03	1.0400 01	6.5130 00	4.1680 01
	54	12.8690	3.5960	3.7415	34.8000	3.51	3087.46	1089.3	1.1230E-03	8.8270 03	9.9090 00	6.2935 00	4.3455 01
	55	13.6060	3.6420	3.8211	34.8000	3.48	3074.60	1132.0	1.0650E-03	8.8670 03	9.4420 00	6.0265 00	4.5210 01
	56	14.3580	3.6880	3.9025	34.8000	3.45	3062.52	1174.3	1.0110E-03	8.9050 03	9.0050 00	5.8005 00	4.6970 01
	57	15.1260	3.7340	3.9871	34.8000	3.42	3051.21	1216.3	9.6150E-04	8.9420 03	8.5980 00	5.6015 00	4.8720 01
	58	15.9145	3.7800	4.0754	34.8000	3.40	3040.73	1258.0	9.1600E-04	8.9760 03	8.2220 00	5.3950 00	5.0450 01
120	59	16.7171	3.8260	4.1675	34.8000	3.38	3031.06	1299.4	8.7405E-04	9.0090 03	7.8760 00	5.1870 00	5.2170 01
	60	17.5350	3.8720	4.2635	34.8000	3.36	3022.21	1340.5	8.3505E-04	9.0410 03	7.5490 00	4.9960 00	5.3870 01
	61	18.3700	3.9180	4.3636	34.8000	3.34	3014.17	1381.4	7.9880E-04	9.0710 03	7.2460 00	4.8360 00	5.5560 01
	62	19.2200	3.9640	4.4679	34.8000	3.33	3006.94	1422.0	7.6490E-04	9.1000 03	6.9590 00	4.6760 00	5.7240 01
	63	20.0860	4.0100	4.5767	34.8000	3.32	3000.52	1462.3	7.3320E-04	9.1280 03	6.6930 00	4.5260 00	5.8910 01
	64	20.9700	4.0560	4.6902	34.8000	3.31	2994.91	1502.4	7.0350E-04	9.1540 03	6.4410 00	4.3860 00	6.0570 01
	65	21.8700	4.1020	4.8086	34.8000	3.30	2990.11	1542.3	6.7560E-04	9.1790 03	6.2030 00	4.2560 00	6.2210 01
	66	22.7900	4.1480	4.9322	34.8000	3.29	2986.12	1582.0	6.4940E-04	9.2030 03	5.9780 00	4.1360 00	6.3840 01
	67	23.7300	4.1940	5.0613	34.8000	3.28	2982.94	1621.4	6.2480E-04	9.2260 03	5.7650 00	4.0260 00	6.5460 01
	68	24.6900	4.2400	5.1962	34.8000	3.27	2980.57	1660.7	6.0170E-04	9.2480 03	5.5630 00	3.9260 00	6.7070 01
	69	25.6700	4.2860	5.3373	34.8000	3.27	2979.01	1699.8	5.7990E-04	9.2680 03	5.3720 00	3.8360 00	6.8670 01
	70	26.6700	4.3320	5.4850	34.8000	3.26	2978.26	1738.7	5.5940E-04	9.2870 03	5.1920 00	3.7560 00	7.0260 01
	71	27.6900	4.3780	5.6396	34.8000	3.26	2978.32	1777.4	5.4010E-04	9.3050 03	5.0230 00	3.6860 00	7.1840 01
	72	28.7300	4.4240	5.8016	34.8000	3.26	2979.19	1816.0	5.2190E-04	9.3220 03	4.8650 00	3.6260 00	7.3410 01

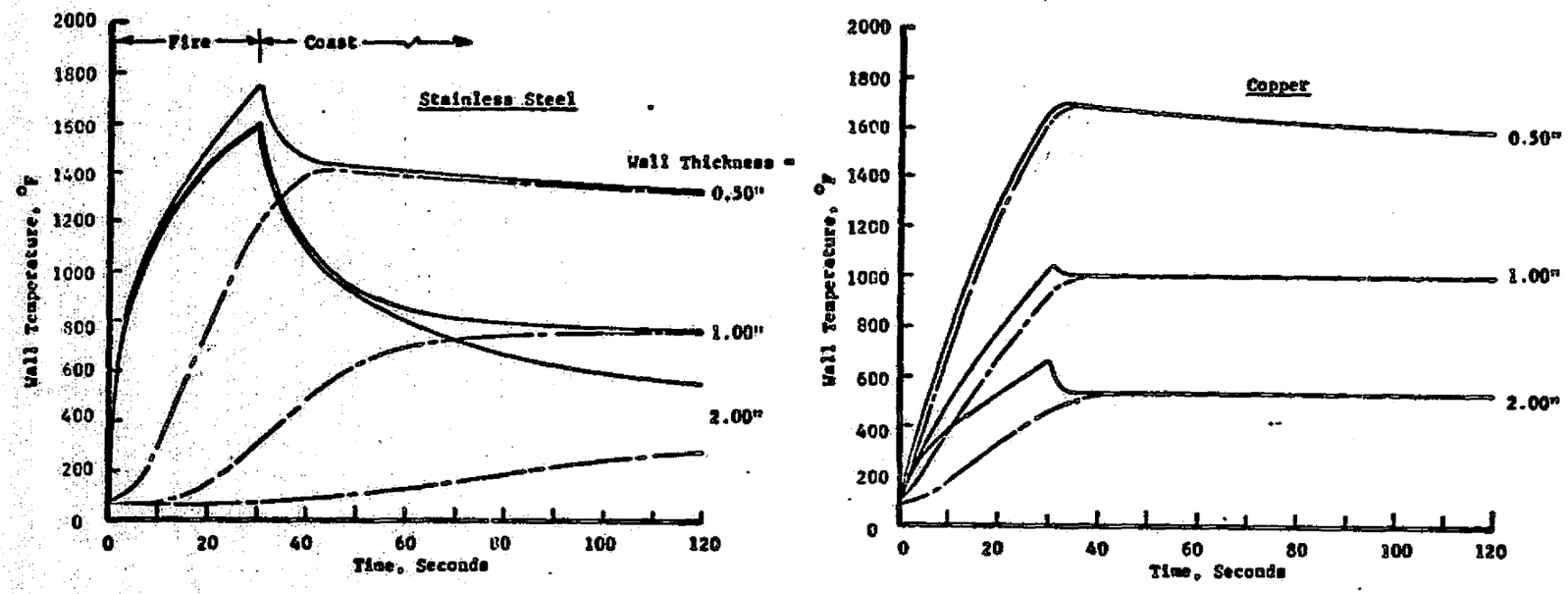
INTEGRATED TOTALS

WGT. FLOW (LBM/SEC)	MOMENTUM (LB)	THRUST (LB)	PRESSURE-AREA (LB)	MOMENTUM-DRAG (LB)	TOTAL THRUST (LB)	CFG. COEFF. (-)
14.374	1710.1	1113.9	0.0	1204.7	4054.7	0.96621

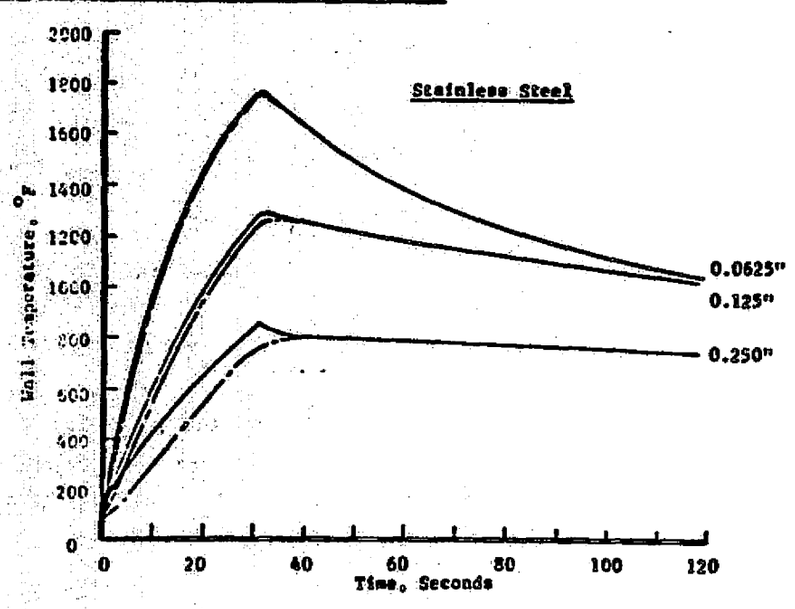
Static Wall Pressure Distribution

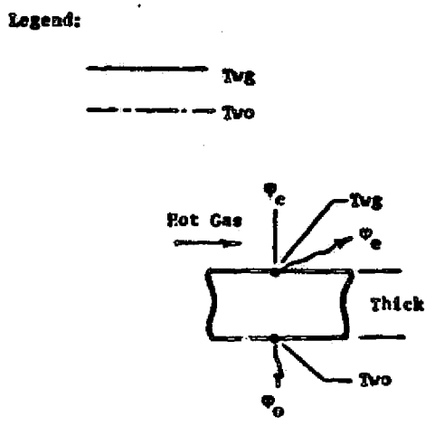
Figure 2

TRANSITION REGION MAXIMUM TEMPERATURES (ε = 2.4:1)



SKIRT REGION MAXIMUM TEMPERATURES (ε = 20:1)





Transition and Skirt Regions
Temperature Response During 30-sec Firing

Figure 3

Extendible Nozzle Wall Temperature Response At
Area Ratio 8:1 for a 30 Second Firing

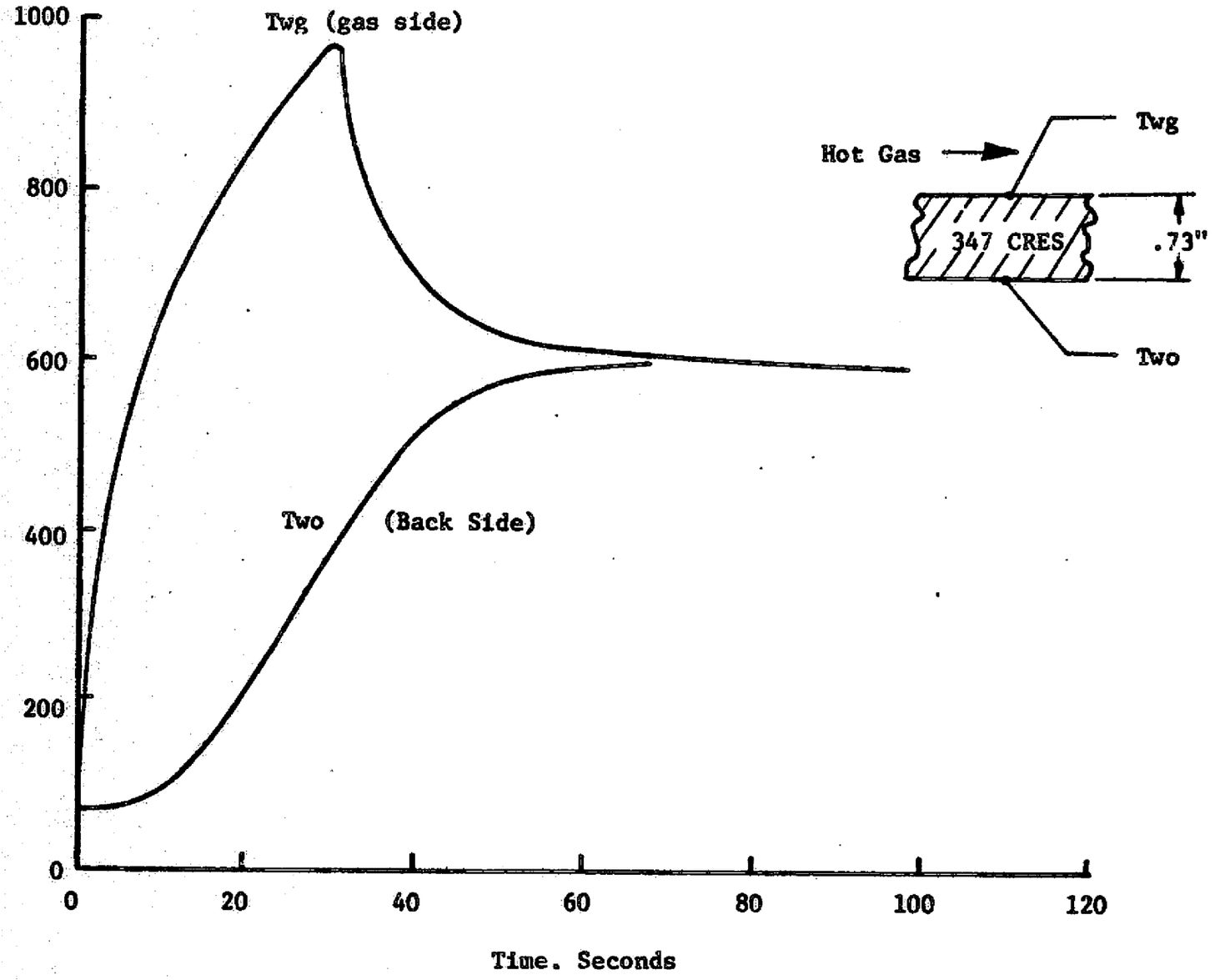


Figure 4

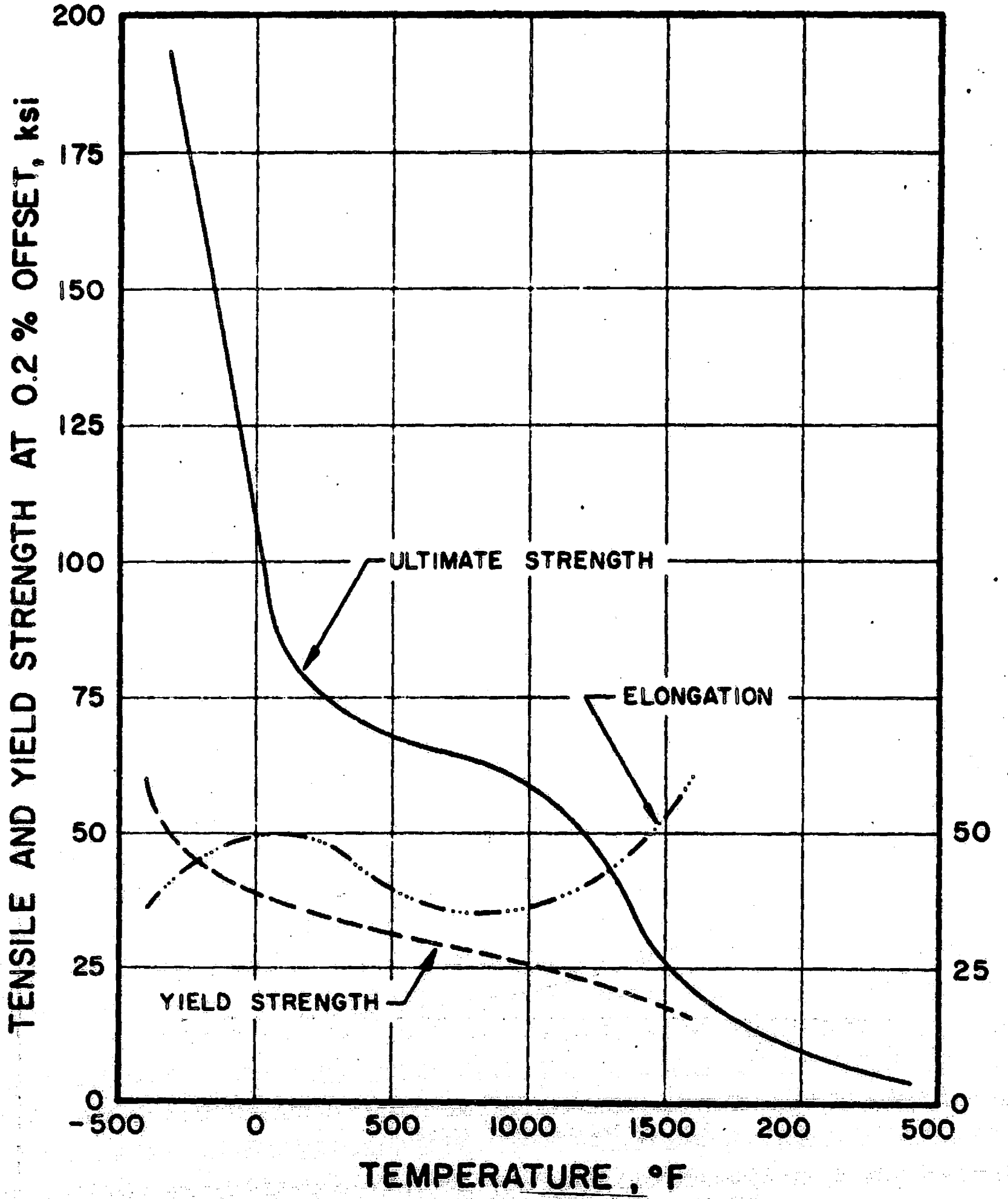


FIGURE 5 -- TYPICAL TENSILE STRENGTH, YIELD STRENGTH AND ELONGATION OF TYPE 347 STAINLESS STEEL

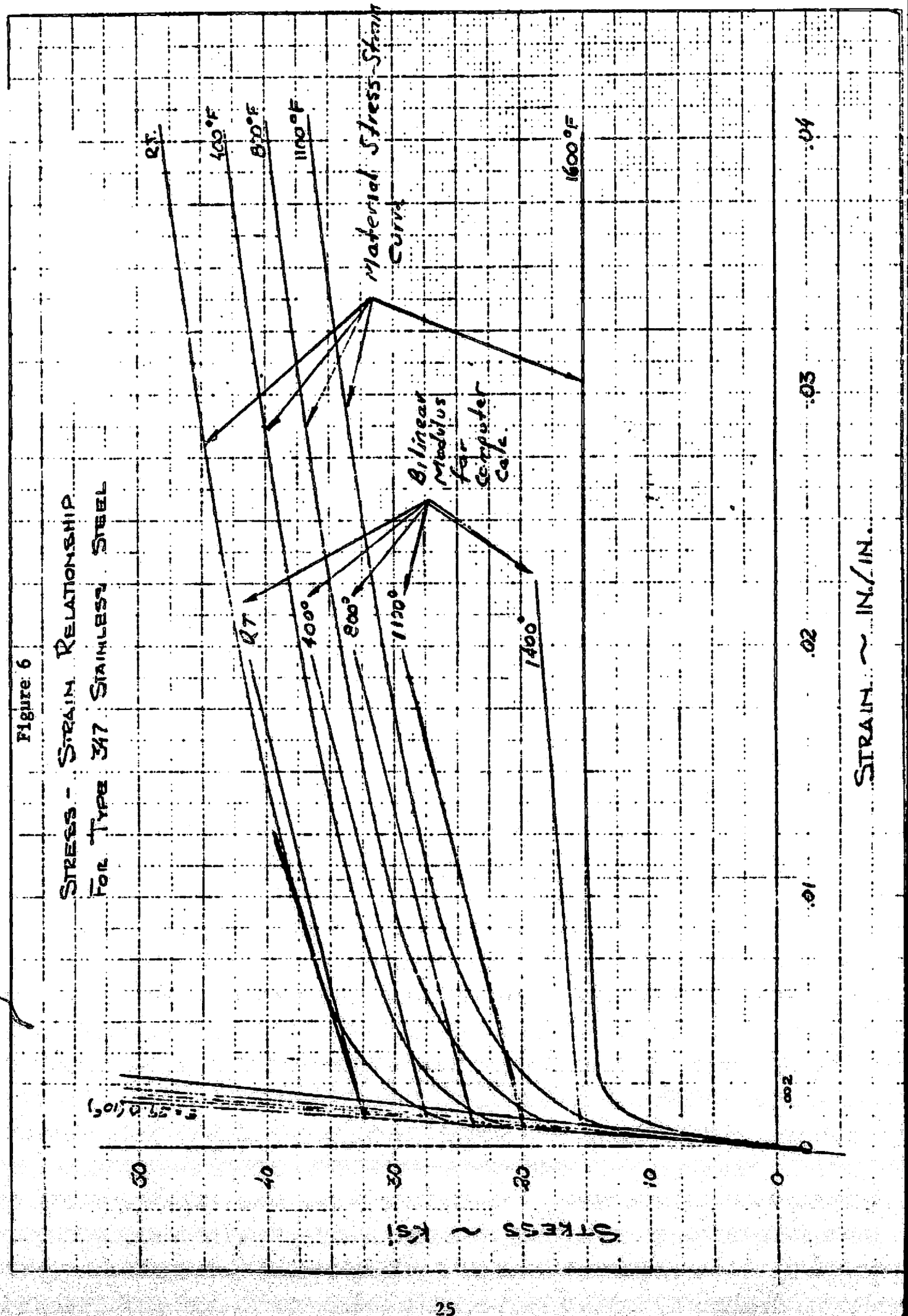


Figure 6

STRESS - STRAIN RELATIONSHIP
FOR TYPE 347 STAINLESS STEEL

Thermal Coefficient of Expansion of AISI 347 Stainless Steel

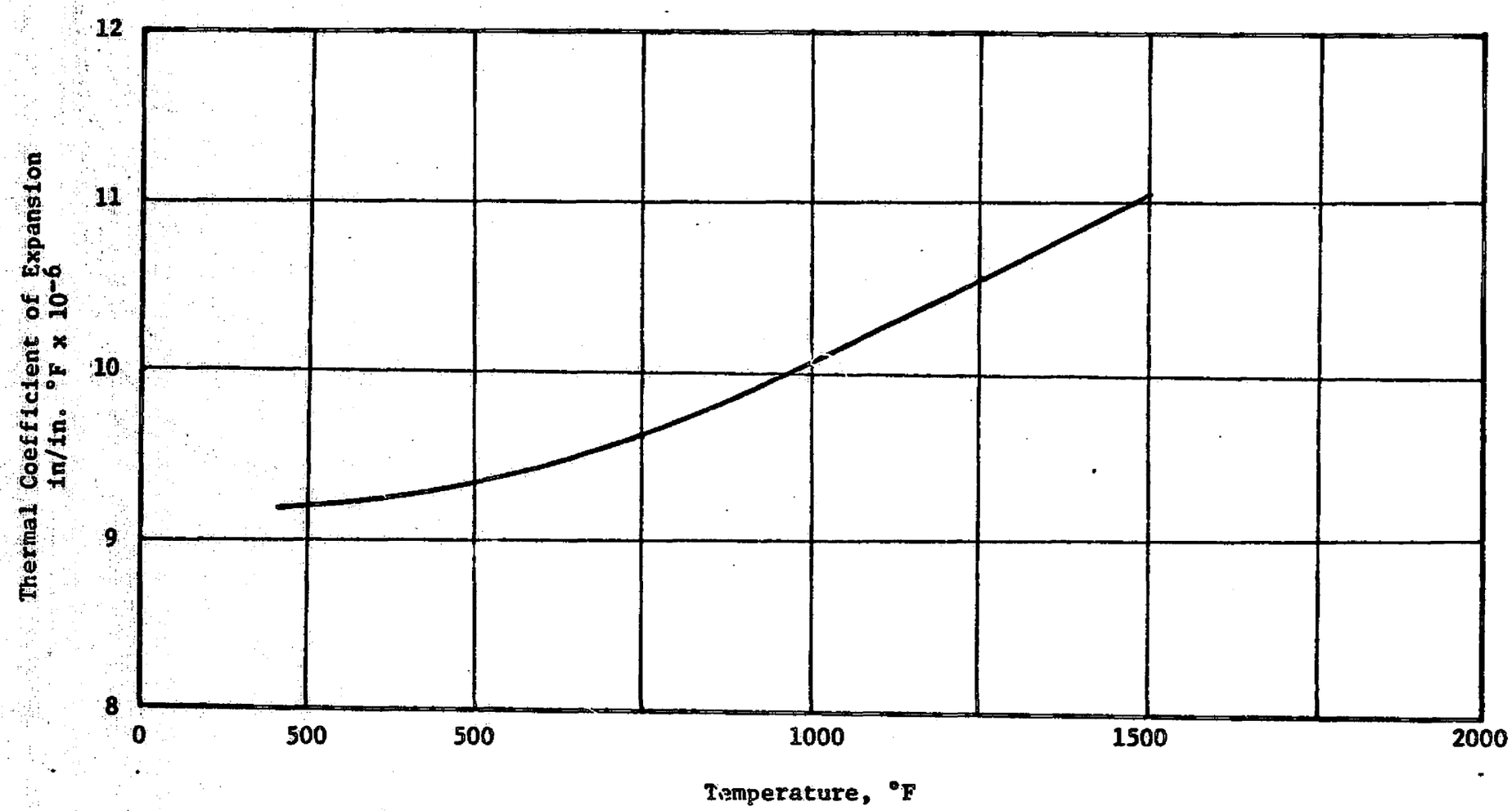
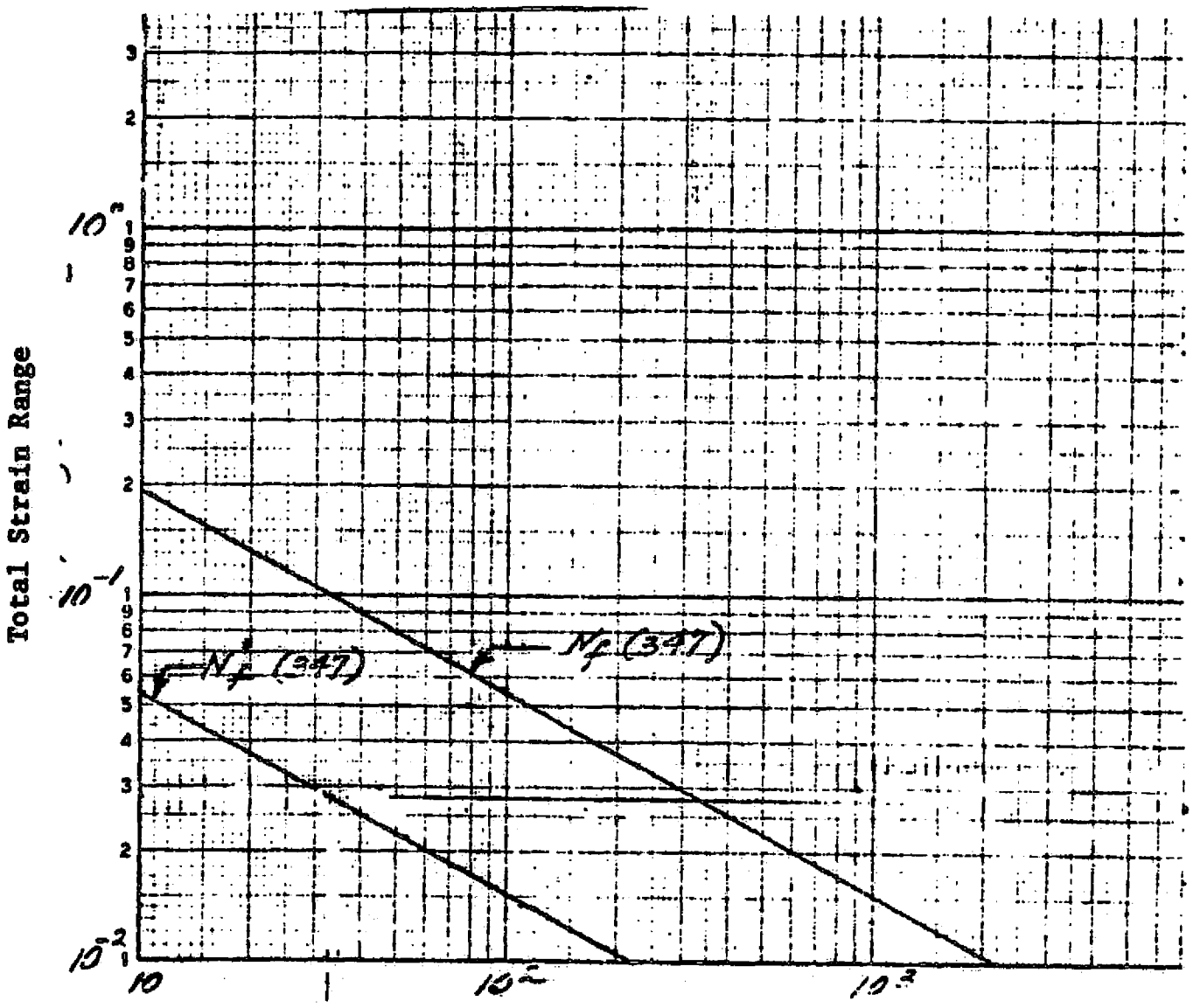


Figure 7

Figure 8

Thermal Fatigue Criteria
for Cyclic Life

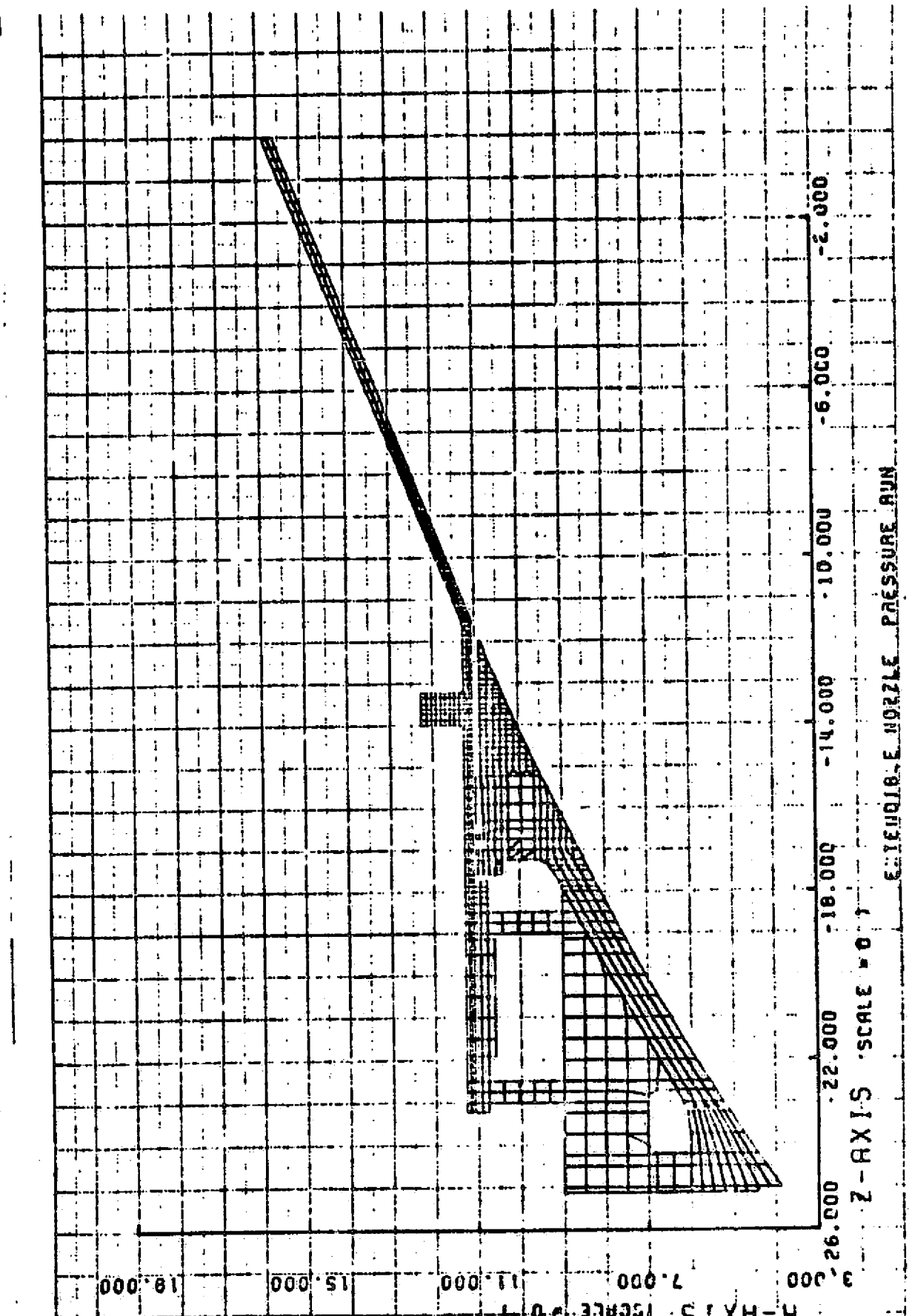


Cycles to Failure at 1500°F

N_f' Assumed lower bound $\frac{1}{10} N_f$

N_f Predicted Average Cyclic Life

Reference 4



Finite Element Grid Photo-reduced

Figure 9

REPRODUCIBILITY OF THE ORIGINAL PAGE IS POOR.

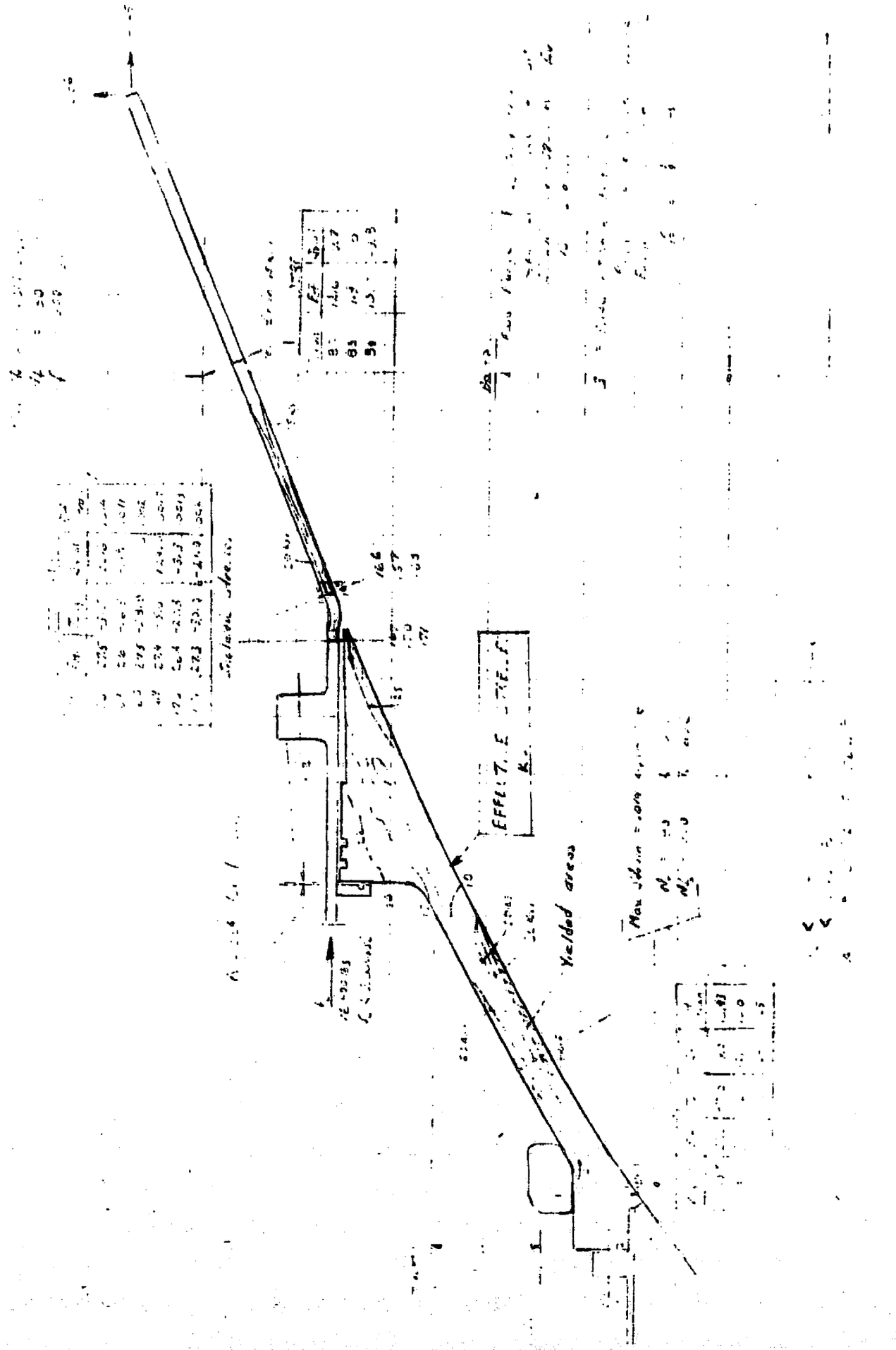


FIGURE 10 -- EFFECTIVE STRESSES FOR COMBINED THERMAL - MECHANICAL LOADS; INELASTIC SOLUTION

REPRODUCIBILITY OF THE ORIGINAL PAGE IS POOR.

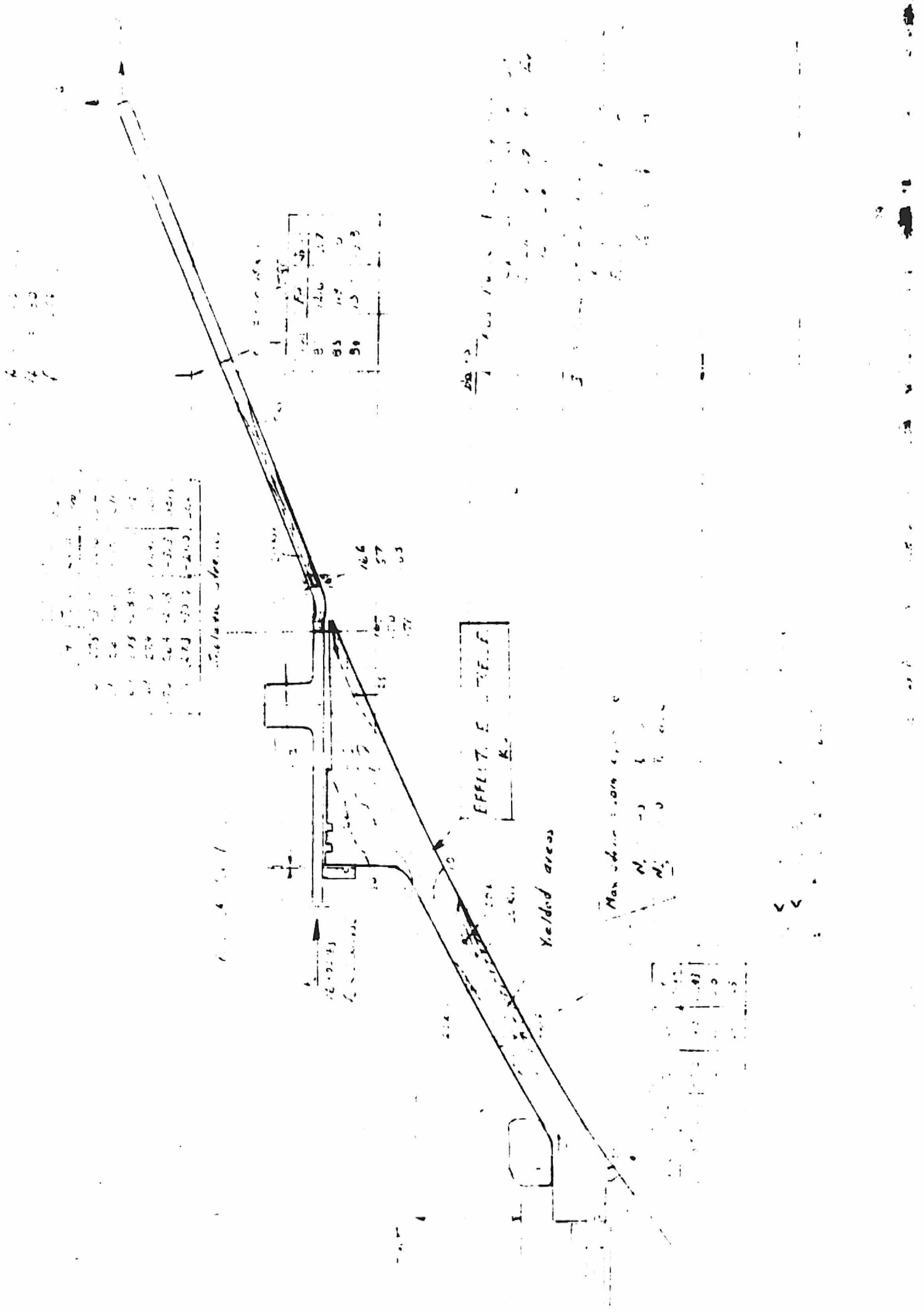
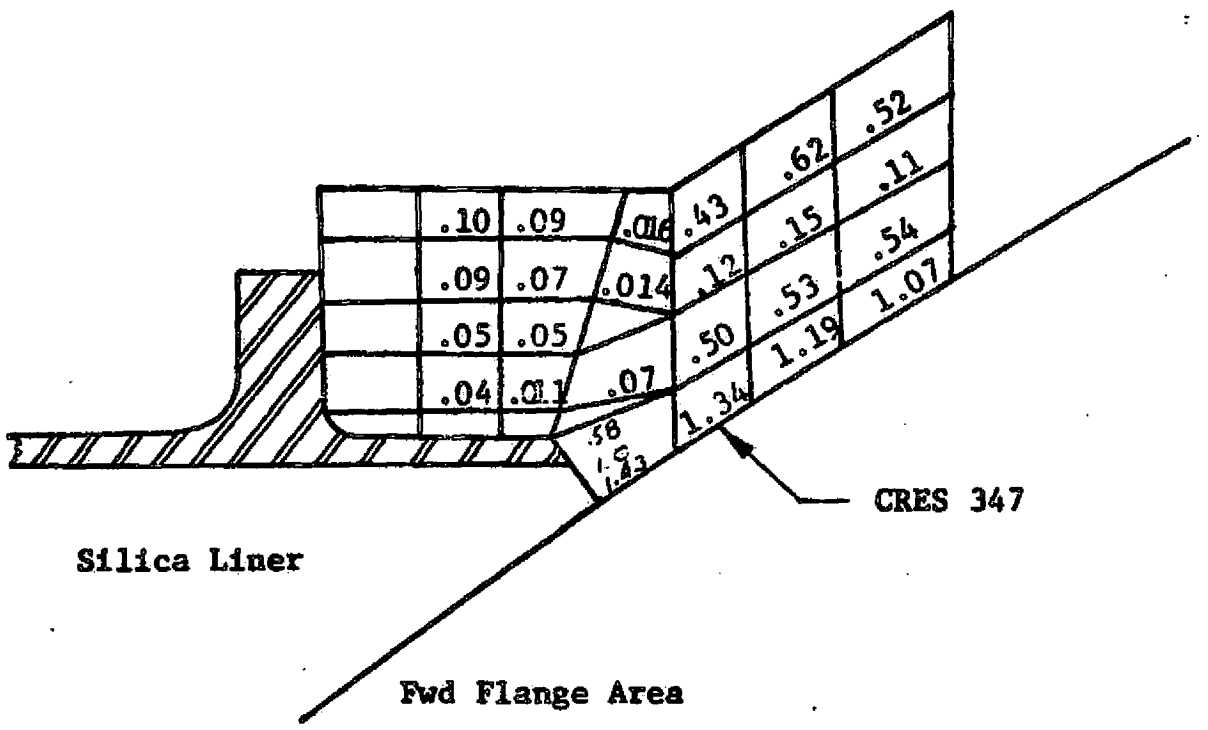


FIGURE 10 -- EFFECTIVE STRESSES FOR COMBINED THERMAL - MECHANICAL LOADS; INELASTIC SOLUTION



The maximum effective strain - inelastic solution

= .0143

N'f = 80 cycles min

Nf = 900 cycles pred. average

FIGURE 11 -- EFFECTIVE STRAIN DISTRIBUTION IN NOZZLE FORWARD FLANGE